CHARACTERISATION OF DEREGULATED MICRORNAS IN HUMAN NON-SMALL CELL LUNG CANCER AND THEIR ROLE IN TUMOUR ANGIOGENESIS AND METASTASIS

HO CHAI SAN

FACULTY OF SCIENCE
UNIVERSITY OF MALAYA
KUALA LUMPUR

2017

CHARACTERISATION OF DEREGULATED MICRORNAS IN HUMAN NON-SMALL CELL LUNG CANCER AND THEIR ROLE IN TUMOUR ANGIOGENESIS AND METASTASIS

HO CHAI SAN

THESIS SUBMITTED IN FULFILMENT OF THE REQUIREMENTS FOR THE DEGREE OF DOCTOR OF PHILOSOPHY

INSTITUTE OF BIOLOGICAL SCIENCES
FACULTY OF SCIENCE
UNIVERSITY OF MALAYA
KUALA LUMPUR

2017

UNIVERSITY OF MALAYA

ORIGINAL LITERARY WORK DECLARATION

Name of Candidate: HO CHAI SAN

Matric No.: SHC 120062

Name of Degree: DOCTOR OF PHILOSOPHY

Title of Thesis ("this Work"): CHARACTERISATION OF DEREGULATED MICRORNAS IN HUMAN NON-SMALL CELL LUNG CANCER AND THEIR ROLE IN TUMOUR ANGIOGENESIS AND METASTASIS

Field of Study: CANCER BIOLOGY

I do solemnly and sincerely declare that:

(1) I am the sole author/writer of this Work;
(2) This Work is original;
(3) Any use of any work in which copyright exists was done by way of fair dealing and for permitted purposes and any excerpt or extract from, or reference to or reproduction of any copyright work has been disclosed expressly and sufficiently and the title of the Work and its authorship have been acknowledged in this Work;
(4) I do not have any actual knowledge nor do I ought reasonably to know that the making of this work constitutes an infringement of any copyright work;
(5) I hereby assign all and every rights in the copyright to this Work to the University of Malaya ("UM"), who henceforth shall be owner of the copyright in this Work and that any reproduction or use in any form or by any means whatsoever is prohibited without the written consent of UM having been first had and obtained;
(6) I am fully aware that if in the course of making this Work I have infringed any copyright whether intentionally or otherwise, I may be subject to legal action or any other action as may be determined by UM.

Chai San

Candidate's Signature Date: 28.07.2017

Subscribed and solemnly declared before,

Witness's Signature Date: 28.07.2017

Name: Prof. Dr. Noor Hasima Nagoor

Designation: Professor

ABSTRACT

Lung cancer is the most commonly diagnosed cancer worldwide and ranks third in Malaysia with increasing mortality rate over the years. This is often due to late presentation of disease at the metastatic stage. MicroRNAs, even though are only small single-stranded non-coding RNAs, have been proven to be mighty micromanagers of gene expression in many biological processes including cancer metastasis and angiogenesis. They are comprehensively studied and thus proposed as potential molecular targets for cancer treatment. However, the mechanisms microRNA is used to modulate lung cancer metastasis remain unclear. High and low invasive A549 and SK-LU-1 sub-cell lines selected through serial transwell invasion assay for at least seven generations from their parental cell lines, were used to analyse differentially expressed metastasis-related microRNAs. Invasive phenotype in high invasive A549 and SK-LU-1 cells was found to be accompanied by gain of miR-92b and miR-378 expression as well as loss of miR-1827 expression. Investigation into the roles of these microRNAs in metastasis, particularly invasion, migration and angiogenesis, revealed that miR-378 functions as a cell invasion regulator while miR-1827 modulates cell migration. Both microRNAs work in opposite manner to mediate angiogenesis. The conversion from low invasive to high invasive phenotype by miR-378 and anti-miR-1827 was shown to involve epithelial-mesenchymal transition. MiR-92b, on the other hand, is not significant during the course of metastasis and angiogenesis in non-small cell lung cancer. Subsequently, using bioinformatics approaches, dual luciferase reporter assay and Western blotting, *RBX1* and *CRKL* were identified as new targets of miR-378 and miR-1827, respectively. Changes in cell invasion and migratory potentials were directly controlled by *RBX1* and *CRKL* under the negative regulation of miR-378 and miR-1827, as the repressive and inductive effects of microRNA mimics and hairpin inhibitors could be rescued by *RBX1*/ *CRKL* overexpression and knockdown. Nevertheless,

restoration of *RBX1* and *CRKL* expression only slightly reverted the angiogenic activities, suggesting that angiogenesis in non-small cell lung cancer is not only dependent on *RBX1* and *CRKL*. These *in vitro* results were translated into *in vivo* zebrafish embryo model. MiR-378 hairpin inhibitors- and miR-1827 mimics-treated high invasive A549 cells demonstrated reduced number of metastases and ectopic vessel formation in the embryonic fish compared to negative controls. Collectively, these findings indicate that miR-378 and miR-1827 play important roles in metastasis and angiogenesis by regulating epithelial-mesenchymal transition in non-small cell lung cancer. In particular, miR-378 promotes cell invasion by targeting *RBX1* while miR-1827 suppresses cell migration by targeting *CRKL*. However, *RBX1* and *CKRL* are not the major players in miR-378- and miR-1827-mediated angiogenesis.

ABSTRAK

Kanser peparu ialah kanser yang paling biasa di diagnosis di seluruh dunia dan ia menduduki tempat ketiga di Malaysia dengan kadar kematian yang semakin meningkat saban tahun. Hal ini sering disebabkan oleh kelewatan pengesanan penyakit pada peringkat metastasis. MikroRNA, walaupun hanya merupakan rantaian RNA tunggal kecil yang tidak mengkod, tetapi telah dibuktikan sebagai pengurus mikro yang berkuasa kepada ekspresi gen di dalam banyak proses biologi termasuk metastasis dan angiogenesis kanser. Ianya telah dikaji secara menyeluruh dan dengan itu dicadangkan sebagai molekul sasaran yang berpotensi untuk rawatan kanser. Namun, mekanisma yang digunakan oleh mikroRNA dalam memodulasikan metastasis kanser peparu masih belum jelas. Sub keturunan sel A549 dan SK-LU-1 yang lebih dan kurang invasif yang dipilih melalui siri 'transwell invasion assay' untuk sekurang-kurangnya tujuh generasi daripada keturunan sel induk mereka, telah digunakan untuk menganalisis mikroRNA berkaitan dengan metastasis yang ekspresinya berbeza. Fenotip invasif dalam sel-sel A549 dan SK-LU-1 yang lebih invasif telah didapati seiring dengan pertambahan ekspresi miR-92b dan miR-378 serta kehilangan ekspresi miR-1827. Penyiasatan ke atas peranan mikroRNA ini dalam metastasis, terutamanya invasi, migrasi dan angiogenesis, mendedahkan bahawa miR-378 berfungsi sebagai satu pengawal invasi sel manakala miR-1827 memodulasikan migrasi sel. Kedua-dua mikroRNA itu bekerja dalam cara yang bertentangan untuk menjadi pengantara angiogenesis. Penukaran daripada fenotip kurang invasif kepada lebih invasif oleh miR-378 dan anti-miR-1827 telah ditunjukkan yang ia melibatkan peralihan daripada epitelium ke mesenkima. Sebaliknya, miR-92b, adalah tidak signifikan semasa metastasis dan angiogenesis dalam 'non-small cell' kanser peparu. Seterusnya, dengan menggunakan pendekatan bioinformatik, 'dual luciferase reporter assay' dan 'Western blotting', *RBX1* dan *CRKL* masing-masing telah dkenalpasti sebagai sasaran baru miR-378 dan miR-1827.

Perubahan dalam potensi invasi dan migrasi sel adalah dikawal secara langsung oleh *RBX1* dan *CRKL* di bawah pengawalan negatif miR-378 dan miR-1827, sebagaimana kesan penyekatan dan induktif mimik dan 'hairpin inhibitors' mikroRNA boleh diselamatkan oleh kelebihan dan penurunan ekspresi *RBX1*/ *CRKL*. Namun, pemulihan ekspresi *RBX1* dan *CRKL* hanya mengembalikan sebahagian kecil aktiviti angiogenik, mencadangkan bahawa angiogenesis dalam 'non-small cell' kanser peparu adalah tidak bergantung kepada *RBX1* dan *CRKL* sahaja. Hasil-hasil '*in vitro*' ini telah diterjemahkan ke dalam model embrio ikan zebra '*in vivo*'. Sel-sel A549 yang lebih invasif yang dirawat dengan 'hairpin inhibitors' miR-378 dan mimik miR-1827 menunjukkan pengurangan dalam bilangan metastasis dan pembentukan saluran ektopia dalam embrio ikan berbanding dengan kawalan negatif. Secara keseluruhannya, hasil kajian ini menandakan bahawa miR-378 dan miR-1827 memainkan peranan penting dalam metastasis dan angiogenesis dengan mengawal peralihan daripada epitelium ke mesenkima dalam 'non-small cell' kanser peparu. Khususnya, miR-378 menggalakkan invasi sel dengan menyasarkan *RBX1* manakala miR-1827 menyekat migrasi sel dengan menyasarkan *CRKL*. Namun, *RBX1* dan *CRKL* bukanlah pemain peranan utama dalam angiogenesis yang dikawal oleh miR-378 dan miR-1827.

ACKNOWLEDGEMENTS

First and foremost, I would like to express my utmost appreciation to my project supervisor, Prof. Dr. Noor Hasima Nagoor. I am grateful for her continuous support in the approaches and ideas undertaken in this project. I am also deeply indebted to Dr. Suzita Mohd. Noor, for the valuable advice and scientific insights she has shared during the early stages of my *in vivo* study.

My sincere gratitude goes to all the past and present members of the Cancer Research Lab for the pleasant working atmosphere. I benefited greatly from the numerous exciting discussions we had. Special thanks dedicated to Darren Khor and David Wong from the Zebrafish Lab, for their technical assistance with zebrafish breeding and embryo handling.

I would also like to acknowledge the Ministry of Education for the scholarship I received, as well as the University of Malaya for financing this project through the High Impact Research Grant (HIR) (UM.C/625/1/HIR/MOE/CHAN/016).

Finally, I would like to express my bottomless love to my dearest family and friends. Thank you for your patience and endless support throughout my study.

The completion of this PhD would not have been possible without the contributions from all of the above-mentioned people in various ways. Once again, thank you!

TABLE OF CONTENTS

LIST OF FIGURES

LIST OF TABLES

LIST OF SYMBOLS AND ABBREVIATIONS

α	:	Alpha
~	:	Approximately
β	:	Beta
Δ	:	Delta, the difference operator
°	:	Degree
°C	:	Degree Celsius
∞	:	Infinity
<	:	Less than
≤	:	Less than or equal to
>	:	More than
≥	:	More than or equal to
+	:	Anode
-	:	Cathode
×	:	i. Multiplication ii. Times
#	:	Number
%	:	Percentage
±	:	Plus-minus
**	:	Significance at the 0.01 level
*	:	Significance at the 0.05 level
× g	:	Times gravity
µg	:	Microgram
µL	:	Microlitre
µm	:	Micrometer
µM	:	Micromolar
µS	:	Microsiemens
3’	:	End of the molecule which terminates in a 3’ phosphate group
3’-UTR	:	3’-untranslated region
5’	:	End of the molecule which terminates in a 5’ phosphate group

5’-UTR	:	5’-untranslated region
5-FU	:	5-fluorouracil
A	:	Adenine
$A_{260/230}$	:	Ratio of absorbance at 260nm to absorbance at 230nm
$A_{260/280}$	:	Ratio of absorbance at 260nm to absorbance at 280nm
AAALAC	:	Association for Assessment and Accreditation of Laboratory Animal Care
ABCC3	:	Adenosine triphosphate-binding cassette subfamily C member 3
ABCC6	:	Adenosine triphosphate-binding cassette subfamily C member 6
AC	:	Adenocarcinoma
ACTA2	:	Actin, alpha 2, smooth muscle, aorta
ACTR2/3	:	ARP2/3 actin-related protein 2/3 homolog
AGE	:	Agarose gel electrophoresis
AKT1	:	AKT serine/threonine kinase 1
ALK	:	Anaplastic lymphoma receptor tyrosine kinase
ALP	:	Alkaline phosphatase
AM	:	Actomethylester
AMOT	:	Angiomotin
ANGPT1	:	Angiopoietin 1
ANGPT2	:	Angiopoietin 2
ANGPTL4	:	Angiopoietin-like 4
APS	:	Ammonium persulfate
ARNT	:	Aryl hydrocarbon receptor nuclear translocator
ATCC	:	American Type Culture Collection
ATP	:	Adenosine triphosphate
BCA	:	Bicinchinonic acid
BCAR1	:	BCAR1, Cas family scaffolding protein
BCIP	:	5-bromo-4-chloro-3-indolyl phosphate
BCL2	:	BCL2, apoptosis regulator
Blastn	:	Nucleotide Basic Local Alignment Search Tool
BMI1	:	BMI1 proto-oncogene, polycomb ring finger

BMP1	:	Bone morphogenetic protein 1
bp	:	Base pair
BRAF	:	B-RAF proto-oncogene, serine/threonine kinase
BSA	:	Bovine serum albumin
C	:	Cytosine
Ca^{2+}	:	Calcium ions
$CaCl_2$	:	Calcium chloride
CAMK2	:	Calcium/calmodulin-dependent protein kinase II
CALML3	:	Calmodulin-like 3
CAND1	:	Cullin-associated and neddylation-dissociated-1
CCND1	:	Cyclin D1
CDC42	:	Cell division cycle 42
CDH1	:	Cadherin 1
CDH2	:	Cadherin 2
CDKN1B	:	Cyclin-dependent kinase inhibitor 1B
cDNA	:	Complementary DNA
CEACAM6	:	Carcinoembryonic antigen-related cell adhesion molecule 6
Cel	:	Caenorhabditis elegans
ChIP-seq	:	Chromatin immunoprecipitation-sequencing
CLDN1	:	Claudin 1
CLDN3	:	Claudin 3
CO_2	:	Carbon dioxide
CRB	:	Crumbs, cell polarity complex component
CRK	:	CRK proto-oncogene, adaptor protein
CRKL	:	CRK-like proto-oncogene, adaptor protein
CRL	:	Cullin-based RING ligase
CRMP1	:	Collapsin response mediator protein 1
CSN	:	Cop9 Signalosome
C_t	:	Cycle threshold
CTC	:	Circulating tumour cells

CTGF	:	Connective tissue growth factor
CTNNA	:	Catenin alpha
CTNNB1	:	Catenin beta 1
CTNND1	:	Catenin delta 1
CTSC	:	Cathepsin C
CTTN	:	Cortactin
CXCL8	:	C-X-C motif chemokine ligand 8
DAVID	:	Database for Annotation, Visualization and Integrated Discovery
DEPTOR	:	DEP domain-containing MTOR interacting protein
DGCR8	:	DiGeorge syndrome critical regions gene 8
DGS	:	DiGeorge syndrome
DiI	:	1,1'-dioctadecyl-3,3,3',3'-tetramethylindocarbocyanine perchlorate
DKK3	:	Dickkopf WNT signalling pathway inhibitor 3
DMSO	:	Dimethyl sulfoxide
DNA	:	Deoxyribonucleic acid
dNTP	:	Deoxynucleotide
DPBS	:	Dulbecco's phosphate-buffered saline
dpf	:	Day post fertilisation
DPP4	:	Dipeptidyl peptidase 4
ds	:	Double-stranded
DSC3	:	Desmocollin 3
DSG3	:	Desmoglein 3
DSP	:	Desmoplakin
DTT	:	Dithiothreitol
dTTP	:	Deoxythymidine triphosphate
E. coli	:	Escherichia coli
E2F1	:	E2F transcription factor 1
ECM	:	Extracellular matrix
EDTA	:	Ethylenediaminetetraacetic acid
EDV	:	EnGeneIC delivery vehicle

EGF	:	Epidermal growth factor
EGFR	:	Epidermal growth factor receptor
EMT	:	Epithelial-mesenchymal transition
ERBB2	:	Erb-B2 receptor tyrosine kinase 2
ERBB3	:	Erb-B2 receptor tyrosine kinase 3
ERBB4	:	Erb-B2 receptor tyrosine kinase 4
EZR	:	Ezrin
FBS	:	Fetal bovine serum
FDA	:	Food and Drug Administration
FGF	:	Fibroblast growth factor
FGF2	:	Fibroblast growth factor 2
Fiji	:	Fiji Is Just ImageJ
FLT1	:	Fms-related tyrosine kinase 1
FN1	:	Fibronectin 1
FOXA1	:	Forkhead box A1
FOXM1	:	Forkhead box M1
FZD	:	Frizzled
G	:	Guanine
G1	:	Gap 1
GAPDH	:	Glyceraldehyde 3-phosphate dehydrogenase
GJA1	:	Gap junction protein alpha 1
GPI	:	Glucose-6-phosphate isomerase
GRB2	:	Growth factor receptor-bound protein 2
GTC	:	Guanidinium thiocyanate
GTPase	:	Guanosine triphosphatase
h	:	Hour
HCL	:	Hydrochloric acid
HIF1A	:	Hypoxia-inducible factor 1 alpha subunit
HMGA2	:	High mobility group AT-hook 2
HMOX1	:	Heme oxygenase 1

HOXA5	:	Homeobox A5
hPa	:	Hectopascal
hpf	:	Hours post fertilisation
hpi	:	Hours post injection
HPSE	:	Heparanase
HRP	:	Horseradish peroxidase
Hsa	:	Homo sapiens
HUVEC	:	Human umbilical vein endothelial cells
IACUC	:	Institutional Animal Care and Use Committee
ID2	:	Inhibitor of DNA binding 2, helix-loop-helix (HLH) protein
IFNG	:	Interferon gamma
IGF	:	Insulin-like growth factor
IKK	:	Inhibitor of nuclear factor kappa B
IMD	:	Intratumoural microvessel density
IPTG	:	Isopropyl β-D-1-thiogalactopyranoside
IRS2	:	Insulin receptor substrate 2
ITGAV	:	Integrin subunit alpha V
ITGB1	:	Integrin subunit beta 1
ITGB3	:	Integrin subunit beta 3
JUP	:	Junction plakoglobin
kb	:	Kilobases
kDa	:	Kilodalton
KRAS	:	KRAS proto-oncogene, guanosine triphosphatase
L	:	Litre
L1CAM	:	L1 cell adhesion molecule
LB	:	Luria-Bertani
LCS6	:	Let-7 complementary site 6
LDEV	:	Lactate dehydrogenase-elevating virus
ln	:	Natural logarithm
LNA	:	Locked nucleic acid

LOX	:	Lysyl oxidase
LOXL2	:	Lysyl oxidase-like 2
LOXL4	:	Lysyl oxidase-like 4
LRP5/6	:	Low density lipoprotein receptor-related protein 5/6
LVES	:	Large vessel endothelial supplement
mA	:	Milliampere
MAP3K2	:	Mitogen-activated protein kinase kinase kinase 2
MAPK	:	Mitogen-activated protein kinase
MAPK1	:	Mitogen-activated protein kinase 1
MAPK3	:	Mitogen-activated protein kinase 3
MCL1	:	BCL2 family apoptosis regulator
MCS	:	Multiple cloning site
MEM	:	Minimum essential medium
MET	:	i. Mesenchymal-epithelial transition ii. MET proto-oncogene, receptor tyrosine kinase
mg	:	Milligram
$MgCl_2$	:	Magnesium chloride
MiRNA	:	MicroRNA
MiRNA*	:	Passenger microRNA strand
mL	:	Millilitre
MLPH	:	Melanophilin
mm	:	Millimeter
mM	:	Millimolar
MMP	:	Matrix metallopeptidase
MMP2	:	Matrix metallopeptidase 2
MMP9	:	Matrix metallopeptidase 9
MMP14	:	Matrix metallopeptidase 14
MPDZ	:	Multiple PDZ domain crumbs cell polarity complex component
MPP5	:	Membrane palmitoylated protein 5
mRNA	:	Messenger RNA
MT	:	Mutated

MTA1	:	Metastasis-associated 1
MTDH	:	Metadherin
MTg-AMO	:	Multiple-target anti-miRNA antisense oligodeoxyribonucleotide
MTOR	:	Mechanistic target of rapamycin
MUC1	:	Mucin 1, cell surface-associated
MUC3B	:	Mucin 3B, cell surface-associated
MUC5B	:	Mucin 5B, oligomeric mucus/ gel-forming
MYC	:	v-Myc avian myelocytomatosis viral oncogene homolog
MYCL	:	v-Myc avian myelocytomatosis viral oncogene lung carcinoma-derived homolog
NaCl	:	Sodium chloride
NaOH	:	Sodium hydroxide
NAPSA	:	Napsin A aspartic peptidase
NBT	:	Nitro blue tetrazolium chloride
NCBI	:	National Center for Biotechnology Information
NECTIN2	:	Nectin cell adhesion molecule 2
NFκB	:	Nuclear factor kappa B
ng	:	Nanogram
NIH	:	National Institutes of Health
NKX2-1	:	NK2 homeobox 1
NLK	:	Nemo-like kinase
nm	:	Nanometer
nM	:	Nanomolar
NOX4	:	Nicotinamide adenine dinucleotide phosphate oxidase 4
NRP1	:	Neuropilin 1
NSCLC	:	Non-small cell lung cancer
nt	:	Nucleotide
NTRK2	:	Neurotrophic receptor tyrosine kinase 2
OCLN	:	Occludin
OD	:	Optical density
ORF	:	Open reading frame

PAGE	:	Polyacrylamide gel electrophoresis
PATJ	:	PATJ, crumb cell polarity complex component
PBS	:	Phosphate-buffered saline
PBST	:	Phosphate-buffered saline with Tween-20
P_c	:	Compensation pressure
PCP	:	Planar cell polarity
PDGF	:	Platelet-derived growth factor
PET	:	Polyethylene terephthalate
PFA	:	Paraformaldehyde
pH	:	Potential of hydrogen
P_i	:	Injection pressure
PI3K	:	Phosphatidylinositol-4,5-bisphosphate 3-kinase
PIK3R3	:	Phosphatidylinositide-3-kinase regulatory subunit 3
PKP	:	Plakophilin
PLAU	:	Plasminogen activator, urokinase
PLAUR	:	Plasminogen activator, urokinase receptor
PLC	:	Phospholipase C
pm	:	Picomole
POU5F1	:	POU class 5 homeobox 1
PPARGC1B	:	Peroxisome proliferator-activated receptor gamma co-activator 1 beta
Pre-miRNA	:	Precursor microRNA
Pri-miRNA	:	Primary microRNA
PRKC	:	Protein kinase C
PRKCA	:	Protein kinase C alpha
PTCH1	:	Patched 1
PTEN	:	Phosphatase and tensin homolog
PTGS2	:	Prostaglandin-endoperoxidase synthase 2
PTK2	:	Protein tyrosine kinase 2
PTU	:	N-phenylthiourea
PXN	:	Paxillin

RAF1	:	Raf-1 proto-oncogene, serine/threonine kinase
RAP1A	:	RAP1A, member of RAS oncogene family
RAPGEF5	:	Rap guanine nucleotide exchange factor 5
RASA1	:	RAS p21 protein activator 1
RBX1	:	Ring-box 1
RFU	:	Relative fluorescence unit
RHO	:	Ras homolog
RHOA	:	Ras homolog family member A
RIN	:	RNA integrity
RISC	:	RNA-induced silencing complex
RNA	:	Ribonucleic acid
ROC1	:	Regulator of Cullins 1
ROCK1	:	Rho-associated coiled-coil containing protein kinase 1
rpm	:	Revolutions per minute
RPMI	:	Roswell Park Memorial Institute
rRNA	:	Ribosomal RNA
RT-qPCR	:	Reverse Transcription-Quantitative Real-time Polymerase Chain Reaction
S	:	Synthesis
S100A4	:	S100 calcium-binding protein A4
SCLC	:	Small cell lung cancer
SDS	:	Sodium dodecyl sulfate
SEM	:	Standard of mean
SFTA3	:	Surfactant-associated 3
SHH	:	Sonic hedgehog
SiRNA	:	Small interfering RNA
SIV	:	Sub-intestinal vessels
SLC15A1	:	Solute carrier family 15 member 1
SMAD2	:	SMAD family member 2
SMAD3	:	SMAD family member 3
SMAD4	:	SMAD family member 4

SMAD7	:	SMAD family member 7
SNAI1	:	SNAIL family transcriptional repressor 1
SNAI2	:	SNAIL family transcriptional repressor 2
SNP	:	Single nucleotide polymorphism
SOI	:	Site of implantation
SOX2	:	SRY-box 2
SOX4	:	SRY-box 4
SOX9	:	SRY-box 9
SPINK1	:	Serine peptidase inhibitor, Kazal type 1
SPRED1	:	Sprouty-related EVH1 domain-containing 1
SPRED2	:	Sprouty-related EVH1 domain-containing 2
SPRY1	:	Sprouty RTK signalling antagonist 1
SPRY3	:	Sprouty RTK signalling antagonist 3
SPRY4	:	Sprouty RTK signalling antagonist 4
SRC	:	SRC proto-oncogene, non-receptor tyrosine kinase
SRM	:	Substrate-recognition module
STAT1	:	Signal transducer and activator of transcription 1
STAT3	:	Signal transducer and activator of transcription 3
STR	:	Short tandem repeat
SUFU	:	SUFU negative regulator of Hedgehog signalling
T	:	Thymine
TAE	:	Tris-Acetate-Ethylenediaminetetraacetic acid
TCF	:	T-cell factor
TCF3	:	Transcription factor 3
TCM	:	Tumour-conditioned medium
TE	:	Tris-Ethylenediaminetetraacetic acid
TEAD	:	TEA domain transcription factor
TEMED	:	Tetramethylethylenediamine
TGF	:	Transforming growth factor
TGFA	:	Transforming growth factor alpha

TGFB1	:	Transforming growth factor beta 1
TGS	:	Tris-Glycine-Sodium dodecyl sulfate
THBS1	:	Thrombospondin 1
t_i	:	Injection time
TIMP3	:	TIMP metallopeptidase inhibitor 3
TJP1	:	Tight junction protein 1
TJP3	:	Tight junction protein 3
TKI	:	Tyrosine kinase inhibitor
TLN	:	Talin
T_m	:	Melting temperature
TMC5	:	Transmembrane channel-like 5
TNS	:	Tensin
TOB2	:	Transducer of ERBB2, 2
TP53	:	Tumour protein p53
TP53INP1	:	Tumour protein p53-inducible nuclear protein 1
TTF1	:	Transcription termination factor 1
TUSC2	:	Tumour suppressor candidate 2
TWIST1	:	TWIST family basic helix-loop-helix (bHLH) transcription factor 1
U	:	i. Enzyme unit ii. Uracil
USP25	:	Ubiquitin-specific peptidase 25
V	:	Volt
v/v	:	Volume/volume
VANGL2	:	VANGL planar cell polarity protein 2
VCFS	:	Velocardiofacial syndrome
VCL	:	Vinculin
VEGF	:	Vascular endothelial growth factor
VEGFA	:	Vascular endothelial growth factor A
VEGFC	:	Vascular endothelial growth factor C
VEGFR	:	Vascular endothelial growth factor receptor
VHL	:	Von Hippel-Lindau tumour suppressor

VIM	:	Vimentin
w/v	:	Weight/volume
WAS	:	Wiskott-Aldrich syndrome
WT	:	Wild type
WWTR1	:	WW domain-containing transcriptional regulator 1
X-gal	:	5-bromo-4-chloro-3-indolyl-β-D-galactopyranoside
YAP1	:	Yes-associated protein
ZEB1	:	Zinc finger E-box binding homeobox 1
ZEB2	:	Zinc finger E-box binding homeobox 2

LIST OF APPENDICES

CHAPTER 1: INTRODUCTION

Lung cancer remains a major health problem worldwide (Ferlay *et al.*, 2014). It is the third most common cancer diagnosed in Malaysia (Azizah *et al.*, 2016), of which, non-small cell lung cancer accounts for more than 80% (Travis *et al.*, 1995). Adenocarcinoma, being the major subtype of non-small cell lung cancer, responds better to chemotherapy than the other subtypes but it tends to relapse in the form of distant metastases (Yu *et al.*, 2005). The five-year survival rate is worrying as lung adenocarcinomas do not display typical years-long latency periods prior to overt metastasis formation. Instead, these tumours progress rapidly to macroscopic metastases upon infiltration of distant organ sites (Nguyen *et al.*, 2009).

Metastasis refers to the dissemination of primary tumour cells to local or distant sites in the body and proliferate to form secondary tumours (Gupta & Massague, 2006). To gain the ability to invade and migrate, they are reprogrammed through epithelial-mesenchymal transition, where transcription factors are activated, specific cell surface proteins are expressed, cytoskeleton proteins are reorganised, extracellular matrix-degrading enzymes are produced and expression of specific microRNAs are changed (Kalluri & Weinberg, 2009).

Tumours though, are angiogenesis-dependent (Folkman, 1971) and would enter a state known as angiogenic/ tumour mass dormancy when they reach 1-2mm in diameter due to insufficient vascularisation (Naumov *et al.*, 2006). The process of waking up dormant tumour cells to turn them into aggressive killers is complex and involves more than 50 interdependent cytokines, enzymes, growth factors and receptors (Carmeliet, 2000b). The resulting blood vessels are inherently leaky, which enhances the likelihood of metastasis (Jain, 2005).

MicroRNAs are small endogenous 18 to 25 nucleotide non-coding RNAs that regulate gene expression in various biological processes including cancer (Osada & Takahashi, 2007; Peng & Croce, 2016). They bind to the complementary 3'-untranslated region of their target genes to modulate their translation into proteins (Bartel, 2009). MicroRNAs can function as oncogenes or tumour suppressors. Changes in microRNA expression with concomitant downstream modulation of gene transcription have often been linked to the acquisition of metastatic and angiogenic traits (Zavadil *et al.*, 2007; Wang *et al.*, 2010d; Wang & Wang, 2012), thus making microRNAs as desirable therapeutic targets in metastatic cancers.

Before this study was conducted, it has long been shown that tumours are heterogeneous in nature and that highly metastatic tumour cell variants pre-exist in the parental population (Fidler, 1978, 1989). Following the hypothesis, a MSc. project by Yap S. H. (2012) had successfully shown that high and low invasive cells could be isolated from the parental A549 lung cancer cell population. MicroRNAs that were deregulated in high invasive sub-cell line in comparison to low invasive sub-cell line had also been identified. However, specific microRNA functions in lung cancer metastasis remain unclear.

It was hypothesised that the deregulated microRNAs are responsible for the differences in terms of invasiveness and migratory ability between high and low invasive cells, which in turn regulate metastasis and angiogenesis in lung cancer. Therefore, this work aimed to characterise these deregulated microRNAs in lung cancer and elucidate their roles in tumour metastasis and angiogenesis. The specific objectives of this thesis are:

1. To confirm the expression of deregulated microRNAs in SK-LU-1 lung adenocarcinoma cells

2. To uncover the roles of deregulated microRNAs in lung cancer metastasis and angiogenesis
3. To examine the potential roles of deregulated microRNAs in hypothetical signalling pathways modelled for lung cancer metastasis and angiogenesis
4. To identify and validate microRNA targets that are responsible for regulating the invasion, migration and angiogenesis of lung cancer cells
5. To investigate the functions of microRNA gene target in microRNA-mediated lung cancer cell invasion, migration and angiogenesis
6. To evaluate the effects of microRNA mimics/ hairpin inhibitors treatment on lung cancer metastasis and angiogenesis *in vivo*

CHAPTER 2: LITERATURE REVIEW

2.1 Cancer

Cancer is characterised by uncontrolled cell proliferation due to unrepaired DNA damages, thereby promoting the formation of tumour (Lopez-Camarillo *et al.*, 2012). It can be recognised when tumour exhibits properties such as deregulating cellular energetics, evasion of cell death, genome instability and mutation, growth inhibitors and immune destruction, limitless replicative potential and sustained growth signals, tumour-promoting inflammation, as well as angiogenesis, tissue invasion and metastasis (Hanahan & Weinberg, 2011).

2.1.1 Lung Cancer

Lung cancer remains the most commonly diagnosed cancer type and the leading cause of cancer mortality worldwide (Ferlay *et al.*, 2014). In Malaysia, lung cancer ranks the third (Azizah *et al.*, 2016). Direct linkage has been shown between the amount of exposure to tobacco and lung cancer incidences (Proctor, 2001), while other causes such as exposures to arsenic, asbestos, heavy metals, ionising radiation, radon or second-hand smoke, hookah smoking, genetic factors, hormones and viral infection are seen as contributing factors (Travis *et al.*, 2004).

Lung tumours can be categorised histologically into small cell lung cancer (SCLC) (16.8%) and non-small cell lung cancer (NSCLC) (80.4%) (Travis *et al.*, 1995). Cigarette smoking is known to be the cause of all known SCLC cases; however, lung cancer in non-smokers is almost entirely NSCLC with a majority being adenocarcinoma (AC) (40%) (Hanna & Hasan, personal communication, 2007).

The five-year survival rate for lung cancer patients is stagnant at less than 15% over the years (Travis *et al.*, 2011). This is likely due to the lack of early diagnostic

tools, causing late presentation of the disease with symptoms seen only when the disease is in the advance/ metastatic stage, thus refractory to most current therapeutic regimes (Spira *et al.*, 2004; Isobe *et al.*, 2005; Henschke & Yankelevitz, 2008). Chest radiographs have been shown to be unable to detect 70-80% of cancer (Bach *et al.*, 2007), while bronchoscopy, although specific, has low sensitivity (Schreiber & McCrory, 2003).

Specific markers of lung AC for instance, *MUC3B* (mucin 3B, cell surface-associated) (Nguyen *et al.*, 1996), *MUC5B* (mucin 5B, oligomeric mucus/ gel-forming) (Copin *et al.*, 2001), *DPP4* (dipeptidyl peptidase 4) (Wesley *et al.*, 2004), *SPINK1* (serine peptidase inhibitor, Kazal type 1) (Borczuk *et al.*, 2005), *ABCC3* (adenosine triphosphate-binding cassette subfamily C member 3) (Leslie *et al.*, 2007), *NTRK2* (neurotrophic receptor tyrosine kinase 2) (Ding *et al.*, 2008), *CLDN3* (claudin 3), *TJP3* (tight junction protein 3) (Kunner *et al.*, 2009), *NKX2-1* (NK2 homeobox 1) (Rekhtman *et al.*, 2011), *NAPSA* (napsin A aspartic peptidase) (Turner *et al.*, 2012), *CALML3* (calmodulin-like 3), *DSC3* (desmocollin 3), *DSG3* (desmoglein 3), *MLPH* (melanophilin), *SFTA3* (surfactant-associated 3) and *TMC5* (transmembrane channel-like 5) (Zhan *et al.*, 2015) have been recommended to shed light on disease detection. Notably, the accuracy of AC diagnosis using *MUC5B* or *NKX2-1* alone was shown to be 70.4% and 83.8%, respectively. However, the accuracy was drastically increased to 94.3% with the combination of *MUC5B* and *NKX2-1*. Survival analysis revealed that the *MUC5B*(High)/*NKX2-1*(-) group had significantly poorer outcomes compared to the *MUC5B*(Low)/*NKX2-1*(+) group (Nagashio *et al.*, 2015). Similarly, the diagnostic sensitivity and specificity of *NAPSA* were 72.2% and 90.4% while *NKX2-1* were 87.0% and 90.1%. Patients with high expression levels of *NAPSA* and *NKX2-1*, as well as high co-expression levels of *NAPSA*/ *NKX2-1* had better survival rates than those with low

levels of expression (Ma *et al.*, 2015). *CLDN3*, unfortunately, was not found to be associated with patient survival (Jung *et al*., 2009).

2.2 Metastasis

Metastasis is a condition where cells from the primary tumour migrate to either local or distant locations in the body and divide to form secondary tumours. Cancers at this stage are mostly incurable due to its systemic nature and resistance to chemo- and radiotherapies, thus providing an explanation for more than 90% of cancer death due to metastasis (Gupta & Massague, 2006; Steeg, 2006).

2.2.1 Mechanism of Metastasis

Both clonal selection theory (Nowell, 1976) and compartmental heterogeneity model (Weiss, 1990) support the idea of tumour heterogeneity such that only a portion of the tumour cells are genetically unstable and thus are able to acquire the metastatic phenotype through a series of epigenetic changes and somatic mutations to complete the process of dissemination. In addition, Fidler and Kripke showed the metastatic heterogeneity of cells within a primary tumour (Fidler & Kripke, 1977). These highly metastatic tumour cells are released into the circulation (Nagrath *et al.*, 2007; Stott *et al.*, 2010; Yu *et al.*, 2012; Baccelli *et al.*, 2013), rapidly carried away and eventually settle in smaller capillaries of secondary organs (Zeidman, 1961). However, less than 0.01% manage to endure the mechanical stress and infiltrate the parenchyma of foreign tissues to subsequently form macroscopic metastases (Weiss *et al.*, 1989; Weiss, 1992a; Weiss *et al.*, 1992b; Wong *et al.*, 2001; Chambers *et al.*, 2002; Kienast *et al.*, 2010).

2.2.1.1 The Invasion-Metastasis Cascade

Perhaps metastasis could be better described in a cascade of events whereby primary tumour cells (1) invade through extracellular matrix (ECM) and stromal cell

layers, (2) intravasate into the lumina of blood vessels, (3) survive in the circulation, (4) arrest at distant organs, (5) extravasate into the parenchyma of secondary sites, (6) survive in the foreign microenvironment to form micrometastases and (7) proliferate to form macrometastases, as depicted in Figure 2.1 (Fidler, 2003; Weinberg, 2007).

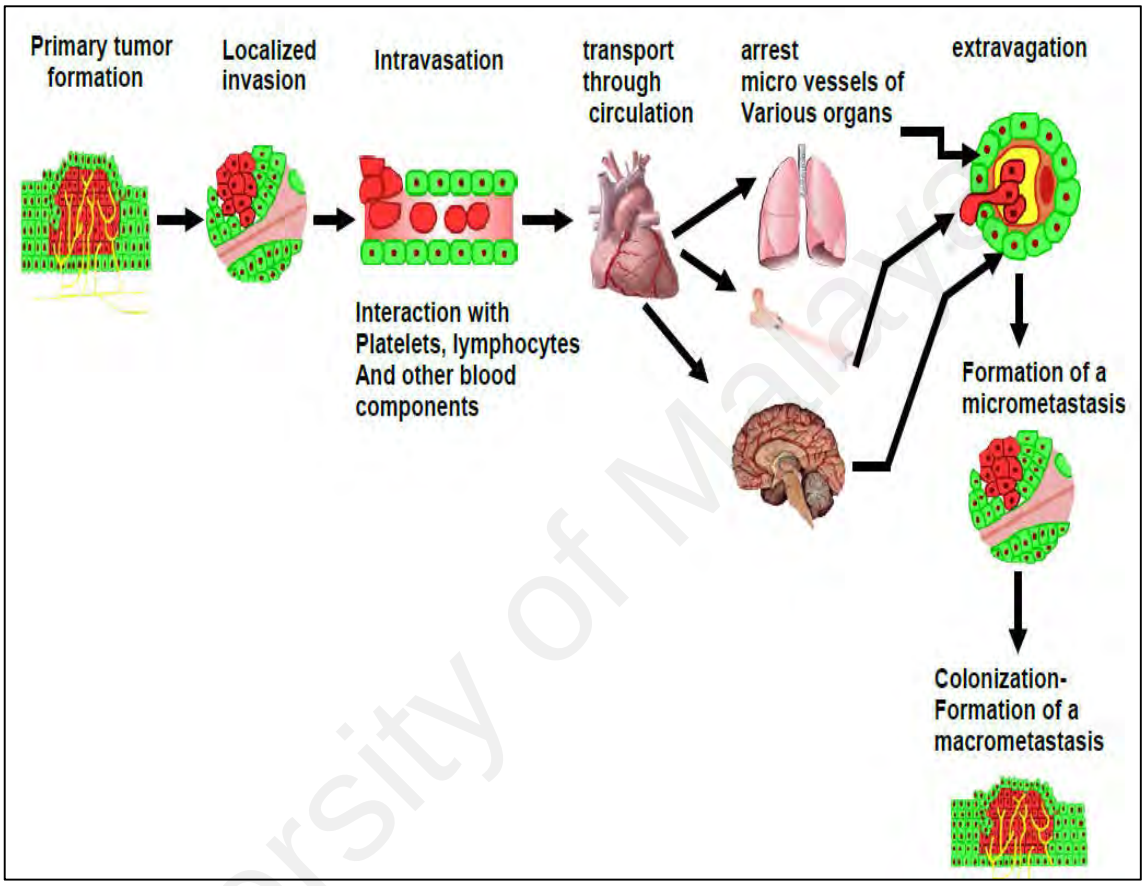

Figure 2.1: Seven steps to metastasis: (1) Breach of basement membrane (2) Intravasation (3) Transport to distant tissues (4) Arrest at target organs (5) Extravasation (6) Formation of micrometastases (7) Colonisation at secondary sites (Figure reproduced with permission from Weinberg, 2007).

Most human tumours are carcinomas derived from epithelial tissues. Epithelial cells are connected by intercellular junctions that prevent dissociation from their neighbours and undergo epithelial-mesenchymal transition (EMT) in order to initiate invasion.

One of the earliest events during EMT involves the delocalisation of tight junction proteins such as claudin 1 (CLDN1), desmoplakin (DSP), occludin (OCLN), plakophilin (PKP) and tight junction protein 1 (TJP1), causing the disruption of tight

junctions. Adherens junction complexes containing cadherin 1 (CDH1) and catenin beta 1 (CTNNB1) are also disrupted, and actin cytoskeleton is reorganised from a cortical location into actin stress fibres anchored to the focal adhesion complexes (Huang *et al.*, 2012). Upon EMT, cells lose apical-basal polarity and exhibit a spindle-shaped, fibroblast-like morphology. The down-regulation of *CDH1* is balanced by an increased expression of *CDH2* (cadherin 2), which results in a 'cadherin switch' that alters cell adhesion (Wheelock *et al.*, 2008; Yilmaz & Christori, 2009). They also express mesenchymal markers such as *ACTA2* (actin, alpha 2, smooth muscle, aorta), *FN1* (fibronectin 1), *S100A4* (S100 calcium-binding protein A4) and *VIM* (vimentin) (Valcourt *et al.*, 2005).

At this point, the resultant mesenchymal cells are able to dynamically elongate and persistently move towards cytokine gradients (Thiery & Sleeman, 2006; Yilmaz & Christori, 2009, 2010) with sheet-like membrane protrusions (lamellipodia) and spike-like extensions (filopodia) at the edge of lamellipodia (Ridley, 2011). These cells polarise, protrude, adhere, translocate and detach in a cyclic manner to invade and migrate in association with ECM degradation and regulated extracellular proteolysis by collagenases (Weiss *et al.*, 1988), MMPs (matrix metallopeptidases), plasminogen activator, urokinase (PLAU) and plasminogen activator, urokinase receptor (PLAUR) (Kim *et al.*, 1998). They extend a lamellipodium at the leading edge which adheres to the substrate, then contract to pull the cell body forward and retract the trailing edge (Figure 2.2) (Ridley *et al.*, 2003; Palmer *et al.*, 2011). Alternatively, tumour cells can move in an amoeboid manner and squeeze through between ECM fibres (Wolf *et al.*, 2003). Intravasation of tumour cells into the lumina of blood or lymphatic vessels is greatly dependent on the structural features of tumour blood vessels which tend to be leaky and tortuous, and reconfigure continuously (Carmeliet & Jain, 2011b).

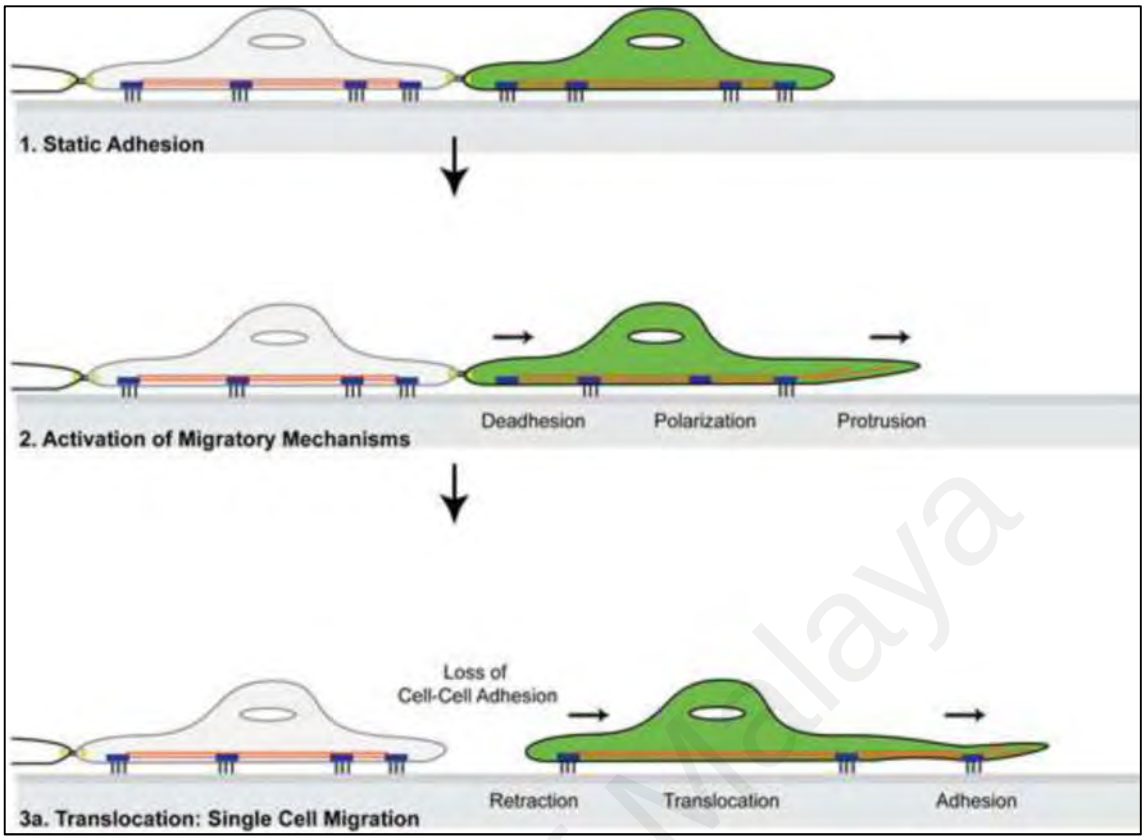

Figure 2.2: Cellular behaviour during cell migration. Migrating cells make new adhesive contacts under the leading edge, translocate and break adhesions at the rear (Figure reproduced with permission from Palmer *et al.*, 2011).

Circulating tumour cells (CTC) must survive a variety of stresses such as anoikis, haemodynamic shear forces, immune surveillance and traps in smaller luminal diameter of capillaries, before they reach distant organ sites (Joyce & Pollard, 2009). Cells that successfully evade these barriers then lodge in the microvasculature of secondary organs, where they may proliferate in the lumina and form a microcolony that eventually breaches the wall of vessels, exposing the cells to the tissue parenchyma (Al-Mehdi *et al.*, 2000). Otherwise, tumour cells may cross the endothelial cell and pericyte layers into the tissue parenchyma. To extravasate into tissues with low intrinsic microvessel permeability, tumour cells induce vascular hyper-permeability by secreting factors to perturb their microenvironment (Valastyan & Weinberg, 2011).

However, the microenvironmental differences at the foreign tissues in comparison to the primary site often render the cells quiescent. These may include the presence of certain cytokines and growth factors, ECM constituents, microarchitecture

of the tissue and the type of stromal cells (Chambers *et al.*, 2002). Seed and soil hypothesis is by far the preferred explanation for the non-randomness of the distribution of metastases. The theory proposed that the tumour cells (seeds) colonise the secondary organs if and only if the microenvironment (soil) is favourable for their growth-enhancing factors and that they are compatible (Paget, 1889). This is further extended to three basic principles found to underlie the efficiency of formation of overt metastases, namely tumour-host interactions to provide chemotactic stimuli for directional migration (Condeelis & Pollard, 2006), pro-metastatic molecular factors acquired through EMT or epigenetic changes (Feinberg, 2007; Nguyen & Massague, 2007; Kalluri & Weinberg, 2009), as well as tissue structure and biomechanics to determine the route and distribution of CTC (Liao & Johnson, 2007; Sullivan & Graham, 2007; Erler & Weaver, 2009; Kumar & Weaver, 2009; Ruppender *et al.*, 2010). As seen in Figure 2.3, those that succeed in overcoming microenvironmental incompatibilities and activating self-renewal pathways, will trigger the reverse programme mesenchymal-epithelial transition (MET) and proliferate continuously to form hidden micrometastases. These later generate clinically detectable metastases, marking the endpoint of the invasion-metastasis cascade (Peinado *et al.*, 2007; Kalluri & Weinberg, 2009; Thiery *et al.*, 2009; De Craene & Berx, 2013; Nieto, 2013).

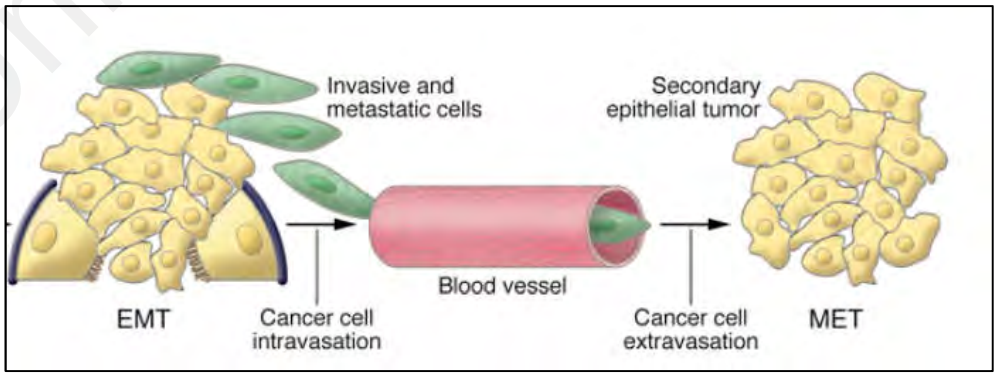

Figure 2.3: EMT contributes to cancer progression. Epithelial cells lose their polarity and detach from the basement membrane. EMT then follows, facilitating the malignant phase of tumour growth. Cells enter the circulation and exit the blood stream at remote sites, where they may form micro and macrometastases by reverting to epithelial phenotype via MET (Figure from Kalluri & Weinberg, 2009, open access journal).

2.2.2 Metastasis in Lung Cancer

Lung cancer spreads by local extension, vascular invasion or through the lymphatic system, especially the lymph nodes around the bronchi and in the mediastinum region between the two lungs (Chandrasoma, 1998). However, metastasis via the lymphatic route takes longer until distant metastases are set, compared to spreading via blood vessels (Popper, 2016). Common sites for lung cancer metastasis include adrenals (36-64%), bone (21-41%), brain (14-45%), kidneys (13-43%), liver (38-58%), lymph nodes (46-85%) and pleura (14-46%), while less commonly to abdominal lymph nodes, heart, pancreas, pericardium, skin and spleen (Stenbygaard *et al.*, 1997). Widespread metastasis is common in NSCLC, especially in lung AC, tumour grows rapidly to form macroscopic metastases upon infiltration of secondary organs (Nguyen *et al.*, 2009), killing patients within 18 months (Wood *et al.*, 2014).

2.3 Angiogenesis

The term angiogenesis was first coined in 1787 (Hunter, 1861). However, only after a decade, angiogenesis was better understood such that, nearly all tumours would enter dormancy upon reaching 2mm in diameter without a supply of nutrients and oxygen and must construct new vessels to survive and grow. In addition, angiogenesis aids in tumour progression as it facilitates metastasis by increasing the chances for tumour cells to enter the blood circulation (Folkman, 1971; Shubik, 1982; Reinhold & van den Berg-Blok, 1984).

2.3.1 Mechanisms of Angiogenesis

Tumour vessels mainly grow by five mechanisms out of the six depicted in Figure 2.4. They are (1) sprouting angiogenesis involving proliferation of stimulated endothelial cells into the surrounding matrix and formation of solid sprouts extending towards the angiogenic stimulus to form a new vessel, (2) vasculogenesis involving

proliferation of endothelial cell precursors or angioblasts (endothelial stem cells) into *de novo* endothelial cells, (3) splitting angiogenesis/ intussusception involving remodelling and expansion of tumour vessels by inserting the interstitial tissue columns into the lumen of pre-existing vessels or division of the lumen of an existing vessel to form two vessels, (4) vasculogenic mimicry or (5) trans-differentiation of tumour cells into endothelial-like cells and creation of structures within the tumour joining to a nearby vessel (Kos & Dabrowski, 2002; Burri *et al.*, 2004; Goh *et al.*, 2007; Carmeliet & Jain, 2011a).

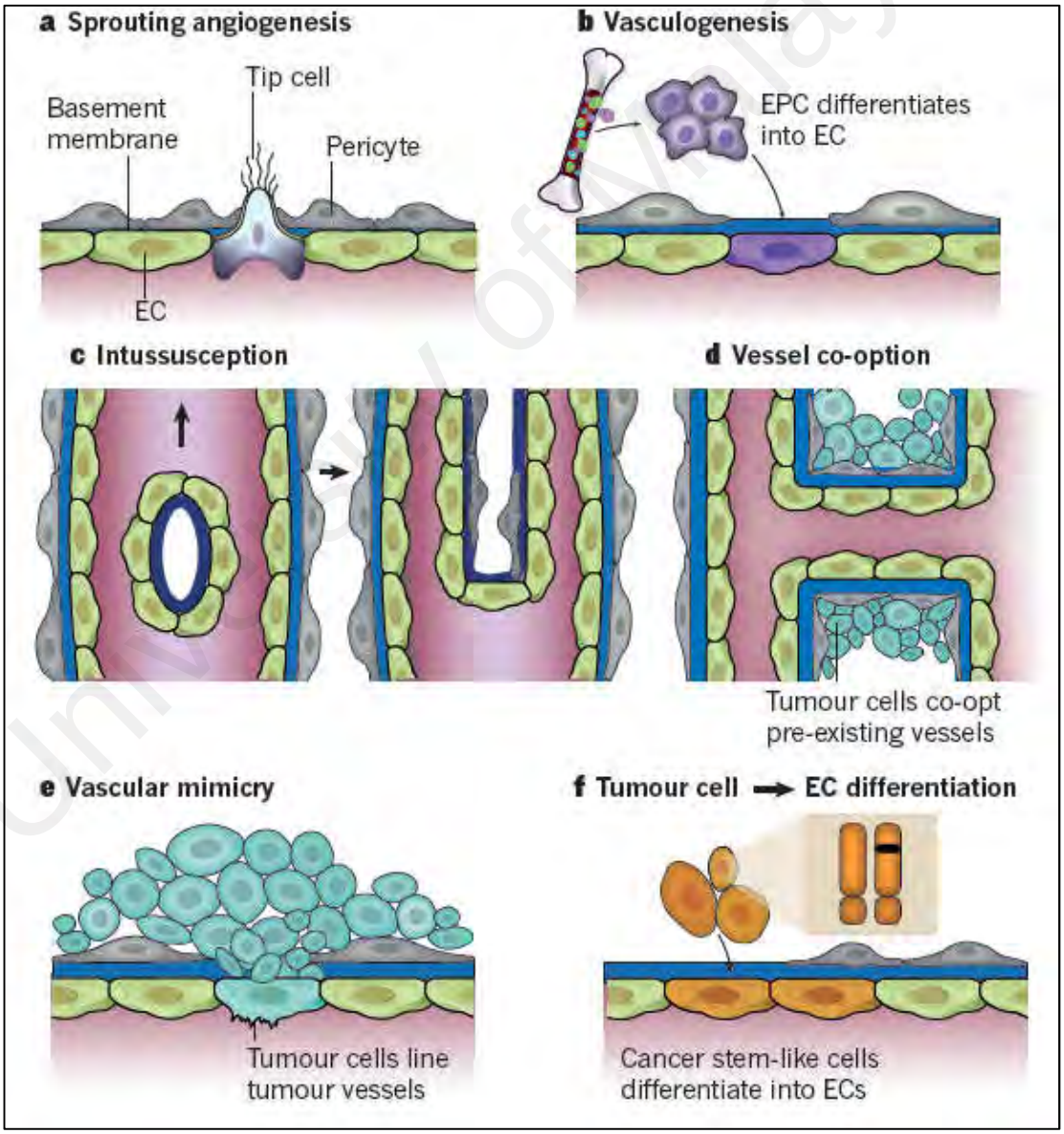

Figure 2.4: Six modes of angiogenesis: (1) Sprouting angiogenesis (2) Vasculogenesis (3) Intussusception (4) Vessel co-option (5) Vascular mimicry (6) Tumour cell to endothelial cell differentiation (Figure reproduced with permission from Carmeliet & Jain, 2011a).

Angiogenesis takes place in sequence of two phases: activation and resolution. The activation phase involves five activities, which are, (1) increased vascular permeability and extravascular fibrin deposition, (2) basement membrane degradation, (3) endothelial cell migration and ECM invasion, (4) cell proliferation, and (5) capillary lumen formation. On the other hand, the resolution phase encompasses four activities, which are, (1) inhibition of endothelial cell proliferation, (2) cessation of cell migration, (3) basement membrane reconstitution, and (4) junctional complex maturation (Pepper *et al.*, 2002).

2.3.1.1 The Angiogenic Switch

During the pre-vascular phase, tumour growth reaches a plateau where the rate of cell proliferation is equivalent to the rate of cell death. When pro-angiogenic factors or activators are produced in excess of anti-angiogenic factors or inhibitors, the equilibrium is tipped in favour of blood vessel growth (Naumov *et al.*, 2006; Aguirre-Ghiso, 2007). This is when tumour cells move into the vascular phase by growing exponentially, invading and metastasising (Holmgren *et al.*, 1995; O'Reilly *et al.*, 1996; Almog *et al.*, 2006). The transition from the pre-vascular to the vascular phase of a tumour is known as the angiogenic switch (Hanahan & Folkman, 1996).

As tumour expands, the centre of the tumour is further away from the blood vessels, creating a hypoxic region which triggers angiogenesis (Takeda *et al.*, 2002). The process begins with the release of vascular endothelial growth factor (VEGF) by tumour cells, which diffuses through the connective tissue towards the pre-existing blood vessels and bind to the transmembrane VEGF receptors (VEGFRs) in endothelial cells (Lamalice *et al.*, 2007). Consequently, this promotes vasodilation, vascular permeability and degradation of surrounding vascular basement membrane, leading to the formation of destabilised vessels. Endothelial cells lose cell contacts and detach

from supporting smooth muscle cells while plasma proteins extravasate and form temporary scaffolding matrix network for endothelial cells to migrate to distant sites directed by chemotactic gradient (Carmeliet, 2000a). The endpoint of the activation phase is marked by the proliferation of endothelial cells and assembly into solid cords and subsequently formation of lumens (Figure 2.5) (Bergers & Benjamin, 2003; Liao & Johnson, 2007).

During the resolution phase, smooth muscle cells are recruited to the migration column to stop endothelial cell proliferation and migration (Carmeliet, 2000a). A basal lamina is produced, surrounding the newly formed blood vessels. All the components then mature by remodelling into a vascular network. However, tumour vessels are ultrastructurally abnormal. They are dilated with irregularly sized lumens, have excessive branching and shunts connected randomly as well as haphazardly criss-crossed the stroma (Baish & Jain, 2000) which appear multi-layered and tortuous (Fukumura *et al.*, 2010; Jain & Styllanopoulos, 2010).

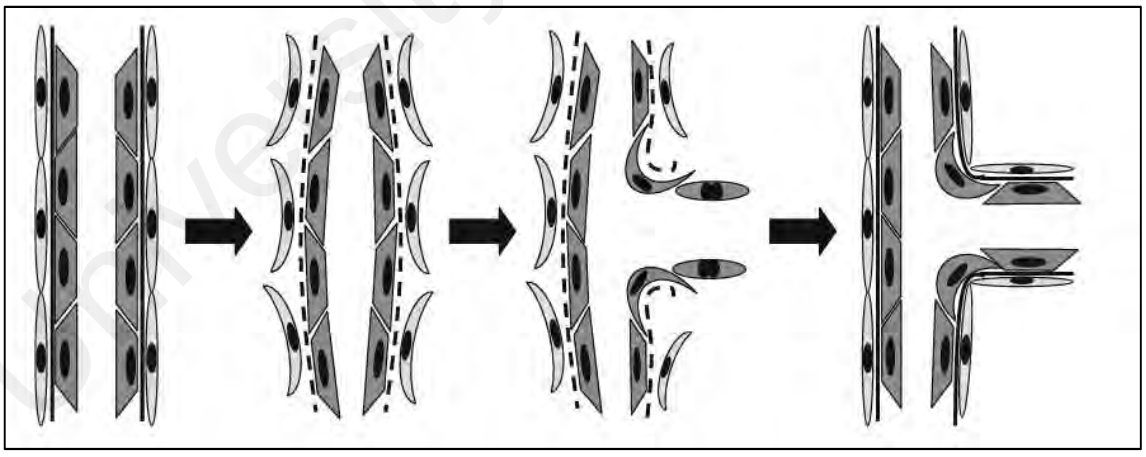

Figure 2.5: Mechanism of angiogenesis. Activated endothelial cells produce enzymes that promote the detachment of pericytes and vasodilation followed by degradation of the basement membrane. Endothelial cells begin to divide and migrate towards angiogenic stimuli. Sprouting endothelial cells form lumen, stabilised by pericyte attachment and deposition of the basement membrane. Blood flow then begins (Figure reproduced with permission from Liao & Johnson, 2007).

2.3.2 Angiogenesis in Lung Cancer

Lung AC has been shown to have high vessel counts which explain the higher chances of metastasis with this subtype (Yuan *et al.*, 1995; Sikora *et al.*, 1997). This intra-tumoural microvessel density (IMD) was also reported to inversely correlate with the survival of patients with surgically resected NSCLC (Fontanini *et al.*, 1997; Tanaka *et al*., 2001).

VEGF and VEGFR were highly expressed in NSCLC (Mattern *et al.*, 1995; Holm *et al.*, 1996; Ohta *et al.*, 1996; Takanami *et al.*, 1997; Takigawa *et al.*, 1998; Choi *et al.*, 2001; Tamura *et al.*, 2001) and have been associated with the clinical stage of NSCLC and poor prognosis (Matsuyama *et al*., 2000; Laack *et al.*, 2002; Stefanou *et al.*, 2004). An inverse relationship was also found between the VEGF serum levels and survival (Shimanuki *et al*., 2005). Furthermore, expression of several angiogenesis-related molecules, such as MMPs (Brown *et al.*, 1993), epidermal growth factor receptor (EGFR) (Fontanini *et al.*, 1998b), prostaglandin-endoperoxidase synthase 2 (PTGS2) (Achiwa *et al*., 1999) and angiopoietin 2 (ANGPT2) (Tanaka *et al.*, 2002), were inversely correlated with NSCLC patients' prognosis.

Interestingly, it was found that lung cancer tumour utilises existing host blood vessels rather than inducing neovascularisation using signals from carcinogenesis. This is supported by the finding that anti-angiogenic therapy failed to improve cytotoxic drug delivery to tumour in patients with NSCLC. Instead, it showed opposite effect which confers an advantage to the tumour as they do not need to undergo vascular construction *de novo* (van der Veldt *et al.*, 2012). Furthermore, lung cancer, which exhibits aggressive biological behaviour, was able to progress rapidly without developing angioarchitectonic structures in secondary niches (Evans, 2012). These however require further validation.

2.4 MicroRNAs (MiRNAs)

Discovered in early 1990, miRNAs belong to the most abundant class of small endogenous non-coding RNAs of 18-25 nucleotides (nt) in length that inhibit protein translation by binding to complementary mRNA targets (Lee *et al.*, 1993). Approximately 60% of mRNAs in the human genome are estimated to be targeted by miRNAs (Friedman *et al.*, 2009; Winter *et al.*, 2009).

2.4.1 Biogenesis of MiRNAs

MicroRNA genes are evolutionarily conserved and are embedded within the intragenic (introns or exons of protein-coding genes) and intergenic regions (Rodriguez *et al.*, 2004). They are transcribed by RNA polymerase II as ~1000nt long transcripts known as primary miRNAs (pri-miRNAs). Pri-miRNAs contain 5' 7-methylguanosine cap structures as well as 3' poly (A) tails and fold into imperfect hairpins with a hairpin stem of around 33 base pairs (bp), a terminal loop and two single-stranded flanking regions upstream and downstream of the hairpin. They are processed by RNase III Drosha and DGCR8 (DiGeorge syndrome critical regions gene 8) into 44-180nt stem-loop structures with 2nt 3'-overhang named precursor miRNAs (pre-miRNAs). Pre-miRNAs are transported to the cytoplasm by Exportin 5 where they are further processed to mature miRNAs by RNase III Dicer. The 18-25nt double-stranded mature miRNAs with 2nt 3' overhang finally gets incorporated into the RNA-induced silencing complex (RISC), a multi-protein complex that separates the mature strand (less stable 5' end) from the passenger strand (miRNA*) and facilitates the miRNA-mRNA interaction (Figure 2.6) (Khvorova *et al.*, 2003; Schwarz *et al.*, 2003; Denli *et al.*, 2004; Han *et al.*, 2004; Lee *et al.*, 2004; Garzon *et al.*, 2010).

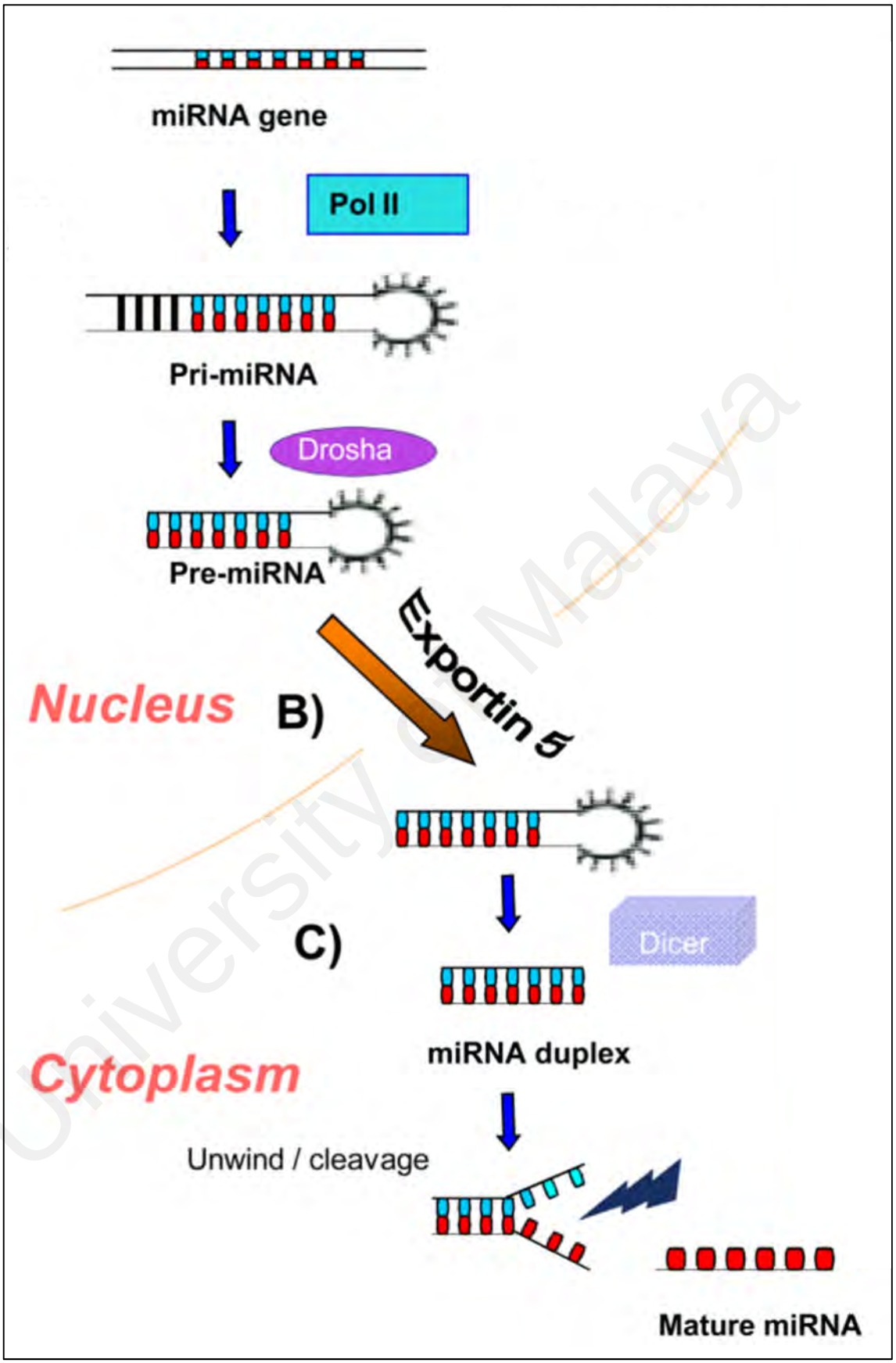

Figure 2.6: The 'linear' canonical pathway of miRNA biogenesis (Figure reproduced with permission from Garzon *et al*., 2010).

2.4.2 Mechanisms of Action of MiRNAs

MicroRNAs generally act in the cytoplasm, although they have also been found to act in the nucleus (Hwang *et al.*, 2007; Kim *et al.*, 2008a; Marcon *et al.*, 2008; Ohrt *et al.*, 2008; Foldes-Papp *et al.*, 2009) and nucleolus (Politz *et al.*, 2009; Liao *et al.*, 2010).

Mature miRNAs exert their regulatory functions by binding to complementary sites within 3'-untranslated region (3'-UTR) of their mRNA targets. The Watson-Crick complementarities between position 2-8 from the 5' miRNA (the seed), and the 3'-UTR of their target mRNAs determine the fate of the mRNA (Bartel, 2009; Rigoutsos, 2009). MicroRNAs have also been reported to bind to the 5'-untranslated region (5'-UTR), the open reading frame (ORF), the promoter, the ribonucleoproteins in seed sequence (Stark *et al.*, 2007; Orom *et al.*, 2008; Place *et al.*, 2008; Beitzinger & Meister, 2010; Eiring *et al.*, 2010) and even the DNA (Gonzalez *et al.*, 2008; Kim *et al.*, 2008a; Khraiwesh *et al.*, 2010).

As illustrated in Figure 2.7, a near-perfect match of the seed and the 3'-UTR of mRNA leads to mRNA cleavage, while partial complementation causes decreased expression via mRNA degradation or translational inhibition (Esquela-Kerscher & Slack, 2006; Bartel, 2009; Winter *et al.*, 2009; Pasquinelli, 2012; Krist *et al*., 2015). The mRNA degradation begins with 5' decapping and 3' deadenylation of the mRNA, revealing itself for exonucleolytic degradation by the enzyme Xrn1p from 5'-3'. Alternatively, deadenylated mRNAs can be degraded by cytoplasmic exonucleases from 3' to 5' (Humphreys *et al.*, 2005; Pillai *et al.*, 2005; Wu & Belasco, 2005; Giraldez *et al.*, 2006; Chendrimada *et al.*, 2007; Kiriakidou *et al.*, 2007; Baek *et al.*, 2008; Selbach *et al.*, 2008). Additionally, miRNAs have been shown to promote mRNAs relocation to P-bodies, the temporary storage and/ or decay sites of repressed mRNAs, which are

devoid of ribosomes (Bagga *et al.*, 2005; Lim *et al.*, 2005; Liu *et al.*, 2005a; Liu *et al.*, 2005b). In conclusion, the net result of miRNA function is a reduction in protein expression.

A single miRNA may have several hundreds of different mRNA targets and can simultaneously govern various biological processes, including cell invasion, migration and angiogenesis (Selbach *et al.*, 2008; Bartel, 2009; Jeffries *et al.*, 2011; Pasquinelli, 2012). At present, more than 4000 miRNAs have been characterised in human (miRBASE, release 21, June 2014), while experimentally validated targets have only been reported for 2117 miRNAs (miRecords at http://c1.accurascience.com/miRecords/).

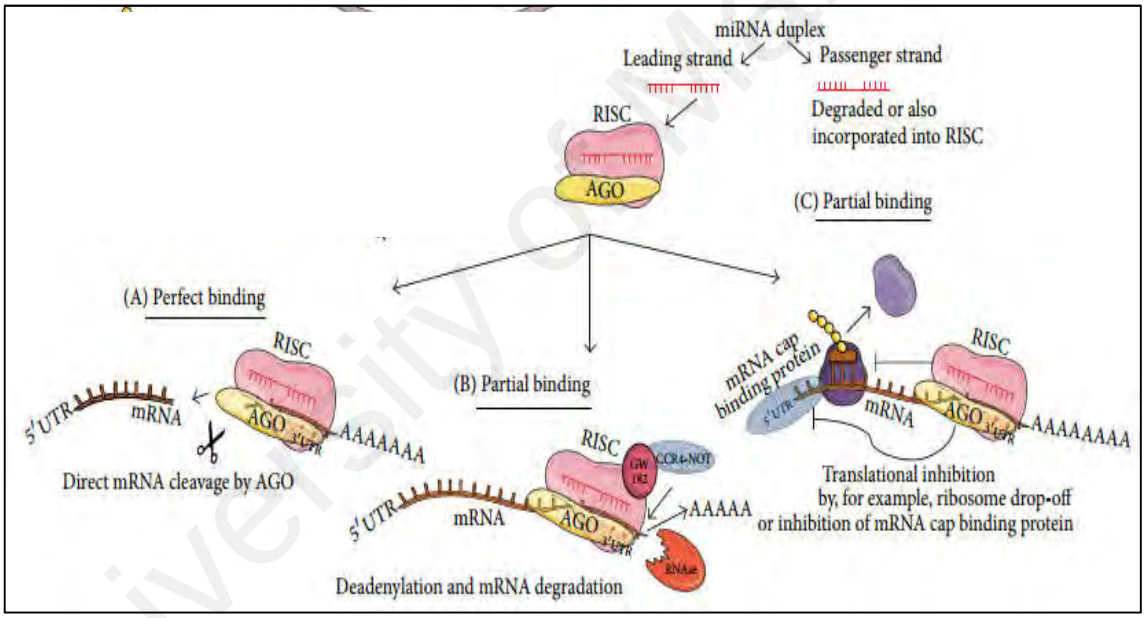

Figure 2.7: Modulation of miRNAs can be achieved by several approaches: mRNA destabilisation, mRNA degradation and inhibition of translation (Figure from Krist *et al.*, 2015, open access journal).

2.4.3 MicroRNAs in Lung Cancer

About half of human miRNA genes are located at fragile sites of the genomic regions which are prone to breakage and rearrangement in cancer cells. MicroRNA functions are commonly altered by aberrant promoter methylation, chromosomal deletion, genomic amplification and point mutation (Esquela-Kerscher & Slack, 2006; Sayed & Abdellatif, 2011).

MicroRNAs have been reported as markers to define some NSCLC subtypes (Yanaihara *et al.*, 2006; Raponi *et al.*, 2009; Bishop *et al.*, 2010; Landi *et al.*, 2010; Puissegur *et al.*, 2011; Lu *et al.*, 2012). For instance, miR-155 was found to be up-regulated exclusively in lung AC with wildtype *EGFR* and *KRAS* (KRAS proto-oncogene, guanosine triphosphatase), while the expression of miR-21 and miR-25 as well as miR-495 were shown to be increased in *EGFR* mutant AC and *KRAS* positive AC respectively (Seike *et al.*, 2009; Dacic *et al.*, 2010). The expression of miR-21, miR-200b, miR-375 and miR-486, representing 80.6% sensitivity and 91.7% specificity in combination, was recommended as the best predictor of lung AC (Yu *et al.*, 2010). In addition, the presence of miRNAs in serum (Hu *et al.*, 2006; Rabinowits *et al.*, 2009; Foss *et al.*, 2011) and sputum (Yu *et al.*, 2010) of patients suggest that miRNAs might serve as excellent biomarkers for screening and staging for NSCLC. For example, miR-212 down-regulation was strongly correlated with the severity of the disease, as they were being significantly suppressed in stage T3/ T4 than in stage T1/ T2 (Incoronato *et al.*, 2011).

Furthermore, miRNAs were found to be associated with risk, relapse and survival of NSCLC. Let-7, the first miRNA identified to be lowly expressed in lung cancer, was associated with poor clinical outcome (Takamizawa *et al.*, 2004; Johnson *et al.*, 2005; Yanaihara *et al.*, 2006). Interestingly, a single nucleotide polymorphism (SNP) in a let-7 complementary site 6 (LCS6) of KRAS mRNA 3'-UTR correlated with higher risk of NSCLC in moderate smokers (Chin *et al.*, 2008). Similarly, the down-regulation of the miR-34 family (miR-34a, 34b and 34c) was clinically correlated with a higher risk of relapse (Gallardo *et al.*, 2009) and was associated with poor overall survival and disease-free survival in stage I NSCLC (Wang *et al.*, 2011c). While let-7a and miR-221 expression correlated with improved survival (Yu *et al.*, 2008), miR-372 (Yu *et al.*, 2008), miR-21 (Voortman *et al.*, 2010), miR-451 (Wang *et al.*, 2011a), miR-9-3 (Heller

et al., 2012), miR-137, miR-182 and miR-186 (Cai *et al.*, 2013) correlated with poor survival in NSCLC.

It is worth noting that miR-31 plays a role in initiating lung tumour development as well as the progression of lung cancer. Edmonds *et al.* reported that miR-31 was overexpressed in NSCLC and it regulates lung epithelial cell growth by directly targeting *RASA1* (RAS p21 protein activator 1), *SPRED1* (sprouty-related EVH1 domain-containing 1), *SPRED2* (sprouty-related EVH1 domain-containing 2), *SPRY1* (sprouty RTK signalling antagonist 1), *SPRY3* (sprouty RTK signalling antagonist 3) and *SPRY4* (sprouty RTK signalling antagonist 4). The induction of miR-31 resulted in lung hyperplasia, followed by formation of adenoma and development of adenocarcinoma. In addition, when mutant *KRAS* was introduced along with miR-31, lung tumourigenesis was accelerated (Edmonds *et al.*, 2016).

2.4.3.1 MicroRNAs and Lung Cancer Metastasis

The presence of nodal and distant metastases often indicates late stages of lung cancer. High serum values of miR-10b in lung cancer patients was associated with lymph node metastasis (Roth *et al.*, 2011). Likewise, miR-26a expression was higher in lymph node metastasis tumour tissues than in primary tumour tissues (Liu *et al.*, 2012a), suggesting that miR-26a is directly involved in the metastatic potential of lung cancer cells. On the contrary, lower miR-34b expression in cancer tissues was associated with higher lymph node metastasis (Wang *et al.*, 2013d). These miRNAs that regulate various steps in the course of metastasis are known as metastamiRs (Hurst *et al.*, 2009).

MiR-29c and miR-126 suppressed lung cancer cell adhesion to the ECM by targeting *MMP2* (matrix metallopeptidase 2) and *CRK* (CRK proto-oncogene, adaptor protein) respectively (Crawford *et al.*, 2008; Wang *et al.*, 2013b). On the other hand, miR-33b, miR-136, miR-145, miR-149, miR-200 and miR-203 function as metastasis

suppressors in lung cancer by repressing EMT, where an increase in expression of epithelial markers and a decrease in expression of mesenchymal markers were observed (Ke *et al.*, 2013; Yang *et al.*, 2013; Hu *et al.*, 2014b; Li *et al.*, 2014; Qu *et al.*, 2015; Hu *et al.*, 2016).

Let-7a, miR-22, miR-133b, miR-145, miR-200 and miR-203 have previously been shown to suppress lung cancer cell invasion and metastasis (Roybal *et al.*, 2011; Liu *et al.*, 2012c; Lu *et al.*, 2012; Wang *et al*., 2013e; Chen *et al.*, 2015a). MiR-21 was overexpressed in lung cancer tissues and could promote invasion and metastasis by down-regulating *PTEN* (phosphatase and tensin homolog) (Zhang *et al.*, 2010; Liu *et al.*, 2013b). Furthermore, miR-196a is frequently overexpressed in NSCLC and it controls invasion by directly targeting *HOXA5* (homeobox A5) (Liu *et al.*, 2012d). Overexpression of miR-221 and miR-222 enhanced lung cancer cell migration through activation of *AKT1* (AKT serine/threonine kinase 1) (Garofalo *et al.*, 2009), whereas miR-146a, miR-203 and miR-7515 inhibited the migration ability of NSCLC cells (Chen *et al.*, 2013; Lee *et al.*, 2013; Wang *et al.*, 2013a). Nevertheless, a relatively large number of miRNAs, such as miR-29, miR-30a, miR-33b, miR-99a, miR-124, miR-125a-3p, miR-126, miR-128, miR-132, miR-133a, miR-136, miR-145, miR-148a, miR-193b, miR-194, miR-200c, miR-203, miR-374a, miR-449a and miR-5481 altered lung cancer cell phenotype by inhibiting both invasion and migration (Crawford *et al.*, 2008; Hu *et al.*, 2012; Kumarswamy *et al.*, 2012; Li *et al.*, 2012a; Huang *et al.*, 2013; Luo *et al.*, 2013; Wu *et al.*, 2013a; Xu & Wang, 2013b; Yang *et al.*, 2013; Han *et al.*, 2014; Hu *et al.*, 2014a; Li *et al.*, 2014; Li *et al.*, 2015a; Liu *et al.*, 2015; Qu *et al.*, 2015; Zhang *et al.*, 2015a; Hu *et al.*, 2016; Sun *et al.*, 2016; Wu *et al.*, 2016).

A summary of miRNAs that play a role in regulating cell adhesion, EMT, invasion and migration in lung cancer is listed in Table 2.1. Figure 2.8 depicts the relationship between miRNAs and lung cancer metastasis (Jiang & Qiu, 2013).

Table 2.1: Summary of miRNAs that play a role in regulating cell adhesion, EMT, invasion and migration in lung cancer.

MiRNAs	Deregulation in Lung Cancer†	Targets††	Molecular Regulation†				Ref (s)
			Adhesion	EMT	Invasion	Migration	
Let-7a	↓	*HMGA2, KRAS*			↓		(Jeong, *et al.*, 2011; Wang *et al.*, 2013e)
MiR-7	↓	*EGFR, PIK3R3, RAF1*			↓	↓	(Webster *et al.*, 2009; Duncavage *et al.*, 2010; Xiong *et al.*, 2011b; Xu *et al.*, 2013a)
MiR-21	↑	*PTEN*			↑	↑	(Zhang *et al.*, 2010; Liu *et al.*, 2013b)
MiR-22	↓	*ERBB3*			↓		(Ling *et al.*, 2012)
MiR-29a	↓	*CEACAM6*			↓	↓	(Han *et al.*, 2014)
MiR-29b	↓	*MMP2, PTEN*			↓	↓	(Wang *et al.*, 2015a)
MiR-29c	↓	*ITGB1, MMP2*	↓		↓	↓	(Wang *et al.*, 2013b)
MiR-30a	↓	*SNAI1*		↓	↓	↓	(Kumarswamy *et al.*, 2012)
MiR-33b	↓	*ZEB1*		↓	↓	↓	(Qu *et al.*, 2015)
MiR-99a	↓	*NOX4*			↓	↓	(Sun *et al.*, 2016)
MiR-124	↓	*SNAI2, SOX9*			↓	↓	(Cui & Hu, 2016; Wang *et al.*, 2016b)
MiR-125a-3p	↓	*MTA1, RHOA*			↓	↓	(Jiang *et al.*, 2010; Huang *et al.*, 2013; Zhang *et al.*, 2015a)
MiR-125b	↑	*TP53INP1*	↑		↑		(Wang *et al.*, 2014; Li *et al.*, 2015b)
MiR-126	↓	*CRK*	↓		↓	↓	(Yanaihara *et al.*, 2006; Crawford *et al.*, 2008)
MiR-128	↓	*VEGFC*			↓	↓	(Hu *et al.*, 2014a)
MiR-132	↓	*ZEB2*			↓	↓	(You *et al.*, 2014)
MiR-133a	↓	*MMP14*			↓	↓	(Xu & Wang, 2013b)
MiR-133b	↓	*EGFR*			↓		(Liu *et al.*, 2012c)
MiR-136	↑	*SMAD2, SMAD3*		↓	↓	↓	(Yang *et al.*, 2013; Shen *et al.*, 2014)
MiR-145	↓	*MTDH, MUC1, POU5F1, SMAD3*		↓	↓	↓	(Sachdeva & Mo, 2010; Hu *et al.*, 2014b; Wang *et al.*, 2015b; Hu *et al.*, 2016)
MiR-146a	↓	*IRS2*		↓		↓	(Chen *et al.*, 2013; Park *et al.*, 2015)
MiR-148a	↓	*ROCK1*		↓	↓	↓	(Li *et al.*, 2013a; Li *et al.*, 2015a)
MiR-149	↓	*FOXM1*		↓	↓		(Ke *et al.*, 2013)
MiR-186	↓	*MAP3K2*			↓	↓	(Huang *et al.*, 2016)
MiR-193b	↓	*CCND1, PLAU*			↓	↓	(Hu *et al.*, 2012)
MiR-194	↓	*BMP1, CDKN1B, FOXA1*			↓	↓	(Wu *et al.*, 2013a; Zhu *et al.*, 2016)
MiR-196a	↑	*HOXA5*			↑	↑	(Liu *et al.*, 2012d)
MiR-200	↑	*FLT1*			↓		(Roybal *et al.*, 2011; Pacurari *et al.*, 2013)
MiR-200c	↓	*USP25*		↓	↓	↓	(Ceppi *et al.*, 2010; Li *et al.*, 2014)
MiR-203	↓	*BMI1, PRKCA, SMAD3*		↓	↓	↓	(Wang *et al.*, 2013a; Chen *et al.*, 2015a; Hu *et al.*, 2016)
MiR-206	↓	*SOX9*		↓	↓	↓	(Wang *et al.*, 2011b; Zhang *et al.*, 2015b; Chen *et al.*, 2016c)
MiR-212	↑	*PTCH1*			↑	↑	(Rabinowits *et al.*, 2009; Li *et al.*, 2012a)
MiR-221	↑	*PTEN, TIMP3*			↑	↑	(Garofalo *et al.*, 2009)
MiR-222	↑	*PTEN, TIMP3*			↑	↑	(Garofalo *et al.*, 2009)
MiR-338-3p	↓	*SOX4*		↓	↓	↓	(Li *et al.*, 2016)
MiR-365	↓	*HMGA2,NRP1, TTF1*			↓		(Qi *et al.*, 2012; Cao *et al.*, 2016)
MiR-374a	↓	*TGFA*			↓	↓	(Wu *et al.*, 2016)
MiR-449a	↓	*MET*			↓	↓	(Luo *et al.*, 2013)
MiR-493	↓	*E2F1*			↓	↓	(Gu *et al.*, 2014)
MiR-5481	↓	*AKT1*			↓	↓	(Liu *et al.*, 2015)
MiR-7515	↓	*MET*				↓	(Lee *et al.*, 2013)

Table 2.1, continued:

†↑ denotes increased expression or promoting action; ↓ denotes decreased expression or inhibitory action
††*HMGA2*- High mobility group AT-hook 2; *PIK3R3*- Phosphatidylinositide-3-kinase regulatory subunit 3; *RAF1*- Raf-1 proto-oncogene, serine/threonine kinase; *ERBB3*- Erb-B2 receptor tyrosine kinase 3; *CEACAM6*- Carcinoembryonic antigen-related cell adhesion molecule 6; *ITGB1*- Integrin subunit beta 1; *SNAI1*- SNAIL family transcriptional repressor 1; *ZEB1*- Zinc finger E-box binding homeobox 1; *NOX4*- Nicotinamide adenine dinucleotide phosphate oxidase 4; *SNAI2*- SNAIL family transcriptional repressor 2; *SOX9*- SRY-box 9; *MTA1*- Metastasis-associated 1; *RHOA*- Ras homolog family member A; *TP53INP1*- Tumour protein p53-inducible nuclear protein 1; *VEGFC*- Vascular endothelial growth factor C; *ZEB2*- Zinc finger E-box binding homeobox 2; *MMP14*- Matrix metallopeptidase 14; *SMAD2*- SMAD family member 2; *SMAD3*- SMAD family member 3; *MTDH*- Metadherin; *MUC1*- Mucin 1, cell surface-associated; *POU5F1*- POU class 5 homeobox 1; *IRS2*- Insulin receptor substrate 2; *ROCK1*- Rho-associated coiled-coil containing protein kinase 1; *FOXM1*- Forkhead box M1; *MAP3K2*- Mitogen-activated protein kinase kinase kinase 2; *CCND1*- Cyclin D1; *BMP1*- Bone morphogenetic protein 1; *CDKN1B*- Cyclin-dependent kinase inhibitor 1B; *FOXA1*- Forkhead box A1; *FLT1*- Fms-related tyrosine kinase 1; *USP25*- Ubiquitin-specific peptidase 25; *BMI1*- BMI1 proto-oncogene, polycomb ring finger; *PRKCA*- Protein kinase C alpha; *PTCH1*- Patched 1; *TIMP3*- TIMP metallopeptidase inhibitor 3; *SOX4*- SRY-box 4; *NRP1*- Neuropilin 1; *TTF1*- Transcription termination factor 1; *TGFA*- Transforming growth factor alpha; *MET*- MET proto-oncogene, receptor tyrosine kinase; *E2F1*- E2F transcription factor 1

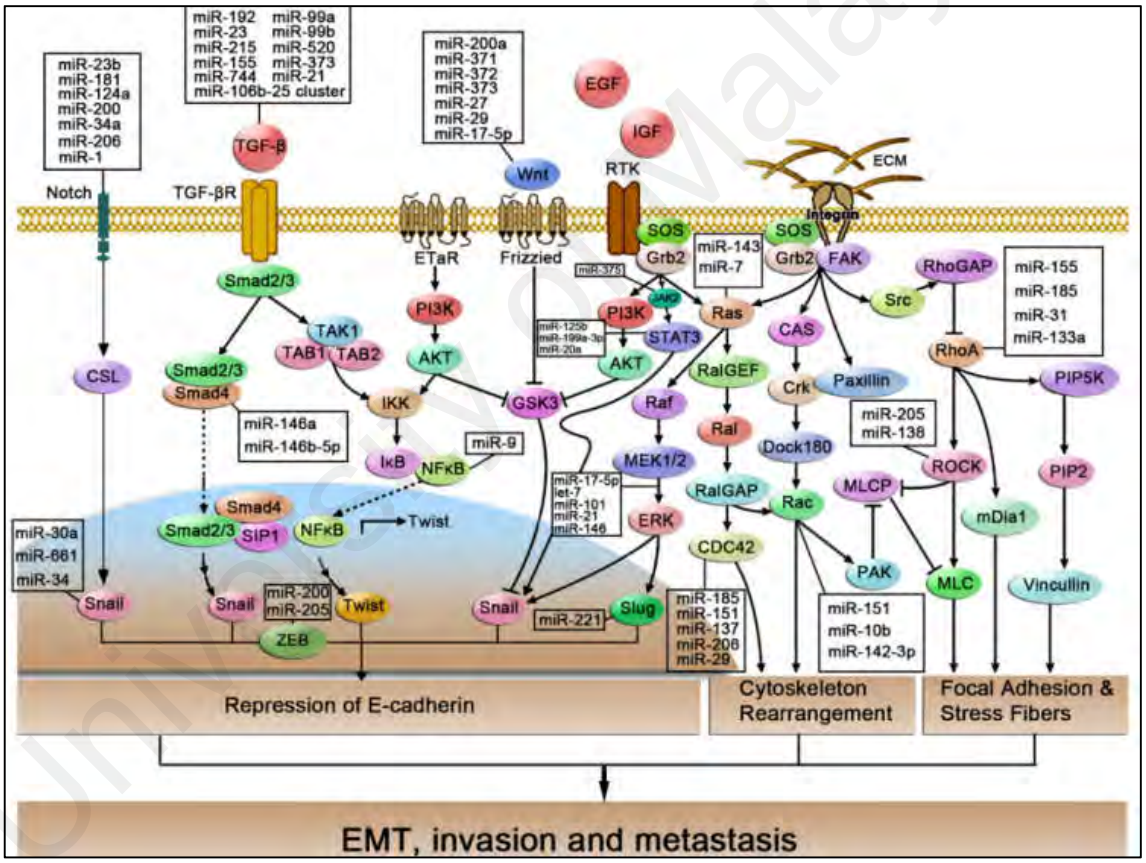

Figure 2.8: The miRNA network and lung cancer metastasis (Figure from Jiang & Qiu, 2013, open access journal).

2.4.3.2 MicroRNAs and Lung Cancer Angiogenesis

AngiomiRs refer to miRNAs that regulate angiogenesis either in a cell-autonomous or non-cell-autonomous manner as shown in Figure 2.9 (Wang & Olson, 2009b). To date, specific roles of miRNAs in lung cancer angiogenesis are poorly

characterised. Studies have only shown that angiomiRs in lung cancer bind to their angiogenesis-related gene targets, without demonstrating the regulation of angiogenesis mediated by the interaction of miRNA-gene. Some presented the role of miRNAs as angiomiRs in lung cancer with overexpression or knockdown studies using endothelial cells (Hu *et al.*, 2014a; Chen *et al.*, 2016c). Just recently, the mechanism of how these miRNAs regulate lung cancer angiogenesis, that is, whether the deregulated miRNAs are exported by tumour cells in exosome and subsequently taken up by endothelial cells to induce proliferation and tube formation, or the miRNAs modulate angiogenesis signalling pathways in the tumour cells to either activate or repress pro- or anti-angiogenic factors being secreted to signal endothelial cells was described.

MiR-378 enhances NSCLC angiogenesis by promoting VEGF expression or through the SUFU-SHH (SUFU negative regulator of Hedgehog signalling-sonic hedgehog) pathway. It was found to be exported from lung cancer cells in exosome, and *HMOX1* (heme oxygenase 1) could down-regulate not only expression of miR-378 but also its exosomal export. Lung microvascular endothelial cells treated with conditioned media proliferated to form tubule-like structures more potently than those cultured with unconditioned media, providing evidence for the pro-angiogenic properties of the cancer cells (Skrzypek *et al.*, 2013).

MiR-494 expression was induced under hypoxic condition in lung cancer cells via *HIF1A* (hypoxia-inducible factor 1 alpha subunit)-mediated mechanism as a novel tumour-derived pro-angiogenic paracrine signal. When lung cancer cells were co-cultured with endothelial cells, it was found that these cancer cells secreted and delivered miR-494 into endothelial cells in microvesicle form. Moreover, specific miR-494 antagomiR effectively repressed angiogenesis of tumour xenografts in nude mice (Mao *et al.*, 2015).

MiR-519c was shown as a hypoxia-independent regulator of *HIF1A* by binding directly to the HIF1A 3'-UTR to reduce angiogenesis in lung cancer. MiR-519c significantly decreased the levels of FGF2 (fibroblast growth factor 2), CXCL8 (C-X-C motif chemokine ligand 8) and VEGF in conditioned media from cells transfected with miR-519c, and this effect was rescued in the presence of *HIF1A* without 3'-UTR. Tube formation was also reduced in endothelial cells treated with miR-519c conditioned medium while tubular formation was restored by co-expressing *HIF1A* construct without 3'-UTR. Consistently, the tube-forming ability of endothelial cells and the secretion of angiogenic factors in lung cancer cells were significantly increased when treated with anti-miR-519c. In addition, mice injected with lung cancer cells overexpressing miR-519c had suppressed tumour angiogenesis as evidenced by CD31 staining. These findings indicate the essential role of *HIF1A* in miR-519c-suppressed tube formation (Cha *et al.*, 2010).

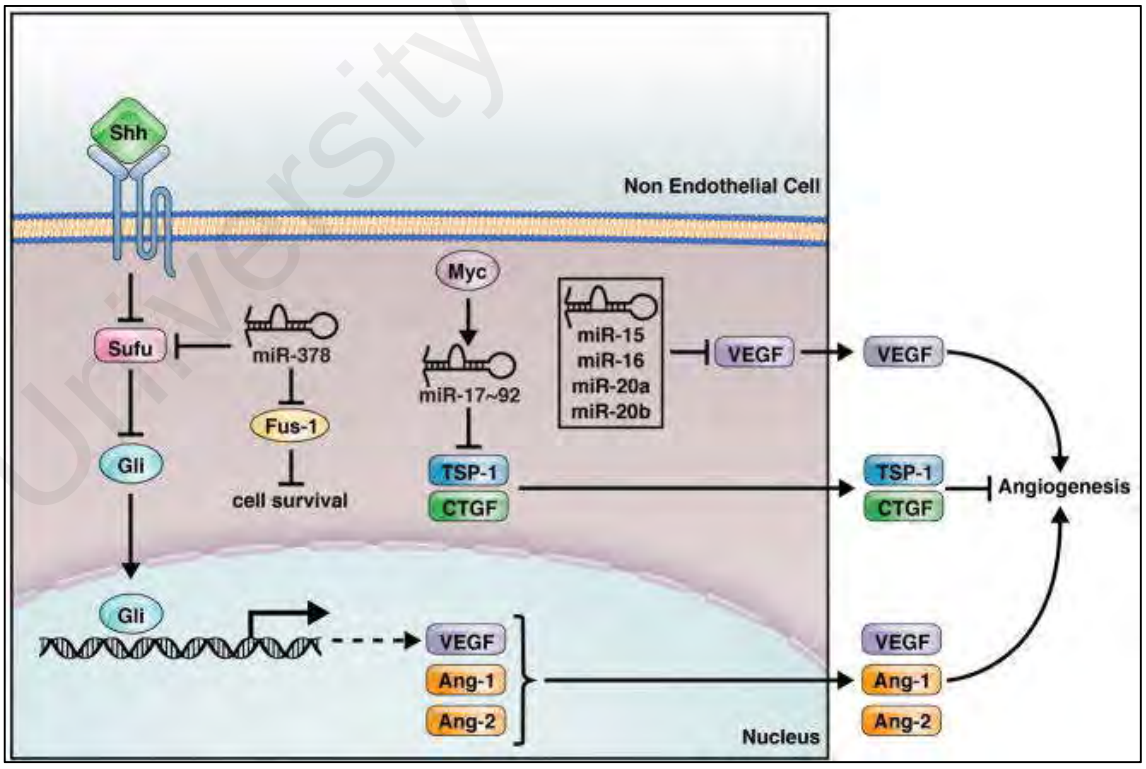

Figure 2.9: Non-cell-autonomous regulation of angiogenesis by miRNAs. Tumour cells express miRNAs which regulate the expression and secretion of pro- or anti-angiogenic factors received by endothelial cells. Interestingly, recent evidence indicated that miRNAs themselves can be exported in exosomes to activate or repress endothelial cells (Figure reproduced with permission from Wang & Olson, 2009b).

2.4.4 MicroRNAs as Therapy

Chemotherapy remains the mainstay of treatment for advanced stage IIIB and IV NSCLC (Shepherd *et al.*, 2005; Sandler *et al.*, 2006; Kim *et al.*, 2008b; Ciuleanu *et al.*, 2009; Mok *et al.*, 2009; Pirker *et al.*, 2009; Scagliotti *et al.*, 2009). Gefitinib (Iressa) is the first anti-lung cancer agent approved by the Food and Drug Administration (FDA) while Erlotinib (Tarceva) was approved for use in NSCLC patients who are no longer responding to chemotherapy. Currently, these two drugs, which are EGFR tyrosine kinase inhibitors (TKIs), are approved as second-line treatment as they show promising ability in the treatment of metastatic NSCLC (Mendelsohn & Baselga, 2003; Gridelli *et al.*, 2008). Recently, Crizotinib (Xalkori) is being used for the treatment of ALK (anaplastic lymphoma receptor tyrosine kinase)-positive NSCLC (Casaluce *et al.*, 2013). The only agent that contribute significantly to response rate and survival in NSCLC is Bevacizumab (Avastin), a monoclonal antibody targeting VEGF to inhibit angiogenesis (Sandler *et al.*, 2006; Wheatley-Price & Shepherd, 2008). Bevacizumab was combined with the standard first-line chemotherapy in stage IIIb or IV NSCLC (DeVore *et al.*, 2000).

Unfortunately, chemotherapy drugs also induce damage on normal cells. Chemotherapy damages blood-producing bone marrow and this increases the risk of bleeding, bruising or infection after minor injuries and fatigue or shortness of breath. Some drugs can damage nerves too. In addition, patients who received chemotherapy might experience undesired side effects such as loss of appetite, loss of hair, mouth sores, nausea and vomiting (American Cancer Society, 2006). Therefore, identifying miRNAs or antagomiRs that can offer a potential to increase tumour responsiveness to chemotherapy is very attractive. MicroRNAs provide an advantage when it comes to treatment due to its small size, as it can be delivered systemically into the cytoplasm of target cells to be active, as is for the siRNAs (small interfering RNAs).

MicroRNA replacement therapy involves the re-introduction of synthetic miRNA duplexes/ miRNA mimics to restore a loss of the tumour suppressive miRNA function. A miRNA mimic has exactly the same sequence as the endogenous miRNA with chemical modifications for stability and cellular uptake (Figure 2.10) (Sotillo & Thomas-Tikhonenko, 2011), and therefore, targets the same set of mRNAs that is also regulated by the naturally occurring miRNA, eliminating non-specific off-target effects. It is important though to take note of the potential toxicity in normal tissues in which the exogenous miRNAs may accumulate (Bader *et al.*, 2010). There is still lack of evidence for this issue since side effects could not be found in several *in vivo* studies, suggesting that delivery of miRNAs mimics to normal tissues is well tolerated (Esquela-Kerscher *et al.*, 2008; Wiggins *et al.*, 2010).

A miRNA, miR-9 reported to target *SOX2* (SRY-box 2), which directly induces ABCC3 and ABCC6 (adenosine triphosphate-binding cassette subfamily C member 6) transporters, is one such candidate. The overexpression of miR-9 in a chemotherapy-resistant glioma stem cell line resulted in reduced ABCC transporter expression and increased drug retention (Jeon *et al.*, 2011). Furthermore, miR-15 and miR-16 were repressed in breast tumours and thus the anti-apoptotic *BCL2* (BCL2, apoptosis regulator) expression was restored. Re-expression of miR-15 and miR-16 sensitised the cells to Tamoxifen (Cittelly *et al.*, 2010a). Similarly, forced overexpression of miR-342 sensitised breast cancer cells to Tamoxifen-induced apoptosis (Cittelly *et al.*, 2010b).

The second strategy is the use of anti-miRNAs (antagomiRs) to inhibit oncomiRs (miRNAs that are associated with cancer). These oligonucleotides are complementary to the endogenous miRNAs, thereby disrupting the loading of mature miRNA into RISC and preventing the degradation of target mRNAs. Chemical modifications, such as 2'-O-methyl-group and locked nucleic acid (LNA), increase stability of antagomiRs against nucleases (Figure 2.10) (Krutzfeldt *et al.*, 2005; Elmen

et al., 2008; Sotillo & Thomas-Tikhonenko, 2011). AntagomiR against miR-21 was proven to be able to sensitise pancreatic cancer cells to 5-fluorouracil (5-FU) treatment, rapidly driving cancer cells to undergo cell death (Hwang *et al.*, 2010). Recently, it was shown that one antisense oligonucleotide is able to target and inhibit multiple miRNAs simultaneously. This multiple-target anti-miRNA antisense oligodeoxyribonucleotide (MTg-AMO) is capable of repressing miR-17-5p, miR-21 and miR-155 at once to better suppress cancer growth compared to individual inhibition of the miRNAs (Lu *et al.*, 2009).

At present, there is no miRNA-based therapeutics being tested in the clinical phase for lung cancer treatment. However, there are several candidates paving their way and in pre-clinical phase (Table 2.2). Intranasal administration of let-7 mimics and local and/ or systemic delivery of liposome-polycation-hyaluronic acid miR-34a mimics nanoparticles into lung cancer xenograft models significantly reduced tumour growth (Esquela-Kerscher *et al.*, 2008; Chen *et al.,* 2010b; He *et al.*, 2010; Trang *et al.*, 2010; Wiggins *et al.*, 2010). Moreover, pre-miR-133b-containing cationic lipoplexes target *MCL1* (BCL2 family apoptosis regulator), were able to regulate survival and sensitivity of lung cancer cells to chemotherapeutic agents (Wu *et al.*, 2011b), while replacement of miR-200c inhibited cell growth in NSCLC and sensitised lung cancer cells to radiation (Ceppi *et al.*, 2010; Cortez *et al.*, 2014). It was also reported that anti-miR-150 expression vector (PR-ASO-150) delivered into lung tumour xenografts in mice, led to inhibition of tumour growth (Li *et al.*, 2012b).

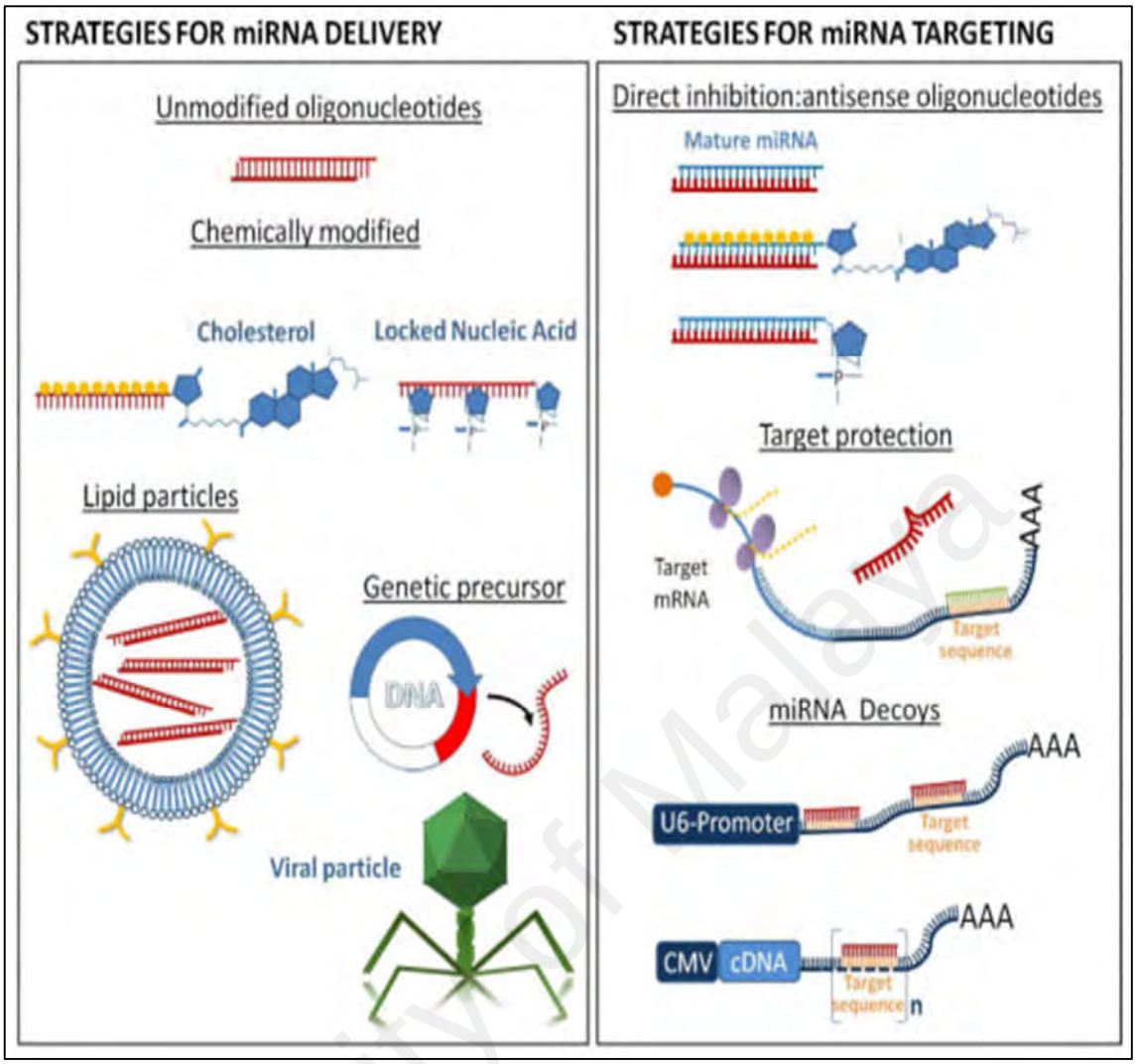

Figure 2.10: Biological and chemical therapeutic tools using miRNA-based approaches (Figure reproduced with permission from Sotillo & Thomas-Tikhonenko, 2011).

Table 2.2: Pre-clinical studies of miRNA mimics in NSCLC.

MiRNAs	Delivery	Results	Ref (s)
Let-7b	Adenovirus	Reduced xenograft growth; 66% reduction in orthotopic tumour burden	(Esquela-Kerscher *et al*., 2008)
	Cationic lipid, intratumoral	Decreased tumour growth	(Trang *et al*., 2010)
	Lentivirus	75% reduction in tumour burden	
	Neutral lipid emulsion, intravenous	Decreased orthotopic tumour burden	(Trang *et al*., 2011)
Let-7b and miR-34a	Neutral lipid emulsion, intravenous	Reduced orthotopic tumour burden with combination	(Kasinski *et al*., 2015)
	Amphoteric liposome, intravenous	40% increased survival with combination or miR-34a alone	
MiR-29b	Liposomes, intravenous	60% smaller xenograft	(Wu *et al*., 2013b)
MiR-34	Cationic lipid, intratumoral and intravenous	Reduced xenograft growth	(Wiggins *et al*., 2010)
	Neutral lipid emulsion, intravenous	60% decrease in orthotopic tumour burden	(Trang *et al*., 2011)
MiR-200c	Amphoteric liposome	MiR-200c plus radiotherapy delayed xenograft growth	(Cortez *et al*., 2014)
Consensus Mimics	EDV™† nanocells, intravenous	60-80% subcutaneous xenograft growth inhibition	(Reid *et al*., 2015)

†EnGeneIC delivery vehicle

CHAPTER 3: MATERIALS AND METHODS

3.1 Cell Lines

Human lung adenocarcinoma epithelial cell lines, A549 (American Type Culture Collection, ATCC, VA, USA) and SK-LU-1 (ATCC, VA, USA), were used in this study. A549 was cultured from tumour tissue explant of a 58-year-old male Caucasian while SK-LU-1 was isolated from primary tumour of a 60-year-old female Caucasian. A549 was cultured in Roswell Park Memorial Institute (RPMI) 1640 (Hyclone, UT, USA) while SK-LU-1 was cultured in minimum essential medium (MEM) α (Nacalai Tesque, Kyoto, Japan), supplemented with 10.0% (v/v) fetal bovine serum (FBS) (HyClone, Northumberland, UK) and 1× penicillin/ streptomycin (Lonza, MD, USA). Human umbilical vein endothelial cells (HUVEC) (ATCC, VA, USA) were cultured in Medium 200 (Gibco, CA, USA) supplemented with 50× large vessel endothelial supplement (LVES) (Gibco, CA, USA) and used below passage-7. All cells were maintained at 37.0°C in a humidified 5.0% carbon dioxide (CO_2) atmosphere.

3.2 Cell Subcultivation

Prior to subcultivation, cells were checked under the Nikon ECLIPSE TS-100 inverted fluorescence microscope (Nikon, Tokyo, Japan) to ensure that they were 80-90% confluent and free of microbial contamination.

The culture medium in the flask was aspirated and the cell monolayer was washed with 3.00mL of 1× phosphate-buffered saline (PBS) (pH 7.4). During this step, the flask was slowly rocked back and forth to clear any traces of FBS. The washing solution was discarded. This was followed by the addition of 3.00mL of dissociating agent- 0.1% (v/v) trypsin solution (Gibco, CA, USA) in 1× PBS with 0.53mM ethylenediaminetetraacetic acid (EDTA) (Gibco, CA, USA) to break the bond between cells and substrate and between each other. The flask was placed back in the LabServ

CO_2 incubator (Fisher Scientific, MA, USA) at 37.0°C for optimal enzyme activity, for 3-5 minutes. The progress of enzyme treatment was checked every few minutes for their appearance (round up). The flask was tapped gently to detach the cells and 3.00mL of growth medium was added to neutralise trypsin. Cells were then resuspended to wash any remaining cells from the bottom of the culture flask, collected in a 15.00mL tube and centrifuged in Eppendorf Centrifuge 5702 (Eppendorf, Hamburg, Germany) at 1,400rpm for 6 minutes.

Supernatant was removed and the cell pellet was resuspended with 5.00mL of growth medium. The empty flask was washed with 3.00mL of 1× PBS once. Depending on the desired number of cells, appropriate volume was inserted into fresh growth medium to make up 10.00mL. The cells were grown as monolayer by maintaining it in the CO_2 incubator with stable temperature (37.0°C), high relative humidity (95.0%), controlled CO_2 level (5.0%) and controlled pH (7.2-7.4).

3.3 Cell Line Authentication

Genomic DNA was extracted from A549 and SK-LU-1 cells using QIAamp DNA kit (Qiagen, North Rhine-Westphalia, Germany). Briefly, cells were harvested and the cell pellet was resuspended in 200.00µL of 1× PBS. This was followed by the addition of 20.00µL of cold proteinase K and 200.00µL of Buffer AL. The mixture was vortexed (FINEPCR, Gyeonggi-do, South Korea) for 15 seconds and incubated in a 56.0°c water bath (Memmert, Bavaria, Germany) for 10 minutes. The tube was centrifuged briefly in Eppendorf Centrifuge 5424 (Eppendorf, Hamburg, Germany) and 100% ethanol (Fisher Scientific, MA, USA) was added. It was then vortexed for 15 seconds and centrifuged briefly.

The content was transferred to a QIAamp Mini spin column placed in a 2.00mL collection tube and centrifuged at 6,000× g for 1 minute. Up to 500.00µL of Buffer

AW1 was added and it was centrifuged at 6,000× g for 1 minute. The column was placed in another 2.00mL collection tube and 500.00µL of Buffer AW2 was added. Subsequently, it was centrifuged at 20,000× g for 3 minutes and supernatant was discarded. The column was centrifuged at maximum speed for 1 minute before transferring to a 1.50mL tube. DNA was eluted with 200.00µL of Buffer AE, incubated at room temperature for 5 minutes and later centrifuged at 6,000× g for 1 minute.

A549 and SK-LU-1 were authenticated by short tandem repeat (STR) profiling (Genetica DNA Laboratories, NC, USA). Fifteen STR loci and the gender identity locus amelogenin were profiled using PowerPlex 16 HS (Promega, WI, USA). Comparison to the ATCC database of A549 and SK-LU-1 cell lines reference profiles was performed.

3.4 Cell Recovery and Cryopreservation

3.4.1 Cell Recovery

Serum-free medium was first mixed with 20.0% FBS in a 15.00mL tube and filled into a T75 flask, which later warmed in the CO_2 incubator at 37.0°C for 30 minutes. Vial containing cryopreserved cells was removed from liquid nitrogen and quickly it was wiped with 70.0% ethanol (Labmart, Selangor, Malaysia) using KimWipe (Kimberly-Clark, TX, USA) and swirled around in the 37.0°c water bath incubator for 2-3 minutes, or until only a small chunk of ice was seen. The vial was wiped with 70.0% ethanol again and all its volume was transferred into the T75 flask prepared previously. Part of the suspension was used to wash as well as to collect the remaining cells in the vial. The cells were then examined under the inverted fluorescence microscope and re-examined the following day to check the attachment of cells. The spent medium was replenished with pre-warmed medium with 20.0% FBS.

3.4.2 Cell Cryopreservation

Cells were stocked when they reached 100% confluency. Freezing medium was prepared according to the recipe: 64.0% serum-free medium, 30.0% FBS, 5.0% dimethyl sulfoxide (DMSO) (Merck, Hesse, Germany) as cryoprotectant agent and 1.0% penicillin/ streptomycin, and kept at 4.0°C. After cells were harvested and centrifuged to collect the cell pellet, freezing medium was transferred to the cells and mixed well. The cryovial was frozen gradually at 4.0°C for 3 hours, -20.0°C for 2 hours, -30.0°C for 1 hour and later stored in the liquid nitrogen at -196.0°C.

3.5 Serial Selection for High and Low Invasive NSCLC Sub-cell Lines

Stock Matrigel basement membrane matrix (10mg/mL) (Corning, NY, USA) was thawed at 4.0°C overnight. Using pre-cooled pipette tips, Matrigel was gently mixed and diluted with cold dilution buffer (40mM Tris, 4.0% (w/v) sucrose, 30mM NaCl, pH 8.0) to 1.5mg/mL. The upper chamber of the 24-well transparent PET membrane 8.0μm pore size inserts (Corning, NY, USA) were coated with 100.00μL of Matrigel solution. The inserts were placed in a 24-well companion plate (Corning, NY, USA) and incubated in the CO_2 incubator at 37.0°C for at least 2 hours for gelling. Cells were harvested and the cell pellet was resuspended with complete medium without antibiotics. Cell counting was performed and cell density was adjusted to 5.0×10^5 cells/mL. Medium with 20.0% FBS was added to the wells of the companion plate (1.00mL per well) to act as chemoattractant and the Matrigel-coated inserts were submerged in the wells. A total of 500.00μL of the cell suspension was loaded into the upper chamber of the inserts. The plate was incubated in the CO_2 incubator at 37.0°C for 48 hours.

The non-invaded cells were collected together with Matrigel in the upper chamber into a culture flask (Flask A). The medium in the well was collected into

another culture flask (Flask B) and the well was washed with 1× PBS. Cells at the bottom of the inserts were detached by submerging in 1.00mL of trypsin in the well and incubated in the CO_2 incubator at 37.0°C for 3-5 minutes. Trypsin activity was inactivated with 1.00mL of medium and collected into Flask B. Culture media for both flasks were discarded and replenished the following day. Selection was repeated when the cells were 70% confluent, up to the seventh generation. High invasive sub-cell lines were denoted as A549-I7 and SK-LU-1-I7 while low invasive sub-cell lines were denoted as A549-NI7 and SK-LU-1-NI7.

3.6 Transwell Invasion Assay

Stock Matrigel was thawed at 4.0°C overnight. Cells were starved with serum-free medium for 20 hours in the CO_2 incubator at 37.0°C. Using pre-cooled pipette tips, Matrigel was gently mixed and diluted with cold dilution buffer to 1.5mg/mL. The upper chamber of the 24-well transparent PET membrane 8.0μm pore size inserts were coated with 70.00μL of Matrigel solution. The inserts were placed in a 24-well companion plate and incubated in the CO_2 incubator at 37.0°C for at least 2 hours for gelling. Cells were harvested after 20 hours of starving and the cell pellet was resuspended in serum-free medium containing 0.1% bovine serum albumin (BSA) (AMRESCO, OH, USA). Cell counting was performed and cell density was adjusted to 1.0×10^5 cells/mL. Medium with 20.0% FBS was added to the wells of the companion plate (1.00mL per well) and the Matrigel-coated inserts were submerged in the wells. A total of 500.00μL of the cell suspension was loaded into the upper chamber of the inserts. The plate was incubated in the CO_2 incubator at 37.0°C for 22 hours.

After incubation, cells that passed through the Matrigel attached either to the bottom of the membrane or fell into the well. Generally, the loss of cells was negligible. Medium was then removed and non-invaded cells together with Matrigel were gently

scraped off the upper chamber 2-3 times with cotton swabs moistened with medium. The inserts were fixed with 100% ethanol for 2 minutes and stained with 1.0% (w/v) methylene blue (Sigma Aldrich, MO, USA) for at least 20 minutes. Following that, the inserts were rinsed thoroughly in two beakers of distilled water to remove excess stain and were allowed to air dry completely. Invaded cells were counted in eight fields of triplicate membranes under the inverted fluorescence microscope at 200× magnification.

3.7 Wound Healing Assay

Cells were grown as 100% confluent monolayer in 6-well plate. Medium was discarded and replaced with serum-free medium containing the proliferation inhibitor Mitomycin C (1µg/mL) (Merck, Hesse, Germany) for 2 hours. Medium was discarded and a scratch was made using sterilised 200.00µL pipette tip. The well was washed with 1× PBS twice to remove debris from damaged or dead cells after mechanical scratching. Image at 0 hour was acquired under the inverted fluorescence microscope at 100× magnification. Photographs were also taken after cells were cultured in serum-free medium in the CO_2 incubator at 37.0°C for 28 hours. The gap distance was evaluated using TScratch v7.8 (Geback *et al.*, 2009).

3.8 Cell Proliferation Assay

Cells were harvested and counted to determine the cell density. Cell suspension was diluted with complete medium without antibiotics to necessary seeding concentration in 6-well plates for 3 samples with 3 replicates for 7 days, such that each well contained 2.0×10^4 viable cells. They were incubated in the CO_2 incubator at 37.0°C. Spent media were discarded and replenished with fresh growth media every 2 days to ensure optimum growing condition for cells. Cells were harvested and total viable cell number was counted every 24 hours for 7 days constitutively using trypan blue dye exclusion assay.

The end of haemacytometer (La Fontaine-Dynatech, Baden-Wurttemberg, Germany) and cover slip were cleaned with 70.0% ethanol using KimWipe. Cells were harvested and 20.00µL of the cell suspension was pipetted into a microcentrifuge tube. Trypan blue solution (0.4% (w/v)) (Sigma Aldrich, MO, USA) was vortexed briefly and 20.00µL was added to the microcentrifuge tube to stain dead cells. The mixture was left at room temperature for 3 minutes. Then, 10.00µL of the mixture was loaded onto the edge of haemacytometer for capillary action. Under the inverted fluorescence microscope, the number of unstained living cells (bright spheres) in the area of 16 squares was counted using a hand tally counter. This procedure was done for all four sets of 16 corner squares. The total count in µL was calculated according to the formula below:

$$\frac{(Cells\ per\ mL \times 10^4)}{4\ quadrants} \times 2 \qquad [\boldsymbol{Equation\ 3.1}]$$

A line graph was plotted with total viable cell number against harvest day and the doubling time was determined as follow:

$$Doubling\ Time = \frac{ln\,2}{ln(ratio)} \times Number\ of\ days \qquad [\boldsymbol{Equation\ 3.2}]$$

where, $Ratio = \frac{Total\ viable\ cell\ number\ on\ harvest\ day}{Total\ viable\ cell\ number\ seeded\ on\ day{-}0}$

3.9 Total RNA Extraction

3.9.1 Guanidinium Thiocyanate (GTC)-Acidic Phenol Extraction

Cells were harvested and the cell pellet was lysed in 1.00mL of TRIzol Reagent (Invitrogen, CA, USA) by repetitive pipetting. TRIzol Reagent disrupts the cells and dissolves the cell components without compromising RNA integrity. The homogenised sample was incubated at room temperature for 5 minutes to allow for complete dissociation.

Subsequently, 200.00µL of chloroform (Merck, Hesse, Germany) was added for phase separation and the tube was capped securely. The tube was then vortexed for 15 seconds and incubated at room temperature for 5 minutes. After centrifugation in Sorvall Legend Micro 17R centrifuge (Thermo Scientific, MA, USA) at 12,000× g at 4.0°C for 15 minutes, the mixture separated into three phases: a lower red, phenol-chloroform phase; an interphase; and a colourless upper aqueous phase, which contained the RNA.

This aqueous phase (450.00µL) was transferred to a 1.50mL tube and precipitated using 500.00µL of isopropanol (Merck, Hesse, Germany). Samples were incubated at room temperature for 10 minutes and centrifuged at 12,000× g at 4.0°C for 10 minutes. RNA was seen as a gel-like pellet on the side and bottom of the tube.

Supernatant was removed and the RNA pellet was washed with 1.00mL of 75.0% ethanol (Fisher Scientific, MA, USA). The sample was mixed by vortexing and centrifuged at 7,500× g at 4.0°C for 5 minutes. This step was repeated one more time. Supernatant was removed and the RNA pellet was air dried for 30 minutes. The RNA pellet was then dissolved in 100.00µL of nuclease-free water (Qiagen, North Rhine-Westphalia, Germany) and incubated in the water bath at 58.0°C for 10 minutes.

3.9.2 Silica Membrane Column-based Extraction

Cells were trypsinised and collected as a cell pellet. The cell pellet was loosened thoroughly by flicking the tube. The cells were disrupted by adding 700.00µL of QIAzol Lysis Reagent included in the MiRNeasy Mini kit (Qiagen, North Rhine-Westphalia, Germany) and vortexed to mix. The tube containing the homogenate was placed at room temperature for 5 minutes to promote dissociation of nucleoprotein complexes.

This was followed by the addition of 140.00µL of chloroform to the tube containing the homogenate and shaken vigorously for 15 seconds for subsequent phase separation. The tube was placed at room temperature for 2-3 minutes and centrifuged at 12,000× g at 4.0°C for 15 minutes. After centrifugation, the sample separated into 3 phases: an upper, colourless, aqueous phase containing RNA; a white interphase; and a lower, red, organic phase.

The upper aqueous phase was transferred to a 1.50mL tube, 1.5 volumes (525.00µL) of 100% ethanol (Fisher Scientific, MA, USA) was added and mixed thoroughly by pipetting up and down several times. Up to 700.00µL of the sample was pipetted, including any precipitate that may have formed, into an RNeasy Mini spin column in a 2.00mL collection tube where the total RNA binds to the membrane and phenol and other contaminants are efficiently washed away. The column was centrifuged at 8,000× g at room temperature for 15 seconds and the flow-through was discarded. This was repeated using the remainder of the sample. To wash, 700.00µL of Buffer RWT was added and centrifuged at 8,000× g for 15 seconds. The flow-through was discarded and 500.00µL of Buffer RPE was pipetted onto the column. It was centrifuged at 8,000× g for 15 seconds to wash the column. The flow-through was discarded. Another 500.00µL of Buffer RPE was added and centrifuged at 8,000× g for 2 minutes to dry the column membrane to ensure that no ethanol was carried over during RNA elution.

The column was removed from the collection tube carefully so that the column did not contact the flow-through. Otherwise, carryover of ethanol would occur. The column was placed into a new 2.00mL collection tube, and the old collection tube was discarded with the flow-through. The column was centrifuged at full speed for 1 minute to eliminate any possible carryover of Buffer RPE or if residual flow-through remained on the outside of the column. The column was transferred to a 1.50mL tube and 30.00-

50.00µL of nuclease-free water was pipetted directly onto the column membrane. It was centrifuged at 8,000× g for 1 minute to elute the RNA.

3.10 RNA Quality Check and Quantitation

3.10.1 Agilent 2200 TapeStation System

R6K sample buffer (Agilent Technologies, CA, USA) and Screen Tape strips (Agilent Technologies, CA, USA) were thawed in dark at room temperature. The buffer was vortexed and centrifuged briefly. Later, 4.00µL of buffer was added to 1.00µL of RNA sample. The mixture was heated at 72.0°C (Allsheng, Hangzhou, China) for 3 minutes, placed on ice for 2 minutes and centrifuged briefly to settle down the vapour and to collect the contents in the base of the tubes. Samples, pipette tips and strips were loaded and the run was started. The 28S/18S rRNA ratio and RNA integrity (RIN) value were evaluated to determine the quality of the RNA.

3.10.2 NanoDrop 2000

The arm of NanoDrop 2000 (Thermo Scientific, MA, USA) was lifted and 1.00µL of nuclease-free water was dropped onto the pedestal to clean. KimWipe was used to wipe the surface and this was followed by the measurement of 1.00µL of blank (nuclease-free water/ elution buffer) and samples. Wiping was done after each measurement was completed, before proceeding to the next sample. Cleaning step was performed again at the end to prevent contamination. The RNA concentration, OD_{260}, OD_{280}, $A_{260/280}$ and $A_{260/230}$ ratios of the samples were measured.

3.11 Reverse Transcription-Quantitative Real-time Polymerase Chain Reaction (RT-qPCR)

3.11.1 RT-PCR

TaqMan MiRNA RT kit components (Applied Biosystems, CA, USA), RNA samples and RT primers (Applied Biosystems, CA, USA) were thawed on ice. RT buffer, RNase inhibitor and RT primers were vortexed and centrifuged briefly. Master mix was first prepared accordingly as shown in Table 3.1:

Table 3.1: Master mix ingredients.

Components	15.00µL Reaction
100mM dNTPs (with dTTPs)	0.15µL
MultiScribe Reverse Transcriptase, 50U/µL	1.00µL
10× RT Buffer	1.50µL
RNase Inhibitor, 20U/µL	0.19µL
Nuclease-free Water	4.16µL
Total Volume	7.00µL

†The total volume will be added with 5.00µL sample and 3.00µL primers to make up 15.00µL reaction

The master mix was pipetted up and down to mix well, centrifuged and placed on ice while aliquoting into PCR tubes (Bio-Rad Laboratories, CA, USA). A total of 5.00µL of RNA sample (5ng) was added to each tube, mixed, centrifuged and placed on Eppendorf PCR Cooler (Eppendorf, Hamburg, Germany). Then, 3.00µL of 5× RT primers were added, mixed and centrifuged. The mixture was incubated on ice for 5 minutes before running on the Veriti 96 Well Thermal Cycler (Applied Biosystems, CA, USA) using the protocol in Table 3.2 below:

Table 3.2: Thermal cycling protocol for RT-PCR.

Steps	Time	Temperature
Hold	30 minutes	16.0°C
Hold	30 minutes	42.0°C
Hold	5 minutes	85.0°C
Hold	∞	4.0°C

3.11.2 qPCR

TaqMan Fast Advanced Master Mix (Applied Biosystems, CA, USA) and TaqMan miRNA assays (Applied Biosystems, CA, USA) were thawed on ice. Reactions were prepared as follow as in Table 3.3:

Table 3.3: Reagents were added sequentially.

Components	10.00µL Reaction
TaqMan Fast Advanced Master Mix	5.00µL
Nuclease-free Water	3.50µL
20× TaqMan MiRNA Assay	0.50µL
Product from RT Reaction	1.00µL
Total Volume	10.00µL

The mixture was centrifuged and placed on ice. The reaction tubes were later loaded into the Bio-Rad CFX96 Real-Time PCR Detection System (Bio-Rad Laboratories, CA, USA), and a run was performed using the following conditions in Table 3.4:

Table 3.4: The qPCR cycle.

Steps	Enzyme Activation	PCR	
	Hold	Cycle (40 Cycles)	
		Denature	Anneal/ Extend
Temperature	95.0°C	95.0°C	60.0°C
Time	20 seconds	3 seconds	20 seconds

The U6 small nuclear RNA was used as a control to normalise differences in total RNA levels in each sample. The relative amount of each miRNA to U6 RNA was expressed using $2^{-\Delta\Delta Ct}$, where $\Delta\Delta C_t = (C_{t\ miRNA} - C_{t\ U6})$. The value of each control sample was set at 1 and was used to calculate the fold change in target miRNAs.

3.12 MicroRNA Mimics and Hairpin Inhibitors

Bidirectional perturbation experiments where cultures transfected with miRNA mimics were contrasted to the cultures transfected with miRNA hairpin inhibitors, were carried out. The MiRIDIAN miRNA mimics and miRNA hairpin inhibitors for hsa-miR-92b, hsa-miR-378 and hsa-miR-1827 were chemically synthesised by Dharmacon,

CO, USA. MicroRNA mimics were synthesised as double-stranded miRNA oligonucleotides to mimic the function of endogenous mature miRNA while minimising the interferon response. The active strand preferentially enters the miRNA pathway to increase the expression level of the endogenous miRNA. MicroRNA hairpin inhibitors were designed as single-stranded miRNA oligonucleotides, which specifically target and bind irreversibly to the targeted miRNA molecules. Sequences based on *Caenorhabditis elegans* miRNA cel-miR-67 (Dharmacon, CO, USA) were used as negative experimental controls and when labelled with Dy547 (Dharmacon, CO, USA), they served as transfection control for monitoring delivery into the cells (Table 3.5).

Table 3.5: Mature miRNAs accession number and sequence.

ID	Accession Numbers	Sequences (5'-3')
Hsa-miR-92b-3p	MIMAT0003218	UAU UGC ACU CGU CCC GGC CUC C
Hsa-miR-378a-3p	MIMAT0000732	ACU GGA CUU GGA GUC AGA AGG
Hsa-miR-1827	MIMAT0006767	UGA GGC AGU AGA UUG AAU
Cel-miR-67	MIMAT0000039	UCA CAA CCU CCU AGA AAG AGU AGA

3.13 Transfection of MiRNA Mimics and Hairpin Inhibitors

Cells were plated at 5.0×10^4 cells/mL in complete medium with no antibiotics a day before transfection. Cells were transfected with 80nM miRNA mimics or miRNA hairpin inhibitors using DharmaFECT 1 transfection reagent (Dharmacon, CO, USA). Briefly, solutions of miRNA mimics and miRNA hairpin inhibitors were prepared by adding 1× siRNA buffer (Thermo Scientific, MA, USA). Diluted miRNAs were placed in tube 1 and transfection reagent was placed in tube 2 with serum-free medium. Both tubes were incubated at room temperature for 5 minutes. The contents in tubes 1 and 2 were combined and mixed by pipetting carefully up and down a few times and then incubated at room temperature for 20 minutes to form transfection complexes. Growth medium with no antibiotics was added to the mixture, which was then added drop-wise to each well of plate after removing the spent medium. The plate was swirled gently to

ensure uniform distribution of the transfection complexes. The transfected cells were incubated in the CO_2 incubator at 37.0°C for 48 hours.

3.14 Endothelial Tube Formation Assay

Geltrex lactate dehydrogenase-elevating virus (LDEV)-free reduced growth factor basement membrane matrix (Gibco, CA, USA) was thawed at 4.0°C overnight. HUVEC were starved for 5 hours in serum-free medium. Meanwhile, 50.00µL of undiluted Geltrex was applied to each well of the 96-well plate using pre-chilled pipette tips and left to polymerise in the CO_2 incubator at 37.0°C for at least 30 minutes. Five hours later, HUVEC were counted and 5.0×10^4 cells were transferred into 1.50mL tubes and they were centrifuged at 4,000rpm for 3 minutes to remove supernatant. The cells were then resuspended with 50.00µL of tumour-conditioned medium (TCM) and seeded into each Geltrex-coated well. TCM was the spent medium collected from each transfection experiment at the 24^{th} hour and centrifuged at 500× g at 4.0°C for 10 minutes to remove detached cells. The plate was incubated at 37.0°C for 15 hours.

Medium was carefully aspirated from the well by holding the plate at a slight angle and washed gently with Dulbecco's PBS (DPBS) with calcium and magnesium (pH 7.4) three times. DPBS containing $CaCl_2$ and $MgCl_2$ maintains the structural and physiological integrity of cells and is suitable for live cell imaging for short duration. The cells were then stained using cell-permeable calcein-actomethylester (AM) dye (Invitrogen, CA, USA). Working dye solution was prepared at 2mg/mL by diluting in DPBS with calcium and magnesium, 50.00µL was added to each well and incubated in the CO_2 incubator at 37.0°C for 30 minutes. Calcein-AM is non-fluorescent and when internalised by endothelial cells, intracellular esterases cleave the AM moiety by hydrolysis to generate free calcein in the cytoplasm that fluoresces brightly. This fluorescence was used to visualise cell organization and quantify the number of

junctions or tubes between cells. The dye-containing solution was gently removed and the cells were washed gently with DPBS with calcium and magnesium. Fluorescence (excitation: 485nm; emission: 520nm) was measured under the inverted fluorescence microscope using a 4× objective and images were analysed using WimTube (Wimasis, Munich, Germany). Wimasis WimTube software tool conducted the conversion of data, noise filtering, particle detection and tubule recognition automatically. The evaluation of image data gave out four parameters: cell covered area, tube length, nodes and loops.

3.15 MiRNA Target Prediction

Putative miRNA targets were generated using publicly available programmes: DIANA-microT-CDS v5.0 (http://diana.imis.athena-innovation.gr/DianaTools/index.php?r=microT_CDS/index) (Paraskevopoulou *et al.*, 2013) using default threshold at 0.7 and TargetScan v7.1 (http://www.targetscan.org/vert_71/) (Agarwal *et al.*, 2015). To avoid false positive target genes, overlapped targets from the two prediction programmes analysed using Venny v2.1 (http://bioinfogp.cnb.csic.es/tools/venny/) (Oliveros, 2015) were generally chosen as more convincing potential target genes. These hypothetical miRNA targets were subjected to gene annotation enrichment analysis using Database for Annotation, Visualization and Integrated Discovery (DAVID) v6.8 (https://david-d.ncifcrf.gov/) (Huang *et al.*, 2009) by the Official Gene Symbol identifier.

3.16 Construction of Wild Type (WT) 3'-UTR Dual Luciferase Reporter Plasmid

3.16.1 Preparation of Insert DNA (3'-UTR)

3.16.1.1 Primer Design

The miRNA target site in 3'-UTR of gene of interest was identified using TargetScan and the *Homo sapiens* 3'-UTR was blasted against National Center for

Biotechnology Information (NCBI) RefSeq RNA database using Nucleotide Basic Local Alignment Search Tool (Blastn) to retrieve full length mRNA sequence. Forward and reverse primers were designed using NCBI Primer-Blast by default parameters. The melting temperatures (T_m) between the two primers were within 5°C of each other. Recognition sequence of XhoI and NheI was inserted at the 5' end of forward and reverse primers, respectively (Table 3.6).

Table 3.6: List of primers used in this study.

Primers[†#]	Sequences (5'-3')	Length (nt)
RBX1_F	AGT ACC TCG AGC ATA CAC AAG AGA GAG CAT CCG	33
RBX1_R	CAT GTG CTA GCC TTC AGA AGA GTG TAC TGT CGC	33
MYC_F	CGC TAC TCG AGG GAT TGA AAT TCT GTG TAA CTG CT	35
MYC_R	ACT GTG CTA GCT GTT GCG GAA ACG ACG AGA A	31
CRKL_F	ATC ATC TCG AGG CAG TTA TGA ACA CCC ACC CT	32
CRKL_R	CTT AGG CTA GCA TCA GCT CGT TAC TTC AGC CC	32
Luc_F	GAT CGC CGT GTA ATT CTA GTT GTT T	25
SV40_R	CTT CCT TTC GGG CTT TGT TAG C	22

[†]F denotes forward primer; R denotes reverse primer
[#]*RBX1*- Ring-box 1; *MYC*- v-Myc avian myelocytomatosis viral oncogene homolog; *CRKL*- CRK-like proto-oncogene, adaptor protein

3.16.1.2 Complementary DNA (cDNA) Synthesis

Total RNA was isolated and quantitated. The RevertAid H Minus First Strand cDNA Synthesis kit components (Thermo Scientific, MA, USA), RNA samples and forward primer were allowed to thaw on ice. The following reagents were added as shown in Table 3.7:

Table 3.7: Reaction components and volumes for RT reactions.

Components	20.00µL Reaction
Template RNA (4µg)	XµL
Forward Primer (0.8µM)	1.60µL
Nuclease-free Water	(10.40-X)µL
Total Volume	12.00µL

[†]The total volume will be added with 8.00µL mixture in Table 3.8 after incubation

A positive control was also set up using 2.00µL of human glyceraldehyde 3-phosphate dehydrogenase (GAPDH) control RNA (100ng) and 1.00µL of 10µM reverse GAPDH primer (Thermo Scientific, MA, USA). The mixture was incubated at 65.0°C for 5 minutes, centrifuged briefly and placed on ice. The following components were added according to the volumes listed in Table 3.8 below:

Table 3.8: RT reaction was set up by mixing the following components.

Components	20.00µL Reaction
5× Reaction Buffer	4.00µL
RiboLock RNase Inhibitor, 20U/µL	1.00µL
10mM dNTP Mix	2.00µL
RevertAid H Minus M-MuLV Reverse Transcriptase, 200U/µL	1.00µL
Total Volume	8.00µL

†The total volume will be added with 12.00µL mixture in Table 3.7

The solution was mixed gently and centrifuged to bring solution to the bottom of the tube. The reaction tubes were incubated at 45.0°C for 60 minutes and the reaction was terminated at 70.0°C for 5 minutes.

3.16.1.3 Amplification by PCR

The Phusion Flash High-Fidelity PCR Master Mix (Thermo Scientific, MA, USA), forward and reverse primers were placed on ice. Reaction components were combined in a PCR tube in Table 3.9:

Table 3.9: PCR components.

Components	20.00µL Reaction
Nuclease-free Water	3.00µL
2× Phusion Flash PCR Master Mix	10.00µL
Forward Primer (0.3µM)	3.00µL
Reverse Primer (0.3µM)	3.00µL
Template DNA	1.00µL
Total Volume	20.00µL

The reaction tube was centrifuged briefly and loaded into the thermal cycler. An experiment document was created using the following parameters in Table 3.10:

Table 3.10: Thermal cycling profile for PCR.

Cycle Steps	3-step Protocol		Cycles
	Temperature	Time	
Initial Denaturation	98.0°C	10 seconds	1
Denaturation	98.0°C	1 second	35
Annealing	X°C†	5 seconds	
Extension	72.0°C	15 seconds	
Final Extension	72.0°C	1 minute	1
	4.0°C	Hold	

†Optimal temperature for primers

3.16.1.4 Agarose Gel Electrophoresis (AGE)

Sufficient agarose (0.3g) (Fisher Scientific, MA, USA) was weighed using the Analytical Balance CP224S (Sartorius, Lower Saxony, Germany) to cast a 1.0% gel. The agarose was added to 30.00mL of 1× Tris-Acetate-EDTA (TAE) buffer (Fisher Scientific, MA, USA) and swirled to mix. The bottle was microwaved (Pensonic, Penang, Malaysia) at medium heat until the solution became transparent (2 minutes). The bottle was removed from the microwave and let it cool under running tap water. While the gel was cooling, casting tray and gel comb (Eppendorf, Hamburg, Germany) were assembled. Once the bottle was cooled that it can be touched comfortably with gloved hand, 1.50µL of RedSafe Nucleic Acid Staining Solution (20,000×) (iNtRON Biotechnology, Gyeonggi-do, South Korea) was added. Gel was poured into casting tray and was let to sit until solidified.

RNA samples were mixed with 2× loading dye (Fermentas, MA, USA) in a ratio of 1:1 while DNA samples were mixed with Blue/Orange 6× loading dye (Promega, WI, USA) in 5:1 ratio and warmed at 70.0°C for 10 minutes. Gel comb was removed and the gel was submerged in 1× TAE buffer in the BG-Submidi Submarine Unit (BayGene, Beijing, China). This was followed by the loading of RNA/ DNA samples and RiboRuler High Range RNA Ladder (Fermentas, MA, USA)/ O'GeneRuler 1kb DNA ladder (Fermentas, MA, USA) into the wells. The electrophoresis was run at 100V (constant) and 400mA for 90 minutes on the PowerPac Basic (Bio-Rad Laboratories,

CA, USA). The gel was viewed and photographed at 302nm using AlphaImager 2200 (Alpha Innotech, CA, USA).

3.16.1.5 QIAquick Gel Extraction

After electrophoresis, the DNA fragment of interest was excised with a razor blade under UV illumination. Empty agarose was trimmed off as much as possible. The gel slice was weighed in a 1.50mL tube. Three volumes of Buffer QG (Qiagen, North Rhine-Westphalia, Germany) was added to one volume of gel (300.00µL per 100mg of gel). The mixture was vortexed and incubated in 50.0°C water bath for 10 minutes. It was vortexed every 2-3 minutes during the incubation to help to dissolve gel. The resulting solution was yellow.

One gel volume of isopropanol was added to the dissolved gel solution and mixed well by inverting back and forth. A QIAquick spin column (Qiagen, North Rhine-Westphalia, Germany) was inserted into a 2.00mL collection tube. To bind DNA, the sample was applied to the column and centrifuged at 17,900× g for 1 minute. The flow-through was discarded and the column was placed back in the same tube. Another 500.00µL of Buffer QG was added and centrifuged at 17,900× g for 1 minute to remove all traces of agarose. The flow-through was discarded and the column was placed back in the same tube.

To wash out salt and impurities, 750.00µL of Buffer PE (Qiagen, North Rhine-Westphalia, Germany) was added, let stand for 3 minutes and centrifuged at 17,900× g for 1 minute. The flow-through was discarded after centrifuging and the column was placed back in the same tube. It was then centrifuged at 17,900× g for 1 minute to dry the spin membrane. The spin column was placed to a new 1.50mL tube and 30.00µL of Elution Buffer (Qiagen, North Rhine-Westphalia, Germany) was added directly to the

centre of the column without touching the membrane. It was incubated at room temperature for 4 minutes and centrifuged at maximum speed for 1 minute.

3.16.1.6 Sequencing

Purified samples were sequenced with forward and reverse primers. Using Serial Cloner v2.6, alignment was performed to compare the sequences against the reference sequences. Quality bar graph was also examined where the acceptable average quality value was close to 30 or higher.

3.16.2 Preparation of Vector DNA

3.16.2.1 Restriction Enzyme Digestion

Under sterile conditions, the following components (Promega, WI, USA) were added in the stated order in Table 3.11:

Table 3.11: Restriction enzyme digestion set up.

Components	20.00µL Reaction
Nuclease-free Water	(16.80-X)µL
Restriction Enzyme 10× Buffer B	2.00µL
Acetylated BSA (10mg/mL)	0.20µL
DNA Sample (1µg)	XµL
NheI, 10U/µL	0.50µL
XhoI, 10U/µL	0.50µL
Final Volume	20.00µL

The addition of BSA was to stabilise the enzymes and enhance their activity (Lepinske, 1996; Williams *et al*., 1996) by protecting them from proteases, non-specific adsorption and harmful environmental factors such as heat, surface tension and interfering substances. The solution was mixed gently by pipetting and centrifuged briefly to collect the content at the bottom of the tube. It was incubated at 37.0°C for 1 hour and proceeded to gel analysis and extraction to reduce background transformation of uncut vector at later stage. Restriction enzyme digestion and gel extraction were also performed on insert DNA.

3.16.3 Ligation of Insert and Vector

The amount of insert DNA (ng) required was calculated as follow:

$$\frac{(50ng\ of\ vector \times kb\ size\ of\ insert)}{7350kb\ size\ of\ vector} \times \frac{1}{3} \qquad [\boldsymbol{Equation\ 3.3}]$$

The T4 DNA Ligase 10× Buffer (Promega, WI, USA) was vortexed to completely incorporate ATP into the solution and to thoroughly mix the dithiothreitol (DTT) into the solution. The ligation reaction was assembled by adding appropriate amount of insert and vector DNA, followed by 1.00µL of ligase buffer and 0.33µL of T4 DNA Ligase (3U/µL) (Promega, WI, USA), and finally topped up with nuclease-free water to 10.00µL. It was then incubated at 4.0°C overnight.

3.16.4 Transformation into *Escherichia coli* (*E. coli*)

Ligation reaction was centrifuged briefly and placed on ice. Frozen high-efficiency JM109 Competent Cells (Promega, WI, USA) was removed from -80.0°C (Panasonic, Tokyo, Japan) and placed on ice until just thawed (5 minutes). Cells were mixed by gently flicking the tube and 100.00µL of the thawed cells were carefully transferred to the ligation reaction tube using pre-chilled pipette tips to prevent the cells from warming above 4.0°C. The pipette tip was moved through the cells while dispensing and the tube was gently flicked to mix and incubated on ice for 30 minutes. A transformation control was also set up by mixing 100.00µL of competent bacteria with 1.00µL of pGEM-3Z Vector control DNA (supercoiled plasmid DNA) (Promega, WI, USA).

A 42.0°C heat shock of 45 seconds was performed, followed by immediate placement on ice for 2 minutes. Up to 900.00µL of cold Luria-Bertani (LB) medium (Laboratorios CONDA, Madrid, Spain) was added to the bacterial suspension before incubation at 37.0°C for 1 hour with agitation (225rpm) in Orbital Shaker-Incubator ES-

20 (Biosan, Riga, Latvia). The transformation reaction was centrifuged at 8,000rpm for 1 minute. The supernatant was discarded and the cell pellet was resuspended with 100.00µL of warm LB medium. The entire aliquot was plated out on 1.0% (w/v) LB agar (Laboratorios CONDA, Madrid, Spain) plates with 50µg/mL ampicillin (MP Biomedicals, CA, USA) at 37.0°C in the incubator (Memmert, Bavaria, Germany) overnight.

3.16.5 Screening of Transformants

3.16.5.1 Colony PCR

A well isolated white colony was picked using a flamed and cooled bacterial loop and transferred to 20.00µL of sterile distilled water. It was boiled at 95.0°C for 10 minutes to break open the bacterial cell wall and release the DNA, centrifuged for 5 minutes to pellet the cell debris and placed on ice immediately. Only 2.00µL of the supernatant was used in a 20.00µL amplification reaction with 0.1µM forward and reverse primers, following cycling conditions described in Table 3.10. An aliquot of the completed PCR was analysed by electrophoresis for the product of appropriate size, which indicated the correct insert was present in the clone.

3.16.5.2 Plasmid Miniprep

Using sterile technique, 5.00mL of LB-Ampicillin broth was pipetted into a 50.00mL tube. Sterile loop was used to pick part of a single colony and inoculated in the tube. The culture was placed to grow at 37.0°C overnight with agitation. The liquid cell culture was shaken vigorously to provide a sufficient amount of oxygen to the dividing cells.

Plasmid DNA was isolated using PureYield Plasmid Miniprep System (Promega, WI, USA). To process a total of 3.00mL of culture, 1.50mL of bacterial culture was first

centrifuged at maximum speed for 30 seconds. The supernatant was discarded. An additional 1.50mL of bacterial culture was added to the same tube and centrifuged at maximum speed for 30 seconds. The supernatant was discarded. After that, 600.00µL of Tris-EDTA (TE) buffer (10mM Tris, 1mM EDTA, pH 8.0) was added to the cell pellet and resuspended completely. To lyse the cells, 100.00µL of Cell Lysis Buffer was added and mixed by inverting the tube 6 times (within 2 minutes). The solution changed from opaque to clear blue, indicating complete lysis. It was then neutralised with 350.00µL of cold Neutralization Solution and mixed thoroughly by inverting the tube. The sample turned yellow when neutralisation was complete, and a yellow precipitate formed. The tube was inverted for an additional of 3 times to ensure complete neutralisation. It was centrifuged at maximum speed for 3 minutes. The supernatant (900.00µL) was transferred to a PureYield Minicolumn. The minicolumn was placed into a Collection Tube, and centrifuged at maximum speed for 15 seconds. The flow-through was discarded and the minicolumn was placed into the same collection tube.

Subsequently, 200.00µL of Endotoxin Removal Wash was added and centrifuged at maximum speed for 15 seconds to remove protein, RNA and endotoxin contaminants from purified plasmid DNA. This was followed by the addition of 400.00µL of Column Wash Solution and centrifuged at maximum speed for 30 seconds. The minicolumn was transferred to a new 1.50mL tube, and then 30.00µL of Elution Buffer was added directly to the minicolumn matrix. It was let stand at room temperature for 1 minute before centrifuging at maximum speed for 15 seconds to elute the plasmid DNA.

3.16.5.3 Restriction Enzyme Digestion

Under sterile conditions, the following components (New England Biolabs, NEB, MA, USA) were added in the stated order in Table 3.12:

Table 3.12: Restriction enzyme digestion components list.

Components	20.00µL Reaction
Nuclease-free Water	(17.50-X)µL
Restriction Enzyme 10× Buffer 2.1	2.00µL
Plasmid DNA sample (1µg)	XµL
Restriction Enzyme, 20,000U/mL	0.50µL
Final Volume	20.00µL

The solution was mixed gently by pipetting and centrifuged briefly to collect the content at the bottom of the tube. It was incubated at 37.0°C for 4 hours and the enzyme activity was inactivated at 80.0°C for 20 minutes. The restriction enzymes used (HindIII, SspI and SpeI) were listed in Table 3.13 and the restriction products were analysed by electrophoresis. Clones that showed the right number of gel bands with appropriate size indicated the correct insert was present. Plasmid DNA of positive clones concluded from both experiments in **Section 3.16.5.1** and **Section 3.16.5.3** were sequenced using Luc_F and SV40_R primers (Table 3.6).

Table 3.13: List of restriction enzymes used in this study.

Restriction Enzymes	Recognition Sequences
NheI	5'-G|CTAGC-3' 3'-CGATC|G-5'
XhoI	5'-C|TCGAG-3' 3'-GAGCT|C-5'
HindIII	5'-A|AGCTT-3' 3'-TTCGA|A-5'
SspI	5'-AAT|ATT-3' 3'-TTA|TAA-5'
SpeI	5'-A|CTAGT-3' 3'-TGATC|A-5'

3.17 Construction of Mutated (MT) 3'-UTR Dual Luciferase Reporter Plasmid

3.17.1 Mutagenesis Primer Design

Using QuikChange Primer Design Program (Agilent Technologies, CA, USA), mutagenesis primers (Table 3.14) were designed such that they contained 10-15nt of unmodified sequence on both sides of the mutation and the mutated bases were in the center of the primers. They had a T_m of ≥ 75.0°C, a minimum GC content of 40.0% and

terminated in one or more C or G bases at the 3' end. PAGE (polyacrylamide gel electrophoresis) purification was performed.

Table 3.14: PCR primers used for site-directed mutagenesis.

Primers†	Sequences (5'-3')	Length (nt)
RBX1_MT	GCT GTT TCT GTA GCC ATA TTG TAT TCT GTG TCA AAT AAA TGA ACG TTG GAT TCT GGA ACG GAT GC	65
MYC_MT	GTC TTG AGA CTG AAA GAT TTA GCC ATA ATG TAA ACT TAA GGA AAA TTG GAC TTT GGG CAT AAA AGA ACT TTT TTA TGC	78
MT_CTRL	CTC CCG TAT CGT AGT TAT CTA CAC GAC GGG	30

† MT denotes mutagenesis primer; CTRL denotes control

3.17.2 QuikChange Site-Directed Mutagenesis System

The amount of each primer needed in the reaction (in picomoles) was calculated using the formula:

$$X\ pmoles\ of\ oligo = \frac{ng\ of\ oligo}{330 \times \#\ of\ bases\ in\ oligo} \times 1000 \qquad [\boldsymbol{Equation\ 3.4}]$$

On ice, in a PCR tube, reaction mixtures were prepared, combining the following components (Agilent Technologies, CA, USA) in Table 3.15:

Table 3.15: Primary ingredients for mutagenesis PCR reaction.

Reaction Components	Templates > 5kb	QuikChange Multi Control Template (4kb)
10× QuikChange Multi Reaction Buffer	2.50µL	2.50µL
Nuclease-free Water	(20.00-X-Y)µL	18.50µL
QuikSolution	0.50µL	-
dsDNA Template	XµL (100ng)	1.00µL (50ng/µL)
Mutagenic Primers	YµL (100ng each primer)	1.00µL QuikChange Multi Control Primer Mix (100ng/µL)
dNTP Mix	1.00µL	1.00µL
QuikChange Multi Enzyme Blend (2.5U/µL)	1.00µL	1.00µL
Total Volume	25.00µL	25.00µL

The QuikChange Multi control template and control primer mix were used to test the efficiency of simultaneous site-directed mutagenesis at three independent sites (mutagenesis control). The 4kb control template encodes the first 146 amino acids of β-

galactosidase (encoded by the *LacZ* gene) but was modified to contain stop codons at three positions in the *LacZ* coding sequence. XL10-Gold cells (Agilent Technologies, CA, USA) transformed with the control template appear white on LB-ampicillin agar plates containing isopropyl β-D-1-thiogalactopyranoside (IPTG) (Fisher Scientific, MA, USA) and 5-bromo-4-chloro-3-indolyl-β-D-galactopyranoside (X-gal) (Fisher Scientific, MA, USA), because each of the three mutations prevents the production of active β-galactosidase. However, the QuikChange Multi control primer mix contains three primers, each of which reverts one of these stop codons to the codon found in the original *LacZ* gene. Restoration of active β-galactosidase requires that all three reversion events occur in the same molecule. Following transformation, colonies could be scored for the β-galactosidase phenotype, where a blue colony indicates the production of a triple-mutant plasmid.

The amplification was carried out following the cycling parameters in Table 3.16 below:

Table 3.16: Cycling instructions for the mutagenesis/ control reaction.

Segments	Cycles	Temperature	Time
1	1	95.0°C	1 minute
2	30	95.0°C	1 minute
		X°C†	1 minute
		65.0°C	16 minutes for experimental reaction 8 minutes for control reaction

†Optimal temperature for primers

3.17.3 Restriction Enzyme Digestion

Following temperature cycling, the reactions were placed on ice for 2 minutes to cool the reaction to ≤ 37.0°C. Prior to transformation into *E. coli*, digestion with 1.00µL of DpnI (10U/µL) (Agilent Technologies, CA, USA) was needed to degrade methylated parental (non-mutated) DNA to reduce the amount of wild type template, while keeping the nascent DNA intact. Each reaction mixture was thoroughly mixed by pipetting the

solution up and down several times. The reaction mixtures were centrifuged for 1 minute, then immediately incubated at 37.0°C for 1 hour.

3.17.4 Transformation into *E. coli*

The XL10-Gold ultracompetent cells were gently thawed on ice. For each mutagenesis reaction, 45.00µL of the ultracompetent cells were aliquoted to a pre-chilled tube. This was followed by the addition of 2.00µL of the XL10-Gold β-mercaptoethanol mix (Agilent Technologies, CA, USA) to the 45.00µL of cells to increase transformation efficiency. The contents of the tube were swirled gently. The cells were incubated on ice for 10 minutes, swirling gently every 2 minutes. Subsequently, 1.50µL of DpnI-treated DNA was transferred to the ultracompetent cells. The transformation efficiency of the XL10-Gold ultracompetent cells was verified by adding 1.00µL of 0.01ng/µL pUC18 control plasmid (Agilent Technologies, CA, USA) to another 45.00µL aliquot of cells. The transformation reactions were swirled gently to mix, and then incubated on ice for 30 minutes.

NZY^+ broth (Fisher Scientific, MA, USA) was pre-heated at 42.0°C for 5 minutes. Meanwhile, the tubes were heat-pulsed at 42.0°C for 30 seconds and incubated on ice for 2 minutes. A total of 500.00µL of pre-heated NZY^+ broth was added to each tube and the tubes were incubated at 37.0°C for 1 hour with shaking at 225rpm. Cells were concentrated by centrifuging at 1,000rpm for 10 minutes and resuspended in 100.00µL of pre-warmed NZY^+ broth. The appropriate volume of each transformation reaction was plated, as indicated in Table 3.17, on LB-ampicillin agar plates. For the mutagenesis and transformation controls, cells were spread on LB-ampicillin agar plates that have been prepared with 80µg/mL X-gal and 20mM IPTG. When plating less than 100.00µL from the transformation reaction, a 100.00µL pool of NZY^+ broth was placed on the agar plate, the cells were pipetted into the pool, and then the mixture was spread.

Table 3.17: Fraction of transformation reaction to spread onto the agar plate.

Reaction types	Volume to Plate
Experimental Mutagenesis	1.00µL, 10.00µL and 100.00µL
Mutagenesis Control	10.00µL
Transformation Control	5.00µL

The transformation plates were incubated at 37.0°C for at least 16 hours. Five colonies were selected and analysed by plasmid isolation and sequencing.

3.18 Dual Luciferase Reporter Assay

Cells were seeded at 5.0×10^4 cells/mL before co-transfection with miRNA mimics/ hairpin inhibitors and 100ng of WT/ MT 3'-UTR plasmids according to the protocols described in **Section 3.13**. MT 3'-UTR was used as control to confirm that the down-regulation of the luciferase activity upon exposure to miRNA is mediated solely by base-pairing between the miRNA's seed sequence and the predicted binding site, and is not due to secondary indirect effects. Cell lysates were harvested 48 hours later and resuspended in 50.00µL serum-free medium in 1.50mL tubes. The content of Dual-Glo Luciferase Buffer (Promega, WI, USA) was transferred to Dual-Glo Luciferase Substrate (Promega, WI, USA) to create the Dual-Glo Luciferase Reagent. It was mixed by inversion until the substrate was thoroughly dissolved. Dual-Glo Stop & Glo Reagent was freshly prepared by diluting appropriate volume of Dual-Glo Stop & Glo Substrate (Promega, WI, USA) in Dual-Glo Stop & Glo Buffer (Promega, WI, USA) in a ratio of 1:100. A volume of Dual-Glo Luciferase Reagent equal to the culture medium volume (50.00µL) was added to each tube and mixed. Firefly luminescence was measured on GloMax-Multi Jr Detection System (Promega, WI, USA) after 10 minutes followed by the addition of 50.00µL of Dual-Glo Stop & Glo Reagent and mixed. Ten minutes later, *Renilla* luminescence was measured in the same order as the firefly luminescence was measured. *Renilla* luciferase served as an internal control due to its constitutive expression was not modulated by experimental factors that could result in either up- or down-regulation of the amount of the enzyme produced. The ratio of

luminescence from the firefly luciferase reporter to luminescence from the *Renilla* luciferase reporter was calculated. This normalisation helped to differentiate between specific and non-specific cellular responses.

3.19 Protein Extraction

Cells were harvested and washed by resuspending the cell pellet with 1× PBS. Cells were pelleted by centrifugation at 500× g for 3 minutes. The supernatant was carefully removed, leaving the cell pellet as dry as possible. Protein was isolated using NE-PER Nuclear and Cytoplasmic Extraction kit (Thermo Scientific, MA, USA). Immediately before use, 100× Halt Protease and Phosphatase Inhibitors Cocktail (EDTA-free) (Thermo Scientific, MA, USA) was added to CERI reagent at a 1× final concentration to preserve protein integrity. Subsequently, 200.00µL of cold CERI was added to the cell pellet and mixed by pipetting to disrupt cell membrane and release cytoplasmic contents. The resulting lysate was vortexed on the highest setting for 30 seconds to fully resuspend the cell pellet. It was placed on ice for 10 minutes and 11.00µL of cold CERII was added to the tube. It was then vortexed on the highest setting for 20 seconds and placed on ice for 1 minute. It was vortexed again on the highest setting for 20 seconds and centrifuged at 16,000× g for 5 minutes. The supernatant (cytoplasmic extract) was transferred to a clean pre-chilled tube.

3.20 Protein Quantitation

Samples and Pierce Bicinchinonic Acid (BCA) Protein Assay reagents (Thermo Scientific, MA, USA) were equilibrated at room temperature. BCA working reagent was prepared for all samples using 50:1 ratio of reagents A:B. Reagent A contains BCA, sodium carbonate, sodium tartrate and sodium bicarbonate in 0.1N NaOH (pH 11.25). Reagent B is a solution containing 4.0% copper (II) sulphate pentahydrate. The working reagent was mixed until light green in colour and 200.00µL was added to each PCR

tube. Next, 25.00µL of sample was added and blank was prepared with 25.00µL of nuclease-free water. The solution was mixed well by pipetting and centrifuged briefly. The tubes were incubated at 37.0°C for 30 minutes and cooled to room temperature for 10 minutes. Using NanoDrop 2000, 1.00µL of blank and samples were measured at 562nm (A_{562}) and concentration was estimated from the standard curve.

3.21 Western Blotting

Resolving solution was prepared by mixing the components listed in Table 3.18 below:

Table 3.18: Solutions for preparing resolving and stacking gels for SDS-PAGE.

1mm Thickness Gel	Stacking Gel (4.0%)	Resolving Gel (X%)
40.0% Acrylamide/Bis Solution 19:1 (Bio-Rad Laboratories, CA, USA)	500.00µL	0.375 × X% = YmL
0.5M Tris-HCL (pH 6.8)	1.26mL	-
1.5M Tris-HCL (pH 8.8)	-	3.75mL
10.0% Sodium Dodecyl Sulfate (SDS) (Fisher Scientific, MA, USA)	50.00µL	150.00µL
Distilled Water	3.18mL	11.02mL - YmL
Tetramethylethylenediamine (TEMED) (Merck, Hesse, Germany)	5.00µL	7.50µL
10.0% (w/v) Fresh Ammonium Persulfate (APS) (Thermo Scientific, MA, USA)	25.00µL	75.00µL
Bromophenol Blue (Fisher Scientific, MA, USA)	10.00µL	-
Total Volume	5.00mL	15.00mL

The resolving solution was loaded to fill 80% of the Mini-PROTEAN gel plates (Bio-Rad Laboratories, CA, USA) and a layer of 0.1% (w/v) SDS was added on top of the resolving solution to prevent oxidisation and dehydration of the gel. It was left to solidify at room temperature. After approximately 45 minutes, SDS was removed using KimWipe. Stacking solution was prepared according to Table 3.18 and casted on top of the resolving gel. Gel comb (Bio-Rad Laboratories, CA, USA) was inserted and it was left to polymerise for 30 minutes. Samples were prepared in a ratio of 4:1 with Lane Marker Reducing Sample Buffer (5×) (Thermo Scientific, MA, USA). The mixture was

vortexed and centrifuged briefly followed by boiling at 95.0°C for 5 minutes. Samples were centrifuged briefly and cooled to room temperature. The gel plates were removed from the casting frames and casting stands (Bio-Rad Laboratories, CA, USA) and placed face to face in the Mini-PROTEAN Tetra Cell 4-Gel System (Bio-Rad Laboratories, CA, USA). The space in the tank was filled with 1× Tris-Glycine-SDS (TGS) buffer. Combs were removed. Each well was flushed with buffer using pipette, after which 20.00µL of samples and 6.00µL of biotinylated protein ladder (Cell Signaling Technology, MA, USA) were loaded. The run was started at 110V and 400mA (constant) for 20 minutes for stacking gel, and then was changed to 150V and 400mA (constant) for 45 minutes when the sample front reached the resolving gel.

Gel was removed from glass and stacking gel was torn off using a blade (Bio-Rad Laboratories, CA, USA). The gels, nitrocellulose membranes and extra thick blot papers (Bio-Rad Laboratories, CA, USA) were soaked in transfer buffer containing 20.0% (v/v) methanol (Merck, Hesse, Germany) for 5 minutes. Bio-Rad Trans-Blot SD Semi-Dry Electrophoretic Transfer Cell (Bio-Rad Laboratories, CA, USA) was cleaned with distilled water and KimWipe. The components for gel transfer were placed sequentially: anode (+), filter paper, nitrocellulose membrane, gel, filter paper and finally cathode (-). The transfer was conducted at 25V (constant) and 50mA per gel for 90 minutes (Major Science, CA, USA). To check for success of transfer, membranes were incubated in Ponceau S (Sigma Aldrich, MO, USA) until bands were seen. The membranes were washed extensively with distilled water until the water ran clear and the protein bands were well defined.

Membranes were blocked in BSA or non-fat skim milk (Merck, Hesse, Germany) at room temperature for 1 hour under 40° orbital agitation using Multi Bio 3D Mini-Shaker (Biosan, Riga, Latvia). Subsequently, the membranes were rinsed with 1× TBST for 5 minutes and incubated with primary antibodies: CTNNB1 rabbit monoclonal

antibody (1:1000) (Cell Signaling Technology, MA, USA), VIM rabbit monoclonal antibody (1:1000) (Cell Signaling Technology, MA, USA), RBX1 rabbit monoclonal antibody (1:1000) (Cell Signaling Technology, MA, USA) or CRKL mouse monoclonal antibody (1:1000) (Cell Signaling Technology, MA, USA), at room temperature for 30 minutes under agitation, then 4.0°C overnight. GAPDH rabbit monoclonal antibody (1:10000) (Cell Signaling Technology, MA, USA) was used as endogenous control. Shaking was continued the next day at room temperature for 1 hour. The membranes were washed three times for 5 minutes with 1× TBST, under agitation. This was followed by incubation in secondary antibodies: anti-rabbit IgG, horseradish peroxidase (HRP)-linked antibody (1:1000) (Cell Signaling Technology, MA, USA) or anti-mouse IgG, HRP-linked antibody (1:1000) (Cell Signaling Technology, MA, USA) added with anti-biotin, HRP-linked antibody (1:1000) (Cell Signaling Technology, MA, USA) at room temperature for 1 hour under agitation. Washing was carried out with 1× TBST for 5 minutes three times followed by 1× TBS (pH 7.6) for 5 minutes once, under agitation.

WesternBright Quantum Chemiluminescent HRP substrate components (Advansta, CA, USA) were mixed 1:1 in a sufficient amount to cover the nitrocellulose membrane. It was then dropped onto the membrane and incubated for 2 minutes. Excess reagent was drained and the membrane was placed on top of a film. The blot was visualised on FUSION FX7 Image and Analytics System (Vilber Lourmat, Eberhardzell, Germany), and quantified using ImageJ v1.49.

3.22 Overexpression Plasmids and SiRNAs

Mammalian expression plasmids pCMV6-AC-RBX1-GFP and pCMV6-AC-CRKL-GFP were purchased from OriGene, MD, USA. They were designed to contain

the cDNA ORF of *RBX1* and *CRKL* without the 3'-UTR. An empty plasmid (pCMV6-AC-GFP) (OriGene, MD, USA) served as the negative control.

ON-TARGET plus SMARTpool siRNAs targeting human *RBX1* and *CRKL* were purchased from Dharmacon, CO, USA. Silencing was proven not to affect cell viability and cell phenotype. ON-TARGET plus SMARTpool non-targeting siRNAs (Dharmacon, CO, USA) do not target any known gene in the cells and were used as negative control to distinguish sequence-specific silencing from non-specific effects. In addition, siGLO Green Transfection Indicator (Dharmacon, CO, USA) contains fluorescent (labelled with 6-FAM) oligonucleotide duplexes that localise to the nucleus thus was used to visually assess the transfection efficiency.

MiRNA mimics/ hairpin inhibitors and 100ng of overexpression plasmids/ 10nM of siRNAs were co-transfected into the cells, according to the protocols described in **Section 3.13.** The transfected cells were incubated in the CO_2 incubator at 37.0°C for 48 hours before evaluating the gene rescue effects by functional assays.

3.23 Experimental Animals

Wild type zebrafish adults (*Danio rerio*) were obtained and housed in the Zebrafish Laboratory (Association for Assessment and Accreditation of Laboratory Animal Care (AAALAC) accredited), Department of Biomedical Science, Faculty of Medicine, University of Malaya, under standard conditions (14 hours:10 hours light:dark cycle, regulated conductivity (500µS), pH (7.0) and temperature (28.0°C)), in a ZebTEC zebrafish housing system (Tecniplast, VA, Italy). Adults were fed twice with Hikari dry food pellets and once with live *Artemia salina* (brine shrimp) daily.

Eggs were obtained by random pairwise mating of zebrafish. Three adult males and four adult females were together placed in a 1L plastic breeding tank (Tecniplast, VA, Italy) the evening before eggs were required. The tank had a mesh across the

bottom so that the eggs can pass through the mesh to avoid them from being eaten by the adults. The eggs were harvested the following morning and transferred into 60mm × 15mm petri dish (Corning, NY, USA) containing system water. Eggs were washed four times with system water to remove debris. Further, unfertilised, unhealthy and dead embryos were identified under a Leica EZ4 dissecting microscope (Leica Microsystems, Wetzlar, Germany) and removed by selective aspiration with a Pasteur pipette (Sigma Aldrich, MO, USA). At 3.5 hours post fertilisation (hpf), embryos were again screened and any further dead and unhealthy embryos were removed. Embryos were incubated and allowed to develop in system water containing methylene blue (Sigma Aldrich, MO, USA) and transferred into system water added with 75μM N-Phenylthiourea (PTU) (Sigma Aldrich, MO, USA) beginning 1 day post fertilisation (dpf) to inhibit pigment formation (Karlsson, von Hofsten & Olsson, 2001). Throughout all procedures, the embryos and the solutions were kept at 28.5°C, in the incubator. Wild type zebrafish embryos (*Danio rerio*) at 2dpf were used in the subsequent experiments.

3.24 Animal Ethics Statement

All experimental procedures using zebrafish were performed according to protocol (#2015-160505/IBS/R/NHNP) approved by the Faculty of Medicine Institutional Animal Care and Use Committee (IACUC), University of Malaya.

3.25 *In Vivo* Metastasis Model

3.25.1 Cell Staining

A day following transfection with hsa-miR-378 hairpin inhibitors, hsa-miR-1827 mimics, negative hairpin inhibitors control and negative mimics control, A549-I7 cells in 6-well plate were labelled with 1,1'-Dioctadecyl-3,3,3',3'-Tetramethylindocarbocyanine Perchlorate (DiI) stain (Invitrogen, CA, USA), a lipophilic fluorescent tracking dye (red fluorescence; excitation: 549nm; emission:

565nm), that is stable for at least 2 weeks in live zebrafish. DiI is transferred from mother to daughter cells but not between other cells. Briefly, 20mg/mL DiI stock was diluted at 1:1000 in DPBS with calcium and magnesium. Medium in the well was removed and cells were washed gently with DPBS with calcium and magnesium. DiI labelling solution was added into the wells (2.00mL per well) and incubated in the CO_2 incubator at 37.0°C for 30 minutes. Medium containing the labelled tumour cells that become detached were collected and centrifuged at 1,000× g for 3 minutes and supernatant was discarded. Labelled cells were washed with DPBS with calcium and magnesium twice: 2.00mL of DPBS with calcium and magnesium was added to resuspend the cell pellet, centrifuged at 1,000× g for 3 minutes and supernatant was discarded. This step was repeated once again. Cells in the well were also gently washed twice with DPBS with calcium and magnesium and 2.00mL of fresh growth medium was added to the labelled cells, resuspended and added back into the corresponding well, followed by incubation in the CO_2 incubator at 37.0°C overnight.

3.25.2 Preparation of Embryos

Two-dpf zebrafish embryos were dechorionated using a pair of microsurgical forceps (Watchmaker #5) (Samco, Surrey, UK). The chorion was held with one forceps, and with the help of the other forceps, a tear was gently made in the chorion and the chorion was turned upside down to release the embryo. The embryos were rinsed thoroughly with system water at least 3-4 times to remove debris and transferred to fresh PTU water at 28.5°C.

3.25.3 Injection and Incubation

Cells were harvested and resuspended at a density of 2.0×10^5 cells/mL in medium containing 1.0% FBS. Cells were kept on ice and in dark before injection. The 2dpf albino embryos were anesthetised by transferring them into 10.0% benzocaine

water (Sigma Aldrich, MO, USA) 2 minutes before injection and they were aligned on the 1.0% agarose gel plate. Excessive water was removed with Pasteur pipette.

Using microloader (Eppendorf, Hamburg, Germany), 10.00µL of the cell suspension was loaded into a 20.0µm TransferTip (Eppendorf, Hamburg, Germany). The injection needle was connected to the Eppendorf FemtoJet and InjectMan NI 2 (Eppendorf, Hamburg, Germany). Aided by the fully automated Leica M205 A stereo microscope (Leica Microsystems, Wetzlar, Germany), the needle tip was pointed to the middle of the embryonic yolk sac region and gently inserted at an angle of 45°, injection pressure (P_i) of 80hPa, compensation pressure (P_c) of 35hPa and injection time (t_i) of 0.3 seconds, approximately 100 cells were injected into the yolk sac. This was first confirmed by dispensing cells onto a TruBond 360 adhesive microscope slide (Matsunami, WA, USA) and visually counting. The yolk was chosen as the injection site, because it could retain a large number of injected cells (up to approximately 300 cells or more) without expulsion and could support cell proliferation. In addition, the migration of xenografted cells into the vasculature from the yolk was not likely to occur by passive transport (Lee *et al.*, 2005; Haldi *et al.*, 2006).

After injection, embryos were rinsed gently with system water, transferred into fresh PTU water and maintained at 28.5°C for 1 hour. A sharp needle cut in the yolk would reclose with little to no loss of contents. After confirmation of visible fluorescent cell mass localised at the injection site under the fully automated Leica DMI6000 B inverted fluorescence microscope (Leica Microsystems, Wetzlar, Germany), embryos were transferred to a 37.0°C incubator. Fish with fluorescent cells outside the implantation area at 2 hours post injection (hpi) were excluded from further analysis.

3.25.4 Image Acquisition and Analysis

At 24hpi, living zebrafish embryos were anesthetised using 10.0% benzocaine water and mounted with VECTASHIELD (Vector Laboratories, CA, USA). A cover slip (Marienfeld-Superior, Baden-Wurttemberg, Germany) was placed on top of the embryo and the edges of the cover slip were sealed with nail polish. The glass slide was kept in a horizontal position in the dark until the nail polish dried and serial sections were captured using Leica TCS SP5 II confocal microscope (Leica Microsystems, Wetzlar, Germany) at low magnification (5×) (excitation: 543nm; emission: 550-640nm) to analyse the tumour cells dissemination pattern throughout the body of the fish. The open source Fiji (Fiji is Just ImageJ) software package (National Institutes of Health, NIH, MD, USA) (Schindelin *et al.*, 2012) was used to quantify the number of cells that have left the yolk sac as a measure of metastasis. The cells remaining in the yolk sac were masked off and eliminated, and the number of cells in the fish body was used as an estimate of the metastatic capability of the cells. A 190-255 fluorescence intensity threshold was set to select cells and the 'analyse particle' tool was used with default selection of cell size and cell shape during counting. A Fiji macro was generated using the 'record' function to streamline analyses and remove bias. As illustrated in Figure 3.1, cancer cell burden per embryo was determined by multiplying the mean area of all red tumour cell clusters by the total number of red objects (area × objects). Migration was quantified by measuring the distance between each cell cluster and the site of implantation (SOI) and averaged for all the clusters within one embryo (van der Ent *et al.*, 2015).

3.26 Whole-mount Alkaline Phosphatase (ALP) Vessel Staining

Briefly, the 24hpi zebrafish embryos were euthanised with an overdose of benzocaine and fixed in 4.0% (w/v) paraformaldehyde (PFA) (Sigma Aldrich, MO,

USA) at 4.0°C overnight, followed by 5-6 washes in PBS with 0.1% Tween-20 (PBST, pH 7.0). Fixed embryos were dehydrated and made permeable in 5-minute successive washes of 25.0%, 50.0% and 75.0% methanol in PBST, and finally suspended in 100% methanol. Subsequently, serial rehydration of the embryos was done in 75.0%, 50.0% and 25.0% methanol in PBST for 5 minutes each and rinsed twice for 5 minutes in PBST. The embryos were then equilibrated with ALP buffer (100mM NaCl, 100mM Tris-HCl, pH 9.5, 50mM $MgCl_2$, 0.1% Tween 20) at room temperature for 30 minutes, followed by incubation in staining solution (110µg/mL NBT, 55µg/mL BCIP in ALP buffer) (Sigma Aldrich, MO, USA) at 37.0°C until the required staining was attained (30 minutes). The reaction was stopped with 5-6 rinses of stop buffer (0.25mM EDTA in PBST, pH 5.5). The embryos were fixed in 4.0% PFA at room temperature for 20 minutes, rinsed twice for 5 minutes in PBST and finally mounted with 80.0% glycerol (Fisher Scientific, MA, USA). The embryos were photographed using the stereo microscope and Fiji was used to analyse the length of ectopic vessels (Ridley *et al.*, 2003).

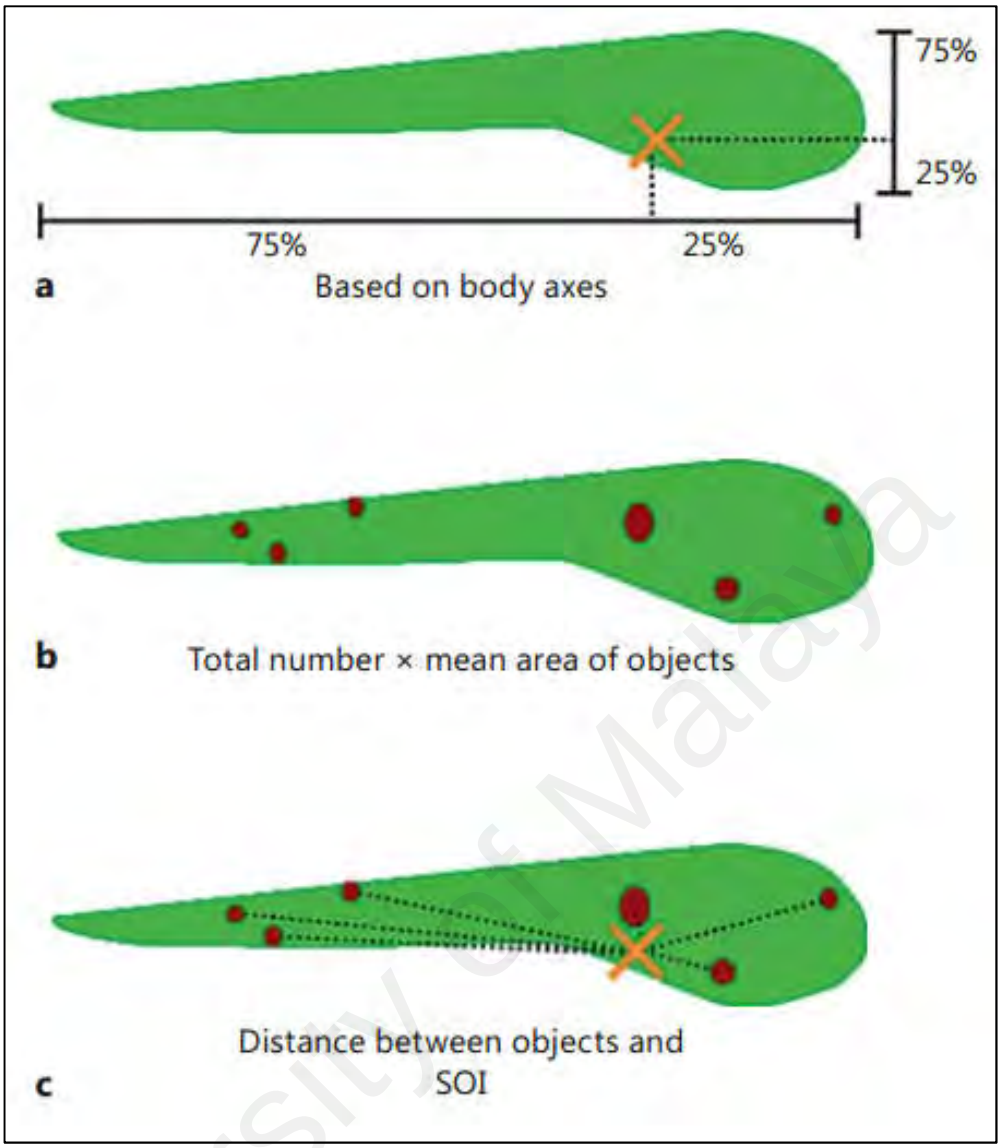

Figure 3.1: Schematic diagram explaining quantitative image analysis of metastasis in zebrafish embryo (Figure reproduced with permission from van der Ent *et al.*, 2015).

3.27 Statistical Analyses

All experiments were performed at least three times and data are expressed as mean ± standard error of mean (SEM). The statistical significance of the differences between two groups of data was evaluated using Student's *t*-test. *P*-value < 0.05 (*) and *P* < 0.01 (**) were considered statistically significant.

CHAPTER 4: GENERATION OF NSCLC SUB-CELL LINES WITH DISTINCT CELL INVASION AND MIGRATION PROPERTIES

Owing to the genetic instability that is present within a tumour, populations with different characteristics can be isolated. This chapter describes the generation of NSCLC sub-cell lines with distinct metastatic properties, from their parental A549 and SK-LU-1 cells.

A549 cells were derived from human alveolar cell carcinoma and show features consistent with bronchogenic carcinoma (Giard *et al.*, 1973). They share many characteristics with human primary alveolar epithelial cells due to the presence of lamellar bodies and surfactant proteins (Lieber *et al.*, 1976), thus are widely studied as model of lung cancer (Shin *et al.*, 2009; Wang *et al.*, 2009c). A549 have occupational clumps of columnar cells and are mucin-positive. They are fast growing with high anchorage-independent growth capacity (Goldsmith *et al.*, 1991).

SK-LU-1 cells are undifferentiated and exhibit no specific features of epithelial differentiation. They are mucin-negative. SK-LU-1 are slow growing with low anchorage-independent growth capacity (Goldsmith *et al.*, 1991). They have *TP53* (tumour protein p53) mutation in exon 8 at codon 193 (Loprevite *et al.*, 1997).

Both A549 and SK-LU-1 express FGF2 at amounts significantly lower than in control human lung fibroblasts (Goldsmith *et al.*, 1991). In addition, both cells contain *KRAS* mutation at codon 12 (Loprevite *et al.*, 1997).

4.1 Cell Line Authentication

It is estimated that one-third of all cell lines used in the life sciences are misidentified and cell line misidentification and contamination have profound effects on time and outcome in research (Hughes *et al.*, 2007; Capes-Davis *et al.*, 2010). Therefore,

it is important to perform cell line authentication before selecting for sub-cell lines. A549 and SK-LU-1 were sent for DNA fingerprinting by STR profiling. Fifteen autosomal STR loci and the gender identity locus amelogenin were profiled. STR profiling detects the presence of STRs that exist at variable lengths within the human genome. By amplifying using fluorescence-tagged primers and electrophoresing in a sequencing gel, the precise length of each allele is determined and compared with size standards and controls. The identification software then assigns a number to each allele at that locus (Figure 4.1 and Figure 4.2).

When compared to ATCC reference database, 80% similarity is the threshold for declaring match (Masters *et al.*, 2001; Lorenzi *et al.*, 2009). A complete match was found for both sample number 4CH-9059-0 and 4CH-9052-0, indicating that they are A549 and SK-LU-1, respectively (Table 4.1 and Table 4.2).

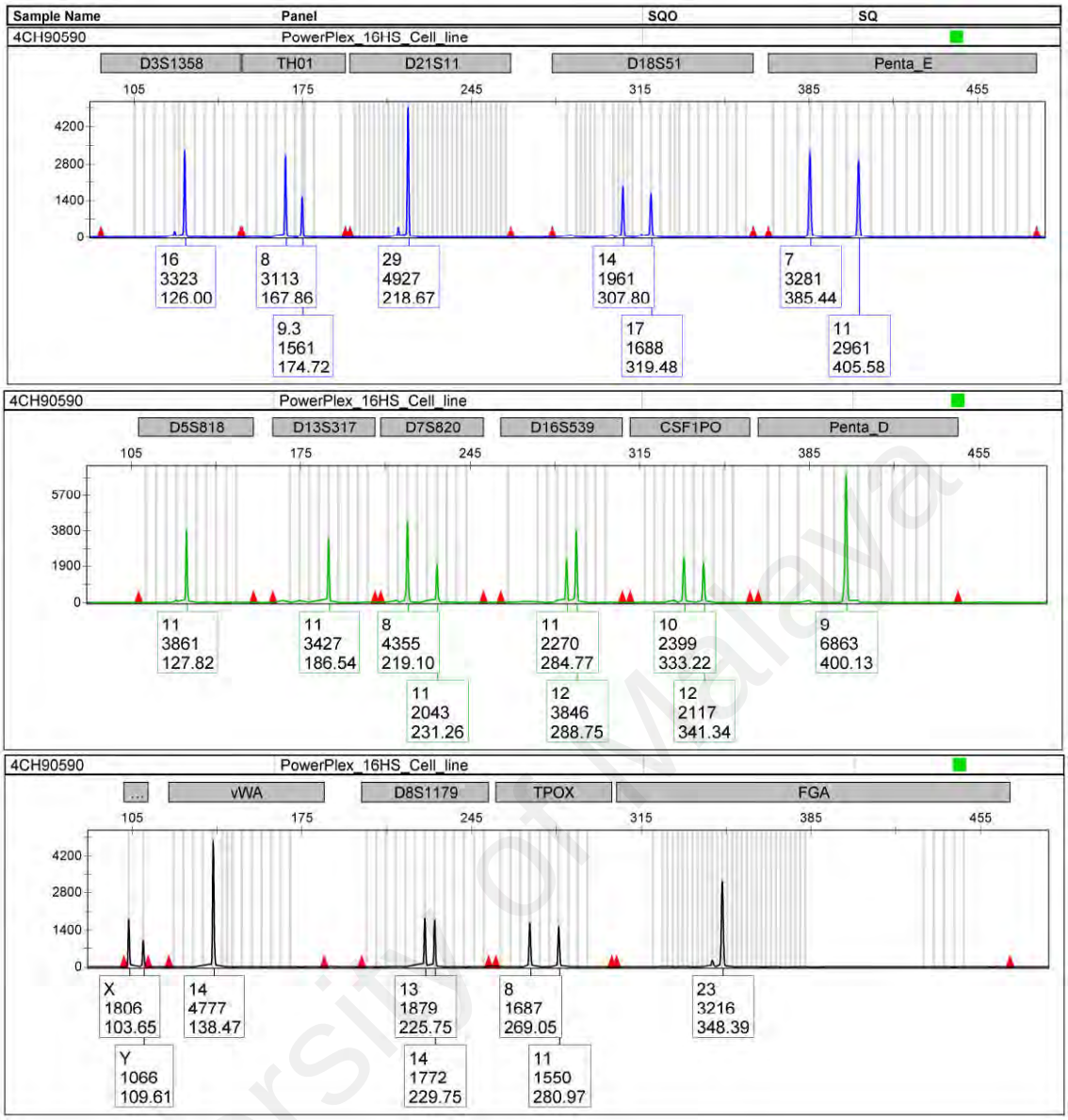

†Row 1 in the boxes represents the number of repeats along the fragment; Row 2 indicates the relative fluorescence units (RFU); Row 3 designates the size of the fragment in base pairs determined based on the sizing curve from the internal size standard.

Figure 4.1: Electropherogram of A549 generated by capillary electrophoresis with base pair size on one axis and RFU on the other.

Table 4.1: The sample genotype was compared to a standard genotype published by ATCC. The genotypes matched and the identity of the A549 cell line was confirmed.

	A549 (ATCC CCL-185)	A549 (ID 4CH-9059-0)
D7S820	8, 11	8, 11
vWA	14	14
D5S818	11	11
D13S317	11	11
D16S539	11, 12	11, 12
TH01	8, 9.3	8, 9.3
TPOX	8, 11	8, 11
CSF1PO	10, 12	10, 12
AMEL	X, Y	X, Y

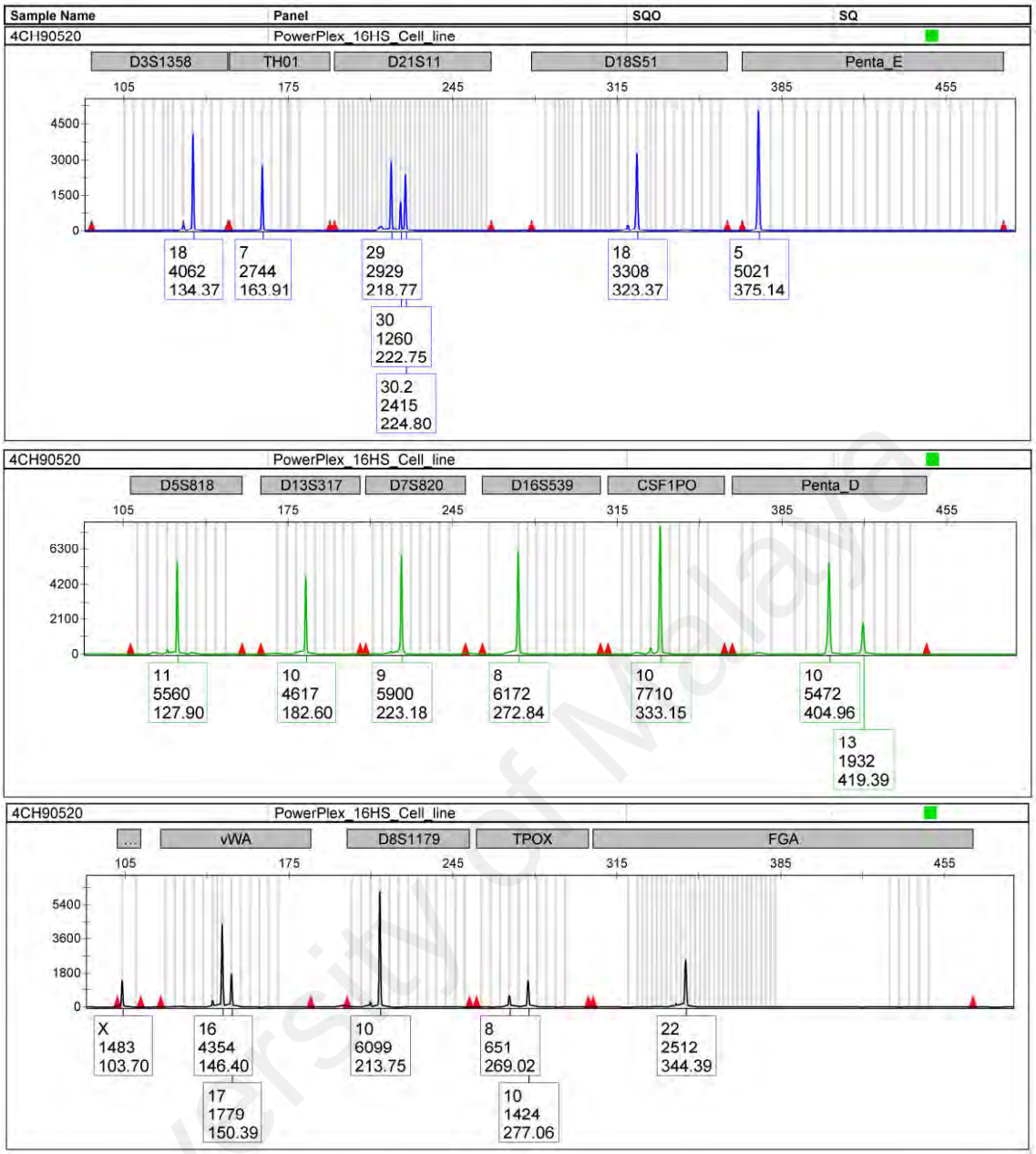

†Row 1 in the boxes represents the number of repeats along the fragment; Row 2 indicates the relative fluorescence units (RFU); Row 3 designates the size of the fragment in base pairs determined based on the sizing curve from the internal size standard.

Figure 4.2: Electropherogram of SK-LU-1 submitted for identification.

Table 4.2: Comparison between STR profiles of tested cell line and its ATCC reference cell line. The identity of the SK-LU-1 cell line was confirmed.

	SK-LU-1 (ATCC HTB-57)	SK-LU-1 (ID 4CH-9052-0)
D7S820	9	9
vWA	16, 17	16, 17
D5S818	11	11
D13S317	10	10
D16S539	8	8
TH01	7	7
TPOX	8, 10	8, 10
CSF1PO	10	10
AMEL	X	X

4.2 Selected NSCLC Sub-cell Lines are Distinct in Their Invasion Abilities

To establish a lung cancer metastasis cell model, serial selection was carried out on A549 and SK-LU-1 using transwell invasion assay. After a 48 h incubation period, cells that have invaded Matrigel were collected as I1, signifying one passage through the basement membrane matrix, while NI1 denotes one passage remained in the medium in the upper chamber. Subsequently, these cells were regrown and repeatedly passed six more times through the invasion selection procedure. The cells harvested from each subsequent round of selection were designated as I2/ NI2, I3/ NI3, I4/ NI4, I5/ NI5, I6/ NI6 and I7/ NI7, respectively. The invasion properties of high invasive sub-cell lines (A549-I7 and SK-LU-1-I7) and low invasive sub-cell lines (A549-NI7 and SK-LU-1-NI7) were validated with transwell invasion assay. The invasive potential was determined based on the cells' ability to invade Matrigel that contained mainly laminin and type IV collagen, the major components of the basement membrane. The growth on Matrigel mimics the cells contact with the basement membrane.

As this study is a continuation from the previous Master's project, A549-I7 and A549-NI7 had been established and their invasion, migration and cell proliferation properties had also been examined (Yap S. H., MSc. thesis, 2012). An increased number of invaded A549-I7 cells were observed compared to A549-NI7 cells (Figure 4.3A). A549-I7 has a 3-fold greater ability to invade through the Matrigel-coated transwell membrane insert compared to A549-NI7 with a *P*-value of 0.023 (Figure 4.3B).

Similarly, a significant increase in the invasion of SK-LU-1-I7 cells into Matrigel was seen compared to SK-LU-1-NI7 cells (Figure 4.4A). SK-LU-1-I7 is 4-fold more invasive than SK-LU-1-NI7 (Figure 4.4B).

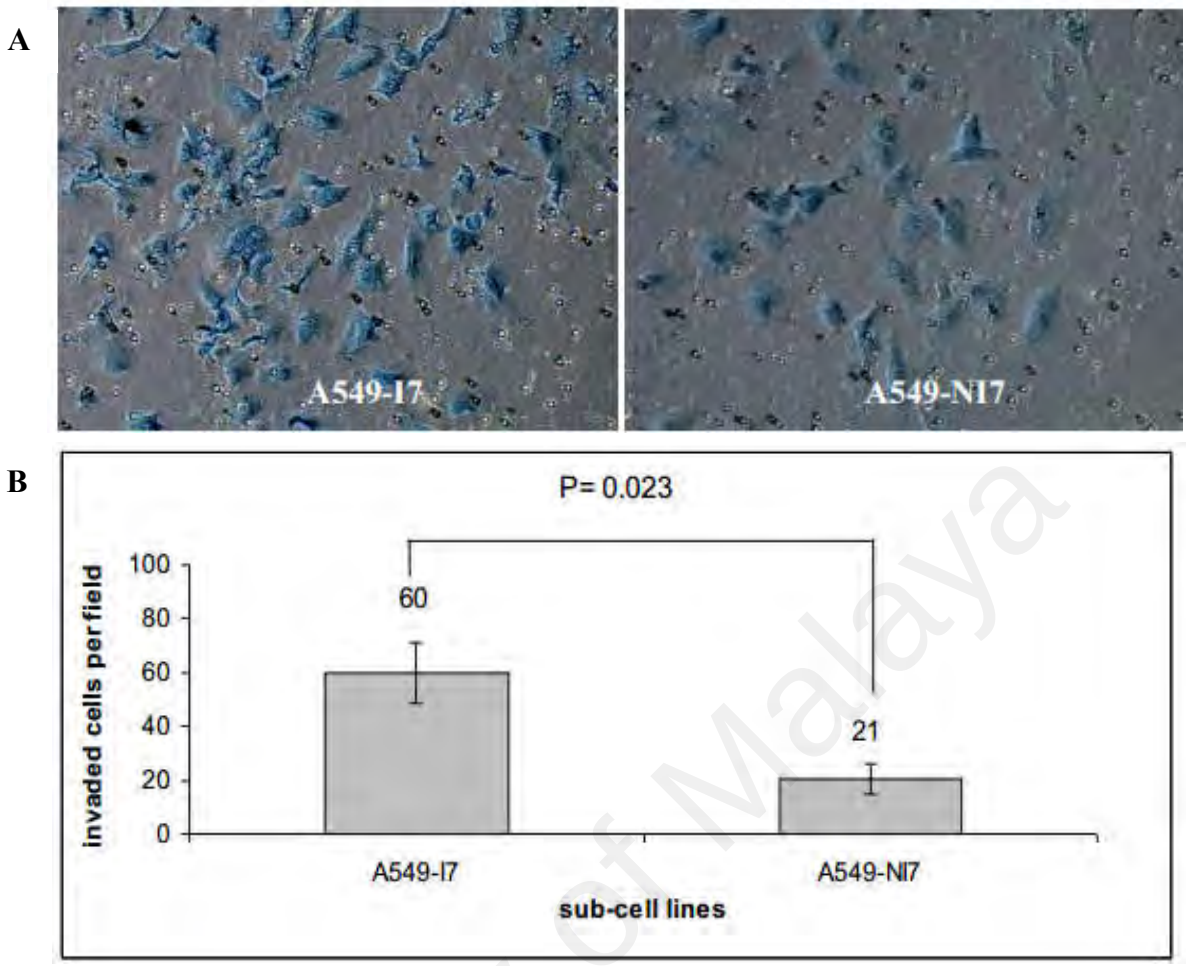

Figure 4.3: Comparison of invasion abilities of high and low invasive A549. (A) Representative cell fields of methylene blue-stained invaded cells on the bottom membrane of Matrigel transwell invasion insert for A549-I7 and A549-NI7 at 200× magnification (Figure from Yap S. H., MSc. thesis, 2012). **(B)** A bar graph representing the average invaded cells per field of A549-I7 and A549-NI7 with data presented as mean ± SEM with *P*-value < 0.05 (Figure from Yap S. H., MSc. thesis, 2012).

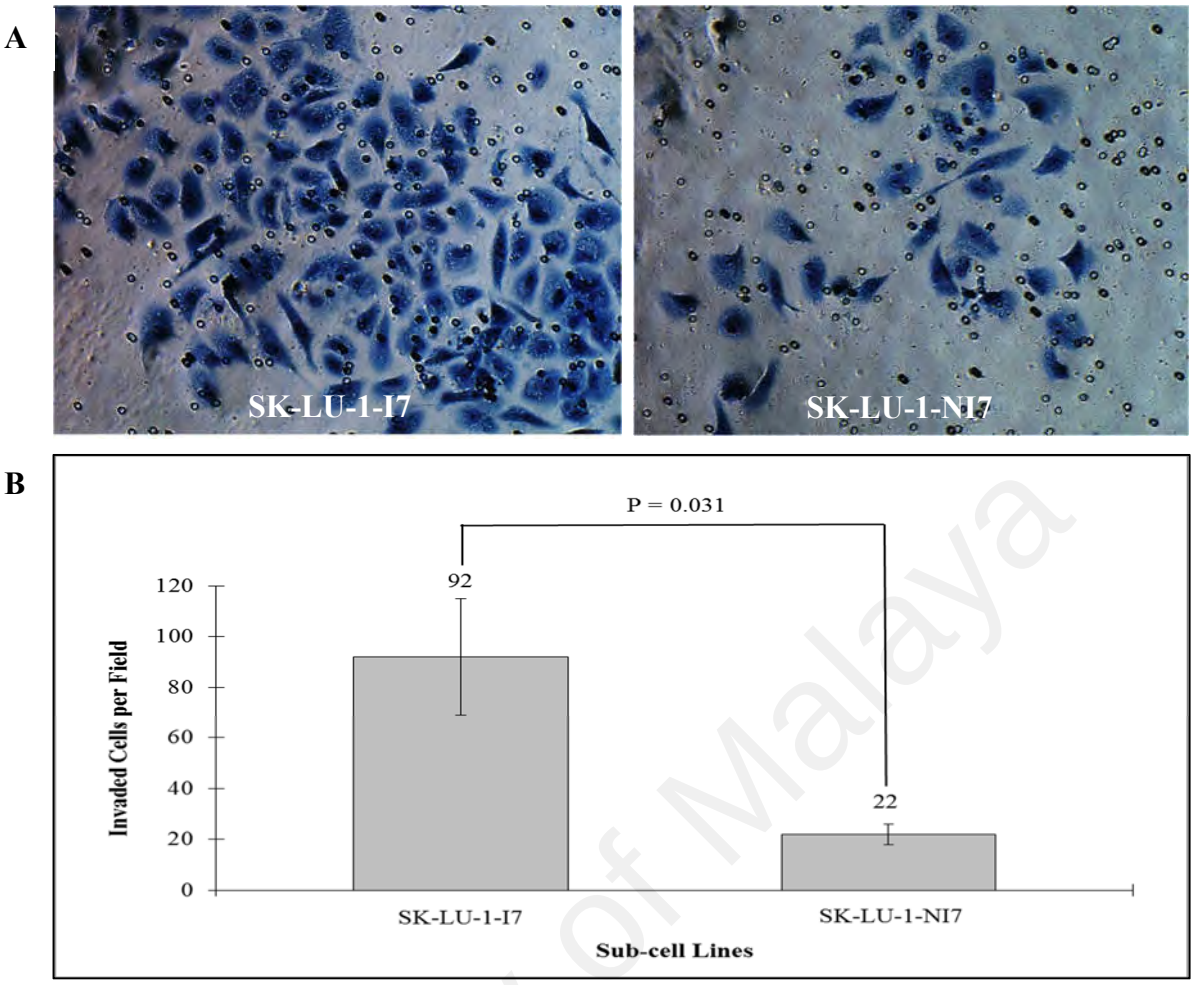

Figure 4.4: SK-LU-1-I7 is about four times more invasive than SK-LU-1-NI7. (A) Transwell invasion assay measures cell invasiveness. Images were captured at a magnification of 200×. **(B)** The number of cells that invaded to the lower chamber was counted (Mean ± SEM, $P < 0.05$).

4.3 Selected NSCLC Sub-cell Lines are also Distinct in Their Migratory Potentials

Cell migration is also an essential step in metastasis. Therefore, it is necessary to examine whether an increase in the cell invasiveness is accompanied by an elevation in the cell migration ability. To achieve this, wound healing assay was performed. It is a generally used experimental model for cell polarisation and directional cell migration. It is favoured over other types of physical exclusion methods because mechanical scratching may release more growth factors from the damaged cells and replacement with fresh growth medium after scratching helps to control the factors available to cells for migration, thus mimicking the cellular microenvironment during metastasis. The collective cell migration probed by this assay is also similar to that in cancer metastasis,

known as sheet migration (Pouliot *et al.*, 2000; Lecomte *et al.*, 2011; Fujisawa *et al.*, 2012; Hai *et al.*, 2012).

A549-I7 cells were observed to close the scratch wound faster than A549-NI7 cells at 28 h time point (Figure 4.5A). A549-I7 has a 3-fold greater migration ability compared to A549-NI7 with a *P*-value of 0.003 (Figure 4.5B).

Likewise, SK-LU-1-I7 cells grew into the gap at significantly higher rate than SK-LU-1-NI7 cells at 28 h (Figure 4.6A). SK-LU-1-I7 exhibits 4-fold enhanced migratory potential compared to SK-LU-1-NI7 (Figure 4.6B).

4.4 Cell Proliferation Rates are Consistent across NSCLC Parental and Sub-cell Lines

The goal of performing serial selection is to isolate the high invasive cells from the low invasive counterparts within the parental population, solely based on their intrinsic metastatic potentials, without affecting cell proliferation. As such, growth rates of the parental and sub-cell lines were measured. The number of viable cells on the log phase of the growth curve (Day 4) was used to calculate the doubling time.

Consistent cell proliferation rates between A549, A549-I7 and A549-NI7, as well as between SK-LU-1, SK-LU-1-I7 and SK-LU-1-NI7 were observed, with a doubling time of approximately 19 hours and 31 hours, respectively (Figure 4.7 and Figure 4.8).

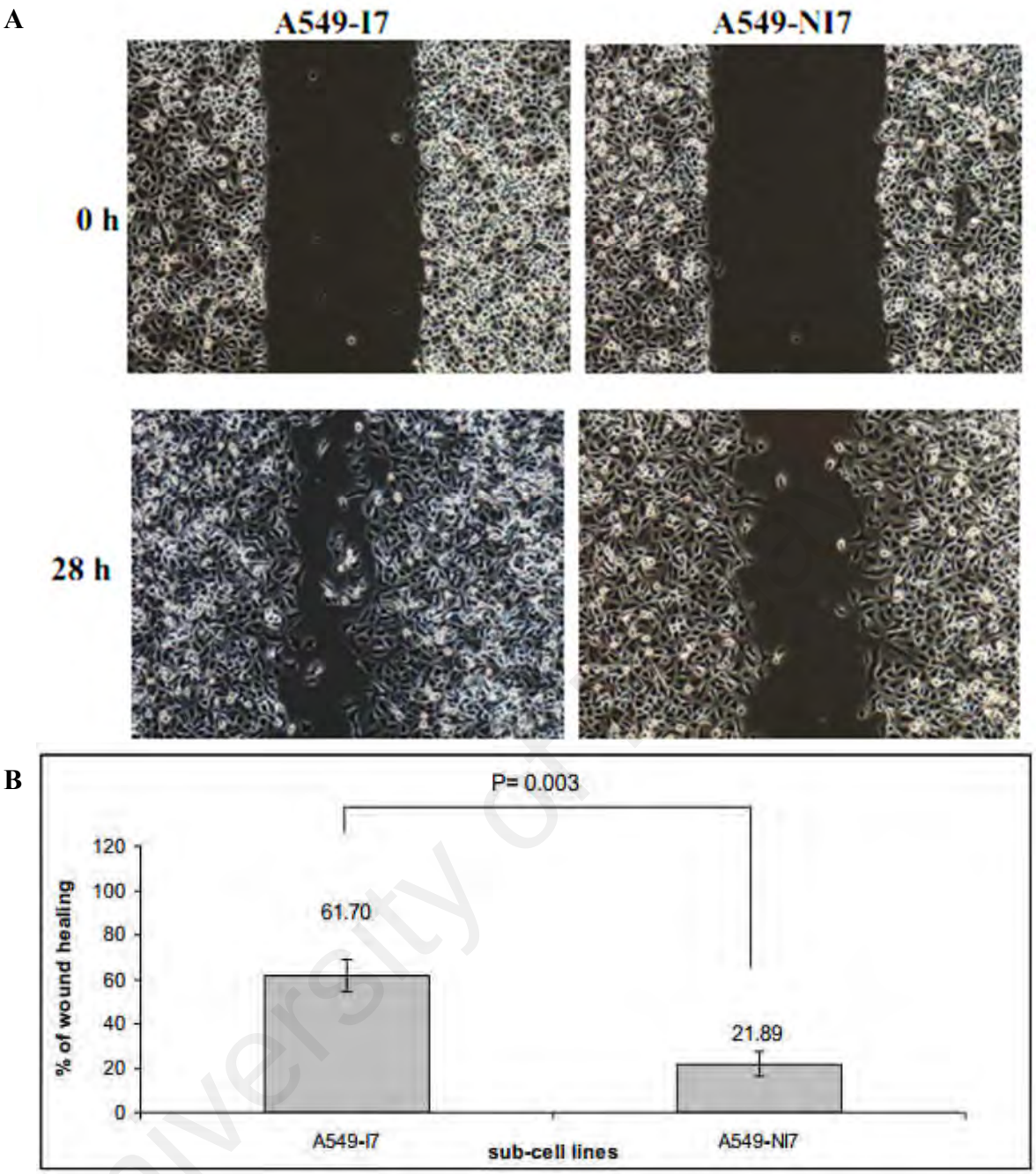

Figure 4.5: Evaluation of migratory potentials of high and low invasive A549. (A) Migration of A549-I7 and A549-NI7 cells into the wound was captured at 0 h and 28 h at 100× magnification (Figure from Yap S. H., MSc. thesis, 2012). **(B)** A bar chart representing the percentage of wound healing for A549-I7 and A549-NI7 with data presented as mean ± SEM (Figure from Yap S. H., MSc. thesis, 2012).

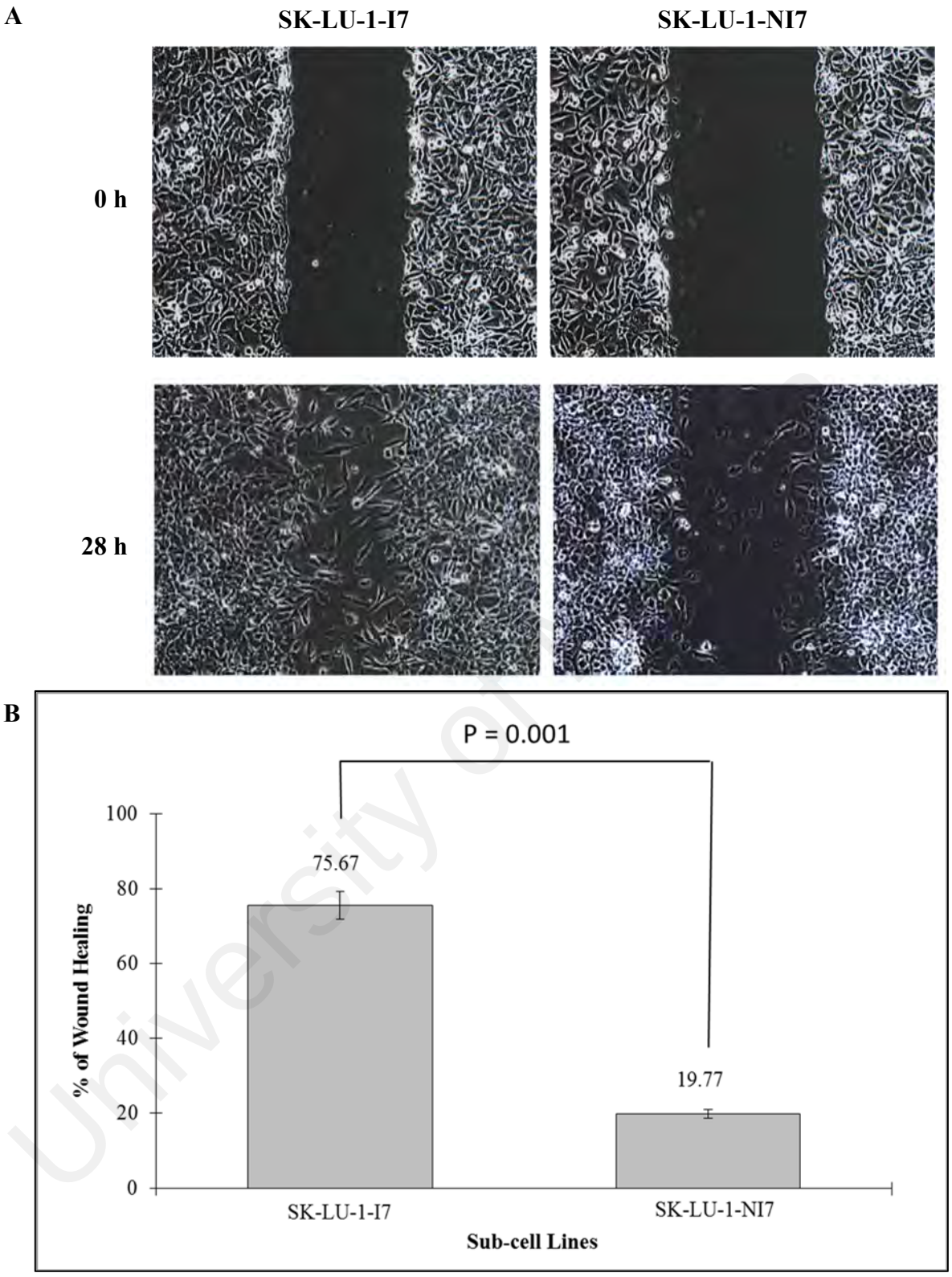

Figure 4.6: SK-LU-1-I7 healed the scratch wound nearly four times faster than SK-LU-1-NI7. (A) Phase micrographs of SK-LU-1-I7 and SK-LU-1-NI7 cells at 0 h and 28 h after monolayer wounding. **(B)** Quantification of cell migration. The distance of wound correlates to cell migration ability (Mean ± SEM, $P < 0.01$).

A

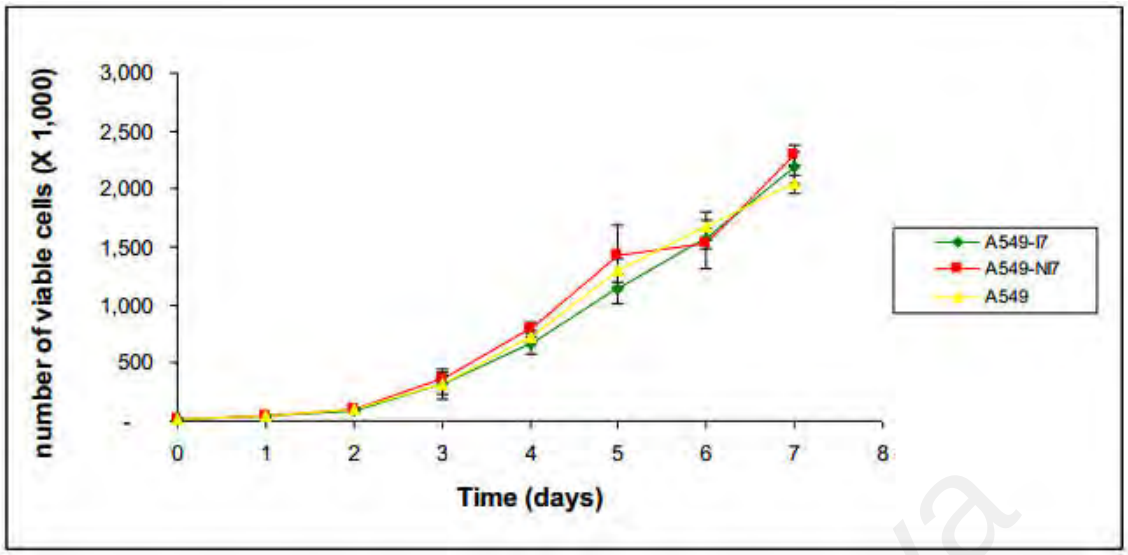

B

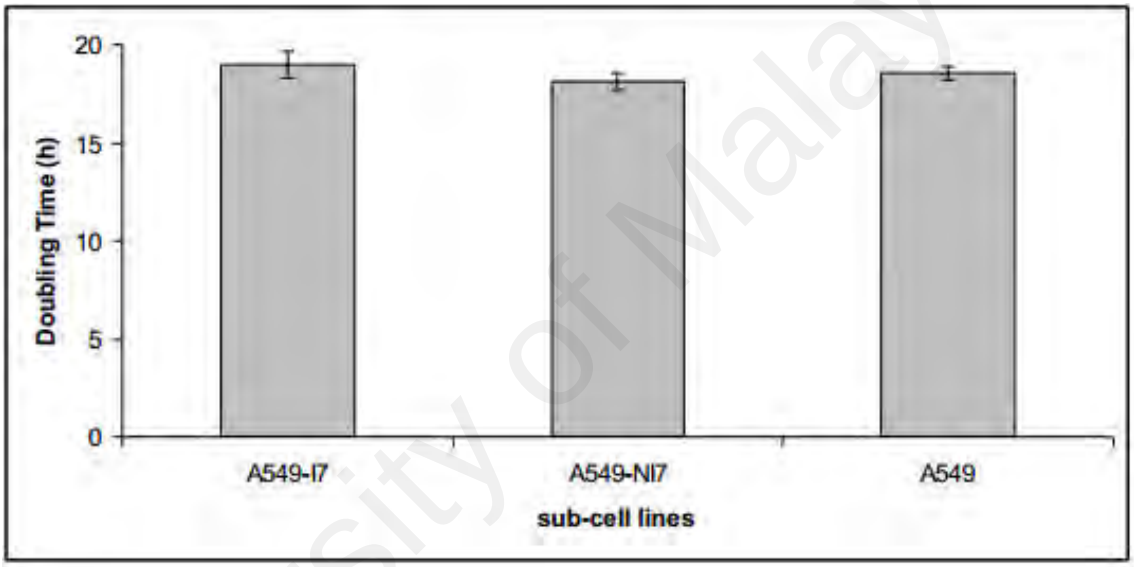

Figure 4.7: Measurement of growth rates among the three A549 cell lines. (A) Cell proliferation curve for A549, A549-I7 and A549-NI7 over 7 days with the number of viable cells on each day presented as mean ± SEM (Figure from Yap S. H., MSc. thesis, 2012). **(B)** A bar chart representing the doubling time (h) for A549, A549-I7 and A549-NI7 (Figure from Yap S. H., MSc. thesis, 2012).

A

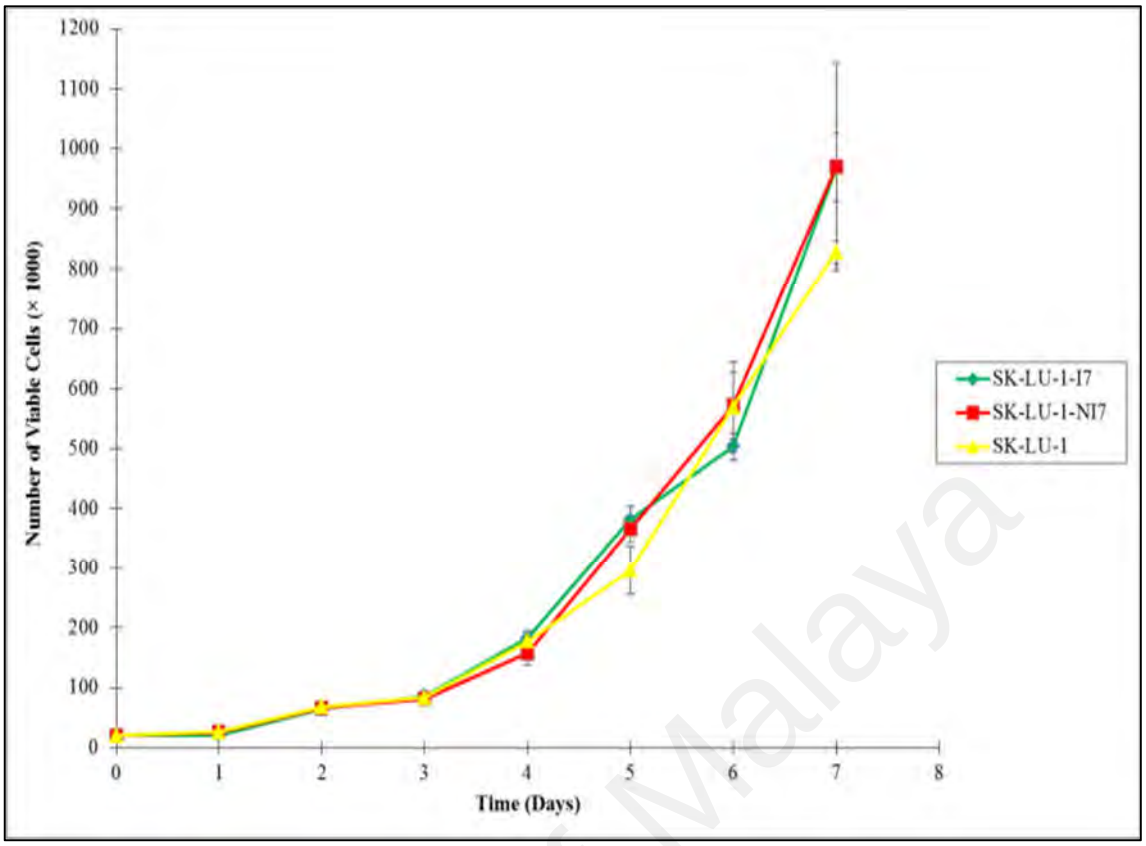

B

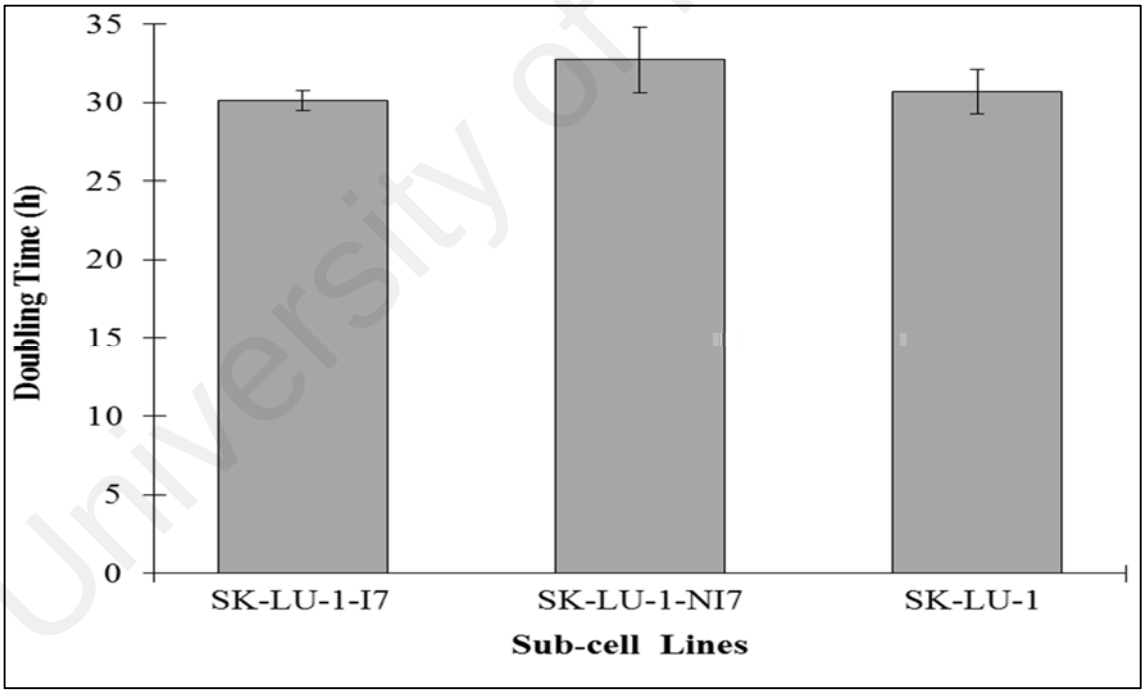

Figure 4.8: SK-LU-1, SK-LU-1-I7 and SK-LU-1-NI7 proliferate at the same rate. **(A)** Cell growth curve constructed for SK-LU-1, SK-LU-1-I7 and SK-LU-1-NI7 by counting viable cells using trypan blue dye exclusion. **(B)** Doubling time was obtained using data from (A).

4.5 Summary

In summary, progressive isolation of A549 and SK-LU-1 parental populations generated sub-cell lines with significantly distinct metastasis-relevant traits, specifically cell invasion and migration. A549-I7 cells are 3-fold more invasive and able to migrate further than A549-NI7 cells, while SK-LU-1-I7 cells show 4-fold higher invasion and migratory abilities compared to SK-LU-1-NI7 cells. The rounds of selection excluded a bias of invasion and migration assays by an additional effect on cell proliferation because all the parental and sub-cell lines proliferate at the same rate, with a doubling time of 19 hours for A549 and 31 hours for SK-LU-1. Generally, SK-LU-1 grow slower compared to A549. These results suggest that the metastatic behaviour of lung cancer cells can be characterised with serial transwell invasion assay, and that the properties of these high and low invasive cells can be clonally studied.

CHAPTER 5: IDENTIFICATION AND CHARACTERISATION OF METASTASIS-RELATED MIRNAS IN NSCLC

As discussed in Chapter 2.0, metastasis is a highly selective process that favours the outgrowth and survival of a metastatic sub-population that pre-exists within the heterogeneous primary tumour (Fidler & Kripke, 1977). Therefore, comparative studies of phenotypes expressed in non-metastatic and metastatic cancer cells will be helpful for the identification of genes responsible for the acquisition of favoured phenotypes leading to tumour metastatic behaviour (Fidler, 1973; Seftor *et al.*, 1990).

Following the isolation of high and low invasive cells in Chapter 4.0, the global miRNA expression in both paired A549 sub-cell lines was examined on a miRNA microarray platform. Based on a fold change of ≥ 2.00 as the threshold for gene expression, a total of eleven human miRNAs were short listed as being significantly (*P*-value ≤ 0.05) differentially expressed between A549-I7 and A549-NI7. Among the eleven metastasis-related miRNAs, four of them are miRNA* (Table 5.1).

Table 5.1: Differentially expressed metastasis-related miRNAs between A549-I7 and A549-NI7 with *P*-value ≤ 0.05 and fold change ≥ 2.00 filtering using Partek® Genomics Suite™ software (Table from Yap S. H., MSc. thesis, 2012).

miRNA Expression in A549-I7	microRNAs	Fold change † (A549-I7/A549-NI7)	*p*-value
Up-regulated	miR-378	3.389	0.033
	miR-671-5p	2.852	0.001
	miR-25*	2.840	0.050
	miR-92b	2.600	0.004
	miR-106b*	2.500	0.011
	miR-550*	2.280	0.046
Down-regulated	miR-629*	-2.915	0.007
	miR-576-3p	-2.780	0.038
	miR-886-5p	-2.538	0.013
	miR-487b	-2.231	0.001
	miR-1827	-2.142	0.004

† *Positive values denote up-regulation; negative values denote down-regulation.*

Four miRNAs (miR-92b, miR-378, miR-671-5p and miR-1827) were chosen for further investigation as these miRNAs were less extensively studied at the point when the MSc. project first started. Their expression were validated in A549 sub-cell lines using RT-qPCR. When compared to A549-NI7, miR-92b, miR-378 and miR-671-5p were significantly up-regulated while miR-1827 was significantly down-regulated in A549-I7 (Figure 5.1). Their expression were correlated to corresponding expression patterns from miRNA microarray (Figure 5.2).

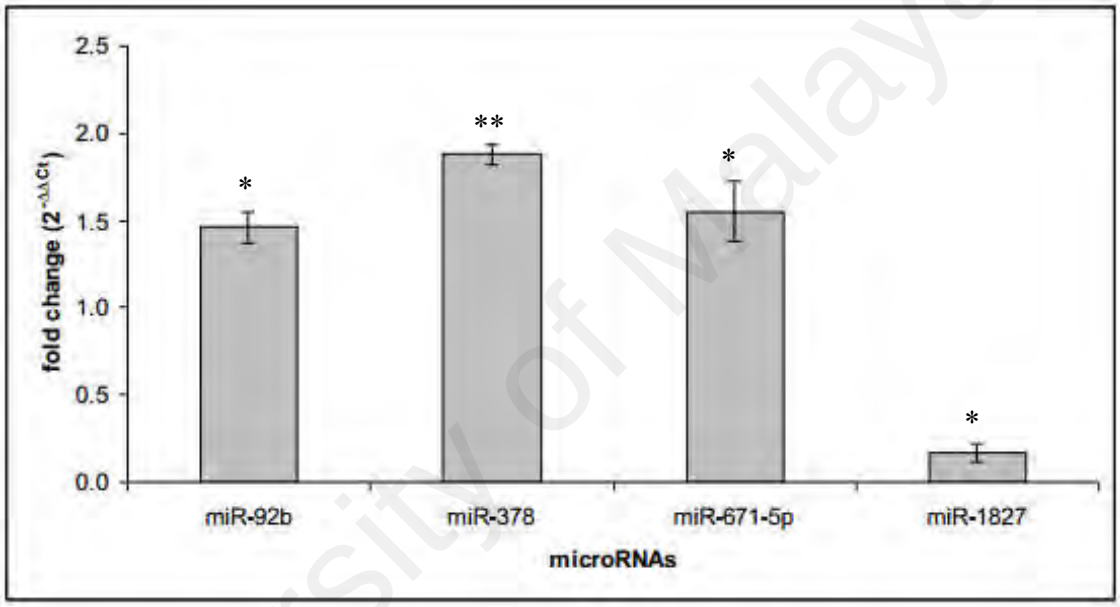

Figure 5.1: Four differentially expressed miRNAs (miR-92b, miR-378, miR-671-5p and miR-1827) between A549-I7 and A549-NI7 were validated using RT-qPCR (Figure from Yap S. H., MSc. thesis, 2012). * $P < 0.05$, ** $P < 0.01$

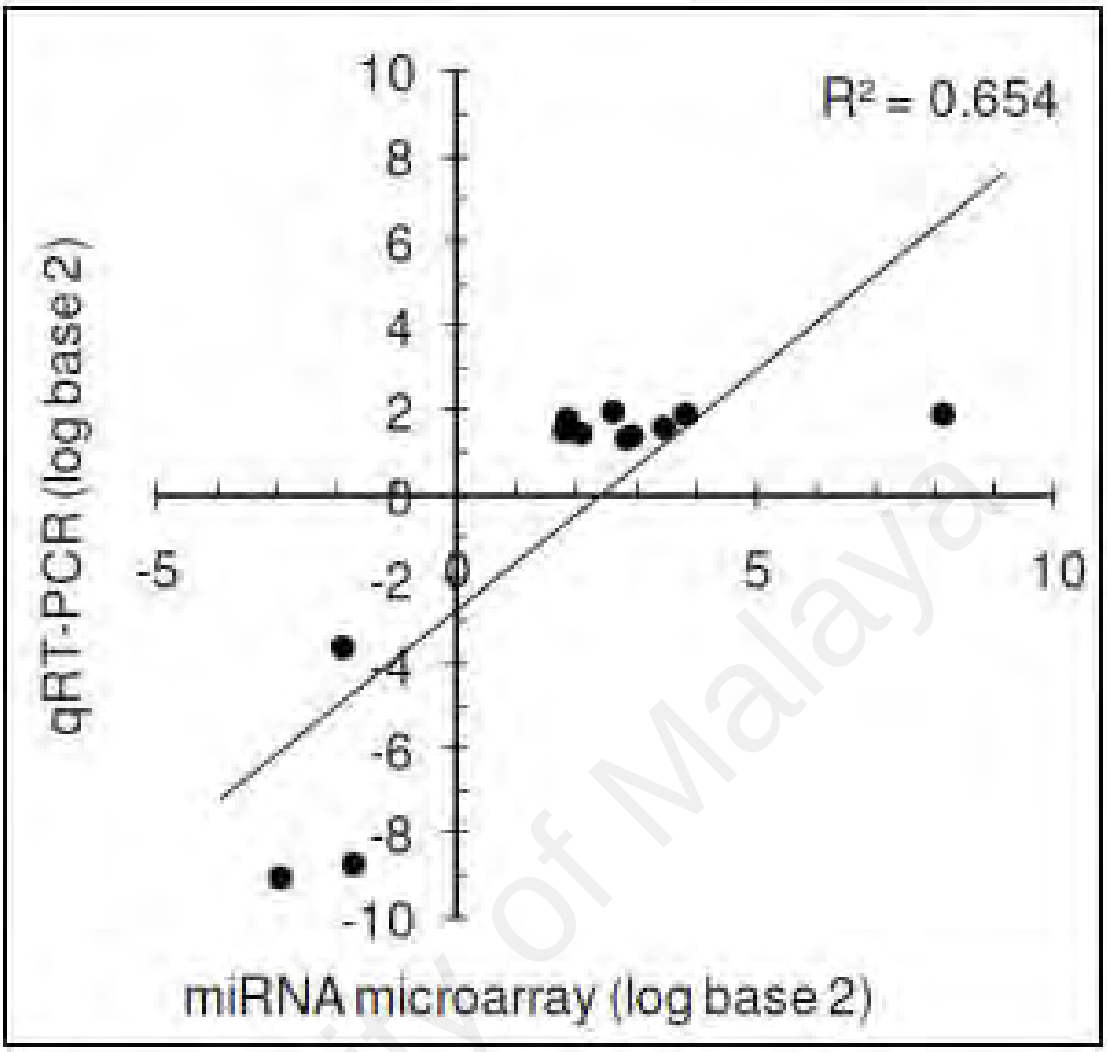

Figure 5.2: A Pearson's correlation plot between miRNA microarray and RT-qPCR data (Figure from Yap S. H., MSc. thesis, 2012).

5.1 MiR-671-5p was Down-regulated in SK-LU-1-I7

To better represent metastasis-related miRNAs in NSCLC, these miRNAs were also validated in SK-LU-1 sub-cell lines using RT-qPCR. Unfortunately, only three miRNAs shared a similar expression with A549-I7, in which miR-671-5p was down-regulated in SK-LU-1-I7 instead of being up-regulated, indicating that miR-671-5p is not a suitable marker in describing metastasis in NSCLC (Figure 5.3). Hence, only miR-92b, miR-378 and miR-1827 were selected for downstream studies.

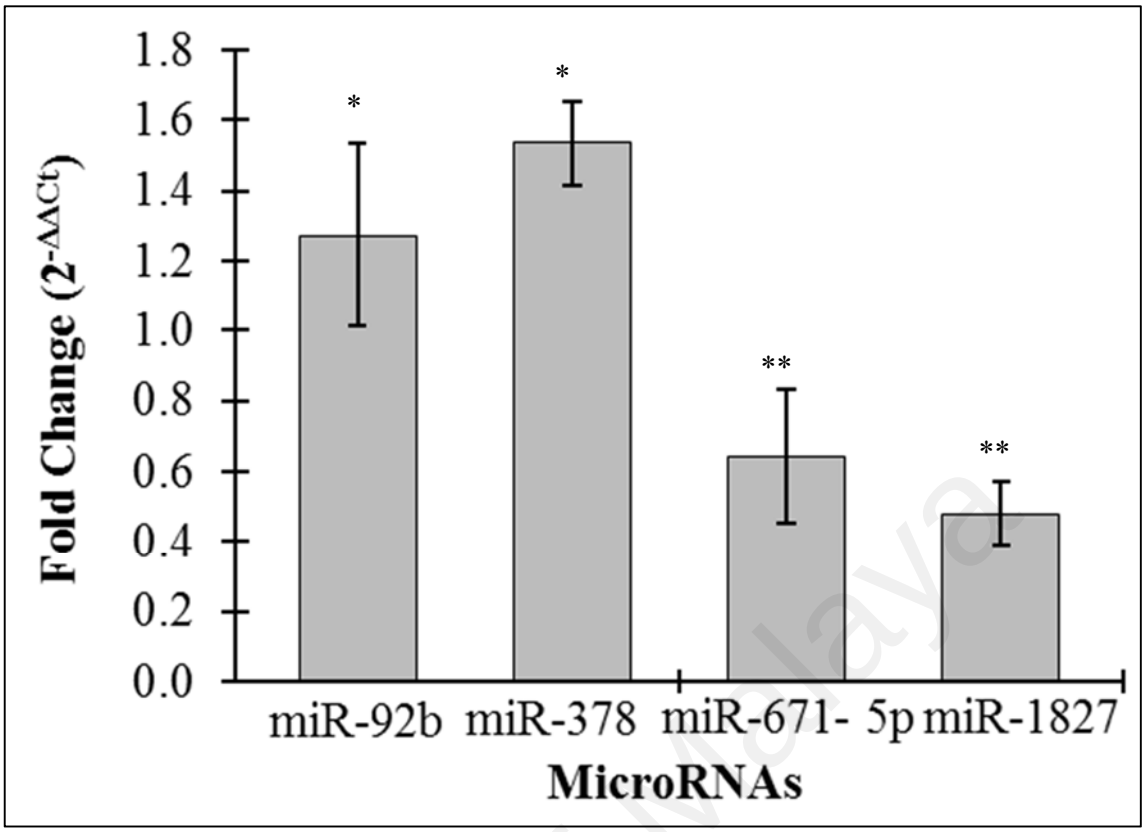

Figure 5.3: The expression of miR-92b and miR-378 were elevated while miR-671-5p and miR-1827 were reduced in SK-LU-1-I7 in comparison to SK-LU-1-NI7. * $P < 0.05$, ** $P < 0.01$

5.2 MicroRNAs Biological Function(s) in Metastasis and Angiogenesis in NSCLC

Given that miR-92b and miR-378 were significantly up-regulated while miR-1827 was significantly down-regulated in high invasive cells, it was hypothesised that by increasing the levels of miR-92b and miR-378 and decreasing the level of miR-1827, low invasive cells may become more aggressive. Thus, overexpression and knockdown studies were carried out by introducing miRNA mimics or hairpin inhibitors and the effects on cell invasiveness and mobility were examined. Since angiogenesis is eventually induced during metastasis as described in Chapter 2.0, the effect on angiogenesis was also assessed.

5.2.1 MiR-92b does not Regulate NSCLC Cell Invasion, Migration and Angiogenesis

A549-NI7 and SK-LU-1-NI7 were first transfected with miR-92b mimics or hairpin inhibitors and their miR-92b expression levels were measured by RT-qPCR after 24 hours. As shown in Figure 5.4, the transfection of miRNA mimics significantly increased the level of miR-92b by more than 8-fold, while miRNA hairpin inhibitors significantly decreased more than 4-fold of the endogenous miR-92b in the low invasive cells.

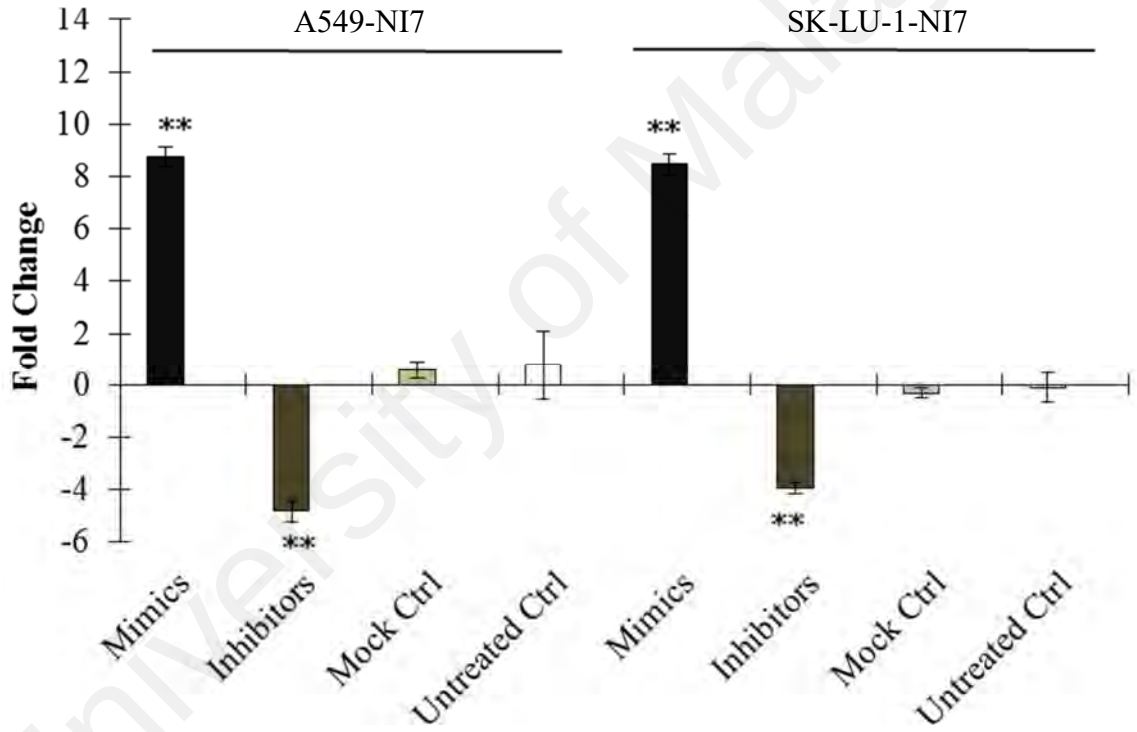

Figure 5.4: Expression and knockdown of miR-92b in A549-NI7 and SK-LU-1-NI7. Cells were transfected with 80nM negative mimics control/ miR-92b mimics or 80nM negative inhibitors control/ miR-92b hairpin inhibitors. Mock control contained only transfection reagent. 24 hours later the cells were harvested and RT-qPCR was performed. The expression was normalised to corresponding negative control. ** $P <$ 0.01 by Student's *t*-test.

To test whether these alterations in the miRNA level had any effects on the cell invasion, transwell invasion assay was conducted. The invasion of both A549-NI7 and SK-LU-1-NI7 cells were not significantly changed by the transfection of miR-92b mimics or hairpin inhibitors (Figure 5.5).

Subsequently, wound healing assay was applied to determine the migratory potential of transfected low invasive cells, and it was also observed that except for miR-92b hairpin inhibitors-treated A549-NI7, no other transfected cells exhibited significant enhanced or reduced migration rates compared to the negative controls (Figure 5.6).

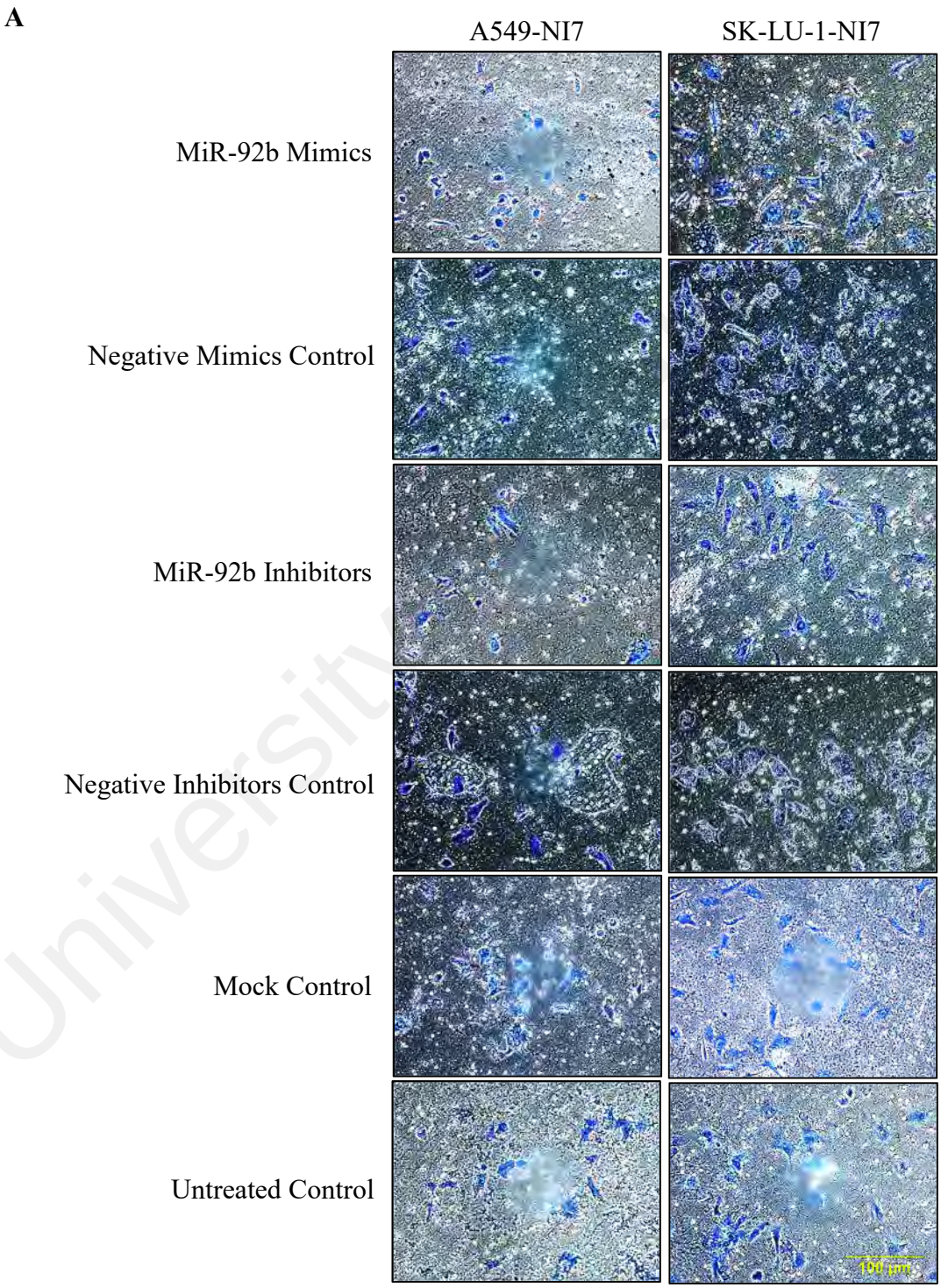

Figure 5.5: MiR-92b mimics and hairpin inhibitors treatment had minimal effect on cell invasion. (A) Representative images of A549-NI7 and SK-LU-1-NI7 cells transfected with either negative mimics control/ miR-92b mimics or negative inhibitors control/ miR-92b hairpin inhibitors. Mock control contained only transfection reagent.

B

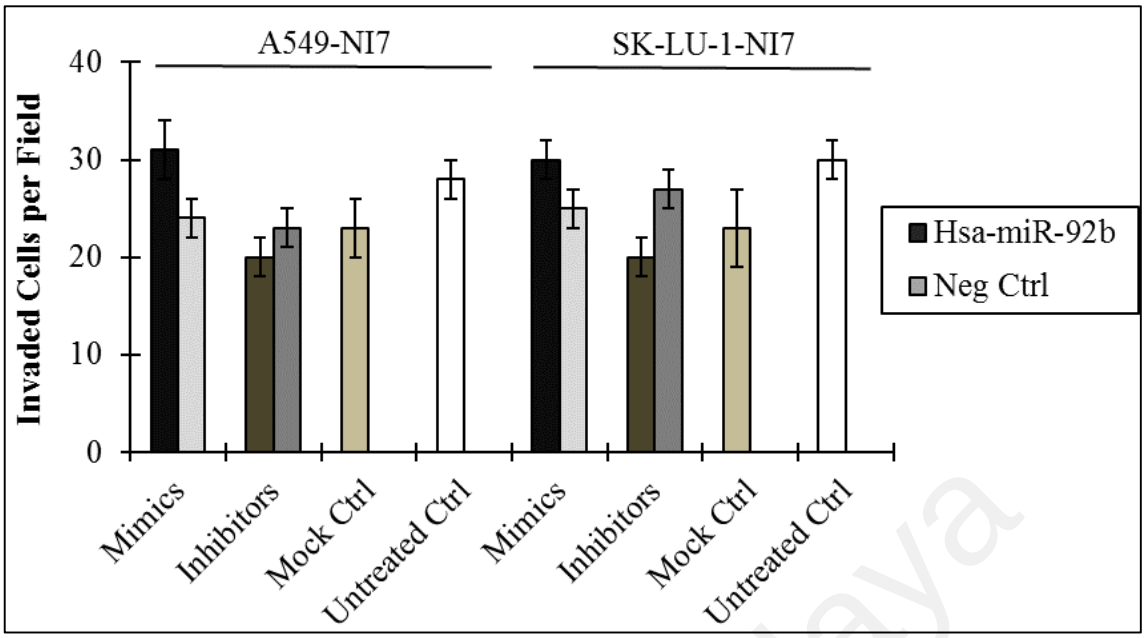

Figure 5.5, continued: (B) Bar graph depicts mean ± SEM of number of invaded cells per field taken from 8 random microscopic fields at 200× magnification.

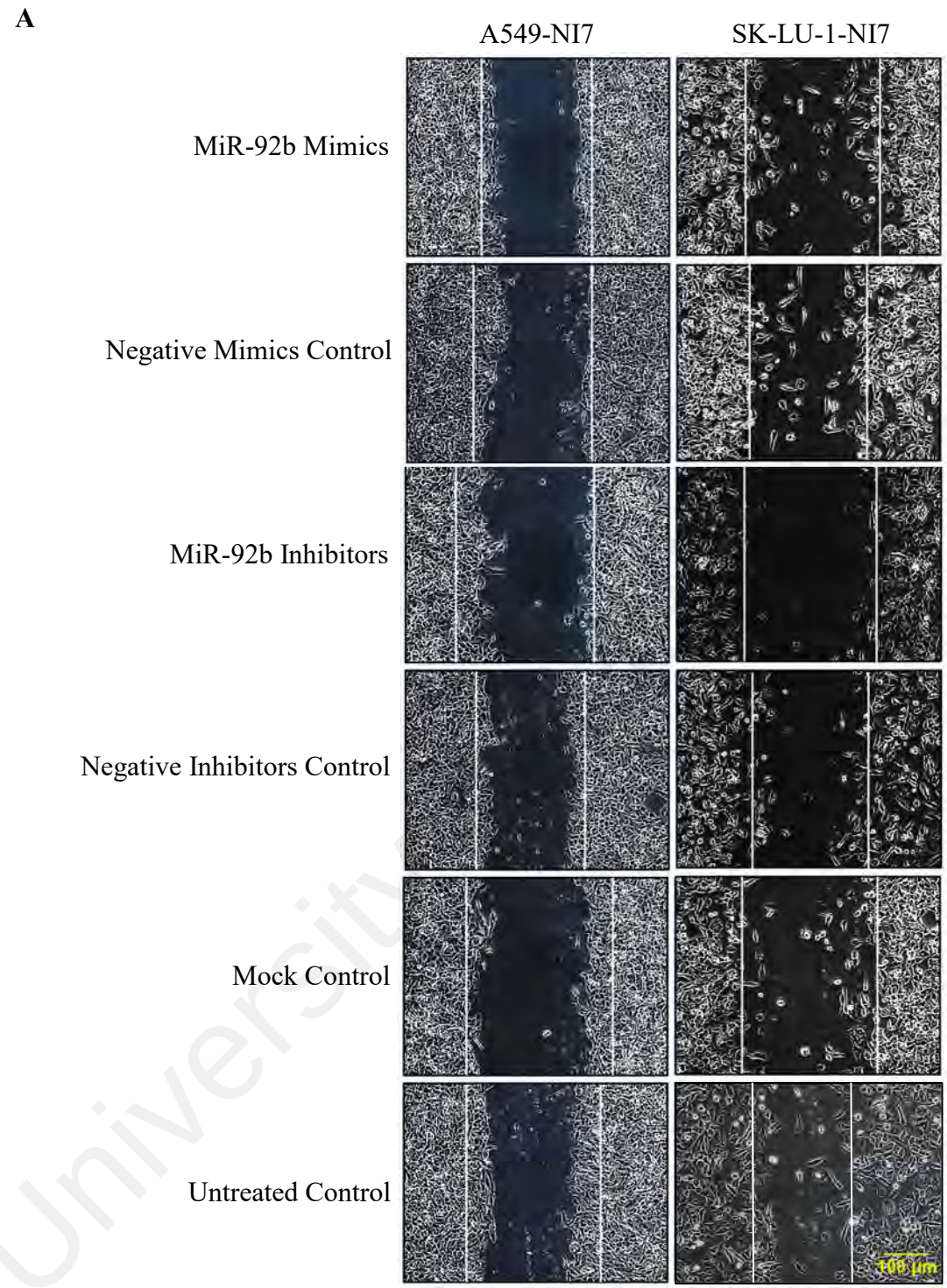

Figure 5.6: Role of miR-92b in NSCLC cell migration. (A) Representative images of wound healing assay (magnification, 100×), white lines illustrate the initial gap distance at 0 h.

B

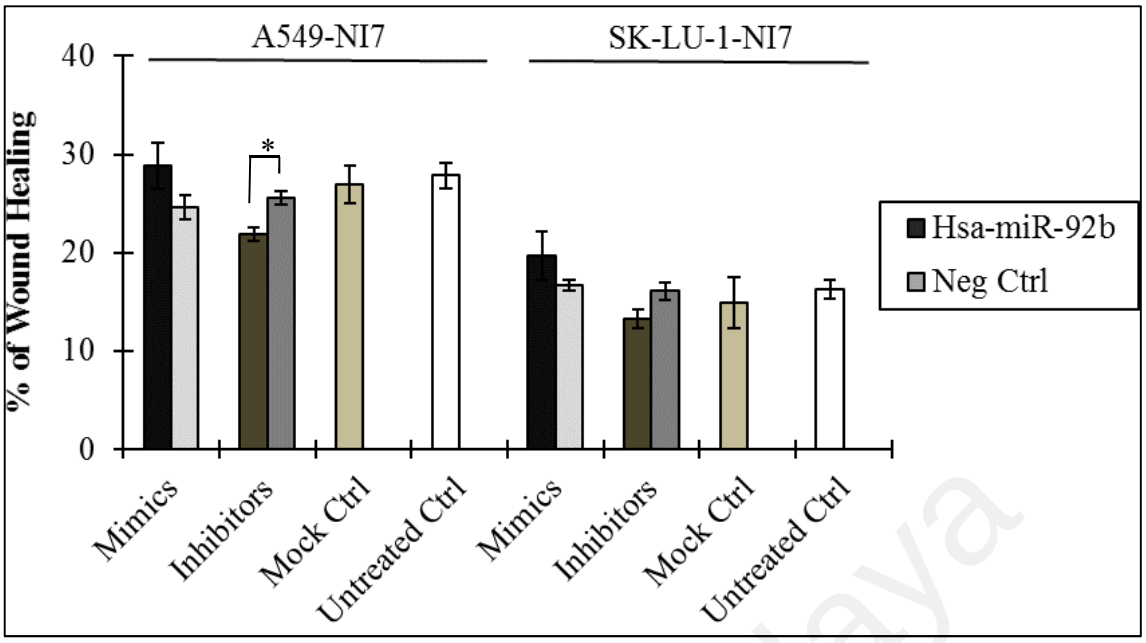

Figure 5.6, continued: (B) Quantification of cell migration for A549-NI7 and SK-LU-1-NI7 was determined after transfection with miRNA control, miR-92b, anti-miR control and anti-miR-92b. * $P < 0.05$

To study the role of miR-92b in tumour angiogenesis, TCM were collected from cells transfected with negative mimics control, miR-92b mimics, negative inhibitors control and miR-92b hairpin inhibitors at 24 h and were used to culture HUVEC. No statistically significant differences in the number of branching points and tubes were observed between the transfection groups, except for the cells treated with TCM from miR-92b hairpin inhibitors-transfected SK-LU-1-NI7 (Figure 5.7).

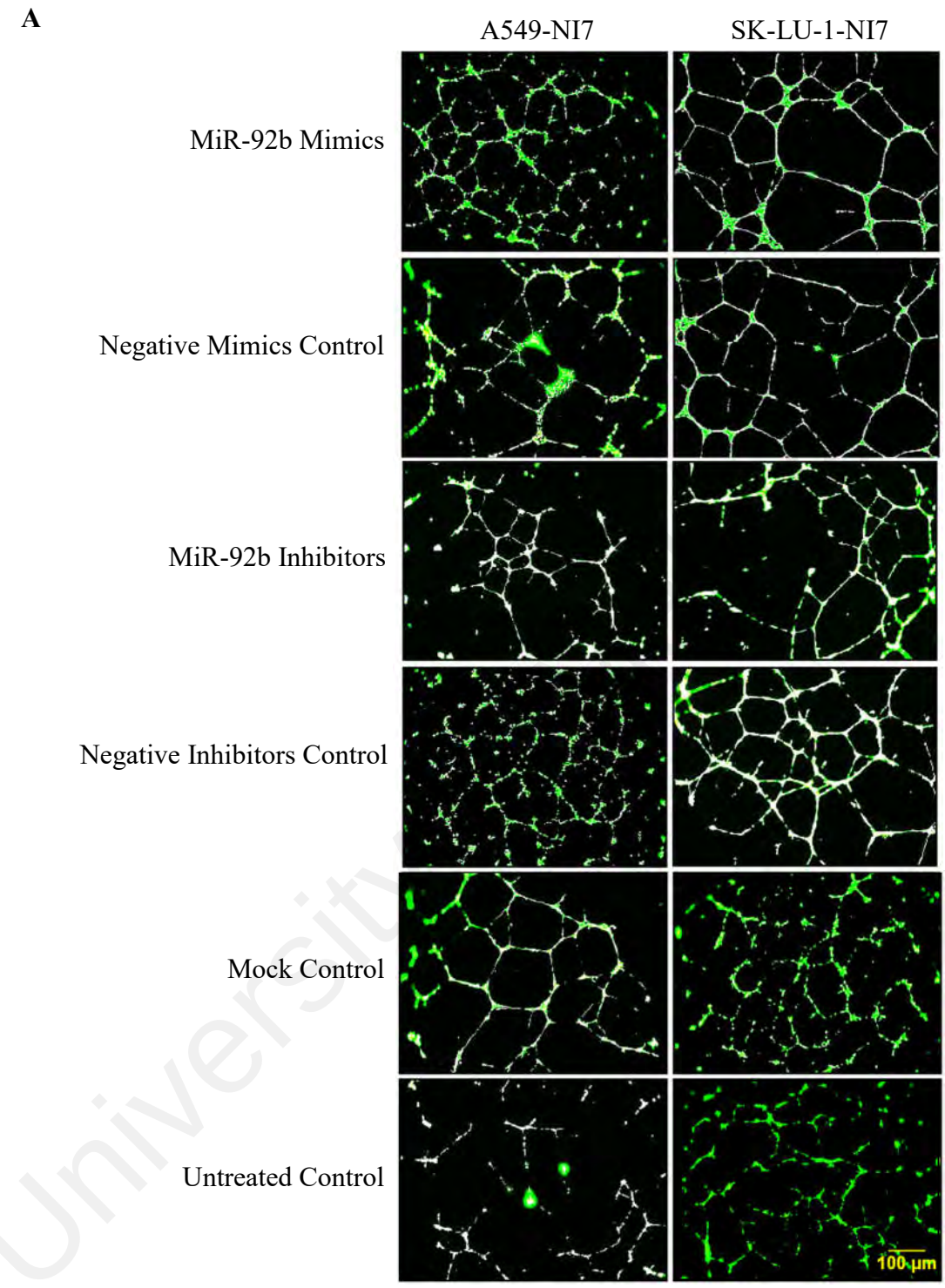

Figure 5.7: Effects of overexpression and knockdown of miR-92b on angiogenesis. **(A)** Tube formation potential was assessed 15 hours after exposure to conditioned media collected from A549-NI7 and SK-LU-NI7 cells treated with negative mimics/ inhibitors control or miR-92b mimics/ hairpin inhibitors. Representative images are shown.

B

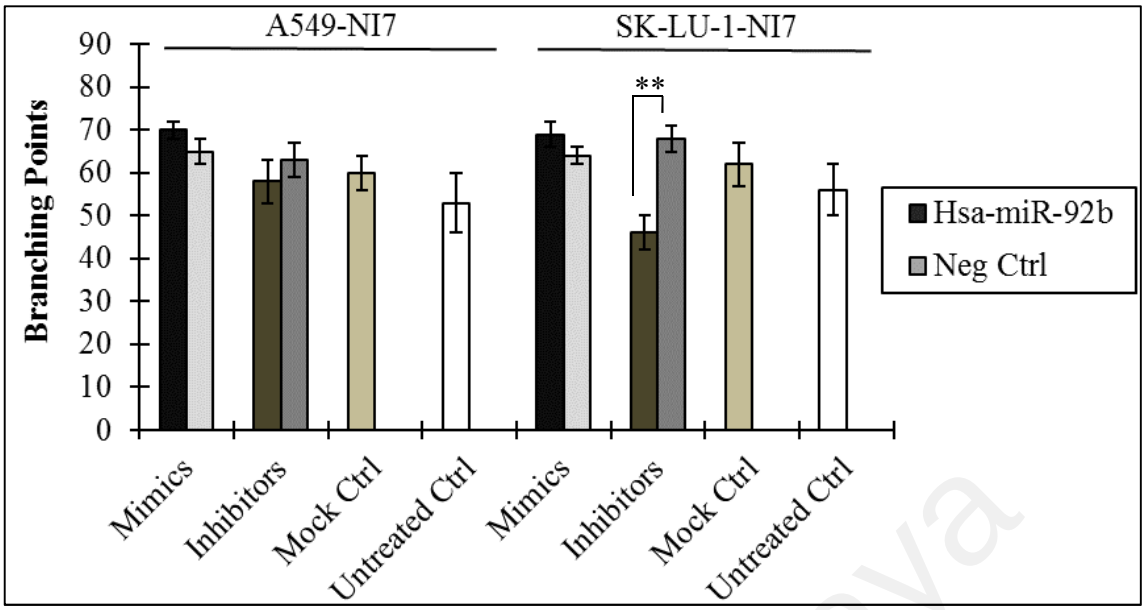

C

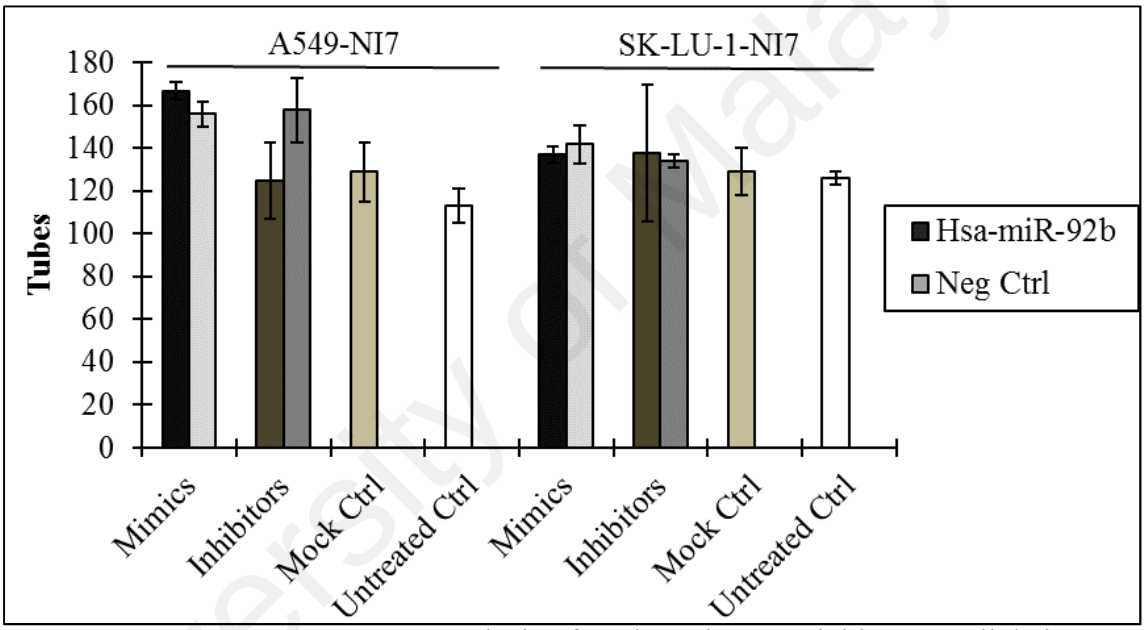

Figure 5.7, continued: (B), (C) Analysis of angiogenic potential in NI7 cells/miR-NC, NI7 cells/miR-92b mimics or NI7 cells/anti-miR-92b, expressed as number of branching points and number of tubes. Values are the mean ± SEM of three replicates. ** $P < 0.01$ compared to negative control.

5.2.2 MiR-378 Modulates NSCLC Cell Invasion and Angiogenesis but not Cell Migration

To examine the effects of miR-378 on invasion and migration of NSCLC cells, miR-378 mimics and hairpin inhibitors were introduced followed by transwell invasion and wound healing assays. Compared to negative controls, when low invasive cells were transfected with miR-378 mimics, miR-378 expression was significantly elevated by approximately 11- to 15-fold (Figure 5.8). This increase was seen to result in a

significantly higher ability to invade through the Matrigel (Figure 5.9). This is in accordance with the phenotype exhibited by high invasive cells, suggesting that miR-378 is one of the master regulators of NSCLC cell invasion.

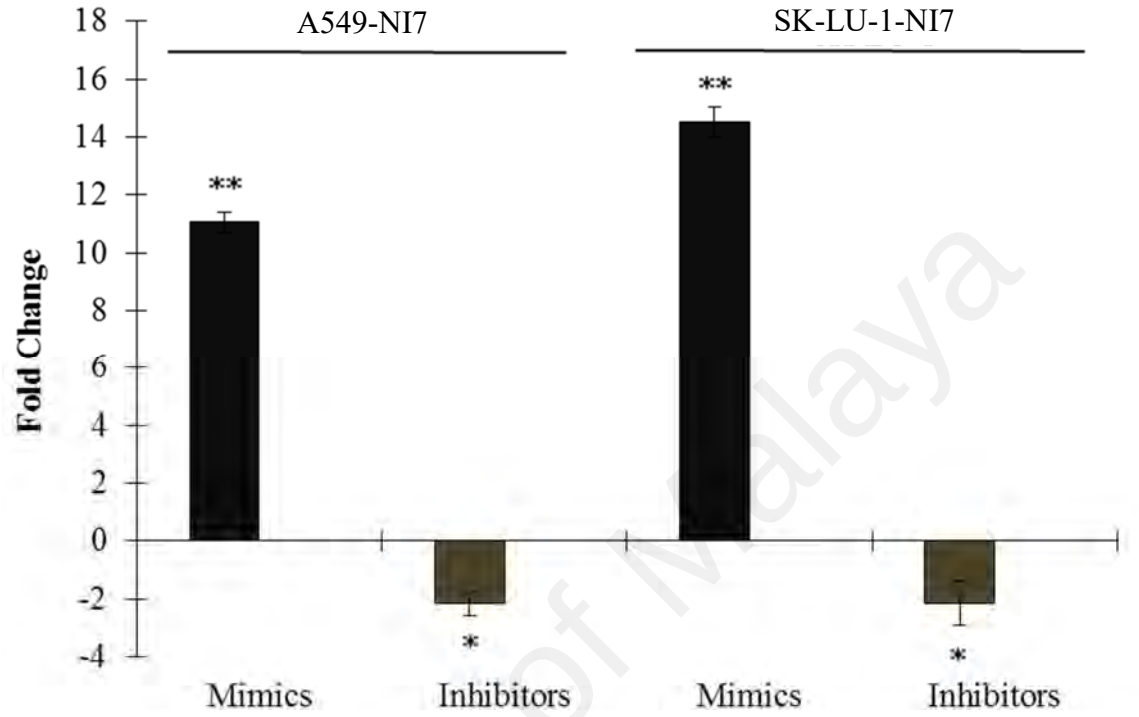

Figure 5.8: Changes of miR-378 expression in A549-NI7 and SK-LU-1-NI7 cells after transfected with miRNA mimics or hairpin inhibitors. Statistical significance between miR-378 mimics-transfected cells and miR-378 hairpin inhibitors-transfected cells in comparison to negative mimics or inhibitors control. * $P < 0.05$, ** $P < 0.01$

On the other hand, overexpression and knockdown of miR-378 did not alter the rates of migration in both A549-NI7 and SK-LU-1-NI7 cells significantly (Figure 5.10). To validate the significance of miR-378 in human NSCLC angiogenesis, miR-378 gain-of-function and loss-of-function studies were conducted. TCM from cells that were transfected with miR-378 mimics induced significantly more formation of branching points and tubes by HUVEC than that from cells transfected with negative mimics control. In contrast, suppression of miR-378 showed significantly fewer branching points and tubes in comparison to negative inhibitors control (Figure 5.11).

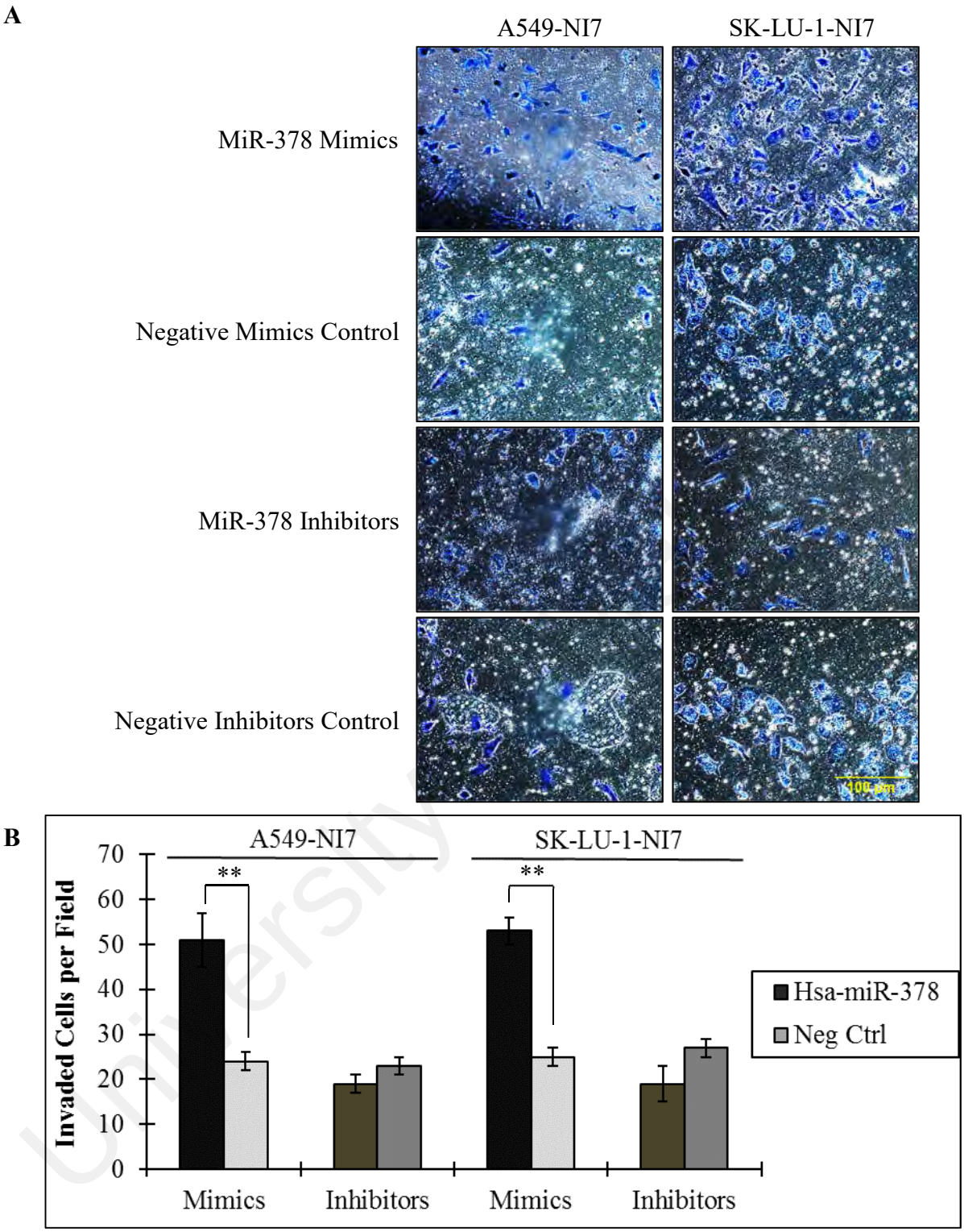

Figure 5.9: Cell invasion was affected by miR-378. (A) Representative fields of A549-NI7 and SK-LU-NI7 cells that successfully invaded into the bottom of the membrane insert post transfection. **(B)** MiR-378 expression promoted cell invasion in A549-NI7 and SK-LU-1-NI7 cells as compared to negative mimics control transfectants. The data are representative of three independent experiments. ** $P < 0.01$

A

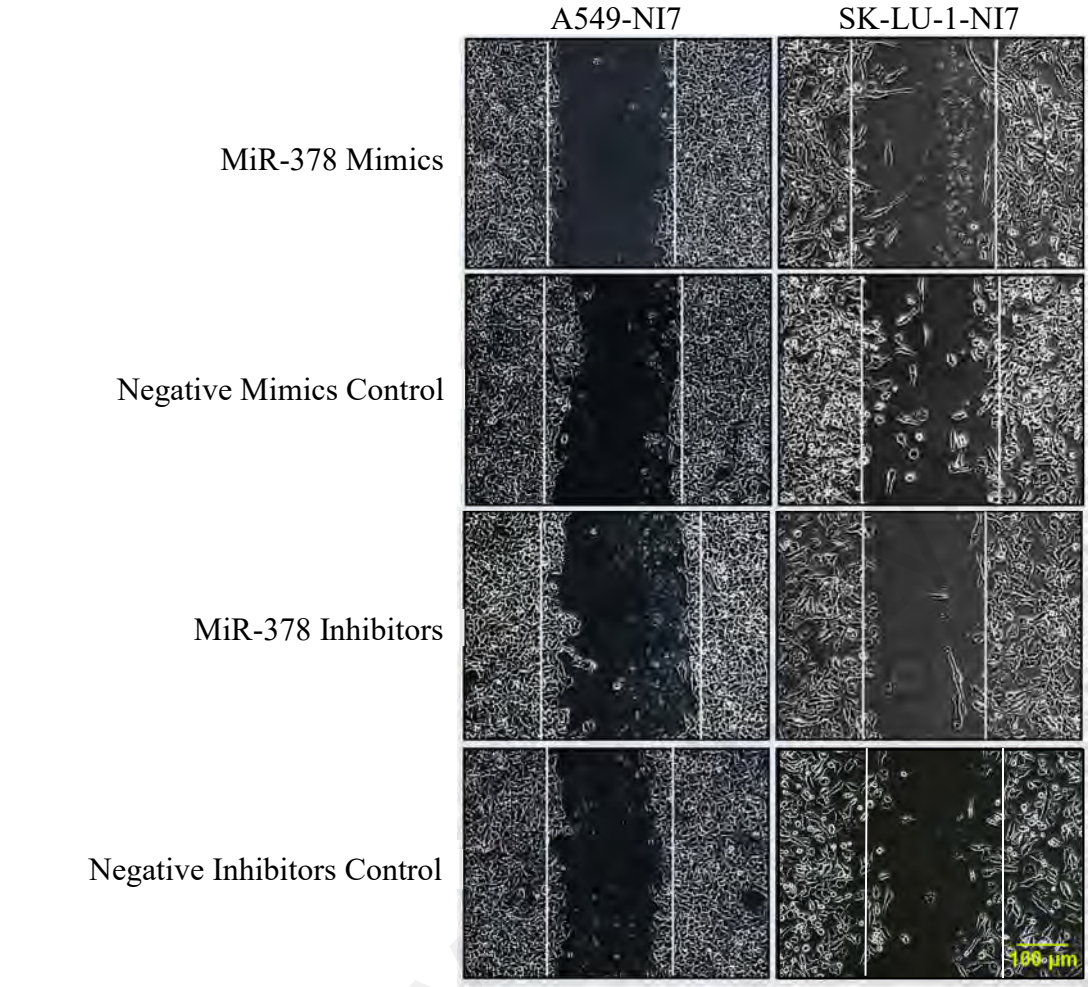

B

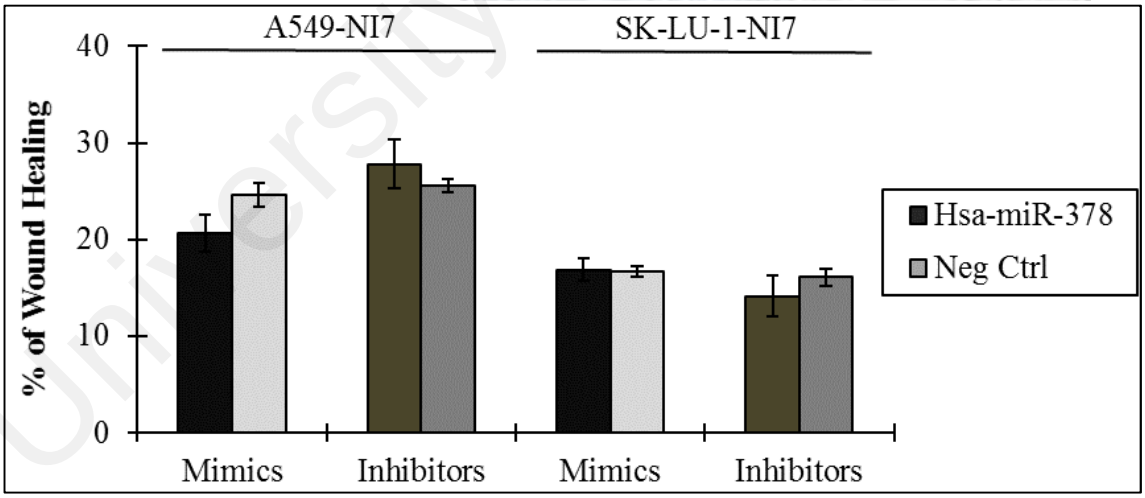

Figure 5.10: Overexpression and knockdown of miR-378 did not alter cell migration *in vitro*. (A) Representative photos of transfected low invasive cells 28 hours after a scratch was made. **(B)** Quantification of migration distance of each transfection group.

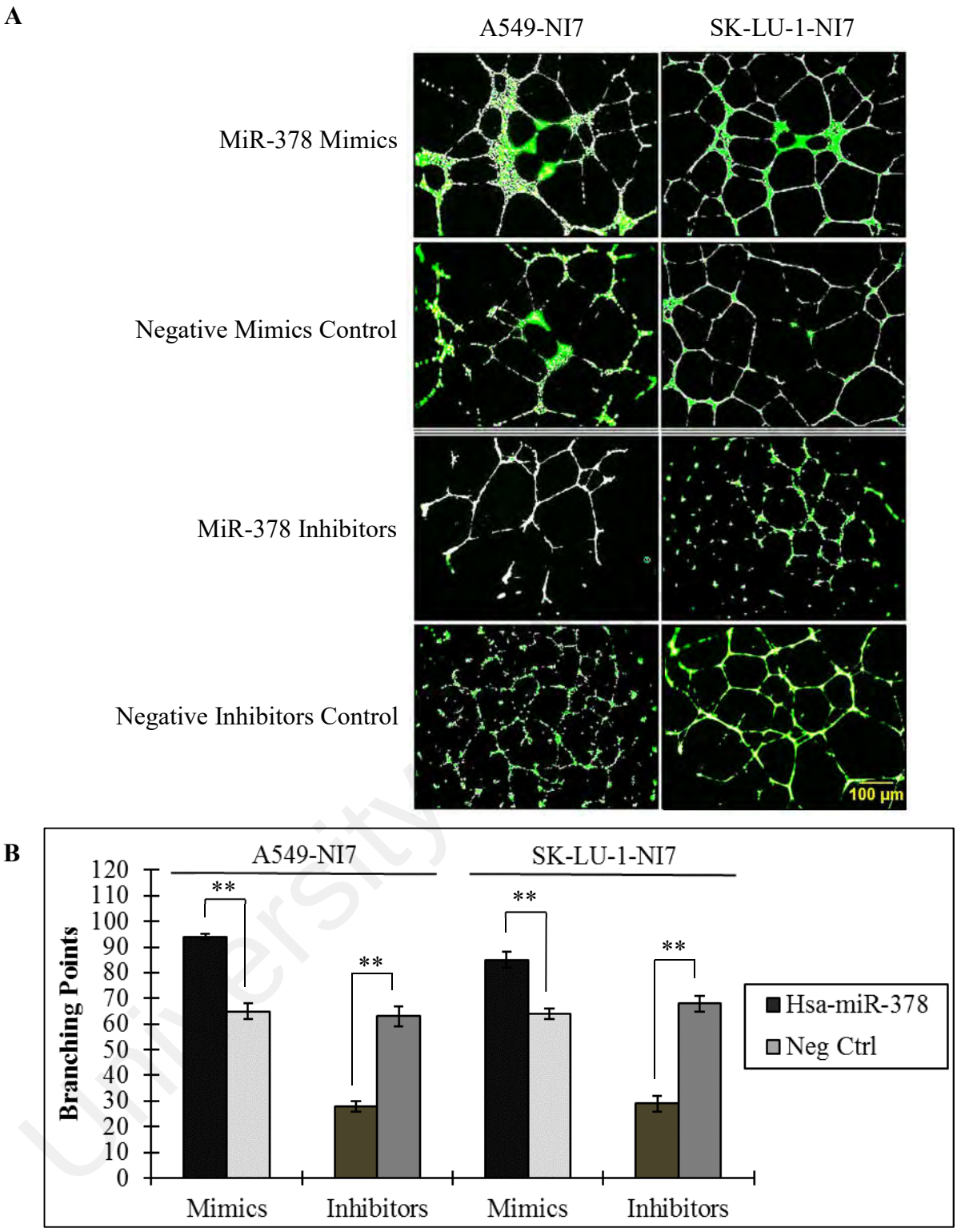

Figure 5.11: MiR-378 functions as an angiogenic promoter. (A) A549-NI7 and SK-LU-1-NI7 cells were transfected with negative mimics/ inhibitors control or miR-378 mimics/ hairpin inhibitors, and TCM were collected to culture HUVEC. Fluorescence microscope pictures were taken after 15 hours (40× magnification). Representative images are shown. **(B)** Number of branching points was counted by WimTube analysis. The results are representative of three independent experiments. Statistical analysis was performed using Student's *t*-test. ** $P < 0.01$

C

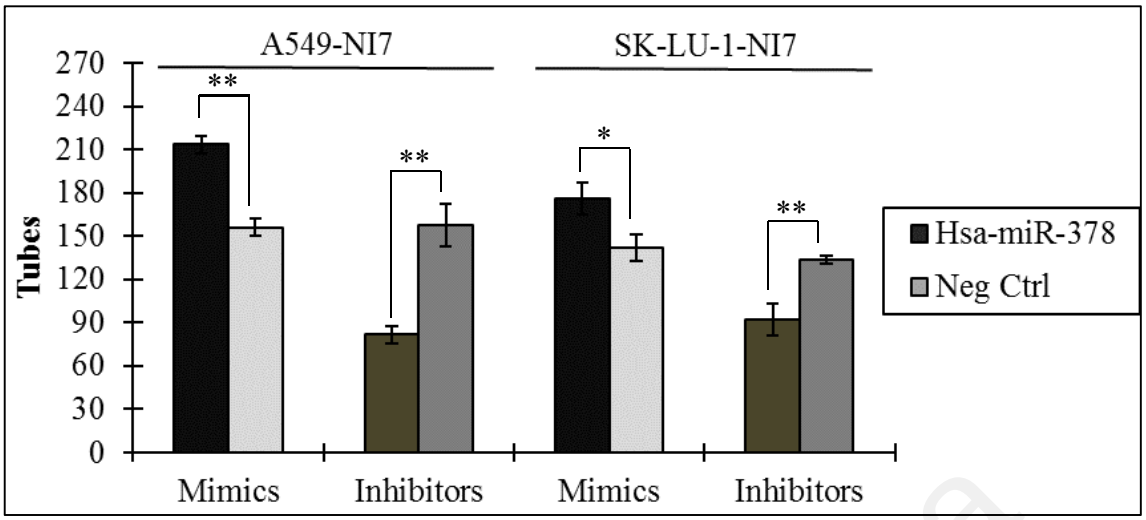

Figure 5.11, continued: (C) Number of tubes was counted by WimTube analysis. The results are representative of three independent experiments. Statistical analysis was performed using Student's *t*-test. * $P < 0.05$, ** $P < 0.01$

5.2.3 MiR-1827 Inhibits NSCLC Cell Migration and Angiogenesis

To analyse the effects of miR-1827 expression on mediating cell invasion, migration and angiogenesis, transient transfection with miR-1827 mimics or hairpin inhibitors was carried out. After transfection, miR-1827 expression was checked with RT-qPCR and the transfected cells were assayed for cell invasion, migration and angiogenesis activities.

The cells showed significant 6- to 9-fold increase in miR-1827 expression when transfected with miR-1827 mimics and significant 2- to 4-fold decrease in miR-1827 expression when transfected with miR-1827 hairpin inhibitors (Figure 5.12). All transfected A549-NI7 and SK-LU-1-NI7 cells remained non-invasive for the transwell invasion assay as no significant decrease or increase in the number of invaded cells was observed (Figure 5.13). Both NSCLC cells transfected with miR-1827 hairpin inhibitors exhibited significantly greater ability in migrating than negative inhibitors control, resembling their high invasive counterparts (Figure 5.14). Similarly, in the presence of TCM derived from miR-1827-silenced cells, HUVEC developed significantly more capillary-like structures compared with those cultured in negative inhibitors control-treated TCM. In contrast, when incubated with TCM from miR-1827 mimics-

transfectants, HUVEC displayed much lower ability to proliferate, causing the number of branching points and tubes to be significantly decreased, compared to that of negative mimics control (Figure 5.15).

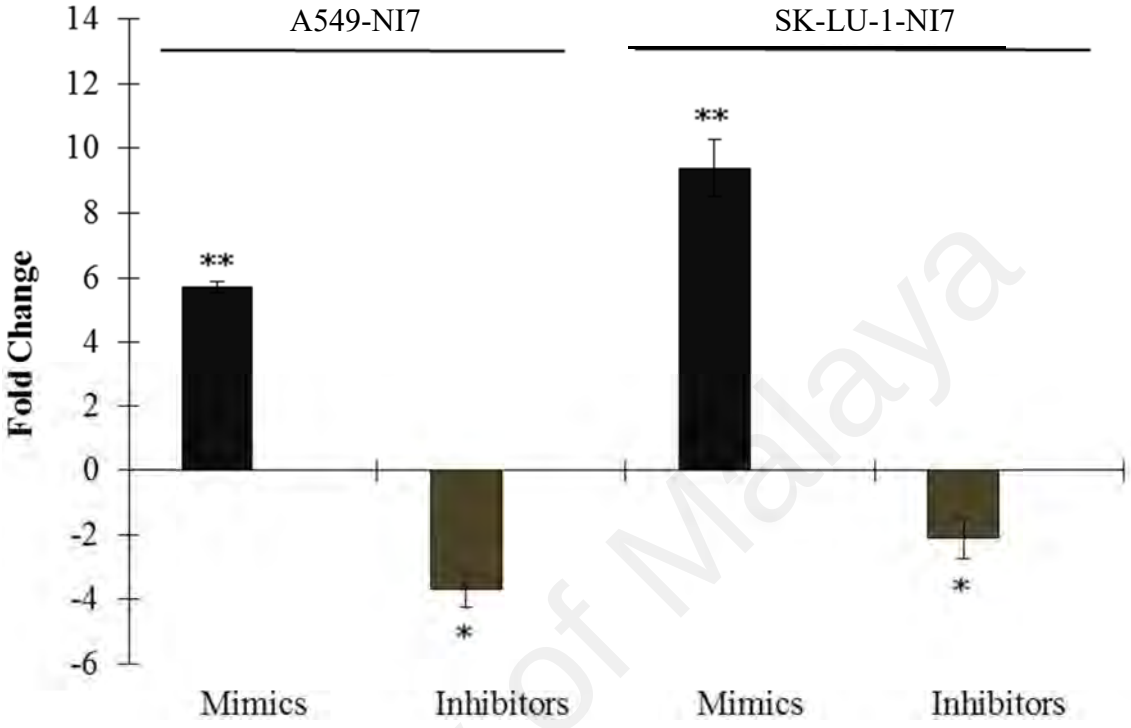

Figure 5.12: The real-time RT-PCR analysis of miR-1827 in A549-NI7 and SK-LU-1-NI7 post transfection. 24 hours after cells were transfected with miR-1827 mimics/ hairpin inhibitors or negative mimics/ inhibitors control, RT-qPCR was performed to detect the expression of miR-1827. * $P < 0.05$, ** $P < 0.01$

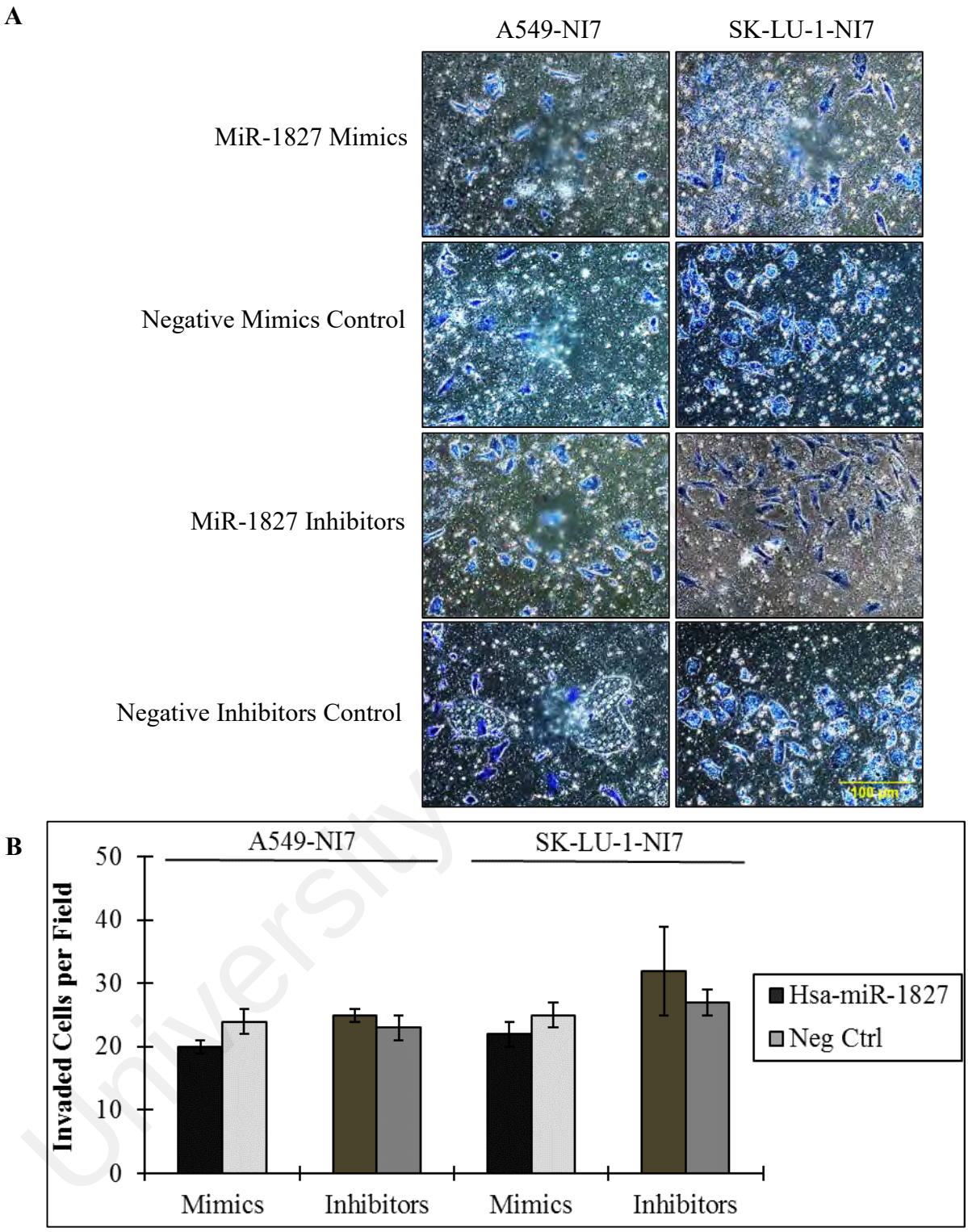

Figure 5.13: Cell invasion was not altered by overexpression and knockdown of miR-1827. (A) Cells transfected with negative mimics/ inhibitors control or miR-1827 mimics/ hairpin inhibitors were applied to transwell chamber coated with Matrigel and then incubated for 22 hours. Representative images are shown. The 8µm pores of the transwell polycarbonate membranes are visible in the background. **(B)** Cell invasion was assessed by counting the stained cells on the bottom of the membrane insert.

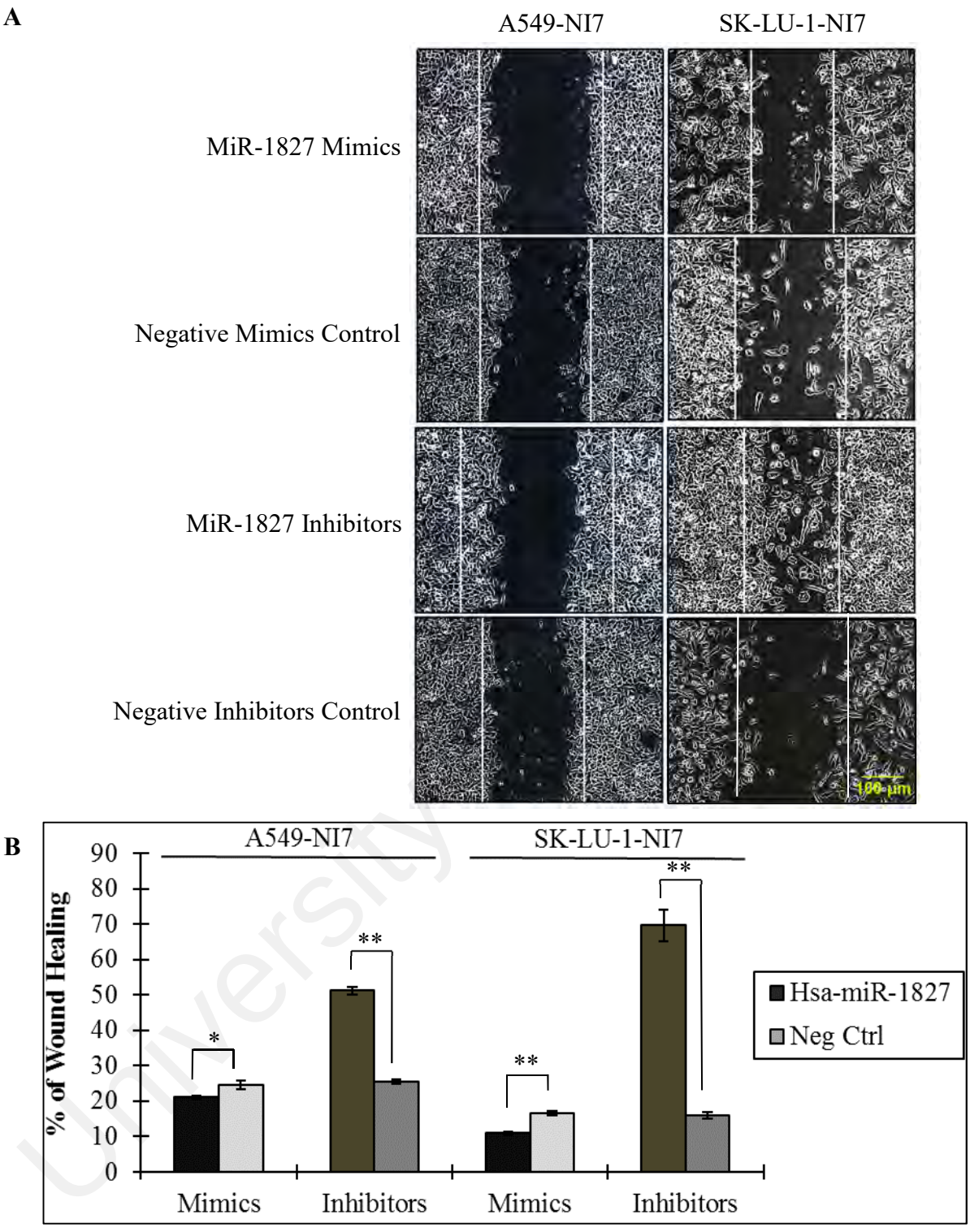

Figure 5.14: Inhibition of miR-1827 promoted cell migration. (A) Wound repair array showed minimal migration of cells across the wound margin under miR-1827 mimics group, whereas anti-miR-1827 induced cell migration across the wound margin resulting in further closure of the wound. Representative images are shown. **(B)** Wound healing analysis as percentage of migrated distance with respect to the gap at 0 h. * $P < 0.05$, ** $P < 0.01$

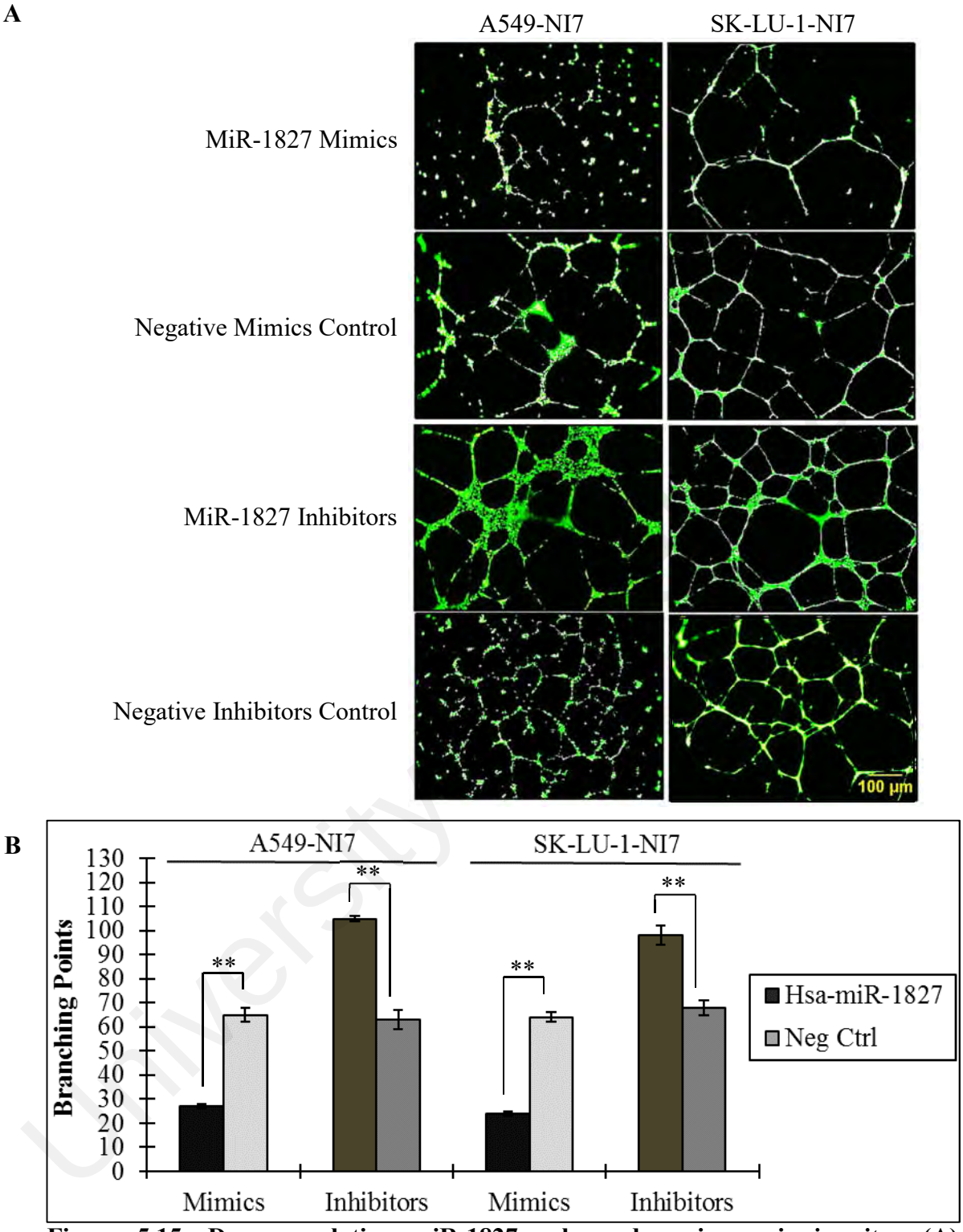

Figure 5.15: Down-regulating miR-1827 enhanced angiogenesis *in vitro*. (A) Representative images of tube formation of HUVEC. **(B)** MiR-1827 represses tumour angiogenesis. Restoration of miR-1827 promoted NI7 cells-inhibited branching point formation of HUVEC. ** $P < 0.01$

C

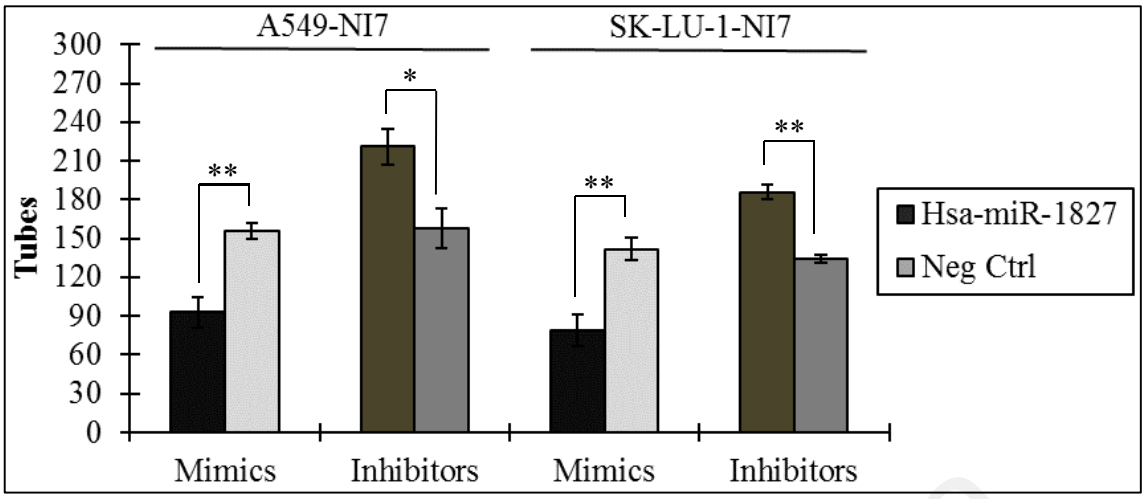

Figure 5.15, continued: (C) MiR-1827 represses tumour angiogenesis. Restoration of miR-1827 promoted NI7 cells-inhibited tube formation of HUVEC. * $P < 0.05$, ** $P < 0.01$

5.3 MiR-378 and MiR-1827 Regulate Metastasis via EMT

MiR-378 and miR-1827 were shown to play important roles in regulating NSCLC cell invasion, migration and angiogenesis. While EMT is considered as an early stage in tumour metastasis, this section aims to examine the effects of miR-378 and miR-1827 on EMT. EMT is characterised by marker changes, such as dissociation of CTNNB1 from CDH1 and accumulation in the cytosol before translocation into the nucleus, as well as induction of VIM. As shown in Figure 5.16, overexpression of miR-378 significantly increased the expression of CTNNB1 and VIM in A549-NI7 and SK-LU-1-NI7 cells. Likewise, inhibition of endogenous miR-1827 significantly amplified the expression of CTNNB1 and VIM in low invasive A549 and SK-LU-1 cells. In contrast, CTNNB1 and VIM were undetected when cells were treated with miR-378 hairpin inhibitors and miR-1827 mimics, so as the control cells.

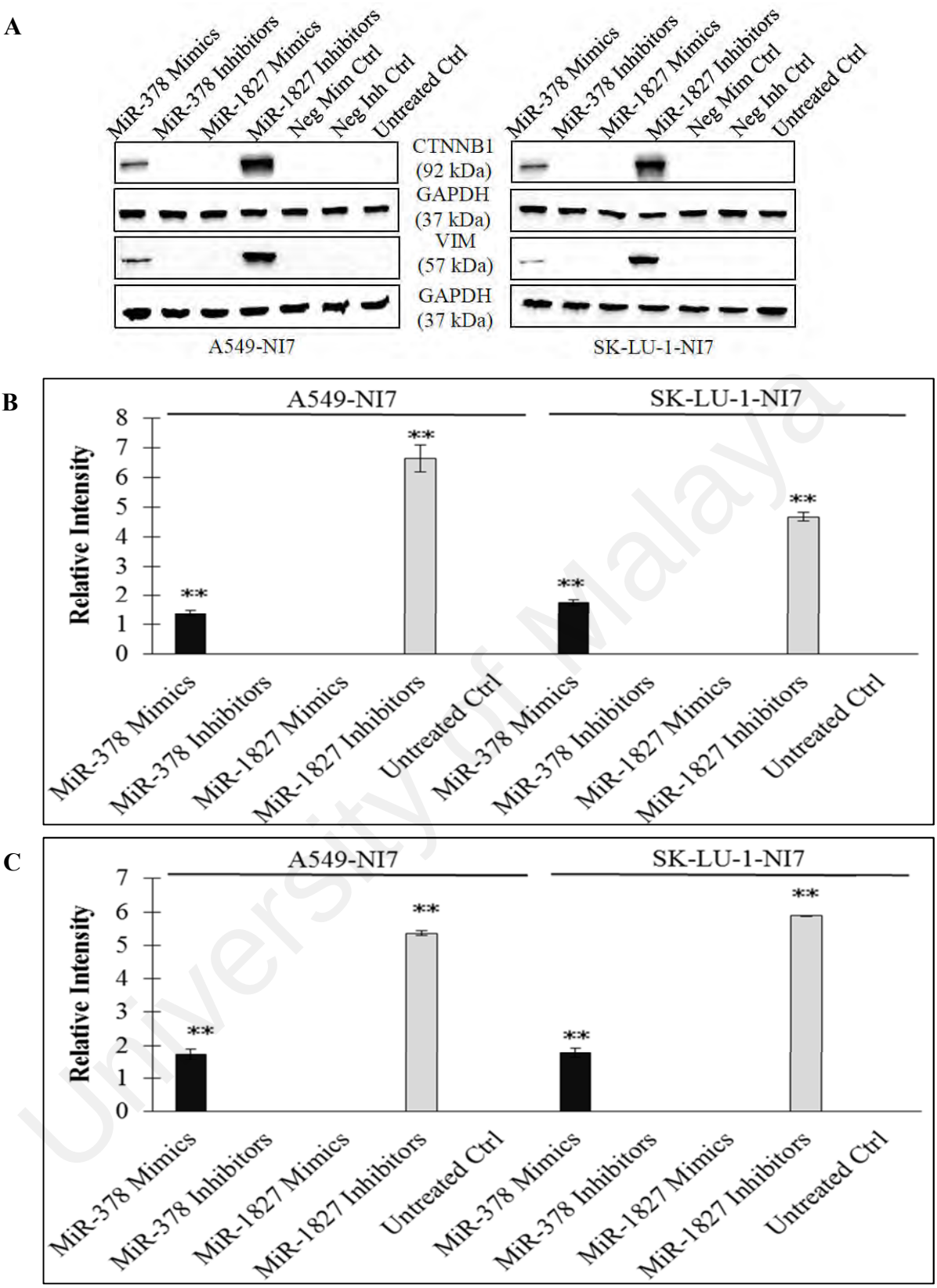

Figure 5.16: MiR-378 and miR-1827 regulate the EMT. (A) Western blot analysis for the expression of CTNNB1 and VIM in A549-NI7 and SK-LU-1-NI7 cells transfected with miR-378 mimics/ hairpin inhibitors, miR-1827 mimics/ hairpin inhibitors or negative mimics/ inhibitors control. **(B)** Expression of CTNNB1 (epithelial marker) post transfection. MiR-378 induces while miR-1827 represses EMT. **(C)** The protein level of VIM (mesenchymal marker) was determined by Western blot after transfection. GAPDH served as an internal control. ** $P < 0.01$

5.4 Summary

It is important to take note that during transfection optimisation, at concentration of 15nM for labelled non-targeting mimics and 25nM for labelled non-targeting hairpin inhibitors, A549-NI7 cells already had a transfection efficiency of more than 80% (**Appendix D**). However, substantial effects can only be seen when cells were transfected at 80nM. That is why the starting concentration for SK-LU-1-NI7 transfection optimisation experiments was set to be 40nM. However, while 40nM of mimics transfection indicator was sufficient enough to yield ≥ 80% transfection efficiency, 80nM was found to be the least amount needed to enter nearly 80% of the cells for hairpin inhibitors transfection indicator (**Appendix D**) to produce significant effects on the *in vitro* assays. As such, to accurately identify the roles of miRNAs in regulating NSCLC cell invasion, migration and angiogenesis, the concentration was standardised at 80nM across the experiments.

Bidirectional transfection experiments were performed on low invasive cells with miRNA mimics and hairpin inhibitors. It is important to take note that, therapeutic wise, it is not practicable as this makes tumour more metastatic. However, it is useful for identifying miRNAs that drive tumour dissemination. On the other hand, the reason why the concept of angiogenesis was introduced at this stage is based on the premise that tumours would remain dormant if neovascularisation is prevented (Holmgren *et al.*, 1995). TCM isolated from cells was used to mimic the chemotactic factors released by tumour. When incubated with TCM, endothelial cells attached to the growth factor-reduced basement membrane extract, differentiated, migrated to align, branched and finally formed the tubular polygonal networks of blood vessels (Casamassimi *et al.*, 2015). Studies have shown that TCM is a potent pro-migratory cocktail (Menon *et al.*, 2007; Lin *et al.*, 2008) that contains soluble growth factors (platelet-derived growth factor (PDGF) and transforming growth factor (TGF)), chemokines, cytokines, acute

phase proteins and proteases (Klopp *et al.*, 2007; Kano, 2015). Many tumour cell lines also secrete VEGF that is highly specific for cultured endothelial cells (Aonuma *et al.*, 1999). Hyper-permeability of HUVEC which had been cultured with TCM for a long time resembled the tumour vascular endothelium *in vivo*, suggesting that normal tissue-derived endothelial cells could be transformed into tumour tissue endothelial cells by TCM (Utoguchi *et al.*, 1995).

Generally, the amplification of miRNAs expression was more pronounced than silencing of miRNAs expression, whereby miRNA mimics could induce up to 15-fold increase in miRNAs expression but miRNA hairpin inhibitors only managed to decrease 2- to 4-fold of endogenous miRNAs. This could be explained through the mechanism by which they participate in the miRNA-mediated gene targeting pathway. MicroRNA mimics are in double-stranded conformation and upon delivery into the cells, they behave like endogenous miRNAs where separation of strands take place and loaded into the RISC to carry out its gene targeting function. On the contrary, miRNA hairpin inhibitors compete with target mRNAs for programmed RISC, and hence the fold change obtained suggests that there were more unsuccessful competitions of miRNA hairpin inhibitors than mRNAs for miRNAs, causing the hairpin inhibitors to be in excess. In other words, the fold change and downstream effects seen might vary with experiments. Furthermore, it could also be due to a portion of hairpin inhibitors that may have been processed as mRNAs after being loaded into RISC to interact with miRNAs. They could have been degraded or exported to P-bodies, leaving the recyclable miRNAs to target mRNAs as usual; while the residual hairpin inhibitors were saturated with newly synthesised free miRNAs in the cytoplasm. After all, these questions are still unanswered and remain to be experimentally tested.

Remarkable changes in miR-92b level were observed, however, only miR-92b hairpin inhibitors transfection significantly altered the cell migration ability of A549-

NI7. Although TCM from miR-92b hairpin inhibitors-transfected SK-LU-1-NI7 prevented the formation of branching points, the reduction in tube formation was not significant. Increasing the transfection dosage might improve the outcomes but given that the other two miRNAs demonstrated notable results at 80nM, it was therefore thought that, miR-92b is not the major miRNA controlling NSCLC cell invasion and migration and angiogenesis.

Meanwhile, although miR-378 mimics transformed the low invasive cells into high invasive ones, transfection with miR-378 hairpin inhibitors insignificantly suppressed cell invasion capability which could be attributed to the points discussed above. On top of that, since A549-NI7 and SK-LU-1-NI7 are after all cancer cells and their invasiveness was compared to high invasive counterparts to begin with, their aggressive phenotypes may not be reduced to be comparable to that of normal cells. While miR-378 was seen not to play a role in cell migration, it was revealed as an important angiomiR in promoting HUVEC growth and maturation.

MiR-1827, on the other hand, was found to inhibit cell migration and angiogenesis. More cells were seen to invade through the Matrigel when treated with miR-1827 hairpin inhibitors and reduced when treated with miR-1827 mimics, but these numbers were statistically insignificant.

MiR-378 and miR-1827 were further demonstrated to affect EMT in NSCLC. In the presence of miR-378 mimics or miR-1827 hairpin inhibitors, cadherin-bound CTNNB1 was reduced to cytosolic CTNNB1. The disruption of linkage of cadherin-CTNNB1-actin cytoskeleton signifies loss of E-cadherin and eliminates cell adhesion, a key step in EMT leading to metastasis (Wheelock *et al.*, 1996). CTNNB1 which was freed from the membrane, accumulated in the cytosol and can later travel to the nucleus to activate TCF (T-cell factor)-regulated genes which are important for cell invasion and

migration (Crawford *et al.*, 1999; Gradl *et al.*, 1999; Peifer & Polakis, 2000). The down-regulation of epithelial marker was accompanied by induction of the intermediate filament protein VIM (mesenchymal marker). High level of VIM correlated with invasive and motile behaviours of A549-NI7 and SK-LU-1-NI7 cells when transfected with miR-378 mimics and miR-1827 hairpin inhibitors, respectively. The function of VIM during cell invasion and migration is thought to be mediated through invadopodia and lamellipodia formation as well as maintenance of cell polarity (Kidd *et al.*, 2014).

Taken together, miR-92b is not the pivotal player in the three key processes, which are, invasion, migration and angiogenesis during metastasis in NSCLC. However, miR-378 drives NSCLC cell invasion and angiogenesis, whereas miR-1827 is closely related to NSCLC cell migration and angiogenesis.

CHAPTER 6: IDENTIFICATION AND VALIDATION OF MIRNAS GENE TARGET(S) IN NSCLC

To understand how deregulated miRNAs exert their biological effects in NSCLC, it is crucial to identify their targets. This chapter aims to investigate the targets of miR-378 and miR-1827 responsible for regulating metastasis and angiogenesis in NSCLC.

6.1 *In Silico* Target Prediction

Bioinformatics analyses were carried out to identify potential miR-378 and miR-1827 targets using TargetScan v7.1 and DIANA-microT-CDS v5.0. TargetScan requires perfect complementarity to the seed region of a miRNA. A total context score is calculated as the sum of context scores for the most favourable miRNA in a family targeting multiple sites on the same gene. A more negative score is associated with a more favourable site (Agarwal *et al.*, 2015). DIANA micro-T uses a 38-nucleotide window progressively moved across a 3'-UTR sequence. The free energy of the potential binding sites is calculated at each step and compared to the results obtained from shuffled sequences. Higher miTG scores correspond to higher possibility of correct prediction (Paraskevopoulou *et al.*, 2013). A total of 132 and 1164 overlapping genes were identified as putative targets for miR-378 and miR-1827, respectively (Figure 6.1).

Upon functional annotation by DAVID v6.8, 8 miR-378 target genes (Table 6.1) and 59 miR-1827 target genes (Table 6.2) were listed according to their metastasis-related pathways. Generally, these target genes are involved in ErbB, HIF-1, Hippo, p53, Rap1, Ras, TGF-β and Wnt signalling pathways to mediate metastasis and angiogenesis in NSCLC. These regulatory networks were summarised in Figure 6.2.

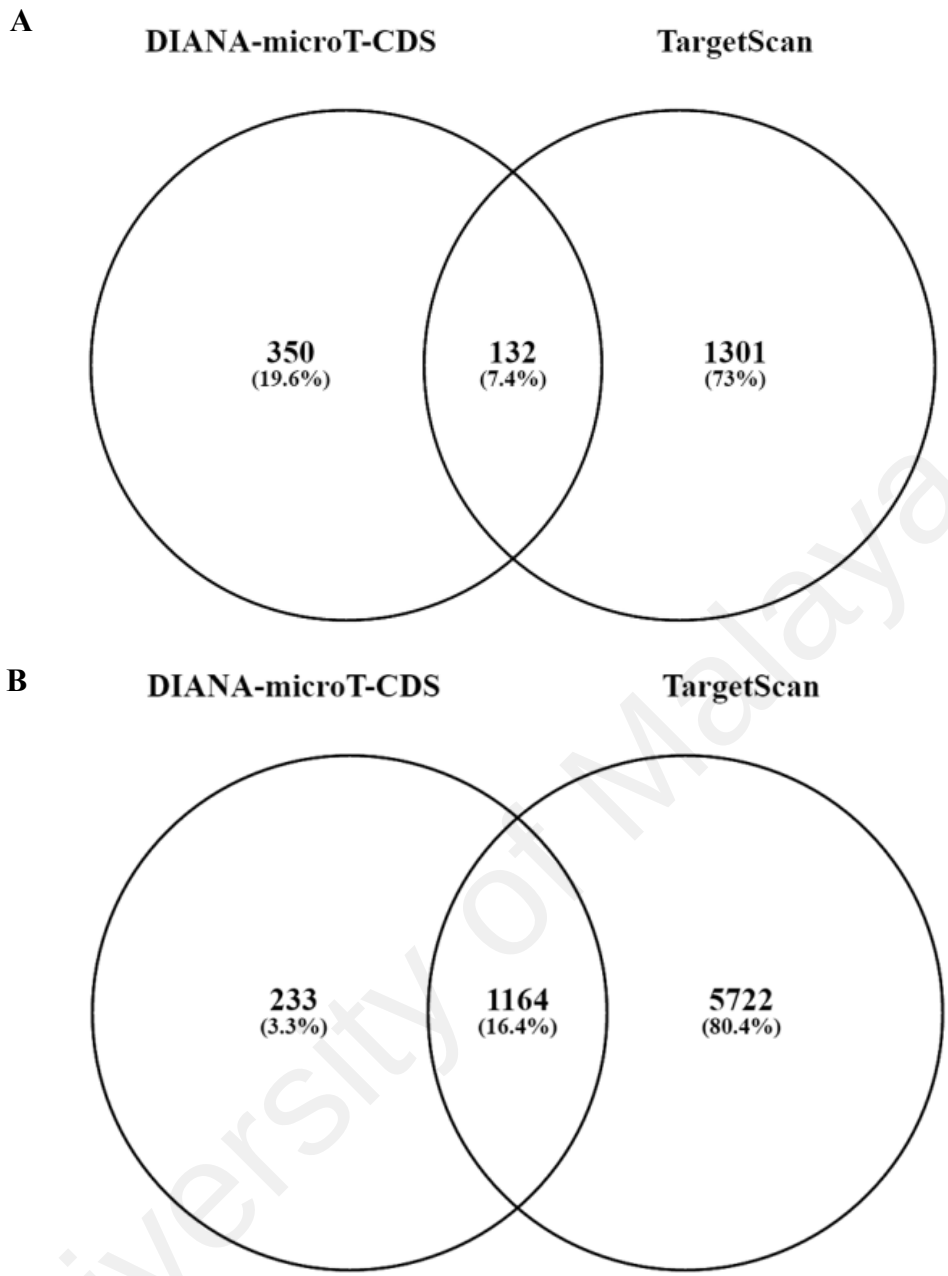

Figure 6.1: Venn diagrams showing the number of gene targets predicted for (A) miR-378 and (B) miR-1827 by TargetScan and DIANA. The number of overlapping genes is represented in the region between the circles.

Table 6.1: Pathways implicated by miR-378 target genes in NSCLC metastasis with their DIANA miTG and TargetScan total context scores.

Gene Symbol	Gene Name	DIANA miTG Score	TargetScan Total Context Score	DAVID Functional Annotation
ERBB4	v-Erb-B2 avian erythroblastic leukemia viral oncogene homolog 4	0.715	-0.10	ErbB signaling pathway
NKX3-1	NK3 homeobox 1	0.895	-0.81	Pathways in cancer
PAX8	Paired box 8	0.851	-0.16	Pathways in cancer
PLA2G12A	Phospholipase A2, group XIIA	0.833	-0.47	Ras signaling pathway
RAD51	RAD51 recombinase	0.741	-0.20	Pathways in cancer
RAPGEF5	Rap Guanine nucleotide exchange factor (GEF) 5	0.715	-0.15	Rap1 signaling pathway Ras signaling pathway
RBX1	Ring-box 1, E3 ubiquitin protein ligase	0.861	-0.47	Pathways in cancer HIF-1 signaling pathway TGF-beta signaling pathway
SKP2	S-phase kinase-associated protein 2, E3 ubiquitin protein ligase	0.860	-0.22	Pathways in cancer

Table 6.2: Functionally annotated using DAVID the miR-1827 gene targets predicted by TargetScan and DIANA.

Gene Symbol	Gene Name	DIANA miTG Score	TargetScan Total Context Score	DAVID Functional Annotation
ADCY2	Adenylate cyclase 2 (brain)	0.796	-0.160	Pathways in cancer
AR	Androgen receptor	0.940	-0.290	Pathways in cancer
ATM	Ataxia telangiectasia mutated	0.770	-0.150	p53 signaling pathway
BBC3	BCL2 binding component 3	0.922	-0.160	Hippo signaling pathway
				p53 signaling pathway
BCL2L1	BCL2-like 1	0.819	-0.240	Pathways in cancer
BCR	Breakpoint cluster region	0.779	-0.090	Pathways in cancer
BDKRB2	Bradykinin receptor B2	0.732	-0.520	Pathways in cancer
CAMK2A	Calcium/ calmodulin-dependent protein kinase II alpha	0.807	-0.240	ErbB signaling pathway
				Wnt signaling pathway
CCNG1	Cyclin G1	0.925	-0.400	p53 signaling pathway
CDKN1B	Cyclin-dependent kinase inhibitor 1B (p27, Kip1)	0.796	-0.260	ErbB signaling pathway
				Pathways in cancer
CRB2	Crumbs homolog 2 (Drosophila)	0.723	-0.100	Hippo signaling pathway
CRKL	v-CRK avian sarcoma virus CT10 oncogene homolog-like	0.899	-0.320	ErbB signaling pathway
				Pathways in cancer
CYCS	Cytochrome c, somatic	0.826	-0.700	p53 signaling pathway
				Pathways in cancer
E2F2	E2F transcription factor 2	0.742	-0.690	Pathways in cancer
ERBB4	v-Erb-B2 avian erythroblastic leukemia viral oncogene homolog 4	0.890	-0.100	ErbB signaling pathway
FAS	Fas cell surface death receptor	0.754	-0.300	p53 signaling pathway
				Pathways in cancer
FGF18	Fibroblast growth factor 18	1.000	-0.640	Pathways in cancer
FGF20	Fibroblast growth factor 20	0.734	-0.250	Pathways in cancer
FZD3	Frizzled family receptor 3	0.845	-0.180	Hippo signaling pathway
				Pathways in cancer
				Wnt signaling pathway

Table 6.2, continued:

Gene Symbol	Gene Name	DIANA miTG Score	TargetScan Total Context Score	DAVID Functional Annotation
FZD5	Frizzled family receptor 5	0.759	-0.200	Hippo signaling pathway
				Pathways in cancer
				Wnt signaling pathway
GRB2	Growth factor receptor-bound protein 2	0.716	-0.430	ErbB signaling pathway
				Pathways in cancer
GSK3β	Glycogen synthase kinase 3 beta	0.982	-0.330	ErbB signaling pathway
				Hippo signaling pathway
				Pathways in cancer
				Wnt signaling pathway
IGF1	Insulin-like growth factor 1 (somatomedin C)	0.845	-0.780	p53 signaling pathway
				Pathways in cancer
IKBKG	Inhibitor of kappa light polypeptide gene enhancer in B-cells, kinase gamma	0.714	-0.640	Pathways in cancer
LAMC2	Laminin, gamma 2	0.816	-0.430	Pathways in cancer
LIMD1	LIM domains containing 1	0.800	-0.300	Hippo signaling pathway
LLGL2	Lethal giant larvae homolog 2 (Drosophila)	0.802	-0.290	Hippo signaling pathway
LRP6	Low density lipoprotein receptor-related protein 6	0.969	-0.170	Wnt signaling pathway
MDM2	MDM2 oncogene, E3 ubiquitin protein ligase	0.992	-0.400	p53 signaling pathway
				Pathways in cancer
MDM4	Mdm4 p53 binding protein homolog (mouse)	0.882	-0.780	p53 signaling pathway
MITF	Microphthalmia-associated transcription factor	0.801	-0.290	Pathways in cancer
MYC	v-Myc avian myelocytomatosis viral oncogene homolog	1.000	-0.580	ErbB signaling pathway
				Hippo signaling pathway
				Pathways in cancer
				Wnt signaling pathway
NCOA4	Nuclear receptor coactivator 4	0.715	-0.260	Pathways in cancer

Table 6.2, continued:

Gene Symbol	Gene Name	DIANA miTG Score	TargetScan Total Context Score	DAVID Functional Annotation
NF2	Neurofibromin 2 (merlin)	0.871	-0.350	Hippo signaling pathway
NFATC3	Nuclear factor of activated T-cells, cytoplasmic, calcineurin-dependent 3	0.863	-0.420	Wnt signaling pathway
NFATC4	Nuclear factor of activated T-cells, cytoplasmic, calcineurin-dependent 4	0.842	-0.820	Wnt signaling pathway
NKD1	Naked cuticle homolog 1 (Drosophila)	0.720	-0.170	Wnt signaling pathway
PAK1	p21 protein (Cdc42/ Rac)-activated kinase 1	0.739	-0.110	ErbB signaling pathway
PLCG1	Phospholipase C, gamma 1	0.803	-0.240	ErbB signaling pathway
				Pathways in cancer
PLEKHG5	Pleckstrin homology domain containing, family G (with RhoGEF domain) member 5	0.923	-0.520	Pathways in cancer
PPP2R2A	Protein phosphatase 2, regulatory subunit B, alpha	0.802	-0.330	Hippo signaling pathway
PTGS2	Prostaglandin-endoperoxide synthase 2 (prostaglandin G/ H synthase and cyclooxygenase)	0.831	-0.160	Pathways in cancer
RALBP1	RALBP1 associated EPS domain containing 2	0.700	-0.230	Pathways in cancer
RCHY1	Ring finger and CHY zinc finger domain containing 1, E3 ubiquitin protein ligase	0.848	-0.160	p53 signaling pathway
RXRB	Retinoid X receptor, beta	0.700	-0.100	Pathways in cancer
STAT3	Signal transducer and activator of transcription 3 (acute-phase response factor)	0.703	-0.140	Pathways in cancer

Table 6.2, continued:

Gene Symbol	Gene Name	DIANA miTG Score	TargetScan Total Context Score	DAVID Functional Annotation
STAT5B	Signal transducer and activator of transcription 5B	0.966	-0.450	ErbB signaling pathway
				Pathways in cancer
STK36	Serine/threonine kinase 36	0.884	-0.200	Pathways in cancer
STK4	Serine/threonine kinase 4	0.759	-0.140	Pathways in cancer
SUFU	Suppressor of fused homolog (Drosophila)	0.710	-0.340	Pathways in cancer
THBS1	Thrombospondin 1	0.981	-0.290	p53 signaling pathway
TP73	Tumor protein p73	0.721	-0.300	Hippo signaling pathway
				p53 signaling pathway
TPM3	Tropomyosin 3	0.885	-0.560	Pathways in cancer
VANGL2	VANGL planar cell polarity protein 2	0.754	-0.180	Wnt signaling pathway
VHL	von Hippel-Lindau tumor suppressor, E3 ubiquitin protein ligase	0.938	-0.520	Pathways in cancer
WNT2B	Wingless-type MMTV integration site family, member 2B	0.721	-0.220	Hippo signaling pathway
				Pathways in cancer
				Wnt signaling pathway
WNT3A	Wingless-type MMTV integration site family, member 3A	0.849	-0.410	Hippo signaling pathway
				Pathways in cancer
				Wnt signaling pathway
WNT5B	Wingless-type MMTV integration site family, member 5B	0.852	-0.450	Hippo signaling pathway
				Pathways in cancer
				Wnt signaling pathway
WNT9B	Wingless-type MMTV integration site family, member 9B	0.720	-0.510	Hippo signaling pathway
				Pathways in cancer
				Wnt signaling pathway

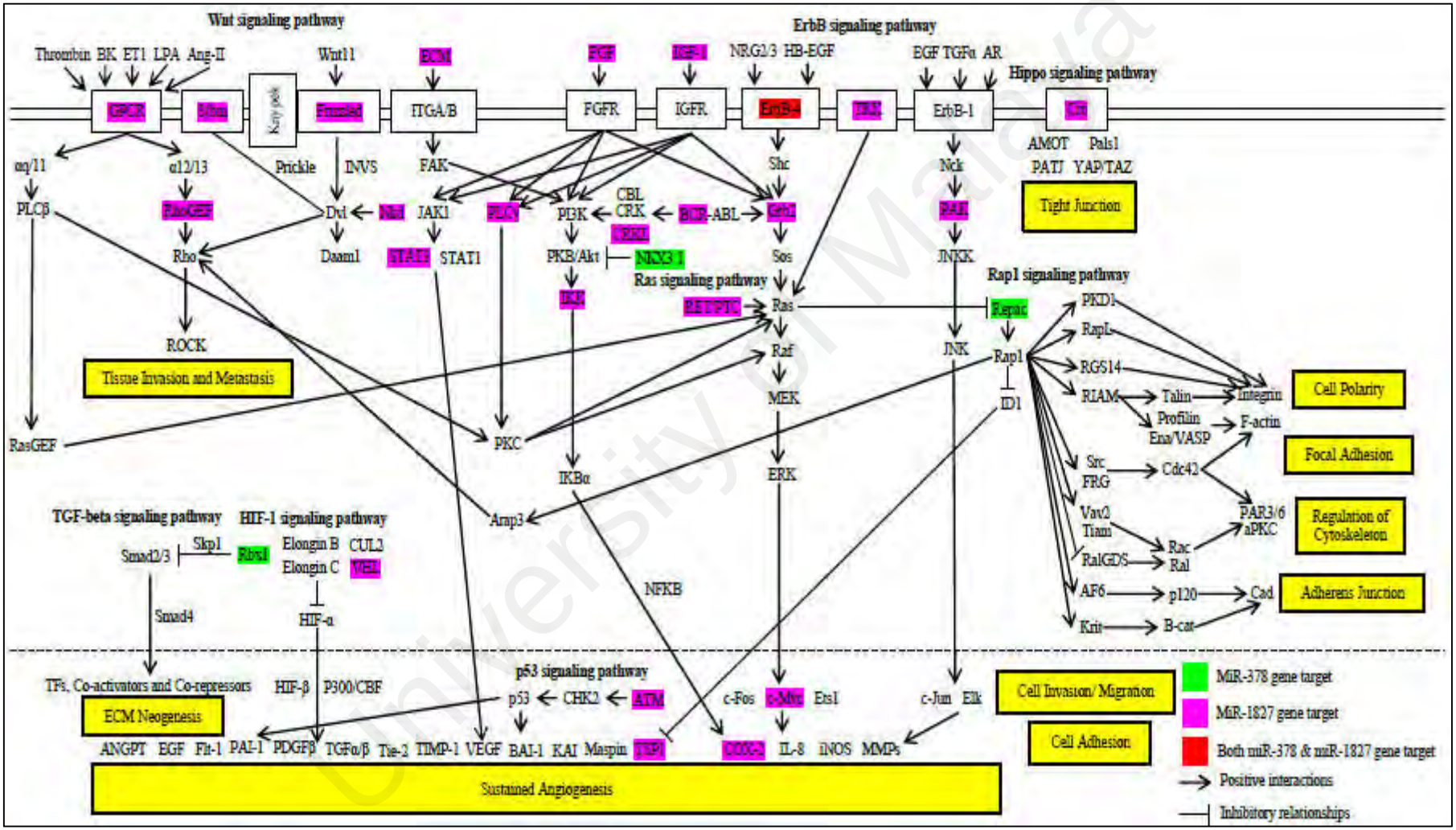

Figure 6.2: A schematic diagram showing the potential relationship between miR-378, miR-1827 and their target genes in metastasis and angiogenesis in NSCLC.

6.2 MiR-378 Directly Represses *RBX1*

RBX1 was selected for miR-378 gene target validation because it had high prediction scores and its function in metastasis is not well studied. To validate whether *RBX1* is directly targeted by miR-378, the human RBX1 3'-UTR containing WT or MT miR-378 binding sequence was cloned downstream of the dual luciferase reporter gene.

RNA was first extracted from A549 and SK-LU-1 and specific primers were used to PCR amplify the 3'-UTR of RBX1 at an optimal temperature of 60°C (Figure 6.3A). This was followed by purification of the amplified RBX1 3'-UTR (Figure 6.3B) and were sequenced and analysed. The amplified RBX1 3'-UTR was 357 bp in length. Both A549 and SK-LU-1 RBX1 3'-UTR were completely identical to NCBI RBX1 3'-UTR reference sequence and they were also identical to each other (Figure 6.3C).

Since the sequences were confirmed to be the same, either A549 or SK-LU-1 RBX1 3'-UTR can be used for cloning. RBX1 and the vector (pmirGLO) were first digested with restriction enzymes NheI and XhoI (Figure 6.4A and Figure 6.4B). They were gel purified and allowed to ligate overnight. Three ratios of vector:DNA were tested and it was found that 3:1 was the best combination for successful transformation (Figure 6.4C).

To screen for positive transformants, that is, those that contained the DNA insert (RBX1 3'-UTR), colony PCR was performed. As shown in Figure 6.5A, five colonies were picked for PCR amplification using the same set of forward and reverse primers and three showed the presence of RBX1 3'-UTR at the correct size. This was further confirmed through restriction enzyme digestion with HindIII, which cut the plasmid at three different sites in the presence of insert DNA, while two bands were produced without insert DNA (Figure 6.5B). Colony 1 was then sequenced to check for correct

orientation (Figure 6.5C). The resulting WT RBX1 3'-UTR plasmid was approximately 8 kb in size.

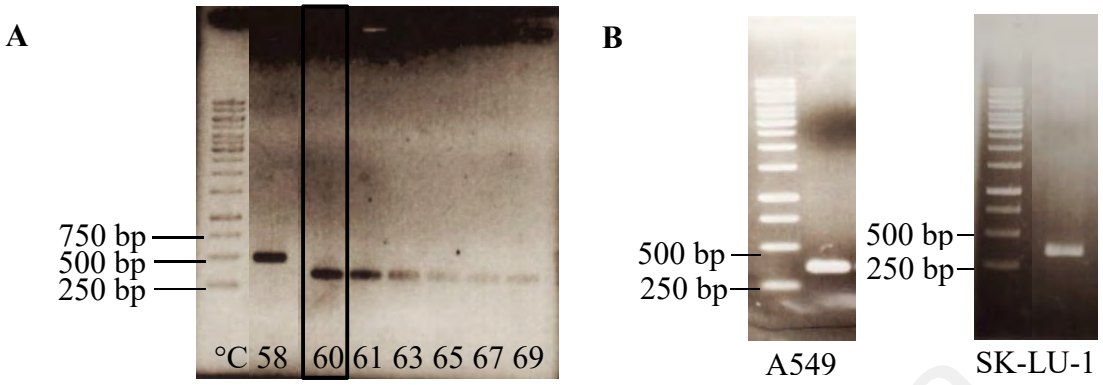

C

Description	Max score	Total score	Query cover	E value	Ident	Accession
Homo sapiens ring-box 1 (RBX1), mRNA	619	619	93%	5e-176	100%	NM_014248.3

Homo sapiens ring-box 1 (RBX1), mRNA
Sequence ID: NM_014248.3 Length: 906 Number of Matches: 1

Range 1: 243 to 577 GenBank Graphics

Score	Expect	Identities	Gaps	Strand
619 bits(335)	5e-176	335/335(100%)	0/335(0%)	Plus/Minus

```
Query  12   CATACACAAGAGAGAGCATCCGTTCCAGAATCCAACTGGACTTTATTTGACACAGAATAC  71
            ||||||||||||||||||||||||||||||||||||||||||||||||||||||||||||
Sbjct  577  CATACACAAGAGAGAGCATCCGTTCCAGAATCCAACTGGACTTTATTTGACACAGAATAC  518

Query  72   AATATGGCTACAGaaacagcaaactgaaaaaacaaagcagaaaaaaaCACAGTTCCATCC  131
            ||||||||||||||||||||||||||||||||||||||||||||||||||||||||||||
Sbjct  517  AATATGGCTACAGAAACAGCAAACTGAAAAAACAAAGCAGAAAAAAACACAGTTCCATCC  458

Query  132  AATTTGTAATTAGGTAACAGCAGGGAAAGTCATTAAATGAATAACAAAACAATTAAGCTT  191
            ||||||||||||||||||||||||||||||||||||||||||||||||||||||||||||
Sbjct  457  AATTTGTAATTAGGTAACAGCAGGGAAAGTCATTAAATGAATAACAAAACAATTAAGCTT  398

Query  192  GATGGAAGAAGTCTTTTCCTAGTGCCCATACTTTTGGAATTCCCACTCTCTGTTGTCCAA  251
            ||||||||||||||||||||||||||||||||||||||||||||||||||||||||||||
Sbjct  397  GATGGAAGAAGTCTTTTCCTAGTGCCCATACTTTTGGAATTCCCACTCTCTGTTGTCCAA  338

Query  252  TGGACACACCTGTCGTGTTTTGAGCCAGCGAGAGATGCAGTGGAAGTGAAAAGCATGGTT  311
            ||||||||||||||||||||||||||||||||||||||||||||||||||||||||||||
Sbjct  337  TGGACACACCTGTCGTGTTTTGAGCCAGCGAGAGATGCAGTGGAAGTGAAAAGCATGGTT  278

Query  312  ACAGACTCCCCATGCGACAGTACACTCTTCTGAAG  346
            ||||||||||||||||||||||||||||||||||
Sbjct  277  ACAGACTCCCCATGCGACAGTACACTCTTCTGAAG  243
```

Description	Max score	Total score	Query cover	E value	Ident	Accession
Homo sapiens ring-box 1 (RBX1), mRNA	619	619	93%	5e-176	100%	NM_014248.3

Homo sapiens ring-box 1 (RBX1), mRNA
Sequence ID: NM_014248.3 Length: 906 Number of Matches: 1

Range 1: 243 to 577 GenBank Graphics

Score	Expect	Identities	Gaps	Strand
619 bits(335)	5e-176	335/335(100%)	0/335(0%)	Plus/Minus

```
Query  12   CATACACAAGAGAGAGCATCCGTTCCAGAATCCAACTGGACTTTATTTGACACAGAATAC  71
            ||||||||||||||||||||||||||||||||||||||||||||||||||||||||||||
Sbjct  577  CATACACAAGAGAGAGCATCCGTTCCAGAATCCAACTGGACTTTATTTGACACAGAATAC  518

Query  72   AATATGGCTACAGaaacagcaaactgaaaaaacaaagcagaaaaaaaCACAGTTCCATCC  131
            ||||||||||||||||||||||||||||||||||||||||||||||||||||||||||||
Sbjct  517  AATATGGCTACAGAAACAGCAAACTGAAAAAACAAAGCAGAAAAAAACACAGTTCCATCC  458

Query  132  AATTTGTAATTAGGTAACAGCAGGGAAAGTCATTAAATGAATAACAAAACAATTAAGCTT  191
            ||||||||||||||||||||||||||||||||||||||||||||||||||||||||||||
Sbjct  457  AATTTGTAATTAGGTAACAGCAGGGAAAGTCATTAAATGAATAACAAAACAATTAAGCTT  398

Query  192  GATGGAAGAAGTCTTTTCCTAGTGCCCATACTTTTGGAATTCCCACTCTCTGTTGTCCAA  251
            ||||||||||||||||||||||||||||||||||||||||||||||||||||||||||||
Sbjct  397  GATGGAAGAAGTCTTTTCCTAGTGCCCATACTTTTGGAATTCCCACTCTCTGTTGTCCAA  338

Query  252  TGGACACACCTGTCGTGTTTTGAGCCAGCGAGAGATGCAGTGGAAGTGAAAAGCATGGTT  311
            ||||||||||||||||||||||||||||||||||||||||||||||||||||||||||||
Sbjct  337  TGGACACACCTGTCGTGTTTTGAGCCAGCGAGAGATGCAGTGGAAGTGAAAAGCATGGTT  278

Query  312  ACAGACTCCCCATGCGACAGTACACTCTTCTGAAG  346
            ||||||||||||||||||||||||||||||||||
Sbjct  277  ACAGACTCCCCATGCGACAGTACACTCTTCTGAAG  243
```

Figure 6.3: Amplification of RBX1 3-UTR. (A) Optimisation of temperature for primers designed to amplify RBX1 3'-UTR. Lane 2 was loaded with PCR product of *GAPDH* at 58°C. **(B)** PCR reaction was scaled up at 60°C and band of interest was gel purified. **(C)** Gel purified RBX1 3'-UTR was sequenced and compared to reference sequence in NCBI. Upper panel: A549; Lower panel: SK-LU-1

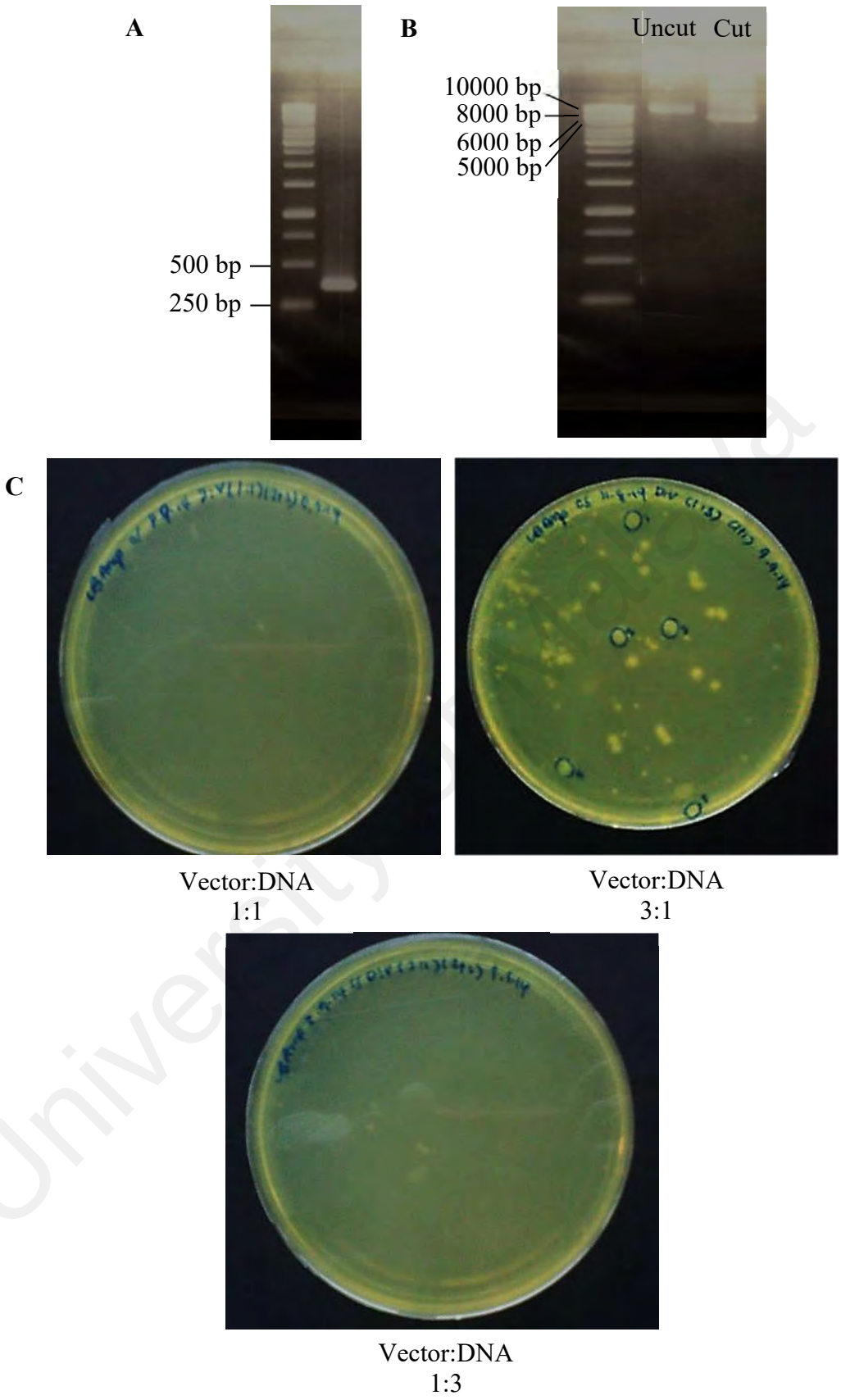

Figure 6.4: Cloning of RBX1 3'-UTR into pmirGLO. (A) RBX1 3'-UTR was digested with restricted enzymes and gel purified. **(B)** Gel image of undigested and digested pmirGLO. **(C)** Ligation products were transformed and plated on LB-Ampicillin agar. Colonies were seen to grow on the plate with 3:1 vector:DNA ligation ratio.

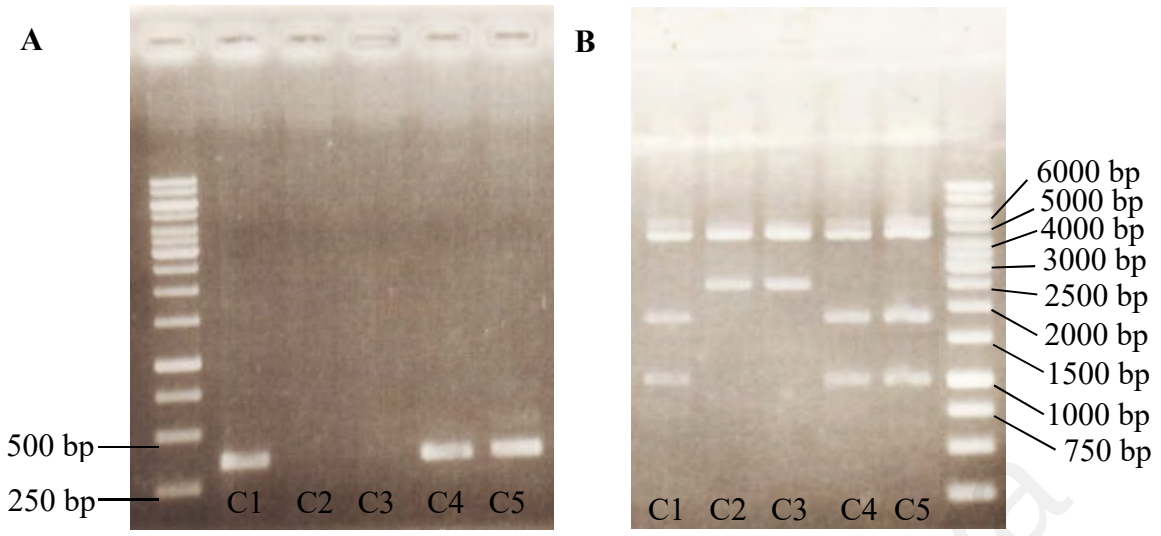

C

```
Alignment of Sequence_1:  [cloned rbx1 snapgene.xdna] with  Sequence_2: [cloned rbx1 sequenced.txt.xdna]

Similarity : 442/442 (100.00 %)

Seq_1  1    GATCGCCGTGTAATTCTAGTTGTTTAAACGAGCTCGCTAGCCTTCAGAAGAGTGTACTGT  60
            ||||||||||||||||||||||||||||||||||||||||||||||||||||||||||||
Seq_2  1    GATCGCCGTGTAATTCTAGTTGTTTAAACGAGCTCGCTAGCCTTCAGAAGAGTGTACTGT  60

Seq_1  61   CGCATGGGGAGTCTGTAACCATGCTTTTCACTTCCACTGCATCTCTCGCTGGCTCAAAAC  120
            ||||||||||||||||||||||||||||||||||||||||||||||||||||||||||||
Seq_2  61   CGCATGGGGAGTCTGTAACCATGCTTTTCACTTCCACTGCATCTCTCGCTGGCTCAAAAC  120

Seq_1  121  ACGACAGGTGTGTCCATTGGACAACAGAGAGTGGGAATTCCAAAAGTATGGGCACTAGGA  180
            ||||||||||||||||||||||||||||||||||||||||||||||||||||||||||||
Seq_2  121  ACGACAGGTGTGTCCATTGGACAACAGAGAGTGGGAATTCCAAAAGTATGGGCACTAGGA  180

Seq_1  181  AAAGACTTCTTCCATCAAGCTTAATTGTTTTGTTATTCATTTAATGACTTTCCCTGCTGT  240
            ||||||||||||||||||||||||||||||||||||||||||||||||||||||||||||
Seq_2  181  AAAGACTTCTTCCATCAAGCTTAATTGTTTTGTTATTCATTTAATGACTTTCCCTGCTGT  240

Seq_1  241  TACCTAATTACAAATTGGATGGAACTGTGTTTTTTTCTGCTTTGTTTTTTCAGTTTGCTG  300
            ||||||||||||||||||||||||||||||||||||||||||||||||||||||||||||
Seq_2  241  TACCTAATTACAAATTGGATGGAACTGTGTTTTTTTCTGCTTTGTTTTTTCAGTTTGCTG  300

Seq_1  301  TTTCTGTAGCCATATTGTATTCTGTGTCAAATAAAGTCCAGTTGGATTCTGGAACGGATG  360
            ||||||||||||||||||||||||||||||||||||||||||||||||||||||||||||
Seq_2  301  TTTCTGTAGCCATATTGTATTCTGTGTCAAATAAAGTCCAGTTGGATTCTGGAACGGATG  360

Seq_1  361  CTCTCTCTTGTGTATGCTCGAGTCTAGAGTCGACCTGCAGGCATGCAAGCTGATCCGGCT  420
            ||||||||||||||||||||||||||||||||||||||||||||||||||||||||||||
Seq_2  361  CTCTCTCTTGTGTATGCTCGAGTCTAGAGTCGACCTGCAGGCATGCAAGCTGATCCGGCT  420

Seq_1  421  GCTAACAAAGCCCGAAAGGAAG  442
            |||||||||||||||||||||
Seq_2  421  GCTAACAAAGCCCGAAAGGAAG  442
```

Figure 6.5: Colony screening. (A) Five colonies were picked for colony PCR and colonies 1, 4 and 5 showed the presence of insert DNA. **(B)** Plasmids of the five colonies were extracted, digested with HindIII and analysed on gel. The digestion pattern was consistent with results from colony PCR. **(C)** Colony 1 sequencing showed 100% similarity to reference sequence created using SnapGene.

To generate MT RBX1 3'-UTR plasmid, WT RBX1 3'-UTR plasmid was used as the template for mutagenesis PCR reaction. Mutagenesis primers were designed such that they were mutated at miR-378 binding site and after rounds of PCR, plasmids with mutated binding site were produced. To avoid false positives, WT RBX1 3'-UTR plasmids in the mixture were degraded with DpnI before transformation. Mutagenesis efficiency was assessed by the colony appearance on LB-Ampicillin plate with X-gal and IPTG. As seen in Figure 6.6A (top right panel), successfully mutated plasmid synthesised functional β-galactosidase to metabolise the substrate and produced a blue phenotype. The colonies obtained on the experimental mutagenesis plate were extracted and sent for sequencing (Figure 6.6B and Figure 6.6C).

Dual luciferase reporter assay was then carried out by co-transfecting miR-378 mimics/ hairpin inhibitors or negative mimics/ inhibitors control and WT/ MT RBX1 3'-UTR plasmid into A549-I7 cells. Cell lysates were collected at 48 h and assayed for luciferase activity. Firefly luciferase activity of each sample was normalised by *Renilla* luciferase activity. The relative luciferase activity of the reporter that contained the WT RBX1 3'-UTR was significantly suppressed when miR-378 mimics were co-transfected. In contrast, the luciferase activity of mutant reporter was insignificantly changed by simultaneous transfection of miR-378 mimics, and it was also found that in the presence of miR-378 hairpin inhibitors, both WT and MT reporter activities were insignificant (Figure 6.7). These results indicate that miR-378 suppresses gene expression through miR-378 binding sequence in the 3'-UTR of RBX1. Western blotting results also showed that A549 and SK-LU-1 cells treated with miR-378 mimics had a significantly reduced expression level of RBX1 (Figure 6.8). This further confirmed *RBX1* as a bona fide target of miR-378.

A

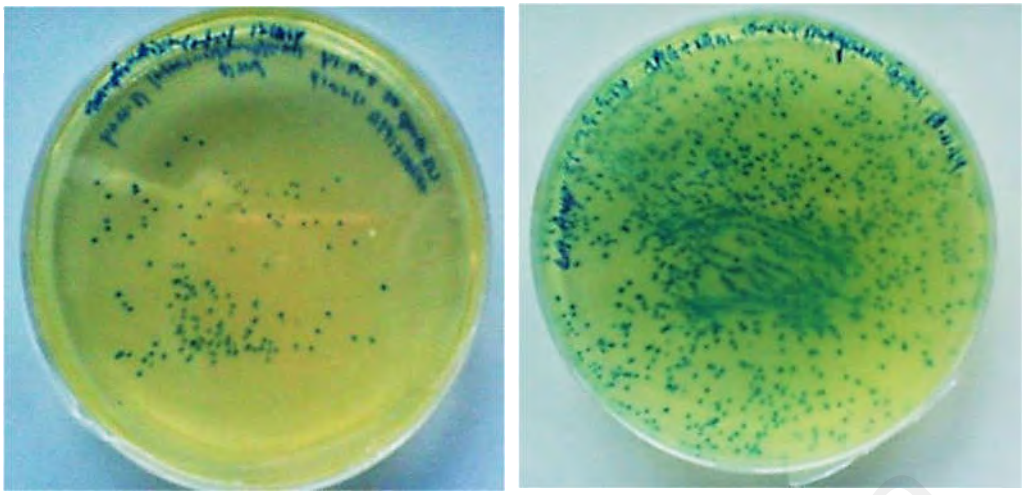

Transformation Control Mutagenesis Control

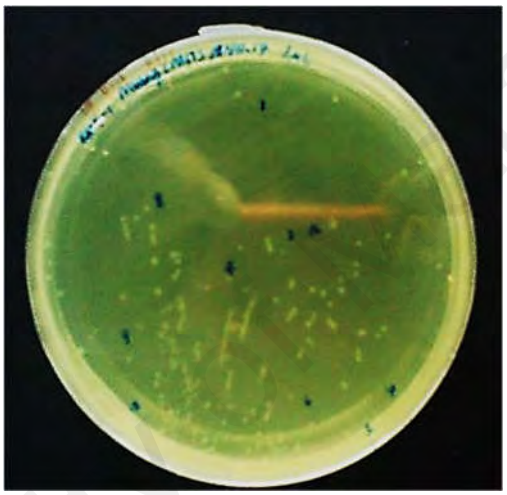

Experimental Mutagenesis

Figure 6.6: Mutagenesis of miR-378 binding site in RBX1 3'-UTR. (A) Photographs of agar plates for transformation control, mutagenesis control and experimental mutagenesis.

B

```
Alignment of Sequence_1:  [rbxl unmutated template.xdna] with  Sequence_2: [rbxl
mutated.xdna]

Similarity : 442/442 (100.00 %)

Seq_1  1     GATCGCCGTGTAATTCTAGTTGTTTAAACGAGCTCGCTAGCCTTCAGAAGAGTGTACTGT  60
             ||||||||||||||||||||||||||||||||||||||||||||||||||||||||||||
Seq_2  1     GATCGCCGTGTAATTCTAGTTGTTTAAACGAGCTCGCTAGCCTTCAGAAGAGTGTACTGT  60

Seq_1  61    CGCATGGGGAGTCTGTAACCATGCTTTTCACTTCCACTGCATCTCTCGCTGGCTCAAAAC  120
             ||||||||||||||||||||||||||||||||||||||||||||||||||||||||||||
Seq_2  61    CGCATGGGGAGTCTGTAACCATGCTTTTCACTTCCACTGCATCTCTCGCTGGCTCAAAAC  120

Seq_1  121   ACGACAGGTGTGTCCATTGGACAACAGAGAGTGGGAATTCCAAAAGTATGGGCACTAGGA  180
             ||||||||||||||||||||||||||||||||||||||||||||||||||||||||||||
Seq_2  121   ACGACAGGTGTGTCCATTGGACAACAGAGAGTGGGAATTCCAAAAGTATGGGCACTAGGA  180

Seq_1  181   AAAGACTTCTTCCATCAAGCTTAATTGTTTTGTTATTCATTTAATGACTTTCCCTGCTGT  240
             ||||||||||||||||||||||||||||||||||||||||||||||||||||||||||||
Seq_2  181   AAAGACTTCTTCCATCAAGCTTAATTGTTTTGTTATTCATTTAATGACTTTCCCTGCTGT  240

Seq_1  241   TACCTAATTACAAATTGGATGGAACTGTGTTTTTTTCTGCTTTGTTTTTTCAGTTTGCTG  300
             ||||||||||||||||||||||||||||||||||||||||||||||||||||||||||||
Seq_2  241   TACCTAATTACAAATTGGATGGAACTGTGTTTTTTTCTGCTTTGTTTTTTCAGTTTGCTG  300

Seq_1  301   TTTCTGTAGCCATATTGTATTCTGTGTCAAATAAAGTCCAGTTGGATTCTGGAACGGATG  360
             ||||||||||||||||||||||||||||||||||||||||||||||||||||||||||||
Seq_2  301   TTTCTGTAGCCATATTGTATTCTGTGTCAAATAAAGTCCAGTTGGATTCTGGAACGGATG  360

Seq_1  361   CTCTCTCTTGTGTATGCTCGAGTCTAGAGTCGACCTGCAGGCATGCAAGCTGATCCGGCT  420
             ||||||||||||||||||||||||||||||||||||||||||||||||||||||||||||
Seq_2  361   CTCTCTCTTGTGTATGCTCGAGTCTAGAGTCGACCTGCAGGCATGCAAGCTGATCCGGCT  420

Seq_1  421   GCTAACAAAGCCCGAAAGGAAG  442
             |||||||||||||||||||||||
Seq_2  421   GCTAACAAAGCCCGAAAGGAAG  442
```

C

```
Alignment of Sequence_1:  [rbxl unmutated template.xdna] with  Sequence_2: [rbxl
mutated.xdna]

Similarity : 439/442 (99.32 %)

Seq_1  1     GATCGCCGTGTAATTCTAGTTGTTTAAACGAGCTCGCTAGCCTTCAGAAGAGTGTACTGT  60
             ||||||||||||||||||||||||||||||||||||||||||||||||||||||||||||
Seq_2  1     GATCGCCGTGTAATTCTAGTTGTTTAAACGAGCTCGCTAGCCTTCAGAAGAGTGTACTGT  60

Seq_1  61    CGCATGGGGAGTCTGTAACCATGCTTTTCACTTCCACTGCATCTCTCGCTGGCTCAAAAC  120
             ||||||||||||||||||||||||||||||||||||||||||||||||||||||||||||
Seq_2  61    CGCATGGGGAGTCTGTAACCATGCTTTTCACTTCCACTGCATCTCTCGCTGGCTCAAAAC  120

Seq_1  121   ACGACAGGTGTGTCCATTGGACAACAGAGAGTGGGAATTCCAAAAGTATGGGCACTAGGA  180
             ||||||||||||||||||||||||||||||||||||||||||||||||||||||||||||
Seq_2  121   ACGACAGGTGTGTCCATTGGACAACAGAGAGTGGGAATTCCAAAAGTATGGGCACTAGGA  180

Seq_1  181   AAAGACTTCTTCCATCAAGCTTAATTGTTTTGTTATTCATTTAATGACTTTCCCTGCTGT  240
             ||||||||||||||||||||||||||||||||||||||||||||||||||||||||||||
Seq_2  181   AAAGACTTCTTCCATCAAGCTTAATTGTTTTGTTATTCATTTAATGACTTTCCCTGCTGT  240

Seq_1  241   TACCTAATTACAAATTGGATGGAACTGTGTTTTTTTCTGCTTTGTTTTTTCAGTTTGCTG  300
             ||||||||||||||||||||||||||||||||||||||||||||||||||||||||||||
Seq_2  241   TACCTAATTACAAATTGGATGGAACTGTGTTTTTTTCTGCTTTGTTTTTTCAGTTTGCTG  300

Seq_1  301   TTTCTGTAGCCATATTGTATTCTGTGTCAAATAAA-GTCCAGTTGGATTCTGGAACGGAT  359
             |||||||||||||||||||||||||||||||||#|##|#|||||||||||||||||||||
Seq_2  301   TTTCTGTAGCCATATTGTATTCTGTGTCAAATAAATGAAC-GTTGGATTCTGGAACGGAT  359

Seq_1  360   GCTCTCTCTTGTGTATGCTCGAGTCTAGAGTCGACCTGCAGGCATGCAAGCTGATCCGGC  419
             ||||||||||||||||||||||||||||||||||||||||||||||||||||||||||||
Seq_2  360   GCTCTCTCTTGTGTATGCTCGAGTCTAGAGTCGACCTGCAGGCATGCAAGCTGATCCGGC  419

Seq_1  420   TGCTAACAAAGCCCGAAAGGAAG  442
             |||||||||||||||||||||||
Seq_2  420   TGCTAACAAAGCCCGAAAGGAAG  442
```

Figure 6.6, continued: (B) Sequencing results of a failed mutagenesis reaction where the binding site for miR-378 was not mutated and hence 100% similar to the reference sequence. **(C)** Successful mutated plasmid was obtained when the miR-378 binding site was seen to have been mutated. Mutated bases were marked by hash tags (#) as the discrepancies to the non-mutated template.

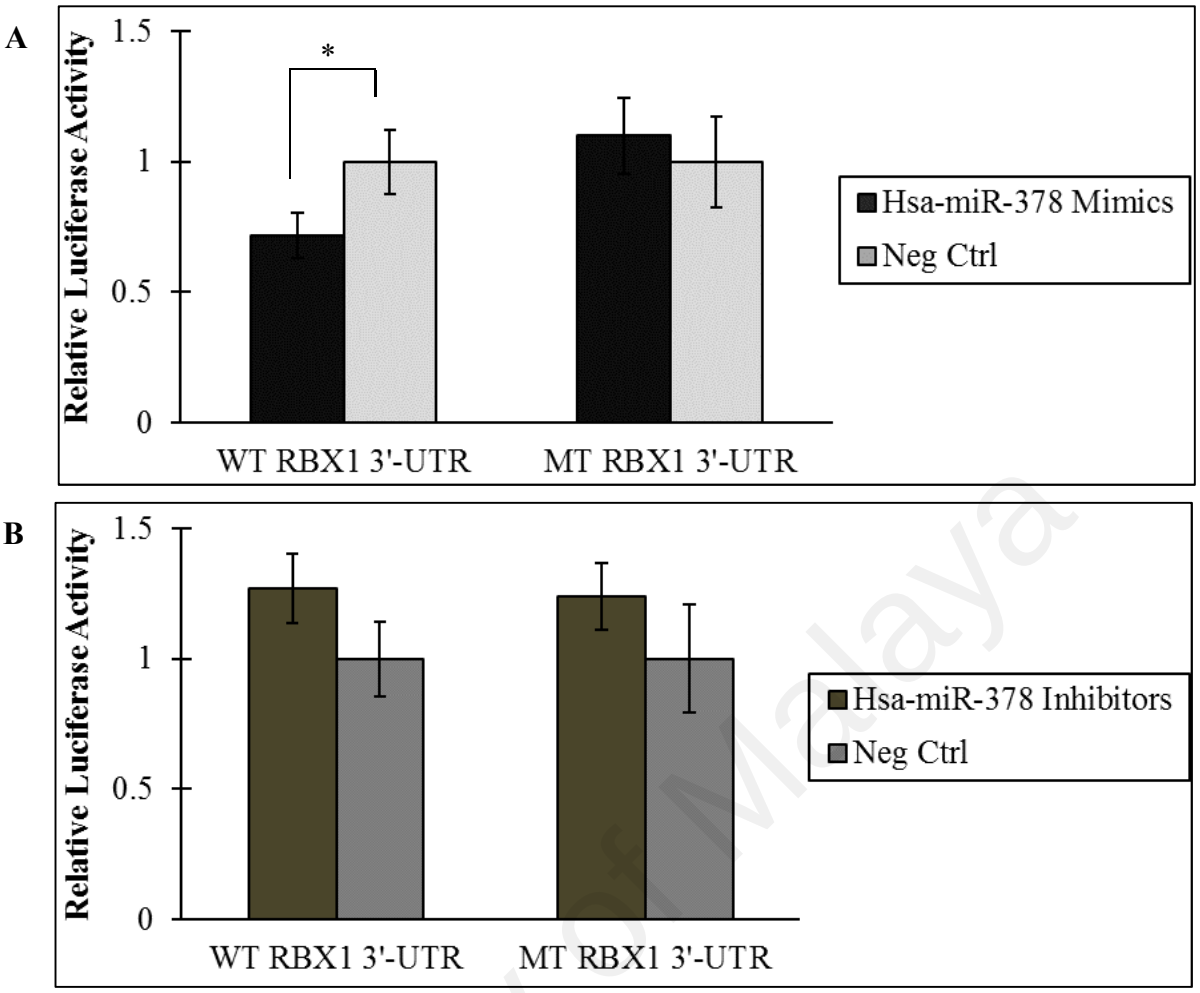

Figure 6.7: Dual luciferase reporter assay on miR-378-*RBX1* interaction. A549-I7 cells were co-transfected with either **(A)** miR-378 mimics/ negative mimics control or **(B)** miR-378 hairpin inhibitors/ negative inhibitors control and WT or MT RBX1 3'-UTR plasmid. Luciferase activity was assayed 48 hours after transfection. Relative luciferase activities were measured and calculated as ratio of firefly luciferase/*Renilla* luciferase activities in the cells, and normalised to those of negative controls. * $P < 0.05$

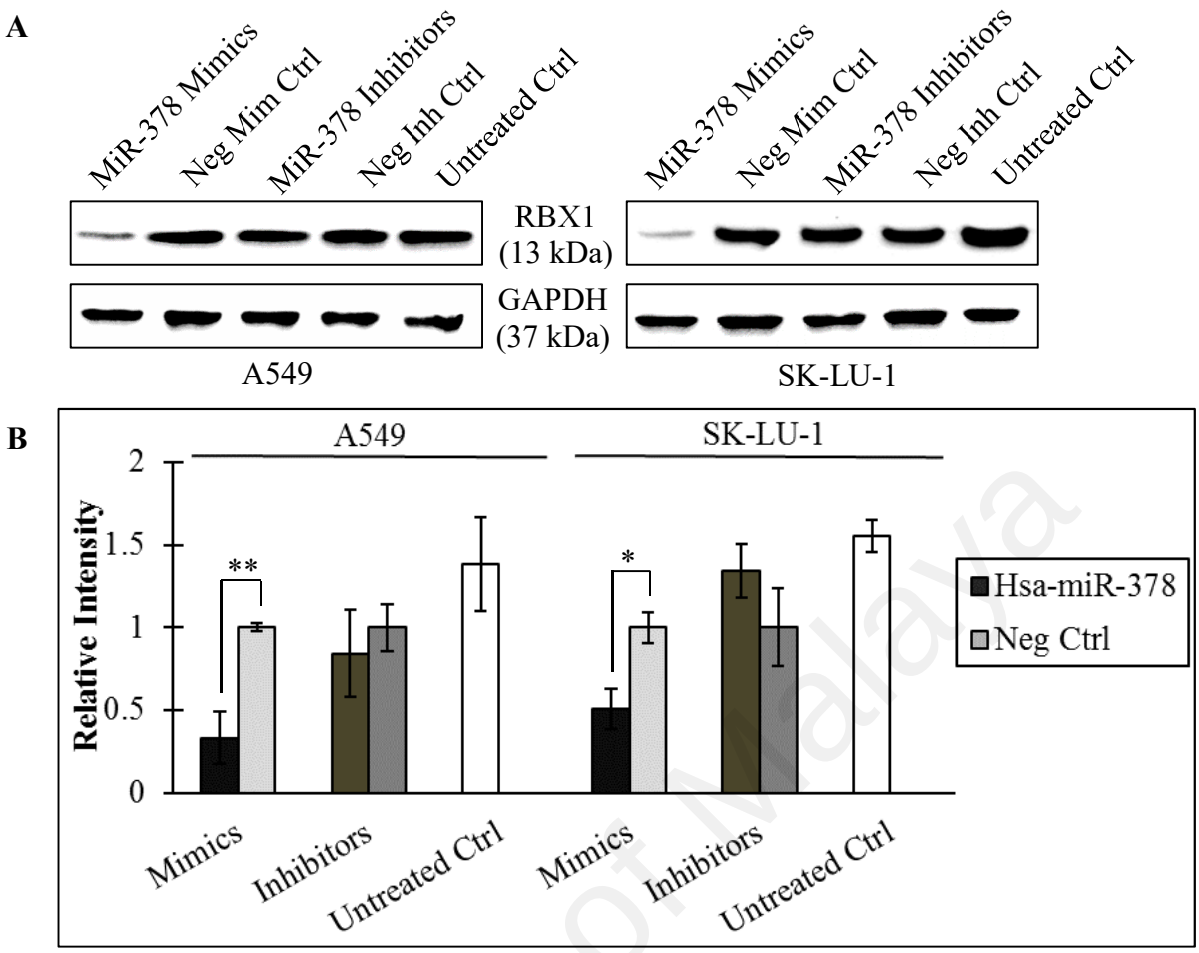

Figure 6.8: *RBX1* is a target of miR-378. (A) Immunoblot analysis of RBX1 expression in transfected A549 and SK-LU-1. GAPDH served as a loading control. RBX1 protein level was dramatically decreased in miR-378-expressing cells. **(B)** Relative expression of RBX1 was determined by normalising to negative controls (n = 3 ± SEM, * $P < 0.05$, ** $P < 0.01$).

6.3 *MYC* is not A Target of MiR-1827

MYC was known to be a multiplayer in tumourigenesis (Lutz *et al.*, 2002; Pelengaris & Khan, 2003). By bioinformatics analyses, *MYC* was found to have high capacity to directly interact with miR-1827 (DIANA miTG score: 1.00; TargetScan total context score: -0.58), therefore it is of interest to determine the role of *MYC* under the regulation of miR-1827 to modulate NSCLC metastasis and angiogenesis. To investigate whether *MYC* can be directly targeted by miR-1827 in NSCLC cells, dual luciferase reporters that have either WT 3'-UTR of this gene or the MT 3'-UTR with altered miR-1827 target sites were constructed (Figure 6.9 to Figure 6.12).

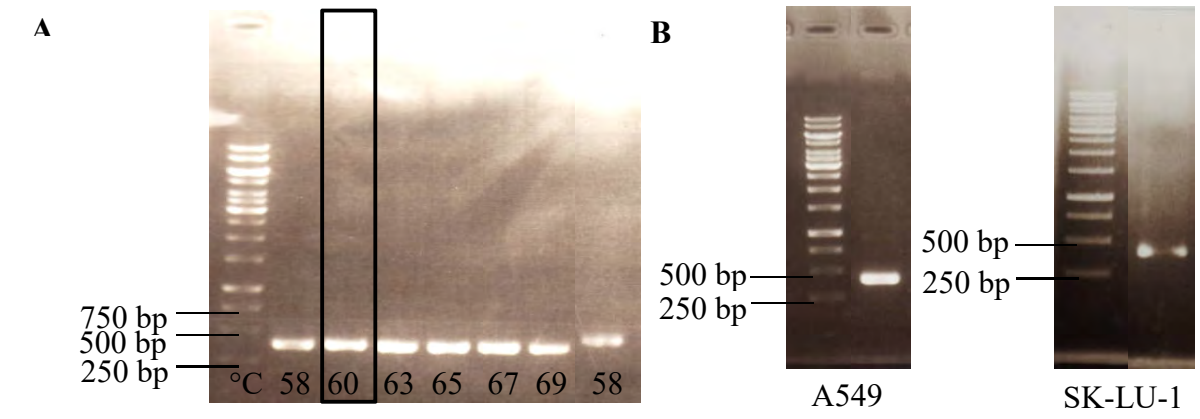

C

Description	Max score	Total score	Query cover	E value	Ident	Accession
Homo sapiens v-myc avian myelocytomatosis viral oncogene homolog (MYC), mRNA	734	734	94%	0.0	100%	NM_002467.4

Homo sapiens v-myc avian myelocytomatosis viral oncogene homolog (MYC), mRNA

Sequence ID: NM_002467.4 Length: 2379 Number of Matches: 1

Range 1: 1826 to 2222 GenBank Graphics

Score	Expect	Identities	Gaps	Strand
734 bits(397)	0.0	397/397(100%)	0/397(0%)	Plus/Minus

```
Query  12    GGATTGAAATTCTGTGTAACTGCTATAAACGTTTTATTAAAGTTATTTACATTTAATGGC  71
Sbjct  2222  GGATTGAAATTCTGTGTAACTGCTATAAACGTTTTATTAAAGTTATTTACATTTAATGGC  2163
Query  72    AATATTTACAGAGAAACATTGTGtaaatcttaaaatttttttaaaaacaattcttaaatac  131
Sbjct  2162  AATATTTACAGAGAAACATTGTGTAAATCTTAAAATTTTTTAAAAACAATTCTTAAATAC  2103
Query  132   aaatctgttaaagaaaaaaaaaaaGATGGTAAGCATAAAAAAGTTCTTTTATGCCCAAAGT  191
Sbjct  2102  AAATCTGTTAAAGAAAAAAAAAAAGATGGTAAGCATAAAAAAGTTCTTTTATGCCCAAAGT  2043
Query  192   CCAATTTGAGGCAGTTTACATTATGGCTAAATCTTTCAGTCTCAAGACTCAGCCAAGGTT  251
Sbjct  2042  CCAATTTGAGGCAGTTTACATTATGGCTAAATCTTTCAGTCTCAAGACTCAGCCAAGGTT  1983
Query  252   GTGAGGTTGCATTTGATCATGCATTTGAAACAAGTTCATAGGTGATTGCTCAGGACATTT  311
Sbjct  1982  GTGAGGTTGCATTTGATCATGCATTTGAAACAAGTTCATAGGTGATTGCTCAGGACATTT  1923
Query  312   CTGTTAGAAGGAATCGTTTTCCTTACTTTTCCTTACGCACAAGAGTTCCGTAGCTGTTCA  371
Sbjct  1922  CTGTTAGAAGGAATCGTTTTCCTTACTTTTCCTTACGCACAAGAGTTCCGTAGCTGTTCA  1863
Query  372   AGTTTGTGTTTCAACTGTTCTCGTCGTTTCCGCAACA  408
Sbjct  1862  AGTTTGTGTTTCAACTGTTCTCGTCGTTTCCGCAACA  1826
```


Description	Max score	Total score	Query cover	E value	Ident	Accession
Homo sapiens v-myc avian myelocytomatosis viral oncogene homolog (MYC), mRNA	734	734	94%	0.0	100%	NM_002467.4

Homo sapiens v-myc avian myelocytomatosis viral oncogene homolog (MYC), mRNA

Sequence ID: NM_002467.4 Length: 2379 Number of Matches: 1

Range 1: 1826 to 2222 GenBank Graphics

Score	Expect	Identities	Gaps	Strand
734 bits(397)	0.0	397/397(100%)	0/397(0%)	Plus/Minus

```
Query  12    GGATTGAAATTCTGTGTAACTGCTATAAACGTTTTATTAAAGTTATTTACATTTAATGGC  71
Sbjct  2222  GGATTGAAATTCTGTGTAACTGCTATAAACGTTTTATTAAAGTTATTTACATTTAATGGC  2163
Query  72    AATATTTACAGAGAAACATTGTGtaaatcttaaaatttttttaaaaacaattcttaaatac  131
Sbjct  2162  AATATTTACAGAGAAACATTGTGTAAATCTTAAAATTTTTTAAAAACAATTCTTAAATAC  2103
Query  132   aaatctgttaaagaaaaaaaaaaaGATGGTAAGCATAAAAAAGTTCTTTTATGCCCAAAGT  191
Sbjct  2102  AAATCTGTTAAAGAAAAAAAAAAAGATGGTAAGCATAAAAAAGTTCTTTTATGCCCAAAGT  2043
Query  192   CCAATTTGAGGCAGTTTACATTATGGCTAAATCTTTCAGTCTCAAGACTCAGCCAAGGTT  251
Sbjct  2042  CCAATTTGAGGCAGTTTACATTATGGCTAAATCTTTCAGTCTCAAGACTCAGCCAAGGTT  1983
Query  252   GTGAGGTTGCATTTGATCATGCATTTGAAACAAGTTCATAGGTGATTGCTCAGGACATTT  311
Sbjct  1982  GTGAGGTTGCATTTGATCATGCATTTGAAACAAGTTCATAGGTGATTGCTCAGGACATTT  1923
Query  312   CTGTTAGAAGGAATCGTTTTCCTTACTTTTCCTTACGCACAAGAGTTCCGTAGCTGTTCA  371
Sbjct  1922  CTGTTAGAAGGAATCGTTTTCCTTACTTTTCCTTACGCACAAGAGTTCCGTAGCTGTTCA  1863
Query  372   AGTTTGTGTTTCAACTGTTCTCGTCGTTTCCGCAACA  408
Sbjct  1862  AGTTTGTGTTTCAACTGTTCTCGTCGTTTCCGCAACA  1826
```


Figure 6.9: Amplification of the 419 bp fragment of the 3'-UTR of MYC. (A) PCR annealing temperature was optimised across different temperatures. Lane 8 represents PCR product amplified by *GAPDH*-specific primers at 58°C. **(B)** The band of interest at 419 bp was excised and purified. **(C)** Sequencing analysis of A549 (upper panel) and SK-LU-1 (lower panel) PCR products.

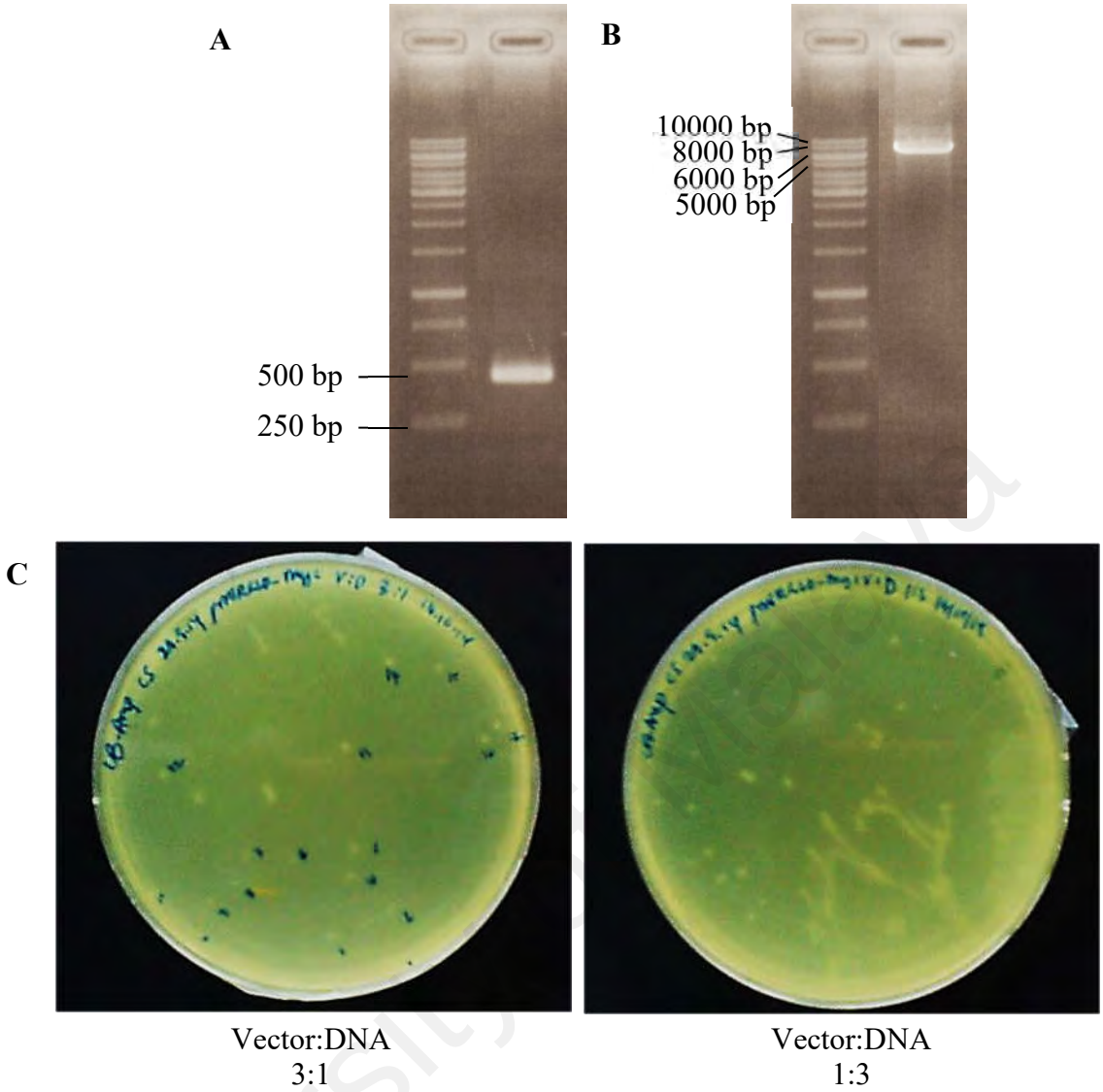

Figure 6.10: Cloning of amplified miRNA target site into 3'-UTR of luciferase reporter vector. Gel images showing **(A)** digested *MYC* and **(B)** digested pmirGLO with restriction enzymes NheI and XhoI. **(C)** *MYC* and pmirGLO were ligated at two ratios and incubated overnight. The ligation products were transformed and plated on LB-Ampicillin agar.

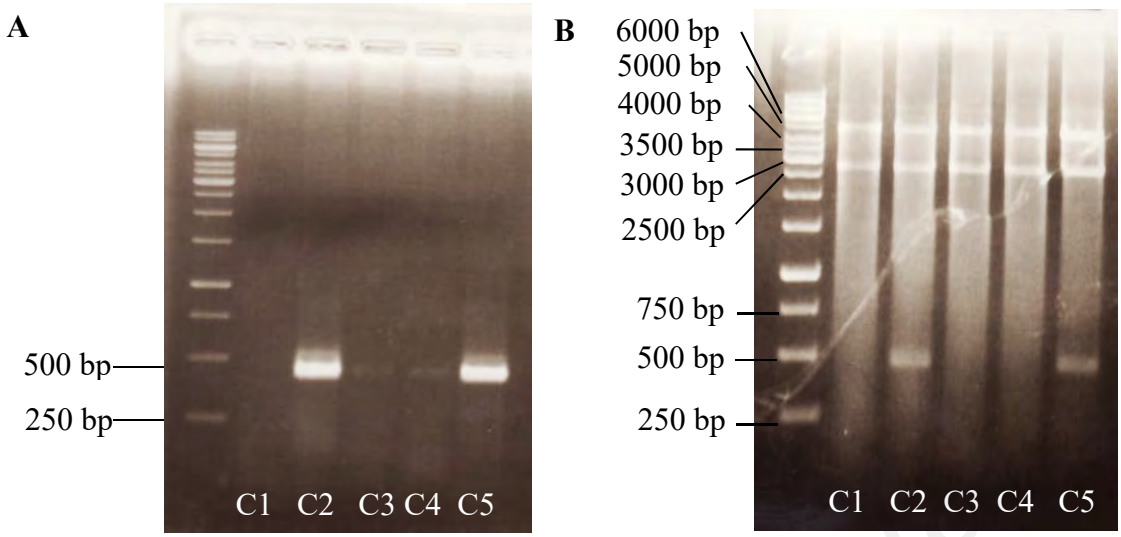

C

```
Alignment of Sequence_1:  [cloned myc snapgene.xdna] with  Sequence_2: [cloned m
sequenced.xdna]

Similarity : 504/504 (100.00 %)

Seq_1  1     gatcgccgtgtaattctagttgtttaaacgagctcgctagctgttgcggaaacgacgaga  60
             ||||||||||||||||||||||||||||||||||||||||||||||||||||||||||||
Seq_2  1     GATCGCCGTGTAATTCTAGTTGTTTAAACGAGCTCGCTAGCTGTTGCGGAAACGACGAGA  60

Seq_1  61    acagttgaaacacaaacttgaacagctacggaactcttgtgcgtaaggaaaagtaaggaa  120
             ||||||||||||||||||||||||||||||||||||||||||||||||||||||||||||
Seq_2  61    ACAGTTGAAACACAAACTTGAACAGCTACGGAACTCTTGTGCGTAAGGAAAAGTAAGGAA  120

Seq_1  121   aacgattccttctaacagaaatgtcctgagcaatcacctatgaacttgtttcaaatgcat  180
             ||||||||||||||||||||||||||||||||||||||||||||||||||||||||||||
Seq_2  121   AACGATTCCTTCTAACAGAAATGTCCTGAGCAATCACCTATGAACTTGTTTCAAATGCAT  180

Seq_1  181   gatcaaatgcaacctcacaaccttggctgagtcttgagactgaaagatttagccataatg  240
             ||||||||||||||||||||||||||||||||||||||||||||||||||||||||||||
Seq_2  181   GATCAAATGCAACCTCACAACCTTGGCTGAGTCTTGAGACTGAAAGATTTAGCCATAATG  240

Seq_1  241   taaactgcctcaaattggactttgggcataaaagaacttttttatgcttaccatcttttt  300
             ||||||||||||||||||||||||||||||||||||||||||||||||||||||||||||
Seq_2  241   TAAACTGCCTCAAATTGGACTTTGGGCATAAAAGAACTTTTTTATGCTTACCATCTTTTT  300

Seq_1  301   ttttctttaacagatttgtatttaagaattgtttttaaaaaattttaagatttacacaa  360
             ||||||||||||||||||||||||||||||||||||||||||||||||||||||||||||
Seq_2  301   TTTTTCTTTAACAGATTTGTATTTAAGAATTGTTTTTAAAAAATTTTAAGATTTACACAA  360

Seq_1  361   tgtttctctgtaaatattgccattaaatgtaaataactttaataaaacgtttatagcagt  420
             ||||||||||||||||||||||||||||||||||||||||||||||||||||||||||||
Seq_2  361   TGTTTCTCTGTAAATATTGCCATTAAATGTAAATAACTTTAATAAAACGTTTATAGCAGT  420

Seq_1  421   tacacagaatttcaatccctcgagtctagagtcgacctgcaggcatgcaagctgatccgg  480
             ||||||||||||||||||||||||||||||||||||||||||||||||||||||||||||
Seq_2  421   TACACAGAATTTCAATCCCTCGAGTCTAGAGTCGACCTGCAGGCATGCAAGCTGATCCGG  480

Seq_1  481   ctgctaacaaagcccgaaaggaag  504
             |||||||||||||||||||||||||
Seq_2  481   CTGCTAACAAAGCCCGAAAGGAAG  504
```

Figure 6.11: Screening for colonies that contained an insert. (A) Five colonies were analysed on colony PCR and two colonies were positive. **(B)** Restriction enzyme analysis by SspI confirmed the presence of MYC 3'-UTR in colonies 2 and 5, indicated by three digested bands instead of two. **(C)** Colony 2 was sequenced and the sequence was identical to reference sequence generated by SnapGene.

A

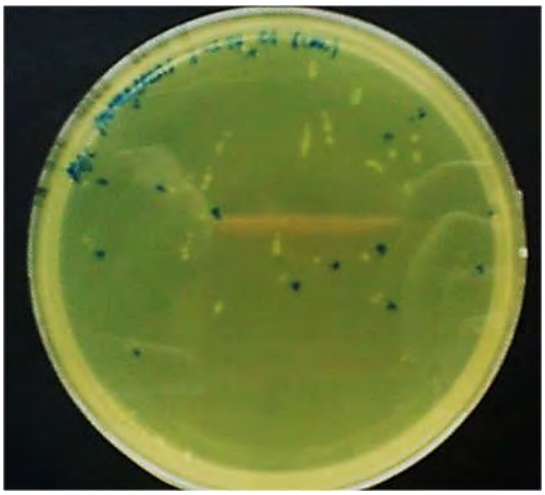

Experimental Mutagenesis

B

```
Alignment of Sequence_1:  [myc unmutated template.txt.xdna] with  Sequence_2: [
mutated.txt.xdna]

Similarity : 504/504 (100.00 %)

Seq_1  1     GATCGCCGTGTAATTCTAGTTGTTTAAACGAGCTCGCTAGCTGTTGCGGAAACGACGAGA  60
             ||||||||||||||||||||||||||||||||||||||||||||||||||||||||||||
Seq_2  1     GATCGCCGTGTAATTCTAGTTGTTTAAACGAGCTCGCTAGCTGTTGCGGAAACGACGAGA  60

Seq_1  61    ACAGTTGAAACACAAACTTGAACAGCTACGGAACTCTTGTGCGTAAGGAAAAGTAAGGAA  120
             ||||||||||||||||||||||||||||||||||||||||||||||||||||||||||||
Seq_2  61    ACAGTTGAAACACAAACTTGAACAGCTACGGAACTCTTGTGCGTAAGGAAAAGTAAGGAA  120

Seq_1  121   AACGATTCCTTCTAACAGAAATGTCCTGAGCAATCACCTATGAACTTGTTTCAAATGCAT  180
             ||||||||||||||||||||||||||||||||||||||||||||||||||||||||||||
Seq_2  121   AACGATTCCTTCTAACAGAAATGTCCTGAGCAATCACCTATGAACTTGTTTCAAATGCAT  180

Seq_1  181   GATCAAATGCAACCTCACAACCTTGGCTGAGTCTTGAGACTGAAAGATTTAGCCATAATG  240
             ||||||||||||||||||||||||||||||||||||||||||||||||||||||||||||
Seq_2  181   GATCAAATGCAACCTCACAACCTTGGCTGAGTCTTGAGACTGAAAGATTTAGCCATAATG  240

Seq_1  241   TAAACTGCCTCAAATTGGACTTTGGGCATAAAAGAACTTTTTTATGCTTACCATCTTTTT  300
             ||||||||||||||||||||||||||||||||||||||||||||||||||||||||||||
Seq_2  241   TAAACTGCCTCAAATTGGACTTTGGGCATAAAAGAACTTTTTTATGCTTACCATCTTTTT  300

Seq_1  301   TTTTTCTTTAACAGATTTGTATTTAAGAATTGTTTTTAAAAAATTTTAAGATTTACACAA  360
             ||||||||||||||||||||||||||||||||||||||||||||||||||||||||||||
Seq_2  301   TTTTTCTTTAACAGATTTGTATTTAAGAATTGTTTTTAAAAAATTTTAAGATTTACACAA  360

Seq_1  361   TGTTTCTCTGTAAATATTGCCATTAAATGTAAATAACTTTAATAAAACGTTTATAGCAGT  420
             ||||||||||||||||||||||||||||||||||||||||||||||||||||||||||||
Seq_2  361   TGTTTCTCTGTAAATATTGCCATTAAATGTAAATAACTTTAATAAAACGTTTATAGCAGT  420

Seq_1  421   TACACAGAATTTCAATCCCTCGAGTCTAGAGTCGACCTGCAGGCATGCAAGCTGATCCGG  480
             ||||||||||||||||||||||||||||||||||||||||||||||||||||||||||||
Seq_2  421   TACACAGAATTTCAATCCCTCGAGTCTAGAGTCGACCTGCAGGCATGCAAGCTGATCCGG  480

Seq_1  481   CTGCTAACAAAGCCCGAAAGGAAG  504
             ||||||||||||||||||||||||
Seq_2  481   CTGCTAACAAAGCCCGAAAGGAAG  504
```

Figure 6.12: Site-directed mutagenesis of MYC 3'-UTR. (A) Mutagenesis by PCR amplification produced a number of colonies on agar plates. Colonies were picked and purified for sequencing. **(B)** Mutagenesis was considered unsuccessful when the miR-1827 binding site was not mutated.

C

```
Alignment of Sequence_1:  [myc unmutated template.txt.xdna] with  Sequence_2: [myc
mutated.txt.xdna]

Similarity : 500/504 (99.21 %)

Seq_1  1     GATCGCCGTGTAATTCTAGTTGTTTAAACGAGCTCGCTAGCTGTTGCGGAAACGACGAGA  60
             ||||||||||||||||||||||||||||||||||||||||||||||||||||||||||||
Seq_2  1     GATCGCCGTGTAATTCTAGTTGTTTAAACGAGCTCGCTAGCTGTTGCGGAAACGACGAGA  60

Seq_1  61    ACAGTTGAAACACAAACTTGAACAGCTACGGAACTCTTGTGCGTAAGGAAAAGTAAGGAA  120
             ||||||||||||||||||||||||||||||||||||||||||||||||||||||||||||
Seq_2  61    ACAGTTGAAACACAAACTTGAACAGCTACGGAACTCTTGTGCGTAAGGAAAAGTAAGGAA  120

Seq_1  121   AACGATTCCTTCTAACAGAAATGTCCTGAGCAATCACCTATGAACTTGTTTCAAATGCAT  180
             ||||||||||||||||||||||||||||||||||||||||||||||||||||||||||||
Seq_2  121   AACGATTCCTTCTAACAGAAATGTCCTGAGCAATCACCTATGAACTTGTTTCAAATGCAT  180

Seq_1  181   GATCAAATGCAACCTCACAACCTTGGCTGAGTCTTGAGACTGAAAGATTTAGCCATAATG  240
             ||||||||||||||||||||||||||||||||||||||||||||||||||||||||||||
Seq_2  181   GATCAAATGCAACCTCACAACCTTGGCTGAGTCTTGAGACTGAAAGATTTAGCCATAATG  240

Seq_1  241   TAAACT---GCCTCAAATTGGACTTTGGGCATAAAAGAACTTTTTTATGCTTACCATCTT  297
             ||||||###|####||||||||||||||||||||||||||||||||||||||||||||||
Seq_2  241   TAAACTTAAGA---AAATTGGACTTTGGGCATAAAAGAACTTTTTTATGCTTACCATCTT  297

Seq_1  298   TTTTTTTTCTTTAACAGATTTGTATTTAAGAATTGTTTTTAAAAAATTTTAAGATTTACA  357
             ||||||||||||||||||||||||||||||||||||||||||||||||||||||||||||
Seq_2  298   TTTTTTTTCTTTAACAGATTTGTATTTAAGAATTGTTTTTAAAAAATTTTAAGATTTACA  357

Seq_1  358   CAATGTTTCTCTGTAAATATTGCCATTAAATGTAAATAACTTTAATAAAACGTTTATAGC  417
             ||||||||||||||||||||||||||||||||||||||||||||||||||||||||||||
Seq_2  358   CAATGTTTCTCTGTAAATATTGCCATTAAATGTAAATAACTTTAATAAAACGTTTATAGC  417

Seq_1  418   AGTTACACAGAATTTCAATCCCTCGAGTCTAGAGTCGACCTGCAGGCATGCAAGCTGATC  477
             ||||||||||||||||||||||||||||||||||||||||||||||||||||||||||||
Seq_2  418   AGTTACACAGAATTTCAATCCCTCGAGTCTAGAGTCGACCTGCAGGCATGCAAGCTGATC  477

Seq_1  478   CGGCTGCTAACAAAGCCCGAAAGGAAG  504
             ||||||||||||||||||||||||||
Seq_2  478   CGGCTGCTAACAAAGCCCGAAAGGAAG  504
```

Figure 6.12, continued: (C) MT MYC 3'-UTR plasmid that consisted of altered bases was ready for luciferase reporter assay.

The reporter plasmids were transfected into A549-I7 cells with or without miR-1827 mimics/ hairpin inhibitors. Transfection of miR-1827 mimics into A549-I7 cells did not significantly decrease luciferase expression of transcripts containing an exact or partially complementary (mutated) miR-1827 binding site (Figure 6.13A). This was also in accordance with the experiment using miR-1827 hairpin inhibitors, in which changes in luciferase activities of both miR-1827 hairpin inhibitors/WT MYC 3'-UTR and miR-1827 hairpin inhibitors/MT MYC 3'-UTR were not significant in comparison to the negative control (Figure 6.13B). Taken together, these data suggest that miR-1827 does not regulate *MYC* expression through the miR-1827 binding site in the MYC 3'-UTR.

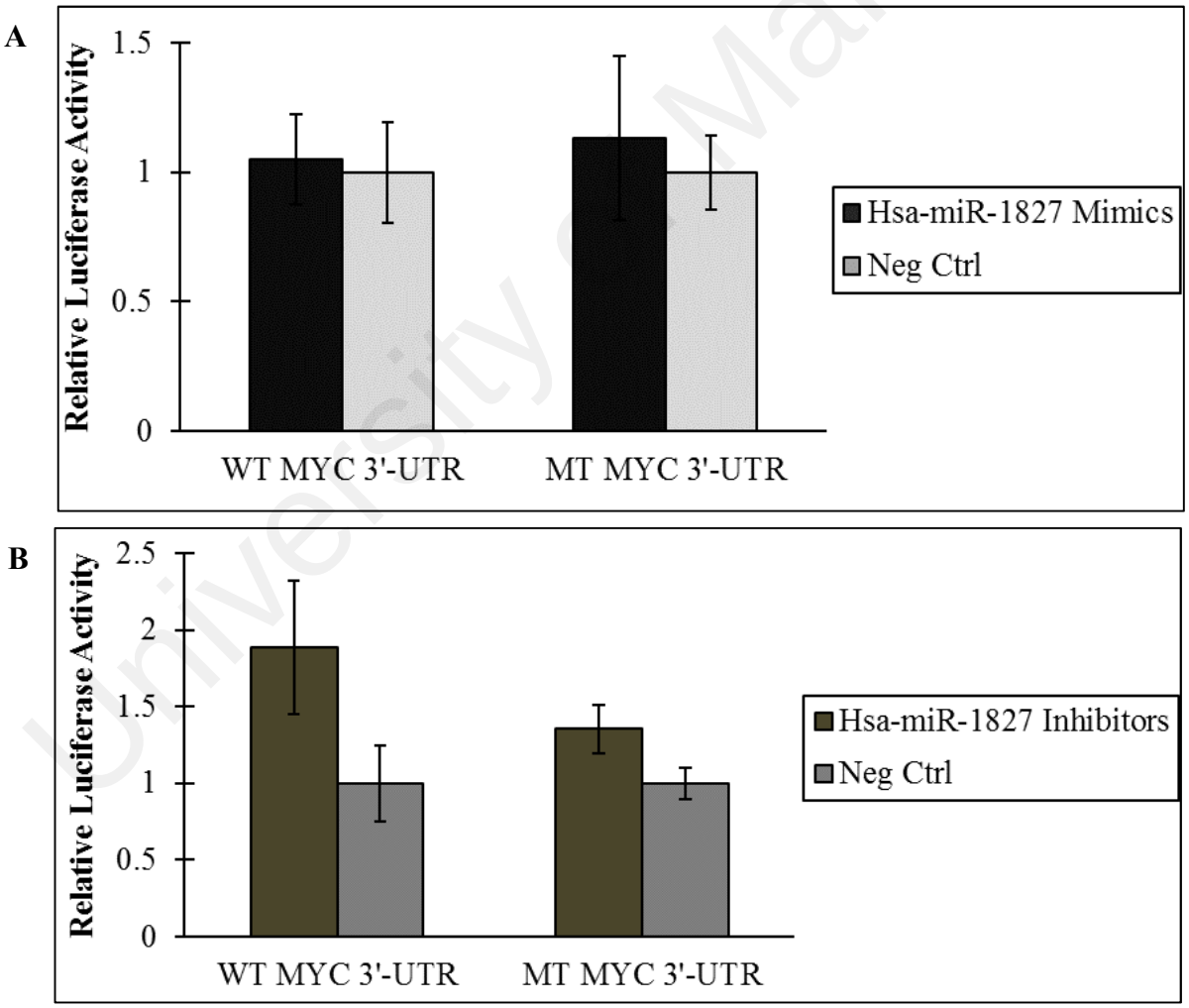

Figure 6.13: MiR-1827 transfection did not down-regulate the luciferase activity. The complementary miR-1827 binding site was inserted downstream of a luciferase reporter on the pmirGLO plasmid and transfected into A549-I7 cells with **(A)** miR-1827 mimics or **(B)** miR-1827 hairpin inhibitors. Partially complementary miR-1827 binding site found in the MYC 3'-UTR (or a mutated binding site) was used for validation of specific miR-1827 seed region-MYC 3'-UTR binding site interaction.

6.4 MiR-1827 Directly Regulates *CRKL*

This led to the validation of alternative gene target for miR-1827. *In silico* analyses revealed that *CRKL* is another potential target of miR-1827. *CRKL* acts as adaptor in diverse signalling pathways (Birge *et al.*, 1993; Knudsen *et al.*, 1994) but how it functions in tumorigenesis is still poorly understood, partly due to its highly pleotropic nature (Chodniewicz & Klemke, 2004; Bell & Park, 2012). MiR-1827 has sequence complementary to a region within the 3'-UTR of the transcript for human *CRKL*, extending between bases 4820 and 4827. To verify the prediction, pmirGLO luciferase vectors which contained WT or MT CRKL 3'-UTR (miR-1827 binding site) were constructed (Figure 6.14 to Figure 6.16). Interestingly, a SNP was found at the 221st base of A549 amplified CRKL 3'-UTR (Figure 6.14C). This was not significant because the particular SNP was not located at the miR-1827 binding site. However, to comply with the reference database, SK-LU-1 amplified CRKL 3'-UTR was used for cloning. Mutagenesis of CRKL 3'-UTR was outsourced due to the repeated failures to perform mutagenesis with the multi-site directed mutagenesis kit (Figure 6.17).

Dual luciferase reporter assay was performed in A549-I7 cells co-transfected with miR-1827 mimics/ hairpin inhibitors or negative mimics/ inhibitors control and WT/ MT CRKL 3'-UTR reporter plasmids. The luciferase activity analysis showed that ectopic expression of miR-1827 significantly suppressed the luciferase activity of WT vector but not the mutant reporter (Figure 6.18A). This suggests that miR-1827 could bind directly to specific site in the 3'-UTR of CRKL mRNA. Nonetheless, the effect of miR-1827 hairpin inhibitors on WT CRKL 3'-UTR was insignificant (Figure 6.18B).

The effect of miR-1827 on *CRKL* expression at the level of translation was determined by immunoblotting. Transfection of miR-1827 mimics led to a significant decrease in CRKL expression in both A549 and SK-LU-1 (Figure 6.19A).

Quantification of immunoblots showed that miR-1827 mimics significantly decreased CRKL expression by ~50% in A549 and ~70% in SK-LU-1 (Figure 6.19B).

Figure 6.14: The 3'-UTR fragment of CRKL was PCR-amplified. (A) *CRKL* was amplified using optimal temperature 63°C. Lane 2 represents amplified *GAPDH* at 58°C. **(B)** *CRKL* was amplified from RNA of A549 and SK-LU-1. PCR products (327 bp) were analysed by gel and purified. **(C)** Sequences were aligned against NCBI reference dataset and compared for similarity. Upper panel: A549; Lower panel: SK-LU-1

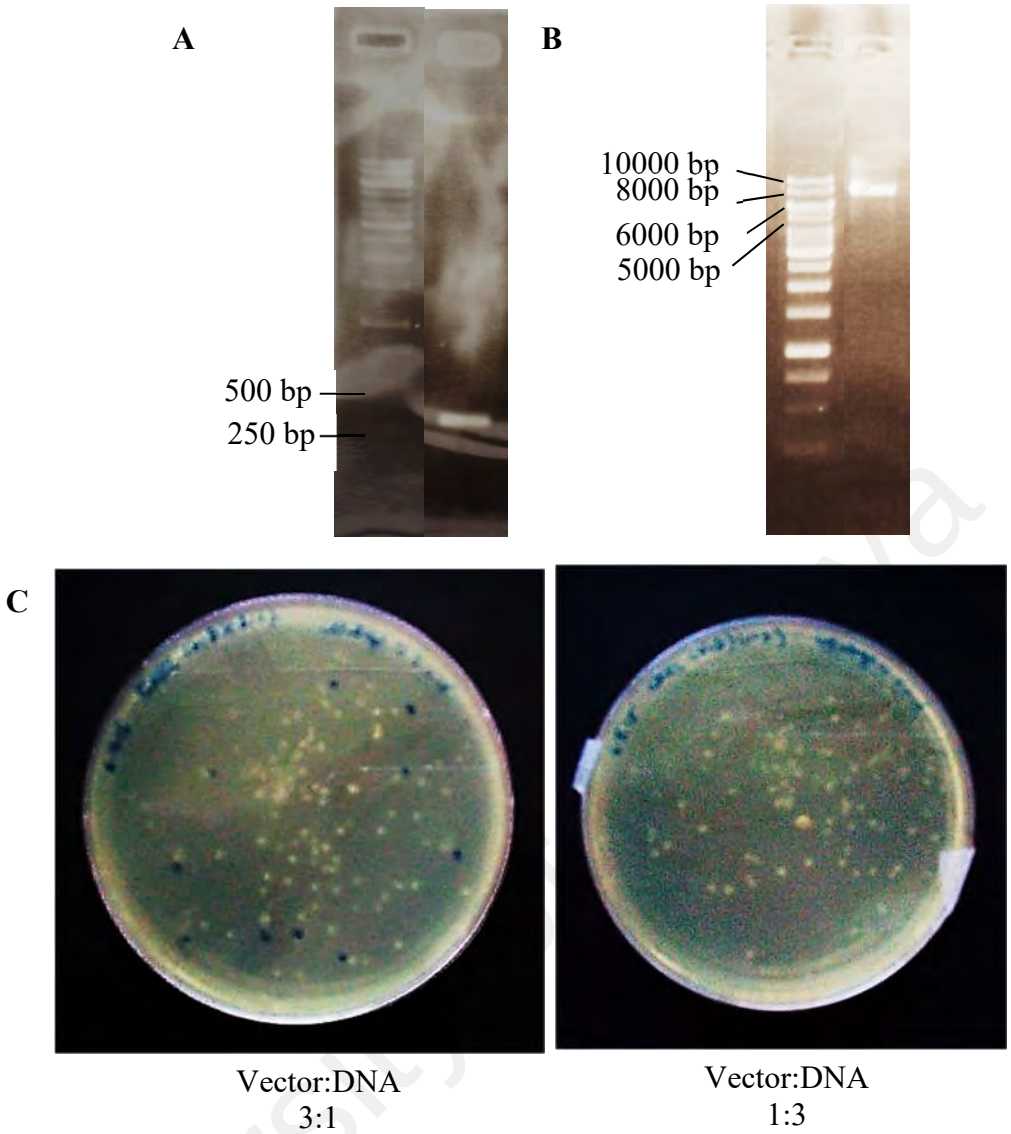

Figure 6.15: Generation of 3'-UTR reporter clones for miRNA target validation. **(A)** Cut *CRKL* and **(B)** Cut pmirGLO were analysed on gel after restriction enzymes digestion. **(C)** Vector and DNA were mixed at 3:1 and 1:3 ratios, transformed into *E. coli* the next day and plated on LB-Ampicillin agar.

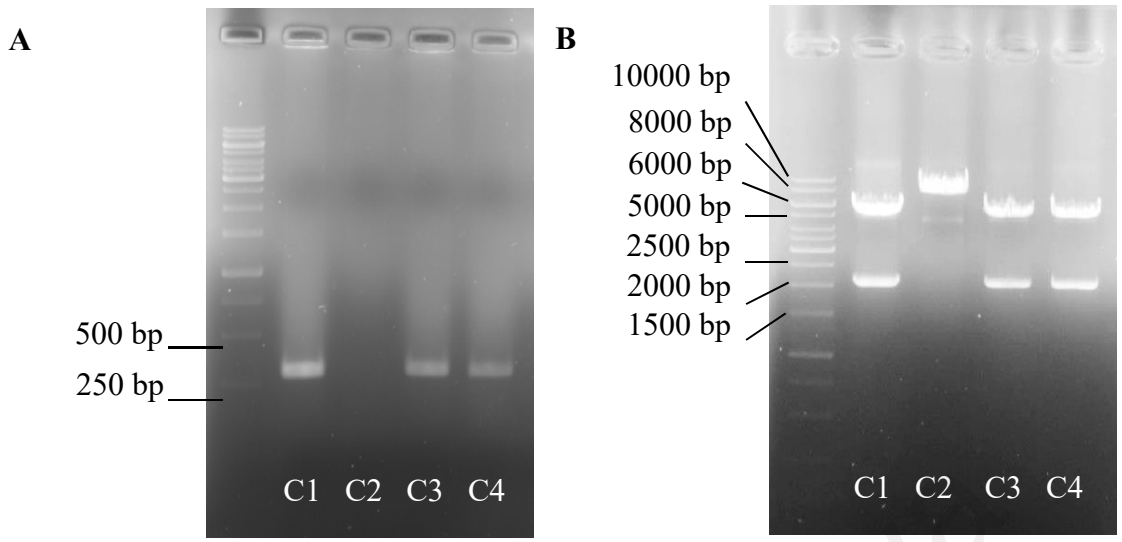

C

```
Alignment of Sequence_1:  [cloned crkl snapgene.xdna] with  Sequence_2: [cloned
crkl sequenced.txt.xdna]

Similarity : 412/412 (100.00 %)

Seq_1  1     GATCGCCGTGTAATTCTAGTTGTTTAAACGAGCTCGCTAGCATCAGCTCGTTACTTCAGC  60
             ||||||||||||||||||||||||||||||||||||||||||||||||||||||||||||
Seq_2  1     GATCGCCGTGTAATTCTAGTTGTTTAAACGAGCTCGCTAGCATCAGCTCGTTACTTCAGC  60

Seq_1  61    CCATGAAAATGGCATCCAGGGCTGCCAGGAGATTCAGAGCTCAAAACAAGGCGAGCTTGA  120
             ||||||||||||||||||||||||||||||||||||||||||||||||||||||||||||
Seq_2  61    CCATGAAAATGGCATCCAGGGCTGCCAGGAGATTCAGAGCTCAAAACAAGGCGAGCTTGA  120

Seq_1  121   GTTCTGCACTCCAGATGTGTGCCAAAACTAGTAAAACTTAACGGACTTACAACCTTGTCA  180
             ||||||||||||||||||||||||||||||||||||||||||||||||||||||||||||
Seq_2  121   GTTCTGCACTCCAGATGTGTGCCAAAACTAGTAAAACTTAACGGACTTACAACCTTGTCA  180

Seq_1  181   GTTTTTTTAATGAGGCAGGGATACTCTGTTTTTCACACTAAACATATGAATGCAGCACTG  240
             ||||||||||||||||||||||||||||||||||||||||||||||||||||||||||||
Seq_2  181   GTTTTTTTAATGAGGCAGGGATACTCTGTTTTTCACACTAAACATATGAATGCAGCACTG  240

Seq_1  241   CTGCCTCAGCTCAGCTTCGTGCCTGGGTTCCCCACTGGTCTGGGAAGACTGTTGTGCTCC  300
             ||||||||||||||||||||||||||||||||||||||||||||||||||||||||||||
Seq_2  241   CTGCCTCAGCTCAGCTTCGTGCCTGGGTTCCCCACTGGTCTGGGAAGACTGTTGTGCTCC  300

Seq_1  301   ATAGAGCAGTGCACATCTGACCCAGAGGGTGGGTGTTCATAACTGCCTCGAGTCTAGAGT  360
             ||||||||||||||||||||||||||||||||||||||||||||||||||||||||||||
Seq_2  301   ATAGAGCAGTGCACATCTGACCCAGAGGGTGGGTGTTCATAACTGCCTCGAGTCTAGAGT  360

Seq_1  361   CGACCTGCAGGCATGCAAGCTGATCCGGCTGCTAACAAAGCCCGAAAGGAAG  412
             ||||||||||||||||||||||||||||||||||||||||||||||||||||
Seq_2  361   CGACCTGCAGGCATGCAAGCTGATCCGGCTGCTAACAAAGCCCGAAAGGAAG  412
```

Figure 6.16: Screening by colony PCR and restriction digestion. (A) Transformants were screened by colony PCR for the presence of CRKL 3'-UTR. Colonies 1, 3 and 4 showed a distinct band between 250 bp and 500 bp. **(B)** Plasmids were extracted from the four colonies and digested with SpeI. Two restriction sites were cut when CRKL 3'-UTR was successfully inserted. **(C)** Sequence of cloned pmirGLO-CRKL 3'-UTR was compared to reference sequence generated using SnapGene.

```
Alignment of Sequence_1:  [crkl unmutated template.xdna] with  Sequence_2: [crkl
mutated.xdna]

Similarity : 340/345 (98.55 %)

Seq_1  1     AATGGCATCCAGGGCTGCCAGGAGATTCAGAGCTCAAAACAAGGCGAGCTTGAGTTCTGC  60
             ||||||||||||||||||||||||||||||||||||||||||||||||||||||||||||
Seq_2  1     AATGGCATCCAGGGCTGCCAGGAGATTCAGAGCTCAAAACAAGGCGAGCTTGAGTTCTGC  60

Seq_1  61    ACTCCAGATGTGTGCCAAAACTAGTAAAACTTAACGGACTTACAACCTTGTCAGTTTTTT  120
             ||||||||||||||||||||||||||||||||||||||||||||||||||||||||||||
Seq_2  61    ACTCCAGATGTGTGCCAAAACTAGTAAAACTTAACGGACTTACAACCTTGTCAGTTTTTT  120

Seq_1  121   TAATGAGGCAGGGATACTCTGTTTTTCACACTAAACATATGAATGCAGCACTGC-TGCCT  179
             ||||||||||||||||||||||||||||||||||||||||||||||||||||#|####
Seq_2  121   TAATGAGGCAGGGATACTCTGTTTTTCACACTAAACATATGAATGCAGCACTGCGTAAGA  180

Seq_1  180   CAGCTCAGCTTCGTGCCTGGGTTCCCCACTGGTCTGGGAAGACTGTTGTGCTCCATAGAG  239
             #||||||||||||||||||||||||||||||||||||||||||||||||||||||||||||
Seq_2  181   -AGCTCAGCTTCGTGCCTGGGTTCCCCACTGGTCTGGGAAGACTGTTGTGCTCCATAGAG  239

Seq_1  240   CAGTGCACATCTGACCCAGAGGGTGGGTGTTCATAACTGCCTCGAGTCTAGAGTCGACCT  299
             ||||||||||||||||||||||||||||||||||||||||||||||||||||||||||||
Seq_2  240   CAGTGCACATCTGACCCAGAGGGTGGGTGTTCATAACTGCCTCGAGTCTAGAGTCGACCT  299

Seq_1  300   GCAGGCATGCAAGCTGATCCGGCTGCTAACAAAGCCCGAAAGGAAG  345
             |||||||||||||||||||||||||||||||||||||||||||||
Seq 2  300   GCAGGCATGCAAGCTGATCCGGCTGCTAACAAAGCCCGAAAGGAAG  345
```

Figure 6.17: Mutagenesis of WT CRKL 3'-UTR plasmid produced MT CRKL 3'-UTR plasmid which contained mutated bases at the miR-1827 binding site.

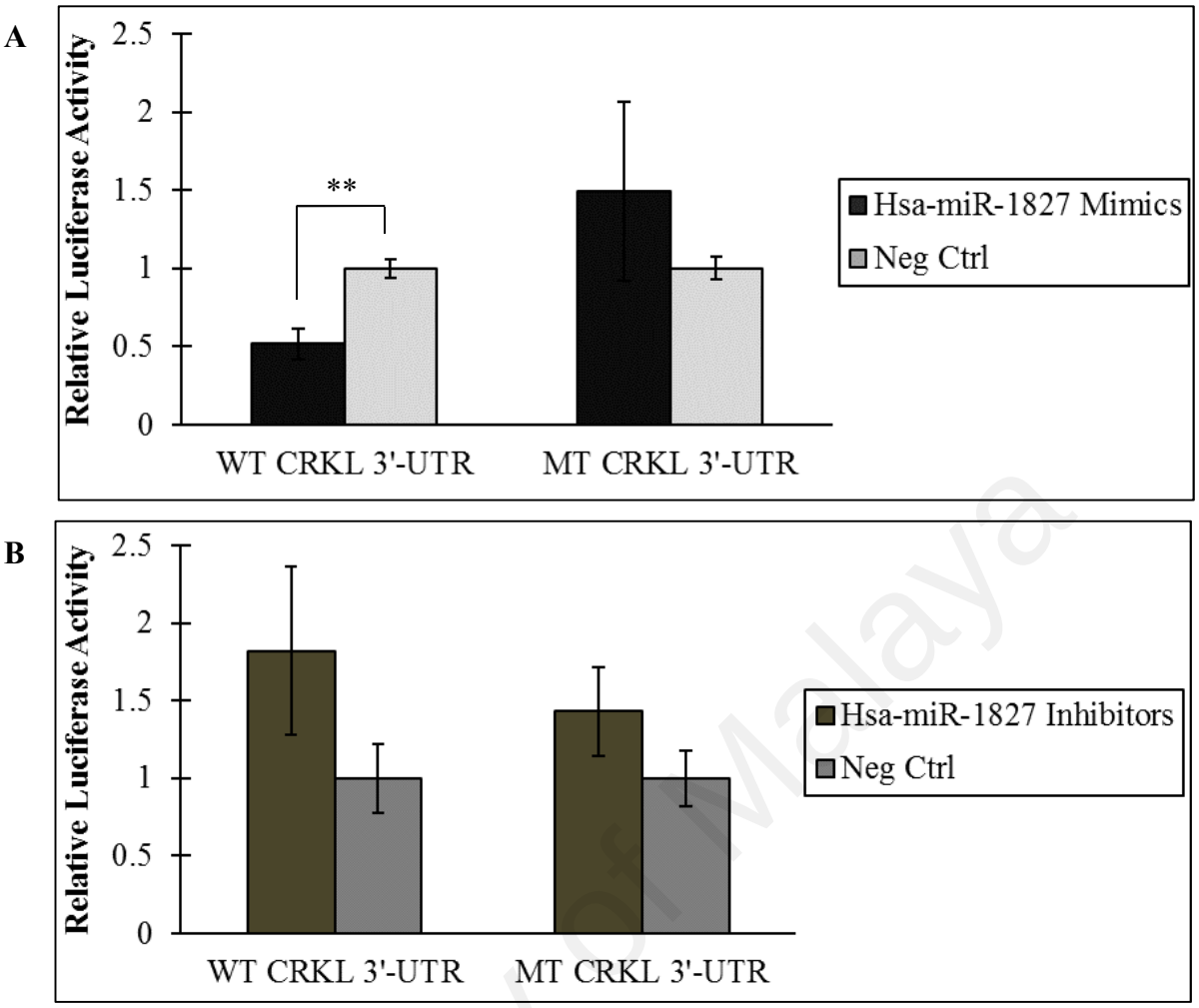

Figure 6.18: MiR-1827 inhibits *CRKL* by targeting CRKL 3'-UTR. (A) Relative luciferase activity of A549-I7 cells co-transfected with a reporter vector containing the WT or MT 3'-UTR of CRKL and miR-1827 mimics or negative mimics control. **(B)** Luciferase reporter vectors co-transfected into cells with anti-miR-1827. Luciferase activity was determined 48 hours after transfection. The activity of firefly luciferase was normalised to that of *Renilla* luciferase. Statistical analysis was performed by Student *t*-test and the data are represented as the mean ± SEM. ** $P < 0.01$

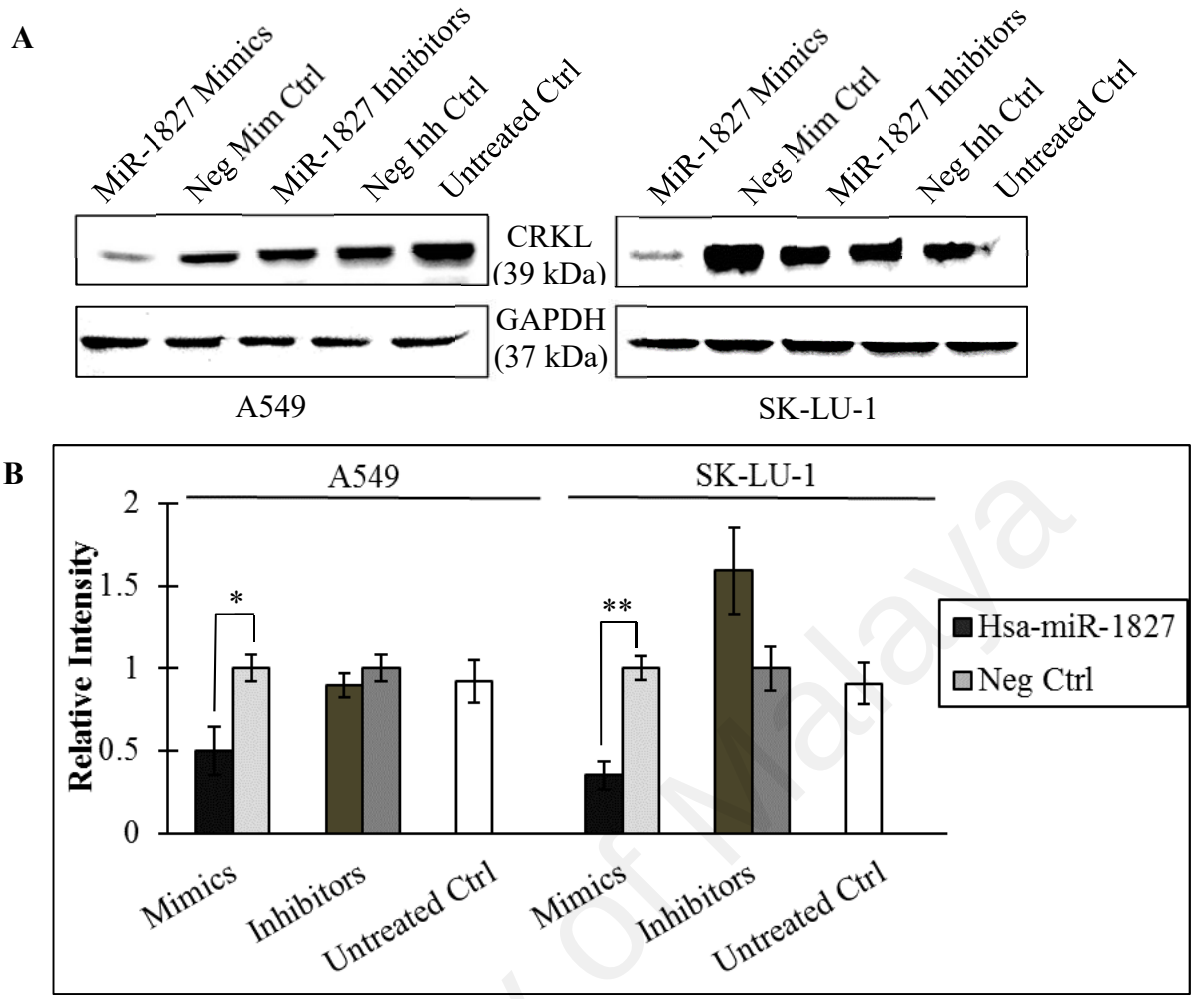

Figure 6.19: CRKL expression was down-regulated by miR-1827 directly targeting its 3'-UTR. (A) CRKL protein level was determined by Western blot after transfection with miR-1827 mimics/ hairpin inhibitors or negative controls in A549 and SK-LU-1 cells. GAPDH served as an internal control. **(B)** Western blot analysis of CRKL. The results are representative of three independent experiments. * $P < 0.05$, ** $P < 0.01$

6.5 Summary

In all the luciferase assays conducted, A549-I7 was used because of the intention to see the extent of miRNA targeting in high invasive cells as they would be the ones to be targeted in the course of miRNA therapeutics development. Of note, luciferase assay analyses demonstrated that the co-transfection of miRNAs hairpin inhibitors and WT 3'-UTR plasmids did not produce significant increase in luciferase expression. In fact, to the best of my knowledge, none of the published work reported the use of hairpin inhibitors in luciferase reporter assay.

In A549-I7, miR-378 was highly expressed. Transfection of negative inhibitors control took into consideration the inhibition by endogenous miR-378 on WT RBX1 3'-UTR. When miR-378 hairpin inhibitors were transfected, they bound to the endogenous miR-378, preventing it from binding to the WT RBX1 3'-UTR, and hence an increase in luciferase expression was seen. However, it was insignificant, partly due to what have been explained in Chapter 5.0. On the other hand, miR-1827 was lowly expressed in A549-I7. The luciferase activity upon transfection of negative inhibitors control in this case, could be high in the first place because there was not much inhibition of WT CRKL 3'-UTR from the endogenous miR-1827. Therefore, when miR-1827 hairpin inhibitors were introduced, the difference in luciferase activities after normalisation was not noticeable. Based on the data, it was hypothesised that luciferase assay is actually context dependent, that is, dependent on the endogenous level of miRNAs. This hypothesis remains disputable because it is contradictory to another study that showed luciferase assay was reproducible in different cell types (Zhang *et al.*, 2015a).

Both A549 and SK-LU-1 cells were used throughout Western blot experiments because it was relevant to examine the changes in protein expression as a whole when miRNA mimics or hairpin inhibitors were treated. In support of the findings from the

dual luciferase reporter assay, Western blot analyses confirmed the direct targeting of the miRNAs on their gene targets, resulted in a reduction in protein expression. MicroRNA hairpin inhibitors were expected to up-regulate the protein expression. In SK-LU-1 though, the increase in RBX1 and CRKL were trivial. These indicate that treatment with miRNA mimics was more effective than hairpin inhibitors. Nevertheless, what was seen in A549 implies that there might be more than one miRNAs or other regulatory elements controlling the expression of *RBX1* and *CRKL*. When miRNA mimics were introduced, it encouraged more of the interaction of miR-378 and miR-1827 with their target genes; but the transfection of miRNA hairpin inhibitors did not stop the other miRNAs from binding to *RBX1* and *CRKL*, hence a milder effect was seen with miRNA hairpin inhibitors.

Collectively, *RBX1* and *CRKL* were found to be novel targets for miR-378 and miR-1827, respectively.

CHAPTER 7: ROLES OF *RBX1* AND *CRKL* IN MIR-378- AND MIR-1827-MEDIATED NSCLC METASTASIS AND ANGIOGENESIS

We have thus far revealed that miR-378 induces NSCLC cell invasion while miR-1827 inhibits NSCLC cell migration. Both miRNAs modulate NSCLC angiogenesis. In addition, miR-378 was shown to directly target *RBX1* whereas miR-1827 binds directly to CRKL 3'-UTR. However, the association of *RBX1* and *CRKL* with NSCLC cell invasion, migration and angiogenesis under the regulation of miR-378 and miR-1827 were unknown. Hence, gene rescue studies using overexpression plasmids and siRNAs were carried out.

7.1 MiR-378-transformed High Invasive NSCLC Cells Reverted to Low Invasive Phenotype when *RBX1* was Overexpressed

To elucidate the relationship between *RBX1* expression and NSCLC metastasis and angiogenesis, A549-NI7 and SK-LU-1-NI7 cells were first co-transfected with miR-378 mimics and *RBX1* overexpression plasmid. The effects on RBX1 protein expression, cell invasiveness, migratory ability and angiogenic potential were then examined.

As shown in Figure 7.1, cells that were co-transfected with *RBX1* overexpression plasmid exhibited a significant increase in RBX1 protein expression compared to miR-378 mimics/pCMV6 transfected cells. The effect of *RBX1* overexpression on cell invasiveness was quantitatively measured by transwell invasion assay and there was a significant reduction in the number of invaded cells in comparison to cells transfected with miR-378 mimics/pCMV6 (Figure 7.2).

MiR-378 is not a regulator of NSCLC cell migration. However, it was appealing to examine the role of *RBX1* in cell migration. Importantly, neither miR-378 mimics nor *RBX1* overexpression led to significant differences in cell motility of both A549-NI7

and SK-LU-1-NI7 (Figure 7.3). Furthermore, miR-378 mimics significantly induced HUVEC to form branch capillary-like division structures but the overexpression of *RBX1* was not able to suppress the effect, especially in SK-LU-1-NI7 (Figure 7.4). This suggests that RBX1 plays a bigger role in angiogenesis in A549 than in SK-LU-1. Together, these results demonstrated that *RBX1* expression prevents low invasive cells from displaying invasive phenotype and partially regulates the angiogenic activity.

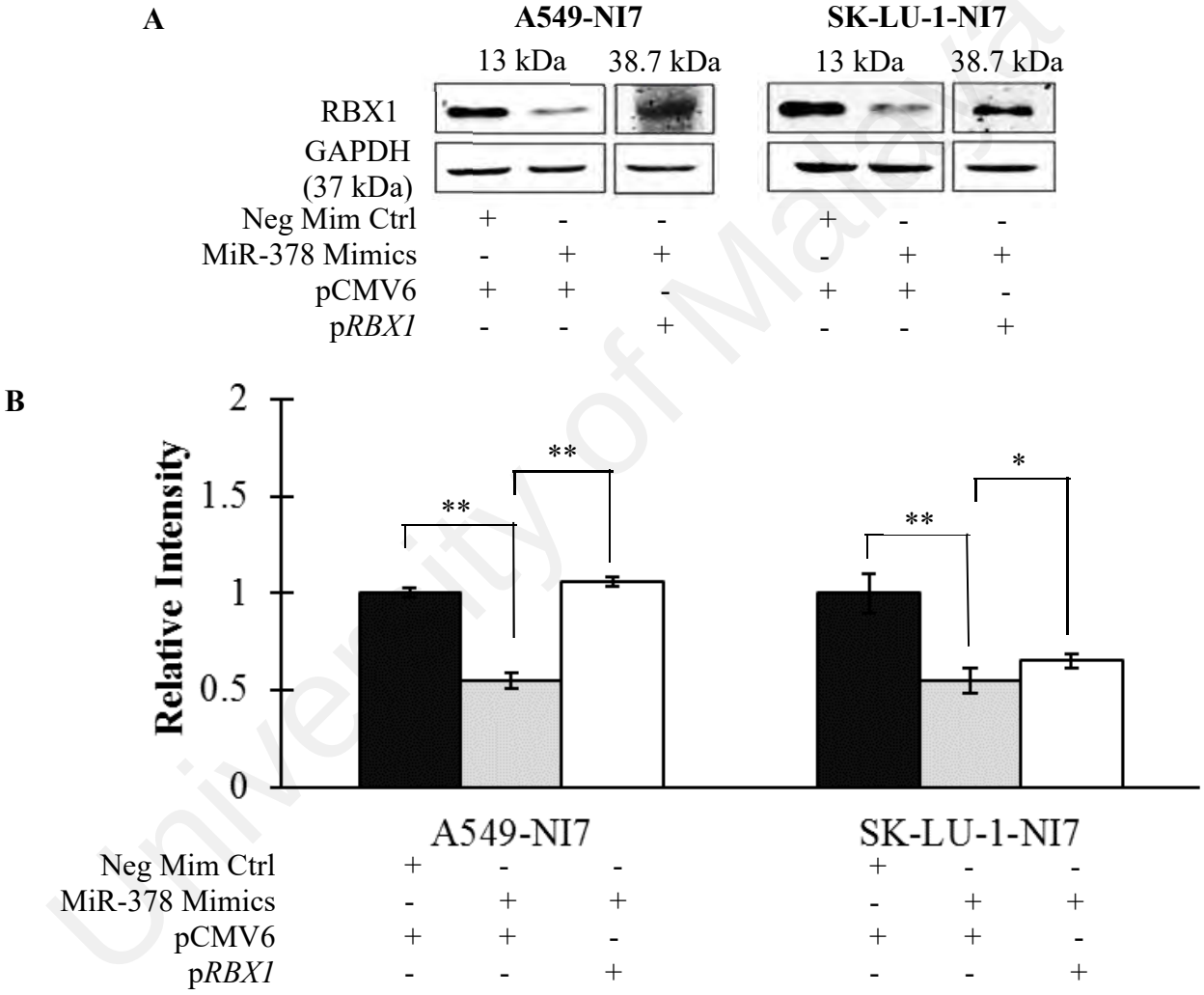

Figure 7.1: Overexpressing *RBX1* restored protein expression. (A) Low invasive cells were transfected with either negative mimics control/pCMV6, miR-378 mimics/pCMV6 or miR-378 mimics/p*RBX1*. 48 hours later, cells were used to measure RBX1 protein expression via Western Blot. **(B)** *RBX1* overexpression restored the miR-378-induced decrease of RBX1 level. * $P < 0.05$, ** $P < 0.01$

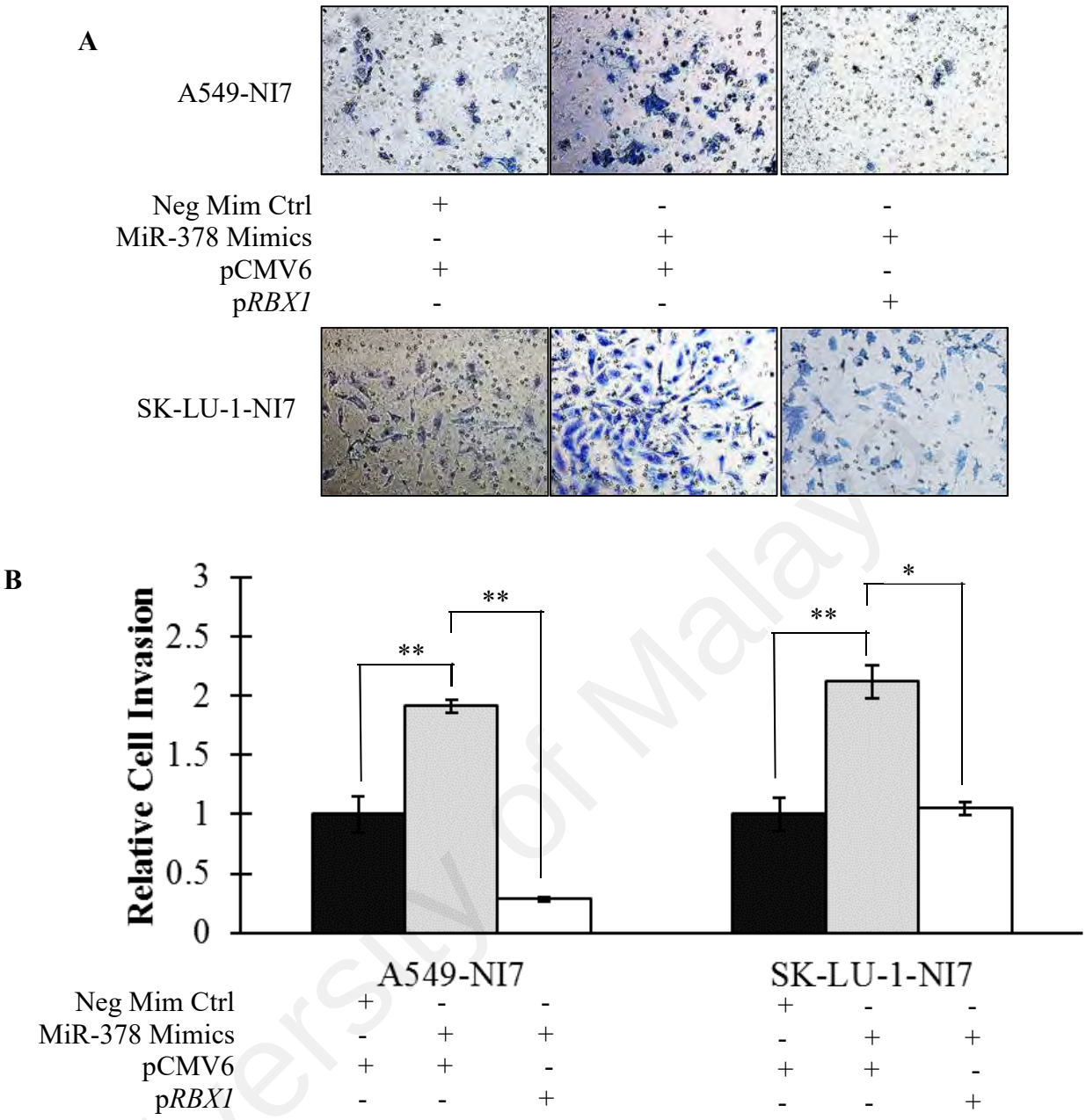

Figure 7.2: Effect of *RBX1* on cell invasion. (A) Cells transfected with negative mimics control/pCMV6, miR-378 mimics/pCMV6 and miR-378 mimics/p*RBX1* possessed different invasion ability. Representative images are shown. **(B)** Overexpression of *RBX1* inhibited miR-378-induced cell invasion. The results were normalised to negative mimics control/pCMV6 (n = 3, * $P < 0.05$, ** $P < 0.01$).

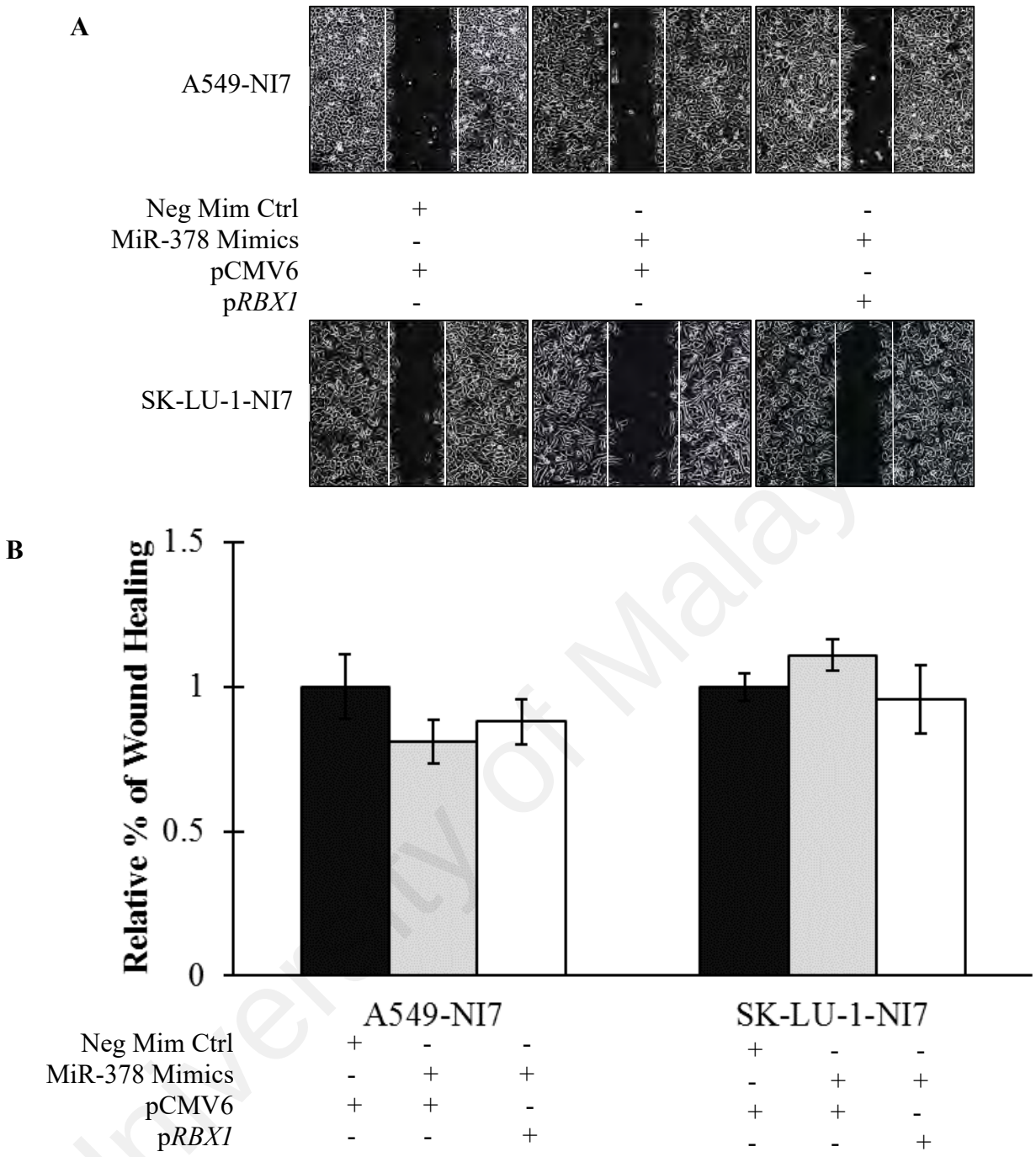

Figure 7.3: *RBX1* is not associated with NSCLC cell migration. (A) Representative images of wound healing assay (magnification, 100×). **(B)** Quantification of cell migration.

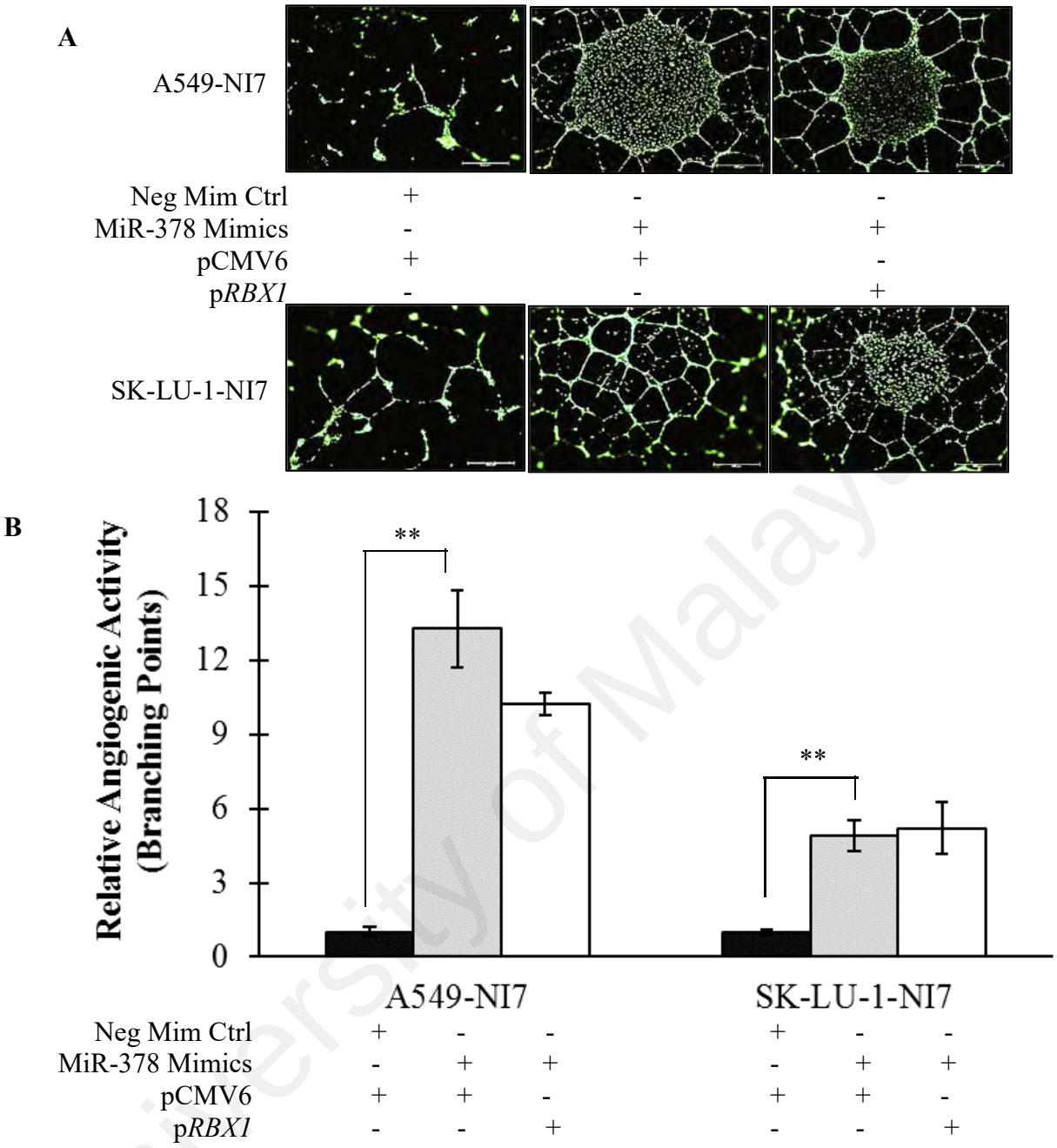

Figure 7.4: *RBX1* is not sufficient to drive an anti-proliferative signal in HUVEC. (A) The effects of TCM collected from negative mimics control/pCMV6, miR-378 mimics/pCMV6 and miR-378 mimics/p*RBX1* on HUVEC tube formation at 15 h. Representative images are shown.

C

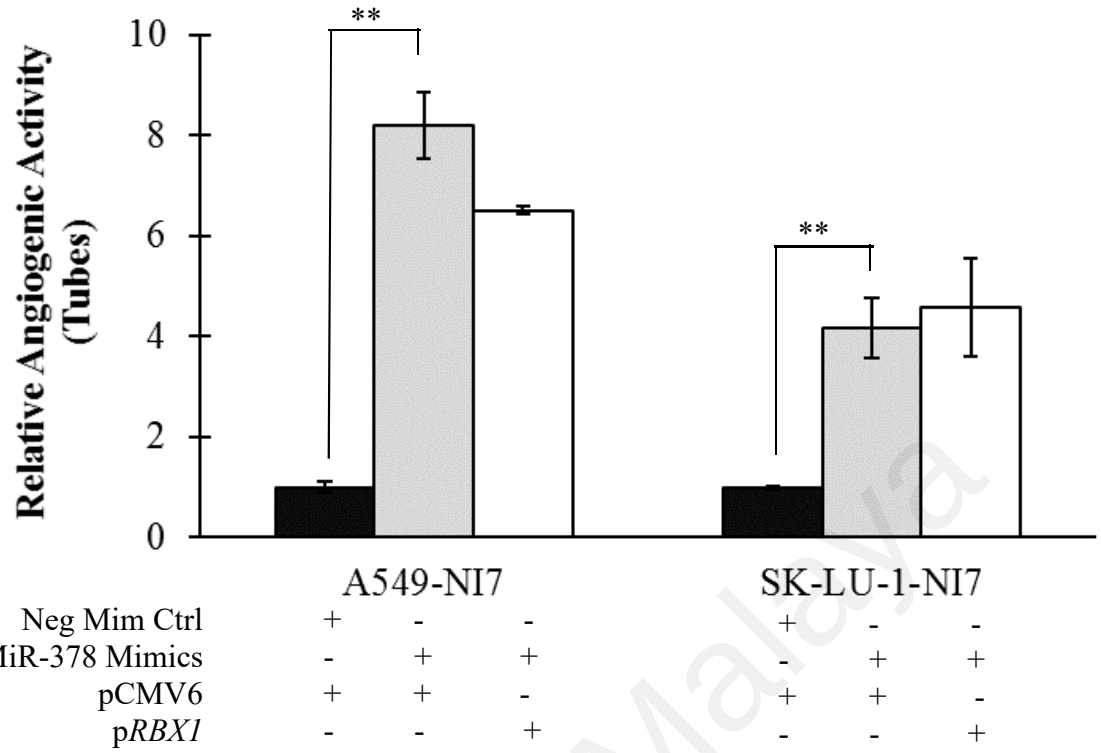

Figure 7.4, continued: (B), (C) Overexpressing miR-378 could induce HUVEC to proliferate. However, *RBX1* expression only partially rescued HUVEC formation into tubes (n = 3, ** $P < 0.01$).

7.2 *RBX1* Silencing Restored NSCLC Cell Invasiveness

Knockdown of *RBX1* by siRNA led to significantly decreased RBX1 protein expression in both A549-I7 and SK-LU-1-I7 (Figure 7.5). This decrease in RBX1 expression was accompanied by a significant increase in cell invasiveness, mimicking the inducing effect of miR-378 on cell invasion (Figure 7.6).

As observed in Figure 7.7 of wound healing assay, the migration abilities of A549-I7 and SK-LU-1-I7 cells were almost entirely similar across different co-transfection groups. Tube formation assays were performed using HUVEC exposed to conditioned media collected from NSCLC cells transfected with either negative inhibitors control/sinon, miR-378 hairpin inhibitors/sinon or miR-378 hairpin inhibitors/si*RBX1*. It was observed that suppression of miR-378 resulted in significant reduction of tube formation potential but this effect was not rescued by silencing of *RBX1* (Figure 7.8).

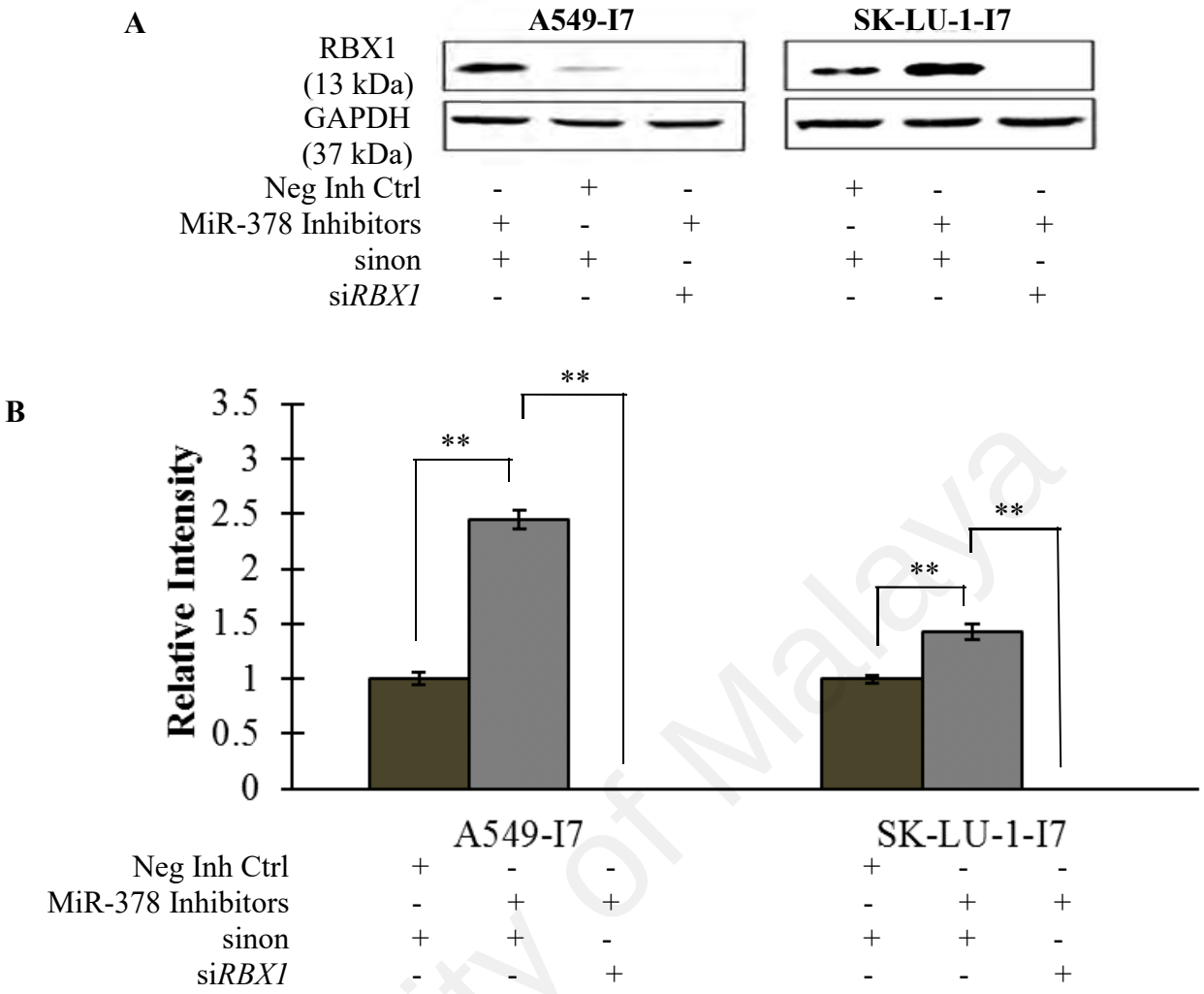

Figure 7.5: Silencing *RBX1* restored protein expression. (A) Total protein was harvested from three different transfection groups and analysed by Western blotting for RBX1 protein. **(B)** MiR-378 hairpin inhibitors increased RBX1 protein level while si*RBX1* knocked down almost 100% of RBX1 protein level. ** $P < 0.01$

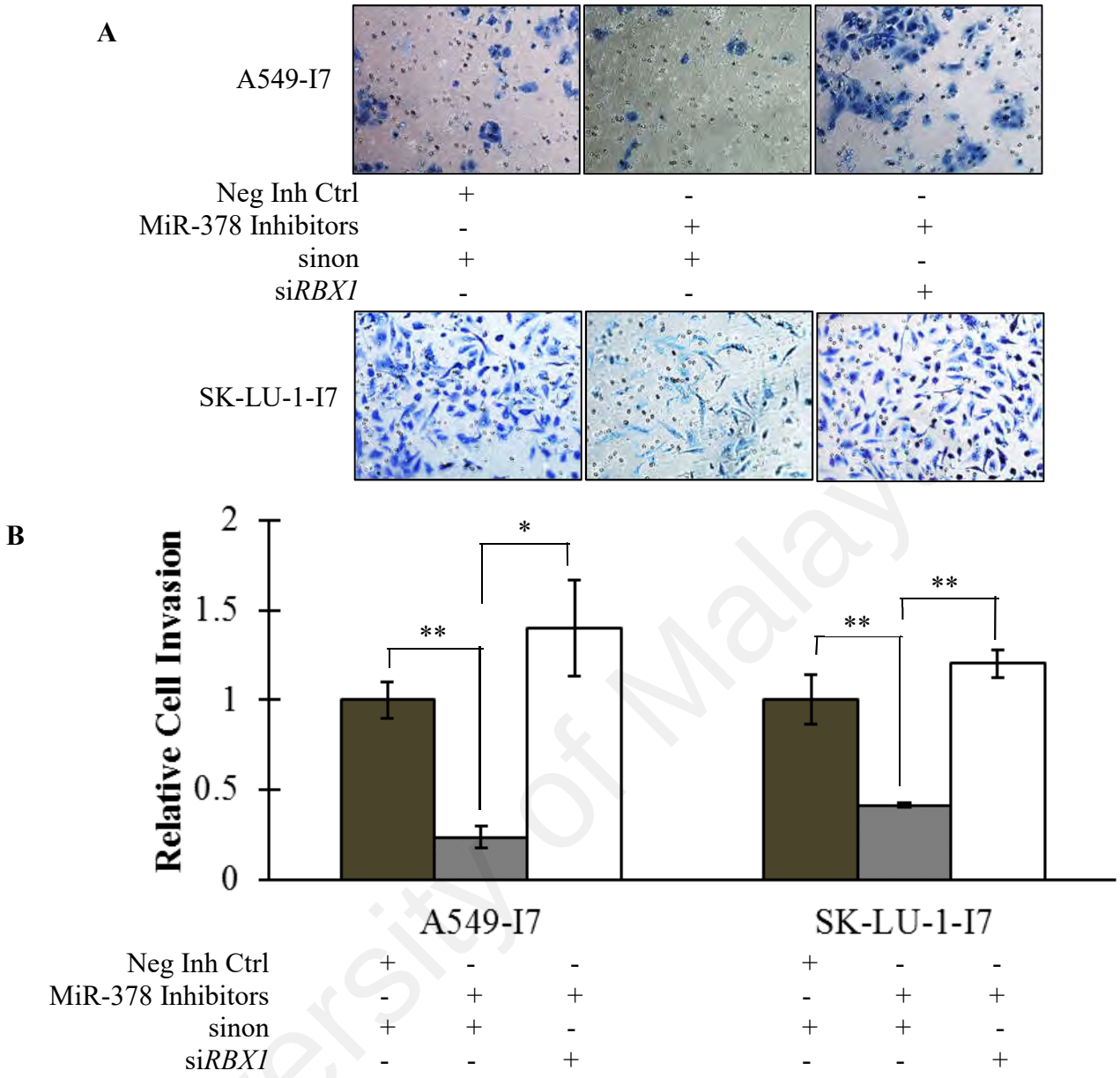

Figure 7.6: Silencing of *RBX1* in miR-378-suppressed cells increased the invasion ability. (A) NSCLC cells were transfected with negative inhibitors control/sinon, miR-378 hairpin inhibitors/sinon or miR-378 hairpin inhibitors/si*RBX1* and plated on Matrigel-coated transwell membrane insert. Cells that invaded to the bottom of the membrane were stained and counted. Representative images are shown. **(B)** MiR-378 hairpin inhibitors weakened the ability of cells to invade while this effect could be rescued by *RBX1* silencing (n = 3 ± SEM, * $P < 0.05$, ** $P < 0.01$).

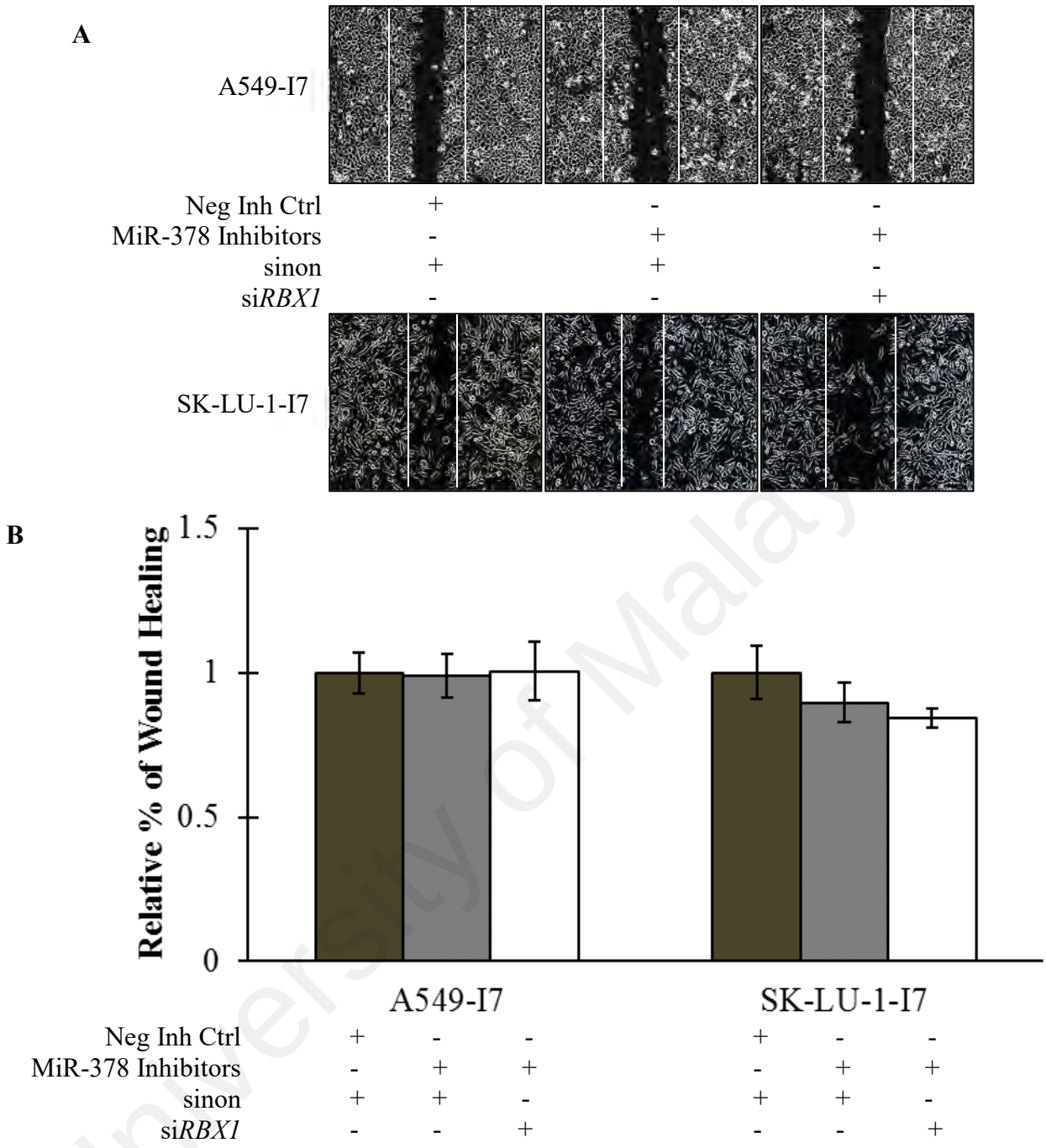

Figure 7.7: *RBX1* is not required for cell migration. (A) Representative bright field images of transfected cells, white lines indicate edges of the wound at 0 h. **(B)** Quantification of migratory ability of cells. Columns represent normalised percentage of wound healing.

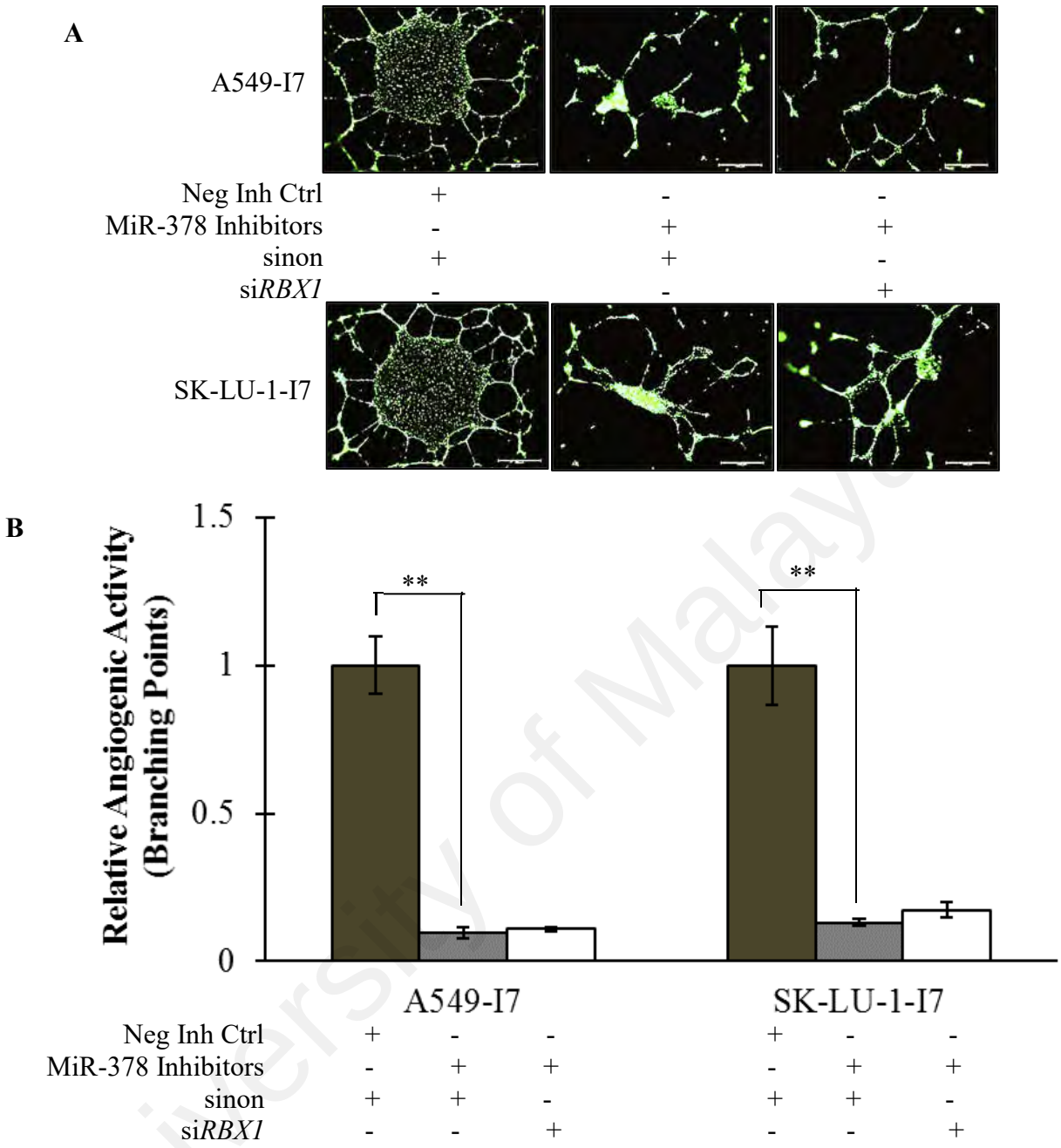

Figure 7.8: Angiogenic effects of transient suppressed expression of miR-378 and *RBX1* rescue in A549-I7 and SK-LU-1-I7 cells. (A) Representative images of tube formation as the effects of *RBX1* knockdown on anti-miR-378-suppressed angiogenic ability in A549-I7 and SK-LU-1-I7 cells. **(B)** Relative number of branching points formed by HUVEC that were incubated in TCM from miR-378 hairpin inhibitors/sinon and miR-378 hairpin inhibitors/si*RBX1*, normalised to negative inhibitors control/sinon. Triplicate assays were performed. Significant differences are indicated by ** ($P < 0.01$).

C

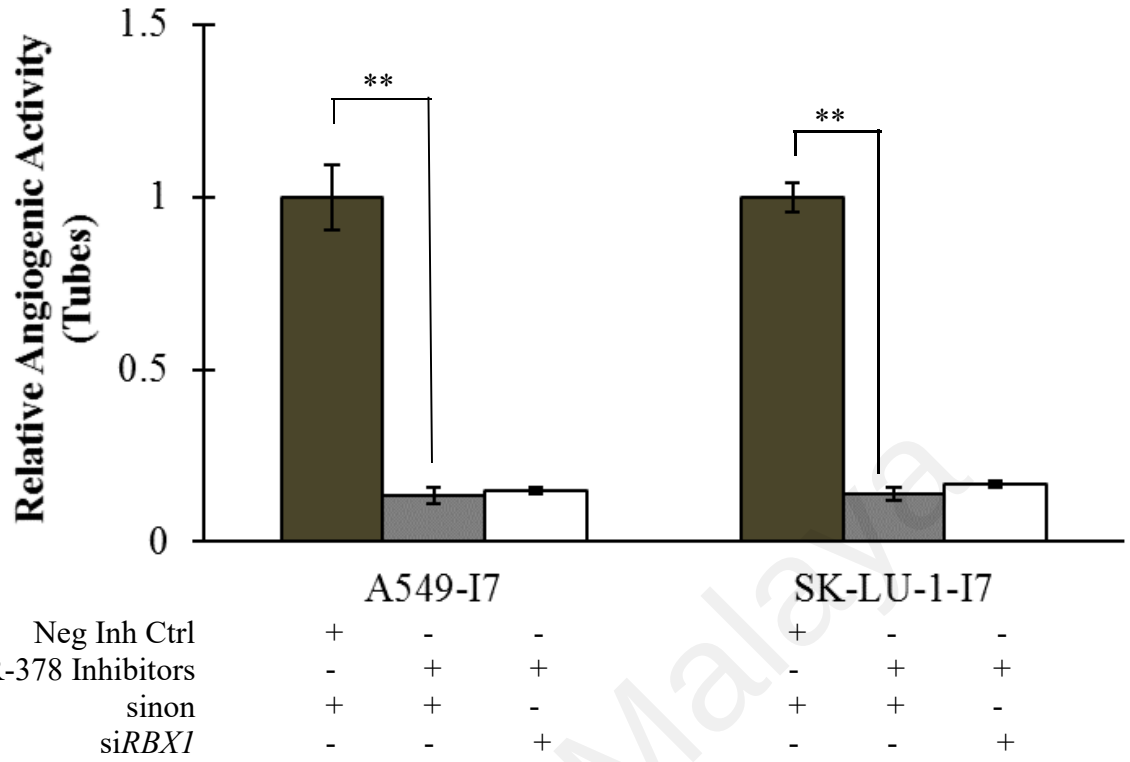

Figure 7.8, continued: (C) Relative number of tubes formed by HUVEC that were incubated in TCM from miR-378 hairpin inhibitors/sinon and miR-378 hairpin inhibitors/si*RBX1*, normalised to negative inhibitors control/sinon. Triplicate assays were performed. Significant differences are indicated by ** ($P < 0.01$).

7.3 Ectopic Expression of *CRKL* Attenuated MiR-1827-repressed NSCLC Cell Migration

To evaluate the role of *CRKL* in NSCLC metastasis and angiogenesis under the regulation of miR-1827, the effects of gene overexpression and knockdown on CRKL protein expression, cell invasiveness, migratory ability and angiogenic potential were investigated.

MiR-1827 mimics significantly decreased the level of CRKL, whereas co-expressing *CRKL* significantly stimulated an increase in CRKL protein expression in A549-I7 and SK-LU-1-I7 cells (Figure 7.9). However, no significant changes in cell invasiveness were noted following treatment with miR-1827 mimics/p*CRKL* compared to miR-1827 mimics/pCMV6 (Figure 7.10).

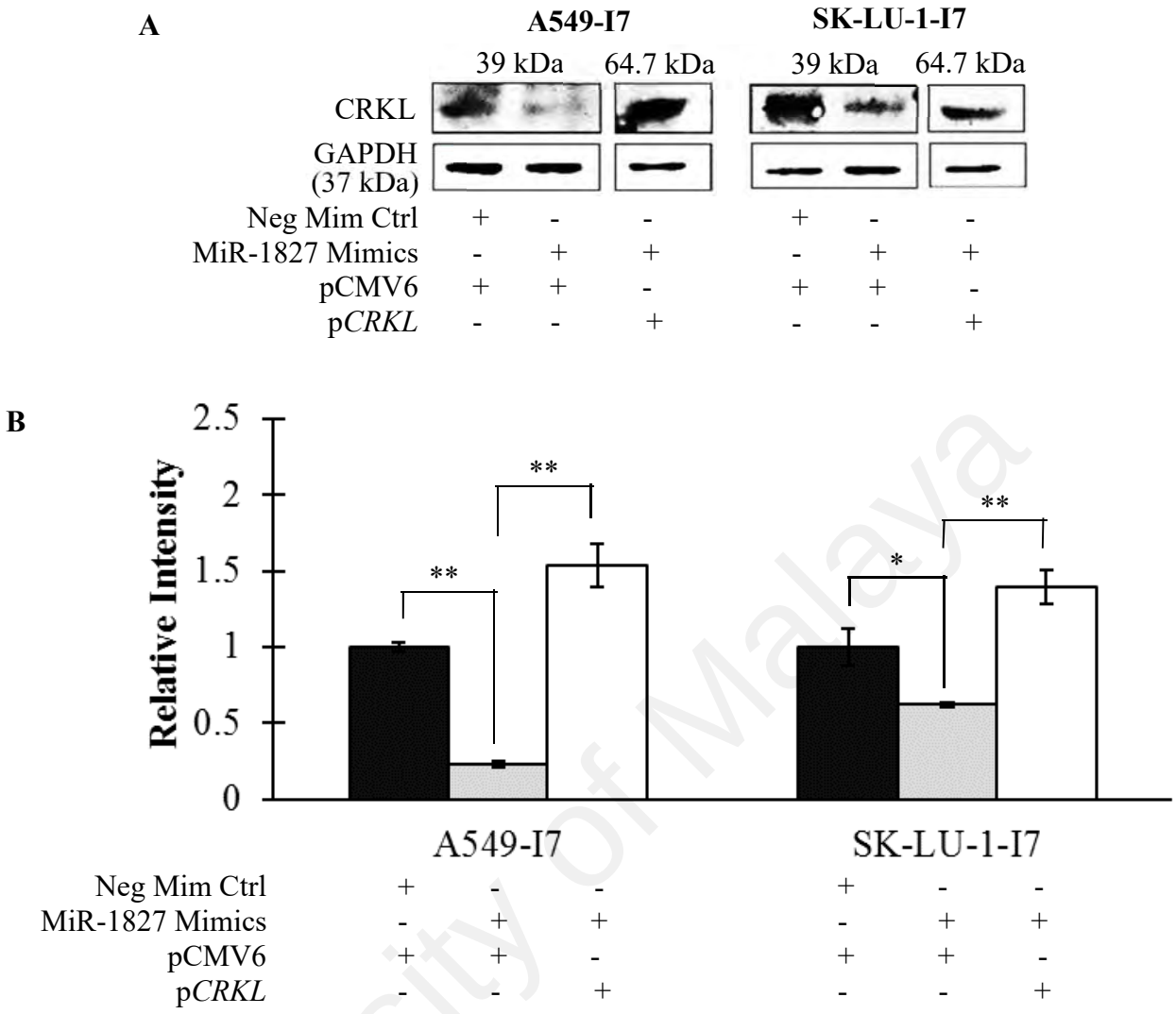

Figure 7.9: CRKL expression in NSCLC cells after co-transfection with miR-1827 mimics and p*CRKL*. (A) Immunoblots of CRKL in A549-I7 and SK-LU-1-I7 cells after 48 hours treatment with negative mimics control/pCMV6, miR-1827 mimics/pCMV6 or miR-1827 mimics/p*CRKL*. GAPDH was used as loading control. **(B)** Western blot analysis. Restoring *CRKL* abrogated the miR-1827-induced down-regulation of CRKL. * $P < 0.05$, ** $P < 0.01$

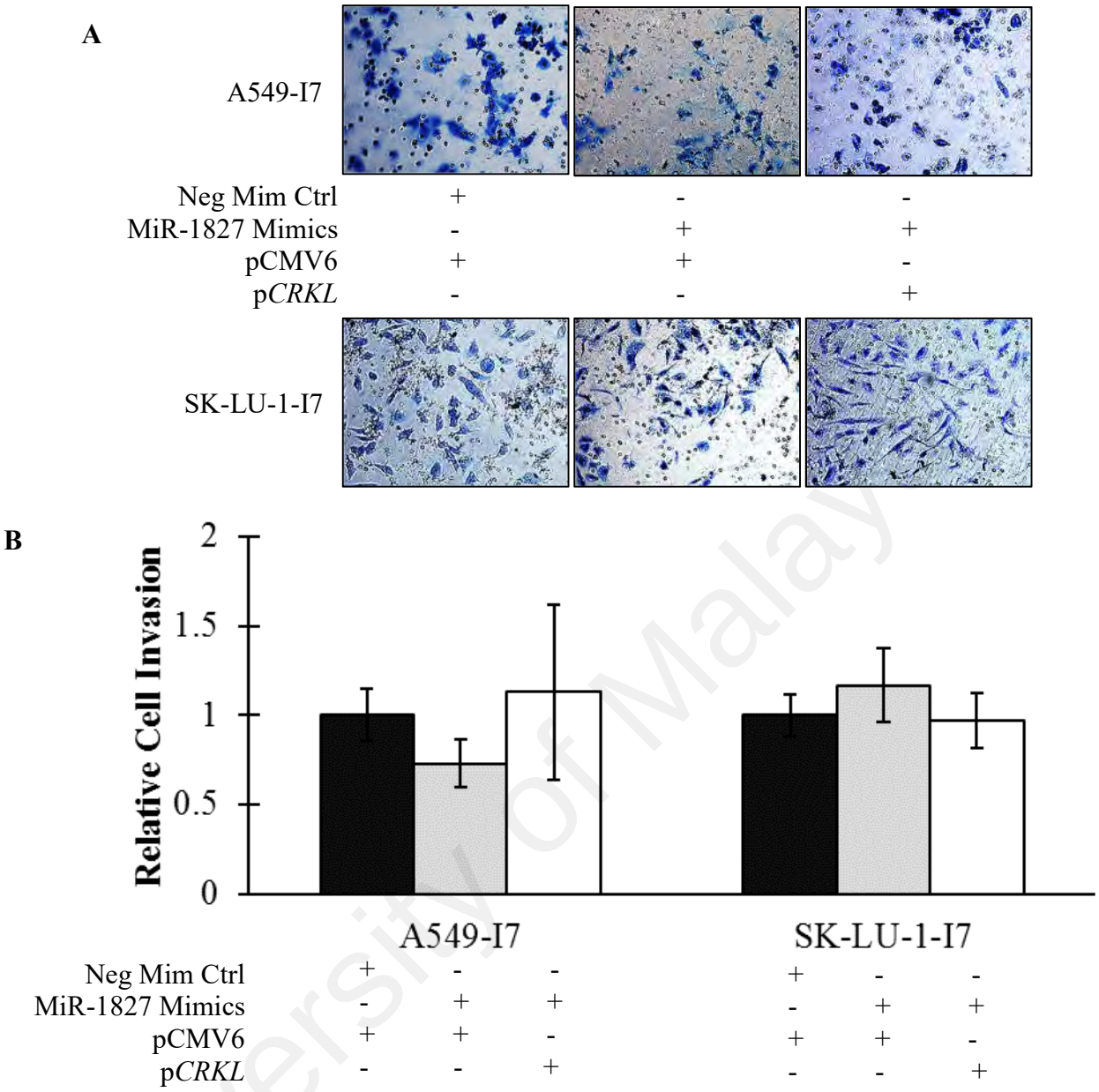

Figure 7.10: *CRKL* and NSCLC cell invasion. (A) Cells were transfected with combination of negative mimics control/miR-1827 mimics and pCMV6/p*CRKL* and then subjected to transwell invasion assay. After 22 hours, invaded cells were fixed, stained and counted. Representative images are shown. **(B)** Transwell invasion assay showed that ectopic expression of *CRKL* did not alter the cell invasion ability of high invasive cells.

Notably, A549-I7 and SK-LU-1-I7 cells were rendered significantly less motile when miR-1827 mimics were transfected. This effect could be completely reversed by co-expressing *CRKL* construct, emphasising the regulatory role of *CRKL* in miR-1827-dependent migration inhibition (Figure 7.11). On the other hand, as shown in Figure 7.12, tube formation was reduced significantly in HUVEC treated with miR-1827 mimics/pCMV conditioned medium, with no significant rebound effect observed with

the dual miR-1827 and *CRKL* expression. These results indicate that *CRKL* is not sufficient to account for the anti-angiogenic effects of miR-1827.

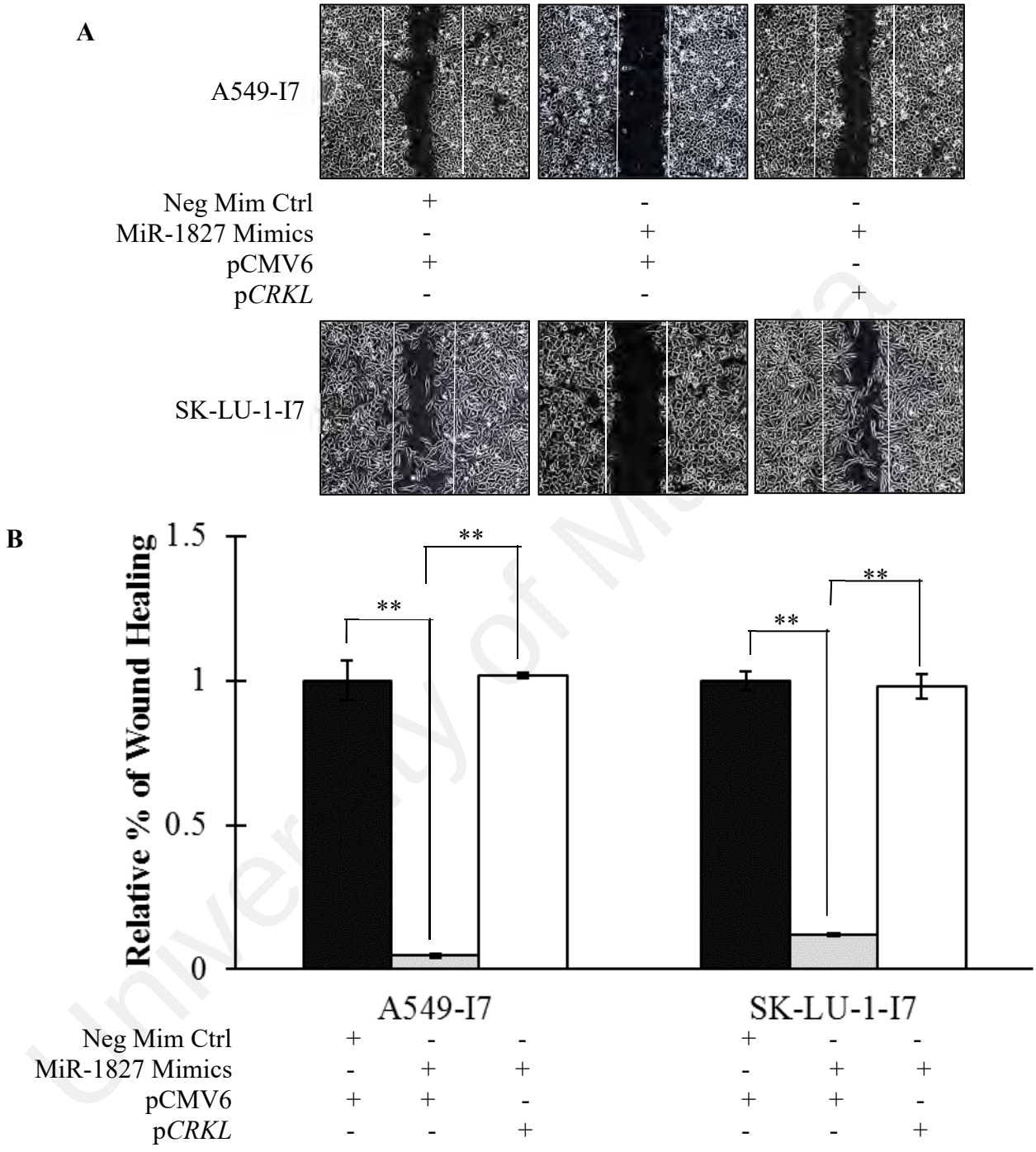

Figure 7.11: MiR-1827 suppresses the migration of NSCLC cells by inhibiting *CRKL*. (A) Wound healing assay indicated that *CRKL* overexpression abolished miR-1827-inhibited cell migration. Representative images are shown. **(B)** The relative percentage of wound healing for miR-1827 mimics/pCMV6 and miR-1827 mimics/p*CRKL* was calculated by adjusting with negative mimics control/pCMV6 to 1. ** $P < 0.01$

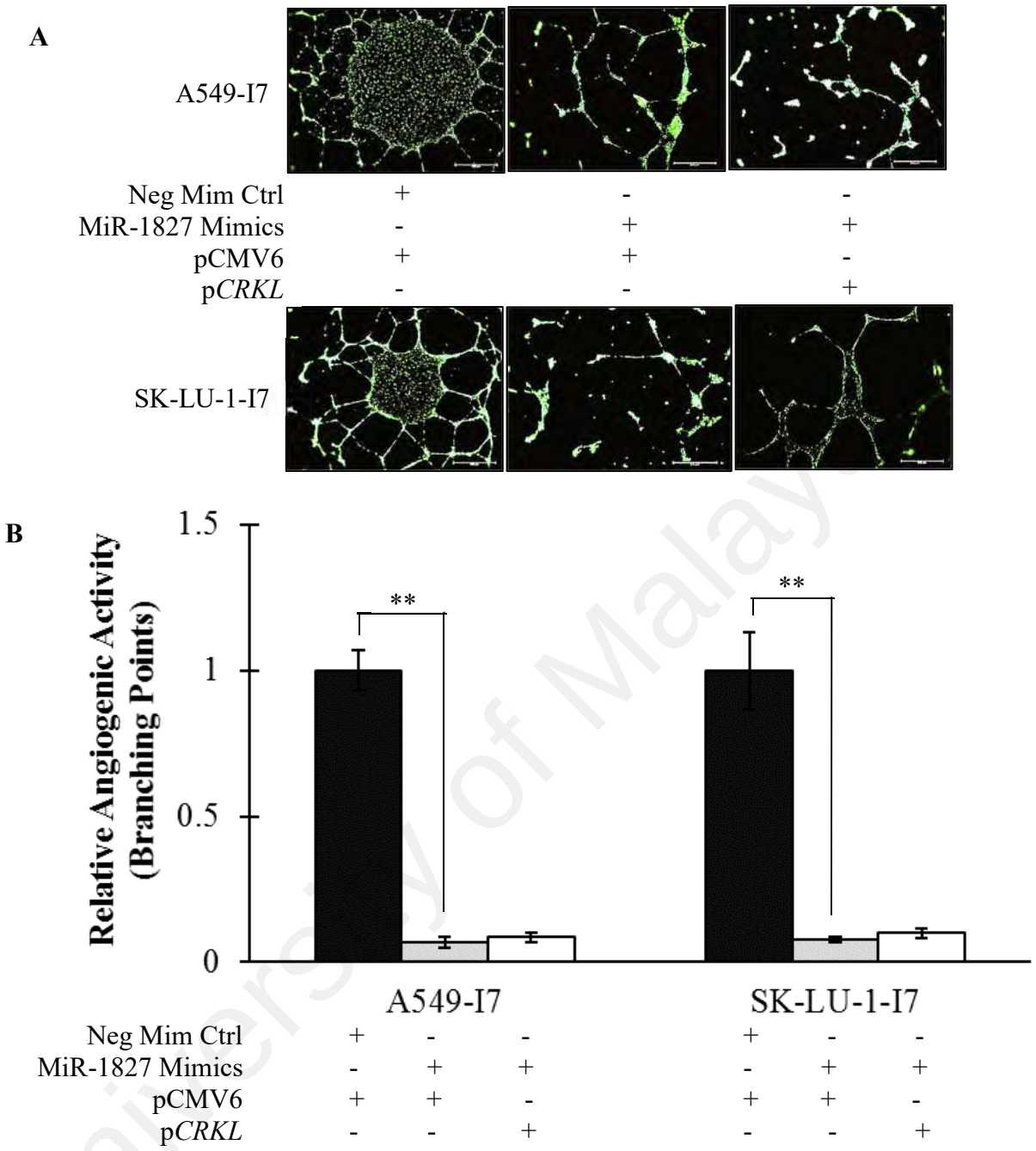

Figure 7.12: *CRKL* is not responsible for miR-1827-mediated angiogenesis. (A) Representative capillary tube formation images of the effects of *CRKL* expression on miR-1827-suppressed angiogenic ability in A549-I7 and SK-LU-1-I7 cells.

C

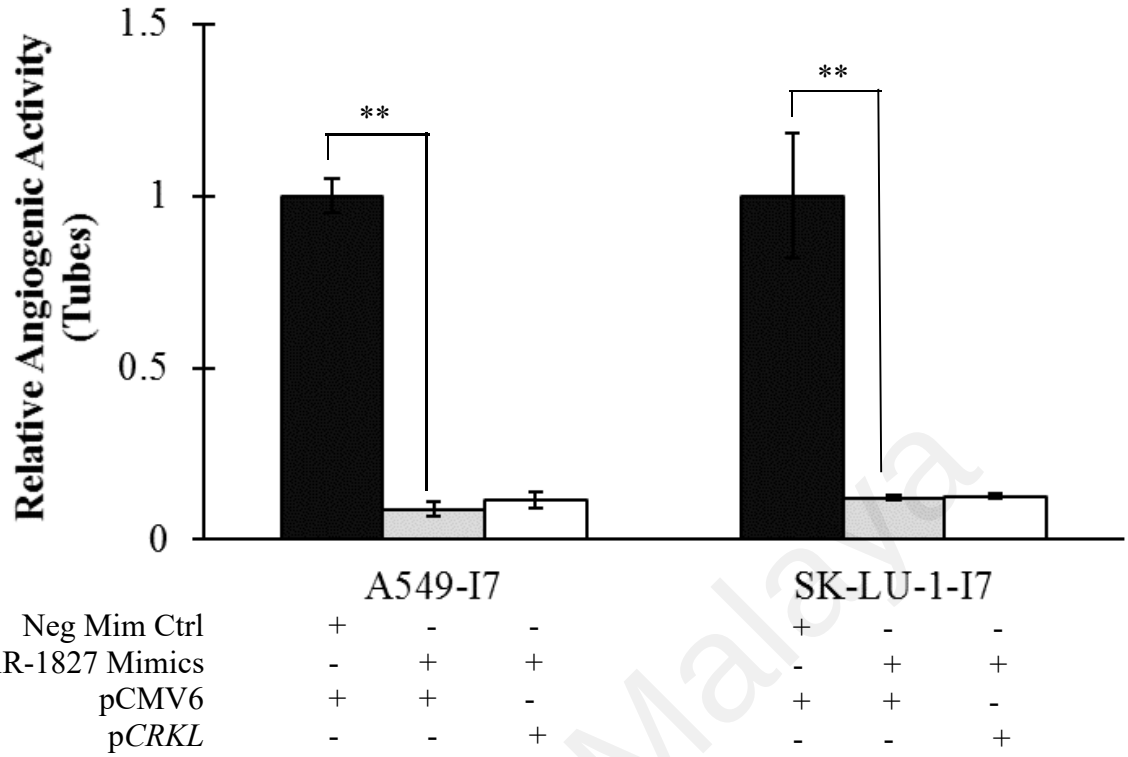

Figure 7.12, continued: (B), (C) Tube forming ability was significantly reduced in response to miR-1827 mimics treatment but tubular formation was not restored in the presence of *CRKL*. ** $P < 0.01$

7.4 *CRKL* Silencing Suppressed Cell Migration

Transfection of miR-1827 hairpin inhibitors in NSCLC cells resulted in significant up-regulation of CRKL protein level whereas *CRKL* silencing induced significant translational inhibition of CRKL (Figure 7.13). It was further shown that increase in miR-1827 expression or decrease in *CRKL* expression did not result in significant changes in cell invasion ability in these cells (Figure 7.14).

Blocking the function of miR-1827 significantly increased the ability of low invasive cells to migrate. Consistently, *CRKL* silencing completely abrogated the effect of anti-miR-1827 treatment, indicating the essential role of *CRKL* in miR-1827-suppressed cell migration (Figure 7.15). In contrast, as presented in Figure 7.16, transfection of miR-1827 hairpin inhibitors resulted in a significant upsurge in tube formation, whereas down-regulation in tube formation potential was insignificantly

achieved using conditioned medium collected from *CRKL*-silenced NSCLC cells following anti-miR-1827 treatment. SiRNA targeting *CRKL* was able to moderately rescue the effects on branching point and tube formation in A549-NI7 cells but interestingly, *CRKL* might only function in early angiogenesis in SK-LU-1-NI7, as down-regulation of *CRKL* expression did not seem to attenuate tube formation promoted by miR-1827 inhibition.

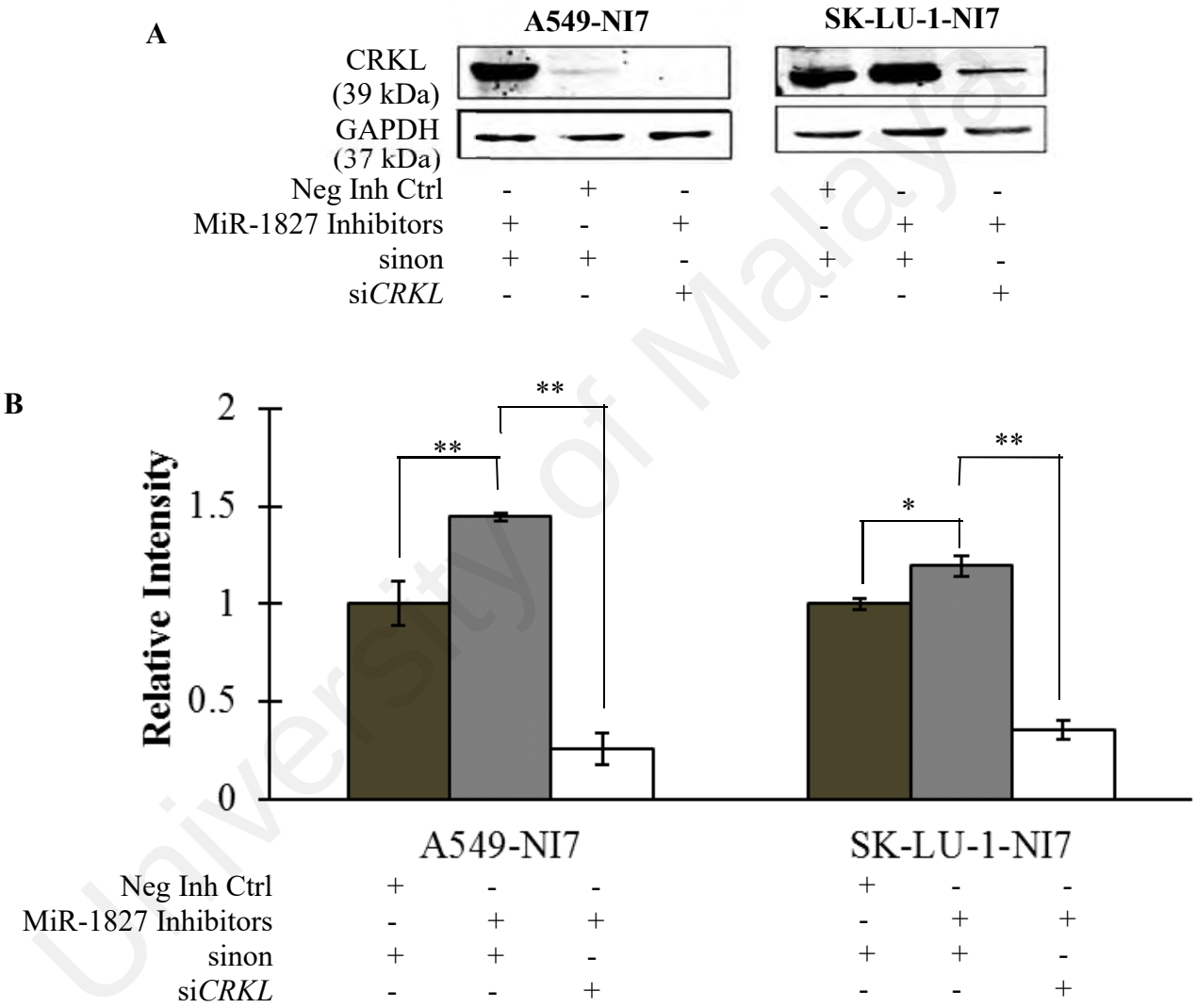

Figure 7.13: si*CRKL* can reverse the inducing effect of anti-miR-1827 on its protein level. (A) CRKL protein expression level in A549-NI7 and SK-LU-1-NI7 cells transfected with negative inhibitors control/sinon, miR-1827 hairpin inhibitors/sinon or miR-1827 hairpin inhibitors/si*CRKL* were analysed by Western blotting. GAPDH was used as a control. **(B)** Band intensity values were analysed using Image J and normalised to negative inhibitors control/sinon. All experiments were performed in triplicate and data are represented as mean ± SEM. * $P < 0.05$, ** $P < 0.01$

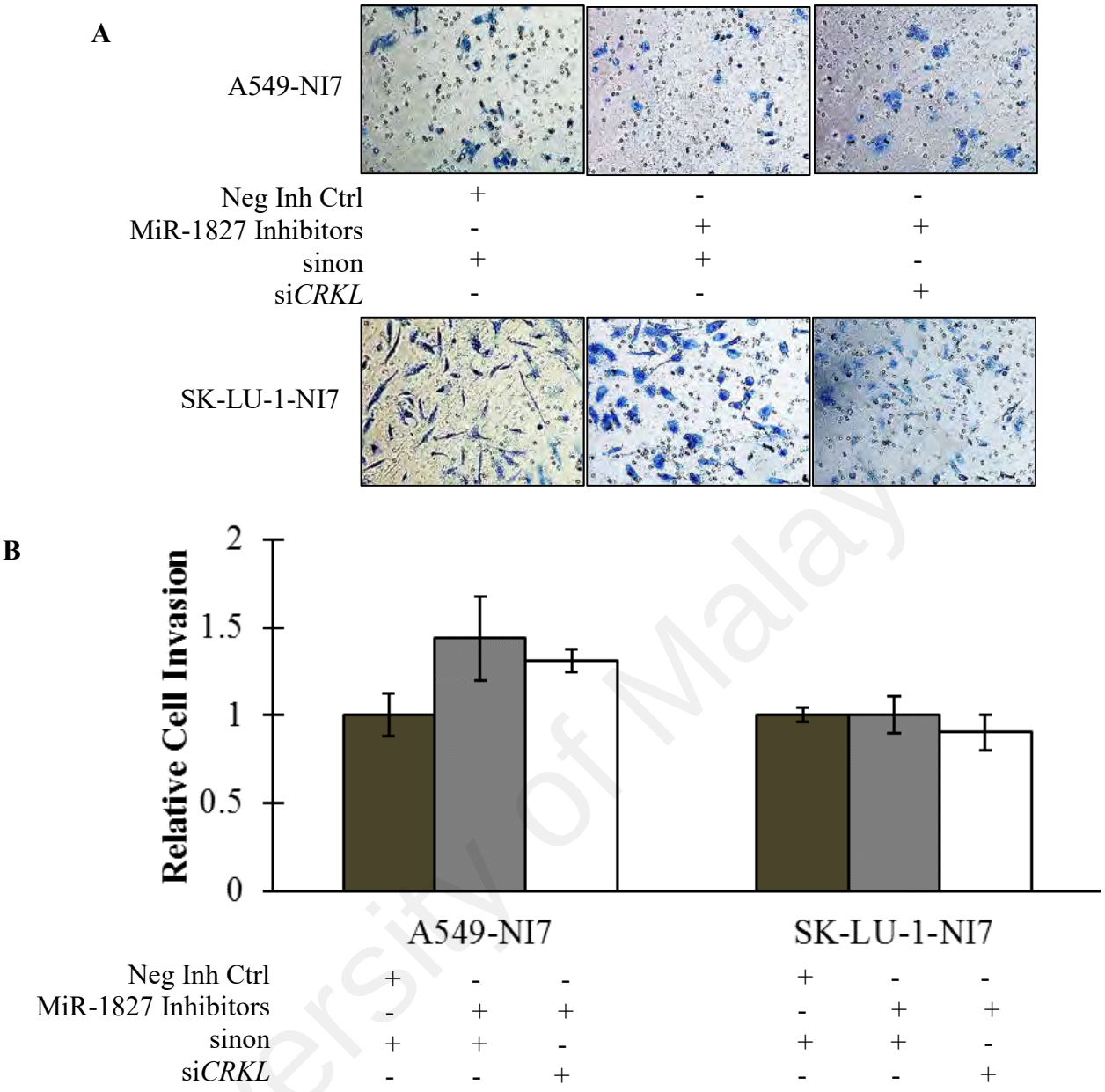

Figure 7.14: Silencing of *CRKL* had no effect on cell invasion. (A) Representative images of invasive cells at the bottom of the membrane stained with methylene blue were visualised as shown. **(B)** Quantification of cell invasion was presented as relative number of invaded cells normalised to negative inhibitors control/sinon. Expression of *CRKL* did not alter the cell invasiveness of A549-NI7 and SK-LU-1-NI7 cells.

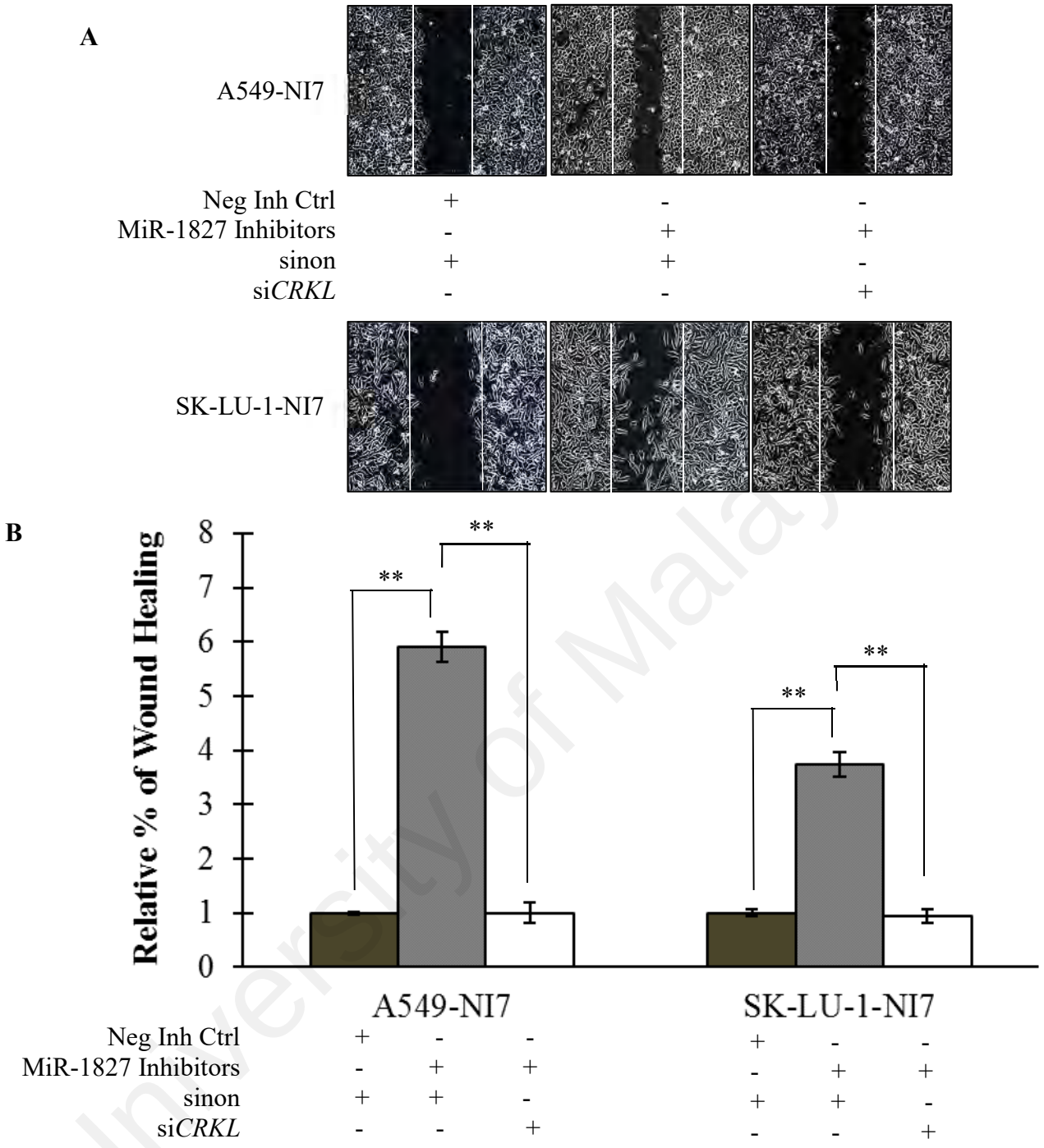

Figure 7.15: Knockdown of *CRKL* mimicked the inhibitory effect of miR-1827 on cell migration. (A) Confluent cell monolayers were wounded with a pipette tip. Wound closure was monitored at 28 h. Representative images are shown. **(B)** Inhibition effects of si*CRKL* on migration of A549-NI7 and SK-LU-1-NI7 cells. ** $P < 0.01$

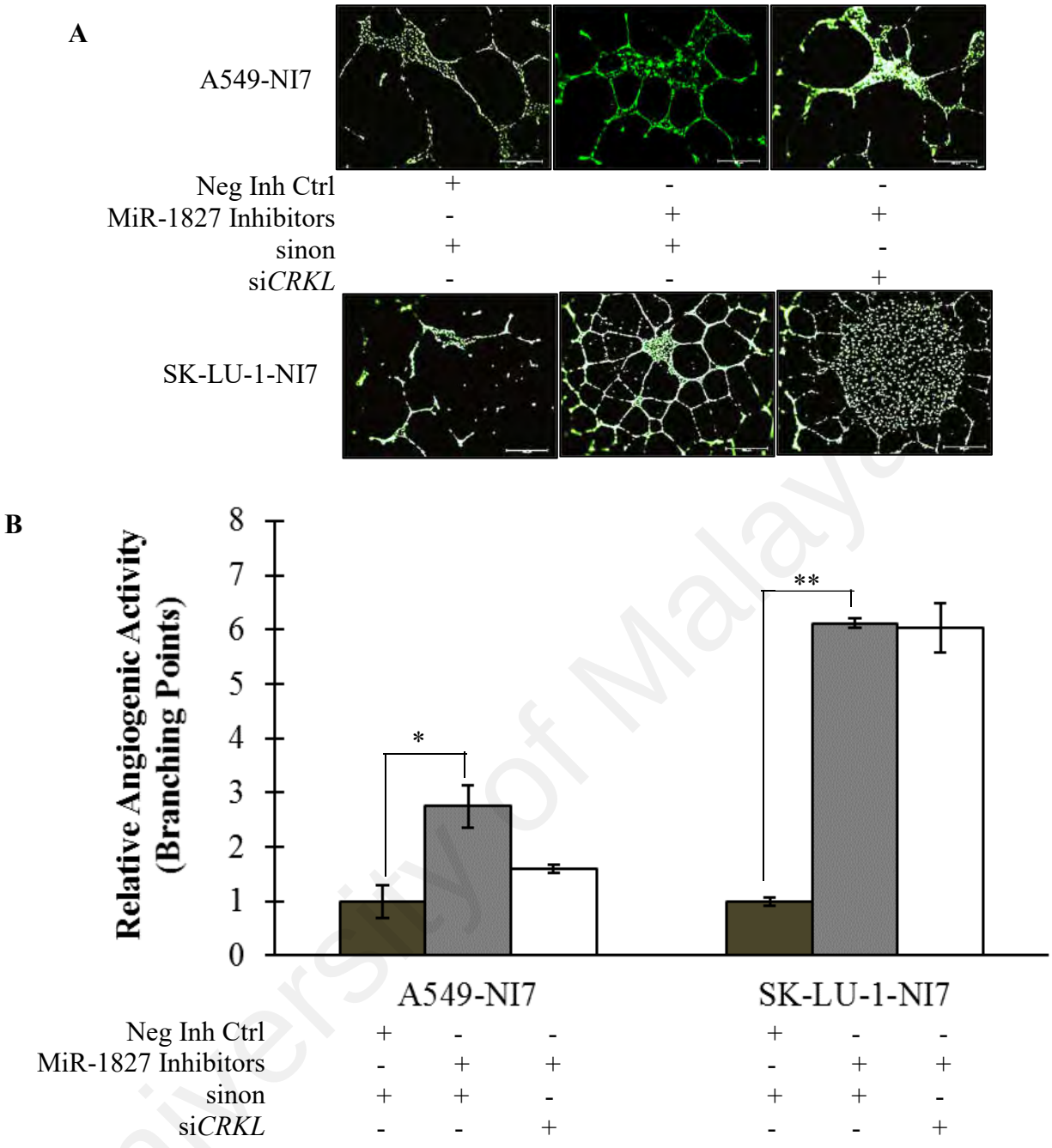

Figure 7.16: si*CRKL* did not reduce the formation of branching points and tubes by HUVEC. (A) Representative photographs of tube formation were taken using fluorescence microscope (under 4× objective). **(B)** Total number of branching points was measured with WimTube software. * $P < 0.05$ and ** $P < 0.01$ as compared to negative inhibitors control/sinon.

C

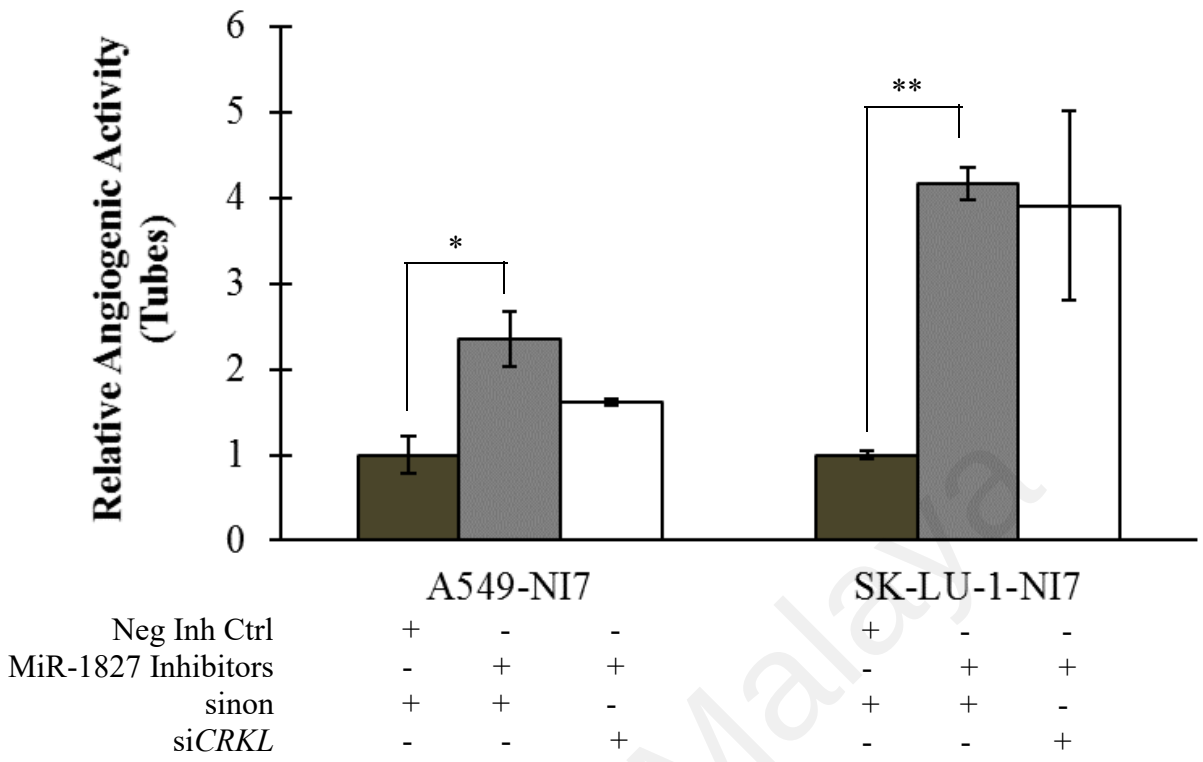

Figure 7.16, continued: (C) Total number of tubes was measured with WimTube software. * $P < 0.05$ and ** $P < 0.01$ as compared to negative inhibitors control/sinon.

7.5 Summary

Briefly, *RBX1* plays a vital role in miR-378-mediated NSCLC cell invasion but not in NSCLC cell migration. Moreover, *RBX1* overexpression partially rescued the non-angiogenic phenotype of A549-NI7 but not SK-LU-1-NI7, suggesting that *RBX1* plays a bigger role in regulating angiogenesis in A549 than in SK-LU-1, nonetheless *RBX1* alone is not adequate to inhibit angiogenesis. It was also postulated that the mechanism of angiogenesis via *RBX1* signalling in SK-LU-1 seems to be far more complicated because there appeared to be other regulatory elements controlling the level of *RBX1* when it was in excess.

CRKL was found to be essential in miR-1827-repressed NSCLC cell migration but not in NSCLC cell invasion. Additionally, the introduction of siRNA targeting *CRKL* could marginally reverse the pro-angiogenic effects triggered by anti-miR-1827. This suggests that *CRKL* is not a major player in NSCLC angiogenesis.

CHAPTER 8: TRANSFECTION OF MIR-378 HAIRPIN INHIBITORS AND MIR-1827 MIMICS REDUCED NSCLC METASTASIS AND ANGIOGENESIS *IN VIVO*

To analyse the *in vivo* effects of miR-378 and miR-1827 on lung cancer tumour cells metastasis and angiogenesis, zebrafish embryos were used as animal model. Zebrafish is a small tropical freshwater fish that produce hundreds of embryos per mating. Immune privilege of zebrafish embryos facilitates implantation of mammalian tumour cells. The transparent nature of zebrafish embryos allows visualisation of tumour cells dissemination and quantification of blood vessel formation in living fish.

8.1 *In Vivo* Metastasis Assay

High invasive A549 cells were transfected with miR-378 hairpin inhibitors or miR-1827 mimics and the transfected cells were labelled with DiI 24 hours later. The labelled cells were then injected into the yolk sac of zebrafish embryos and those that contained transfected cells were counted at 24 h.

8.1.1 MiR-378 Hairpin Inhibitors Reduced Lung Cancer Cell Metastasis in Zebrafish Embryos

Tumour burden carried by zebrafish embryos at 24 h post injection was rather similar for both miR-378 hairpin inhibitors-treated and negative inhibitors control-treated A549-I7 cells (Figure 8.2A). MiR-378-knocked down A549-I7 cells seeded in the tail vein of nearly 27% of zebrafish embryos. However, only one metastasis that reached approximately 1156μm from the yolk sac was seen. Control cells were observed to be capable of seeding in the tail vein of all injected zebrafish embryos. The number of metastases recorded ranged from 1 to 25 with average dissemination 934μm (Figure 8.1, Figure 8.2B, Figure 8.2C and Figure 8.2D).

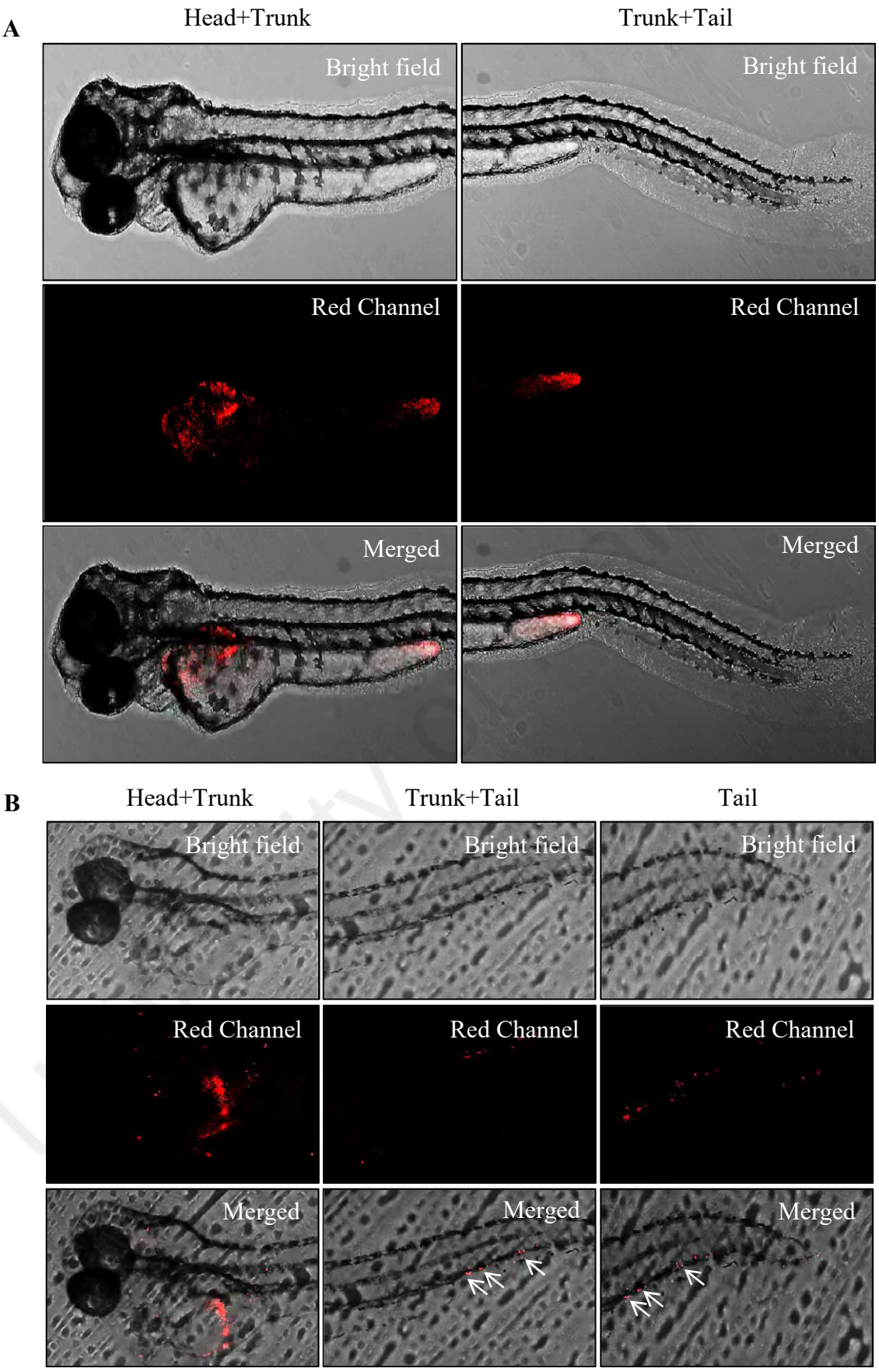

Figure 8.1: Representative embryos are shown at 24 h post injection. (A) MiR-378 hairpin inhibitors-treated and **(B)** negative inhibitors control-treated A549-I7 cells were labelled with DiI dye prior to injection and the fluorescence was visualised at 24hpi at 543nm. White arrows depict metastases when there were more than 5 cells present.

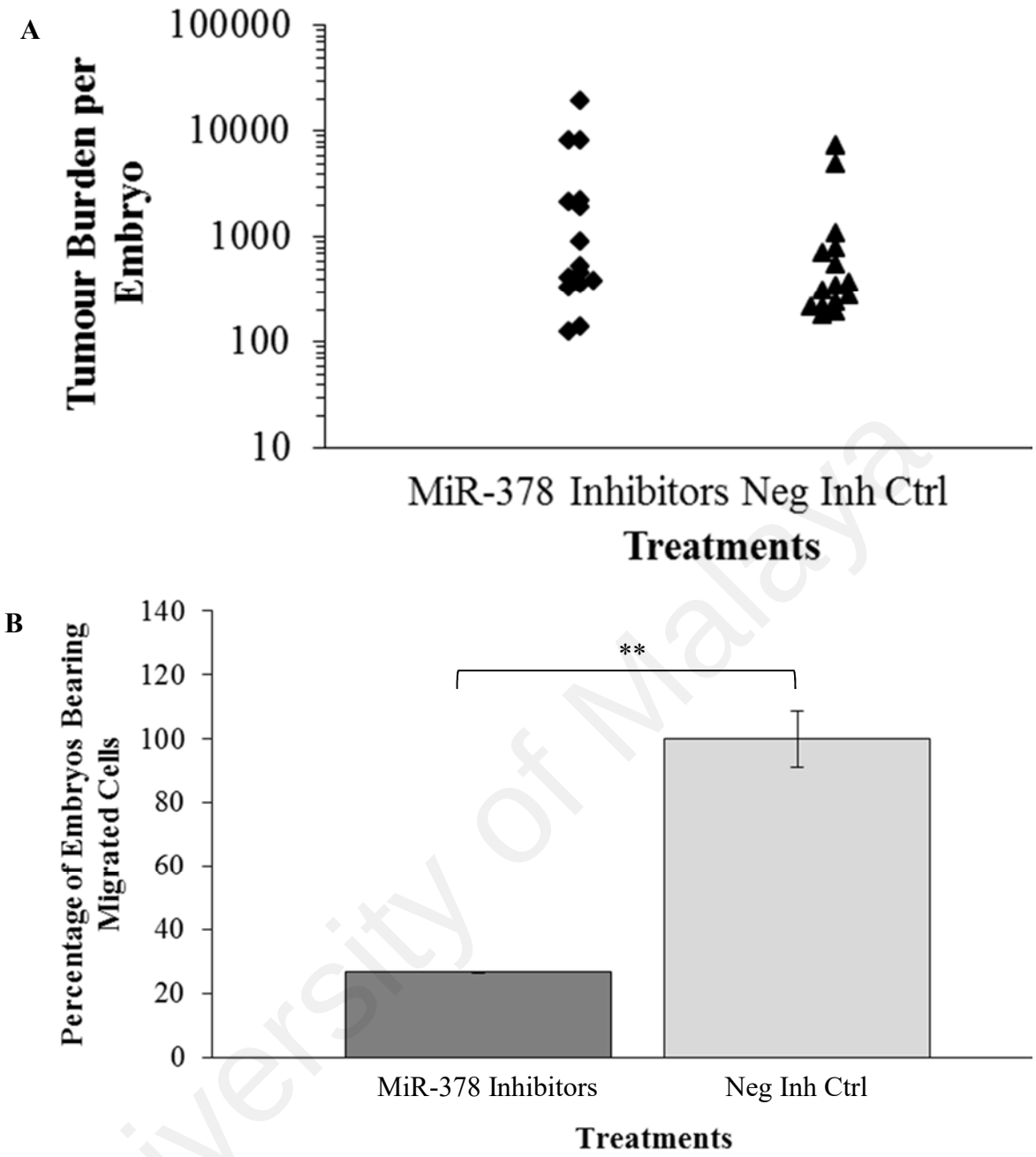

Figure 8.2: Anti-miR-378-transfected cells displayed a lower metastatic response. **(A)** Quantification of tumour burden in zebrafish embryos at 24hpi. **(B)** Quantification of percentage of embryos with evident tail migration.

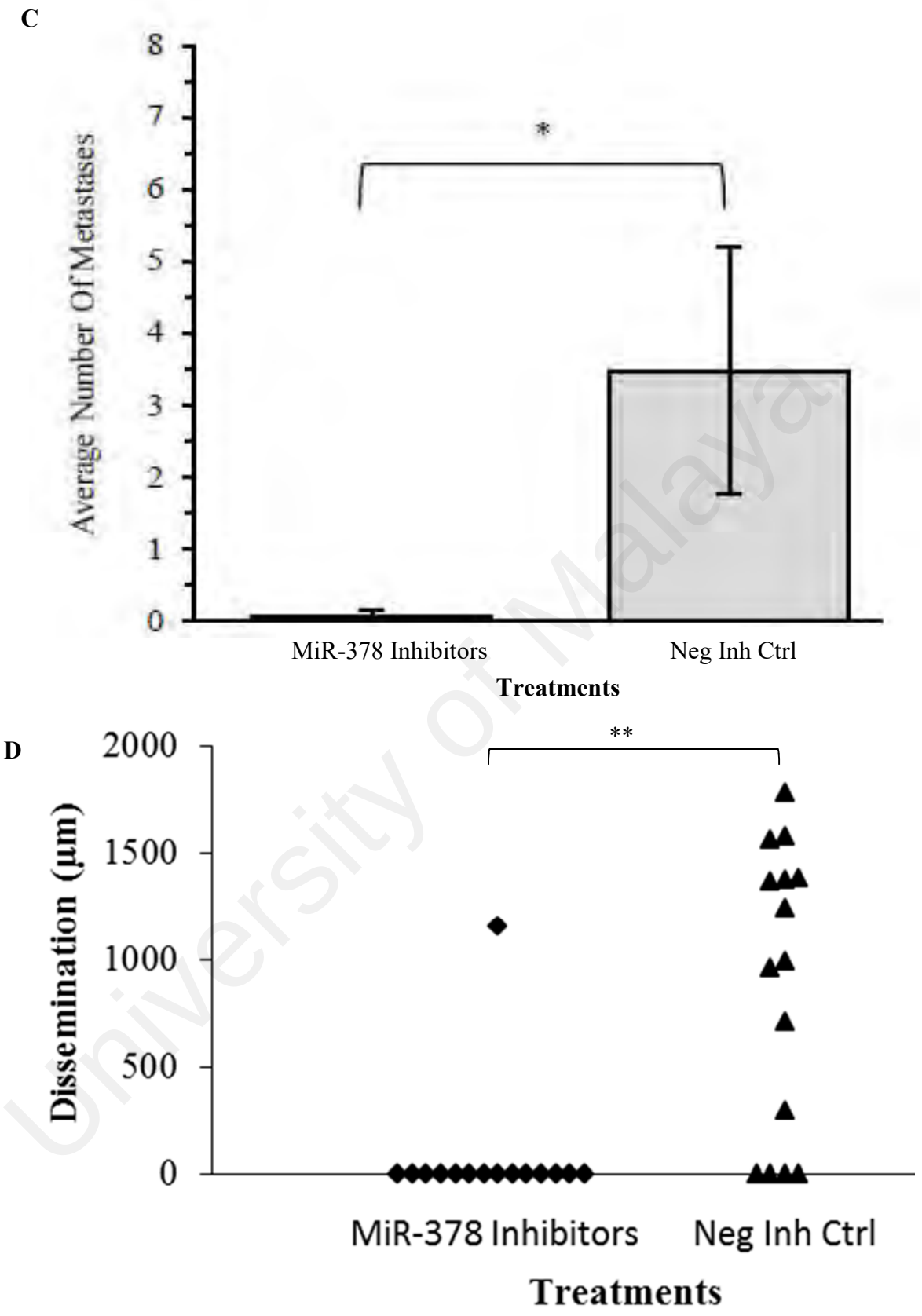

Figure 8.2, continued: (C) Quantification showing the average number of disseminated cells. **(D)** Motility of cells injected into the yolk sac of zebrafish embryos at 24hpi. Statistical significance was assessed by Student *t*-test analysis and significance was expressed as * $P < 0.05$ and ** $P < 0.01$.

8.1.2 MiR-1827 Mimics Decreased Distant Metastasis of Lung Cancer Cells in Zebrafish Embryos

To examine the effect of miR-1827 on lung cancer metastasis, the metastatic potential of miR-1827 mimics- and negative mimics control-transfected A549-I7 cells were injected into the yolk sac of zebrafish embryos. Bearing approximately the same number of tumour cells (Figure 8.4A), there was a significant decrease in the ability of miR-1827 mimics-transfected A549-I7 cells to metastasise in zebrafish embryos, in comparison to negative mimics control (Figure 8.3 and Figure 8.4B). The average number of metastases was reduced almost completely when cells were transfected with miR-1827 mimics, while negative mimics control-transfected cells formed two metastases on average (Figure 8.4C). In addition, cells overexpressing miR-1827 were also not able to distribute further compared to control (Figure 8.4D).

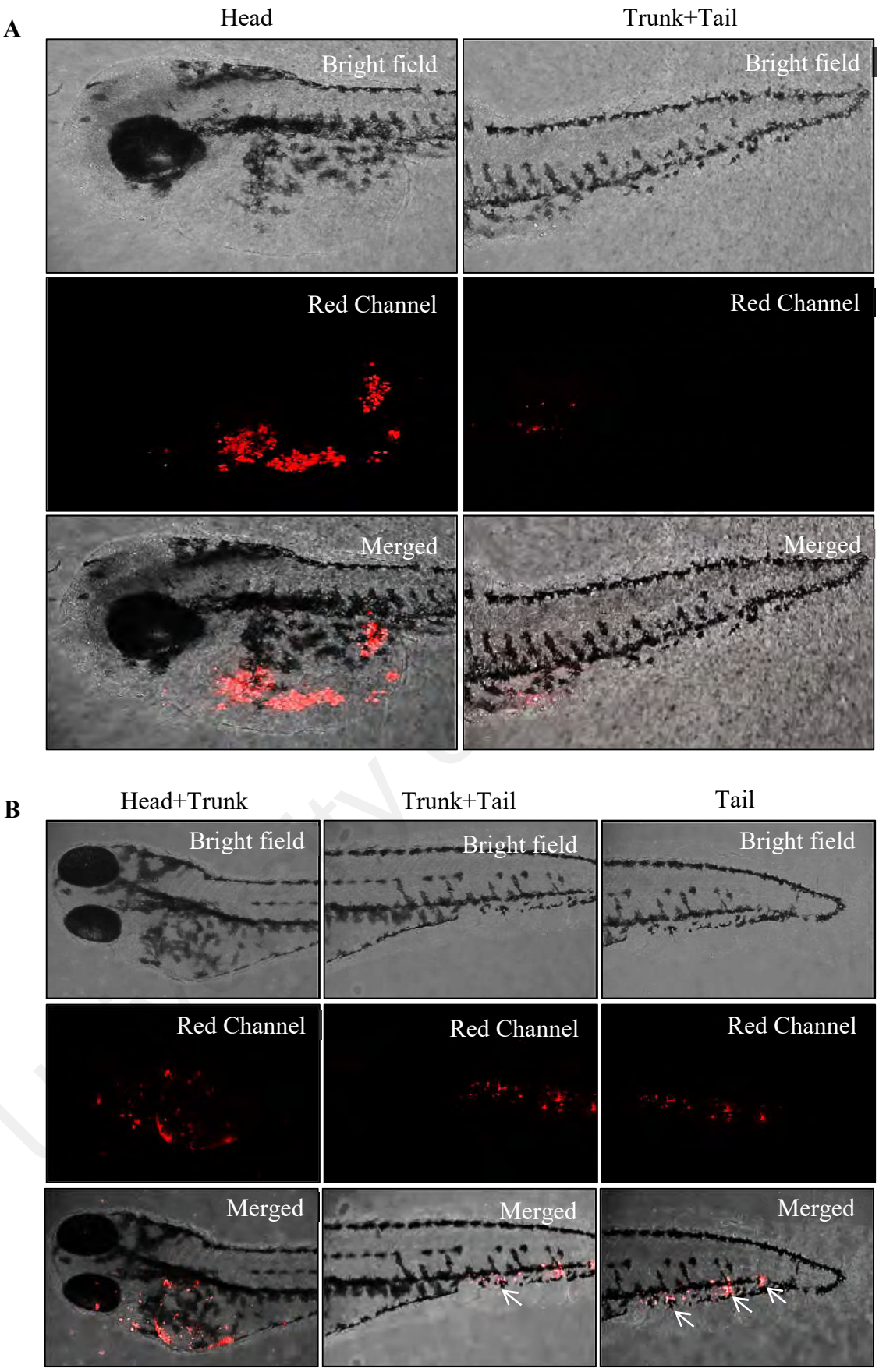

Figure 8.3: Embryos were injected with (A) miR-1827 mimics- or (B) negative mimics control-transfected A549-I7 cells and imaged at 24hpi. Representative images are shown.

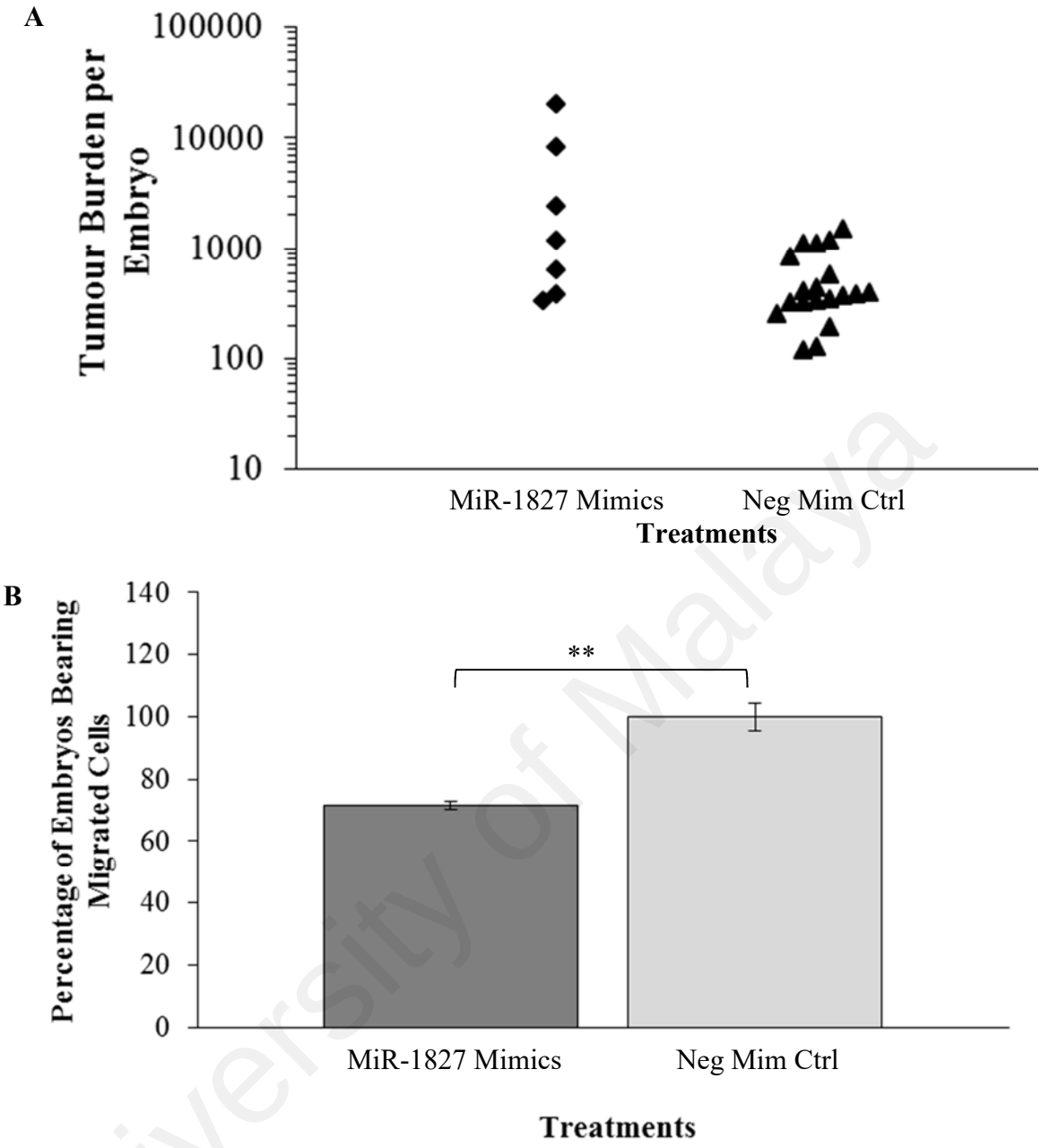

Figure 8.4: MiR-1827 mimics-transfected cells developed fewer metastases. (A) No significance in tumour burden counted in the whole fish body. **(B)** Percentage of embryos with migration was counted at 1dpi.

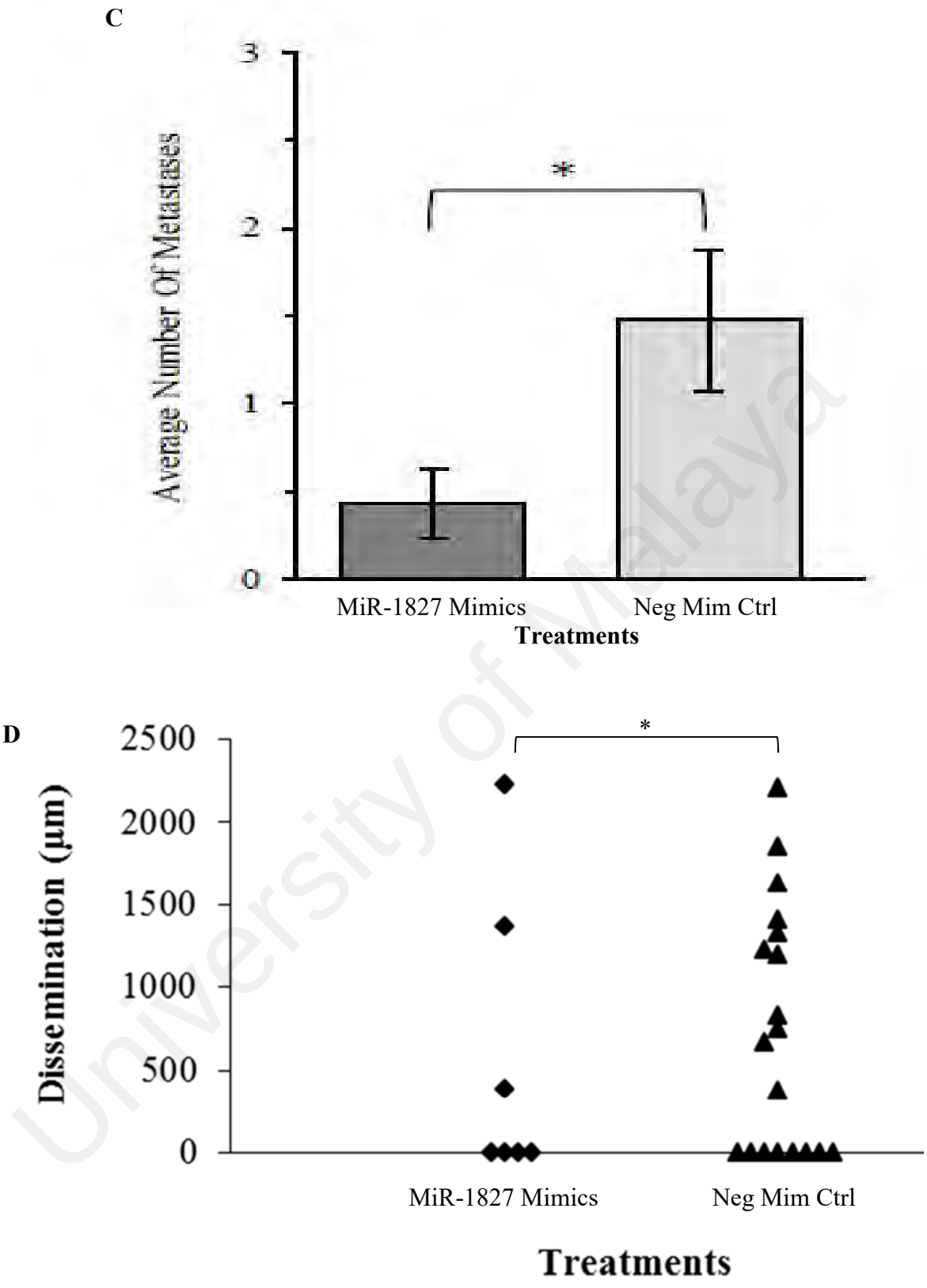

Figure 8.4, continued: (C) Average number of tumour foci in embryos injected with cells overexpressing miR-1827 compared to negative mimics control. **(D)** Metastatic foci were measured relative to the injection site and dissemination was presented as mean distance per foci for individual fish. * $P < 0.05$, ** $P < 0.01$

8.2 Whole-mount ALP Vessel Staining

The developing zebrafish vasculature is an established model of angiogenesis. High invasive A549 cells were transfected with miR-378 hairpin inhibitors or miR-1827 mimics and fluorescently labelled. Implantation of human lung cancer cells into the yolk sac of zebrafish embryos induced neovascularisation. A day after injection, the embryos were fixed and stained for endogenous alkaline phosphatase activity to detect the newly formed blood vessels (Childs *et al.*, 2002).

8.2.1 MiR-378 Regulates Angiogenesis *In Vivo*

Only 7% of embryos transfected with anti-miR-378 showed ectopic vessel formation (Figure 8.6A). The embryos were either vessel-free or only one ectopic vessel was observed (Figure 8.6B). In contrast, more newly formed blood vessels were seen sprouting from the sub-intestinal vessels (SIV) plexus into the tumour mass transfected with negative inhibitors control (Figure 8.5B and Figure 8.6B).

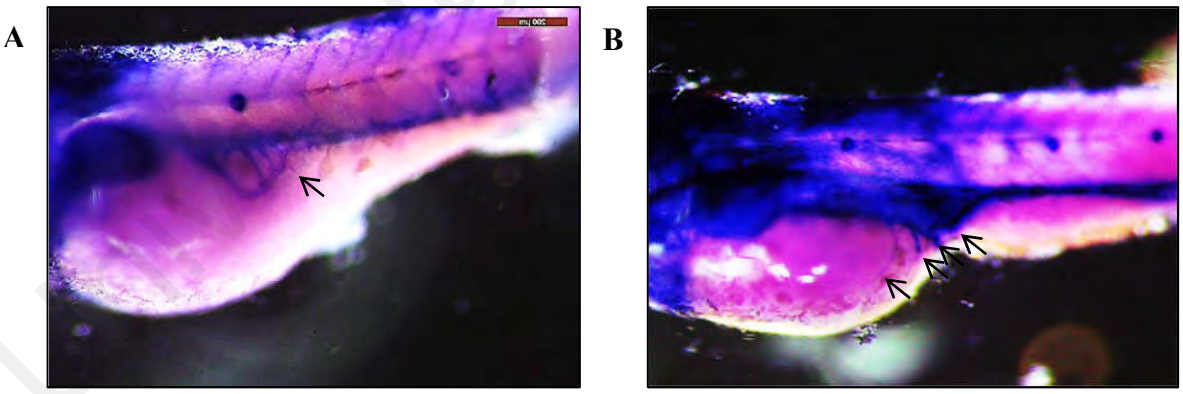

Figure 8.5: Lateral view of stained zebrafish embryos that were transplanted with A549-I7 cells transfected with (A) miR-378 hairpin inhibitors or (B) negative inhibitors control. Representative images are shown. Black arrows indicate newly formed ectopic vessels from the SIV.

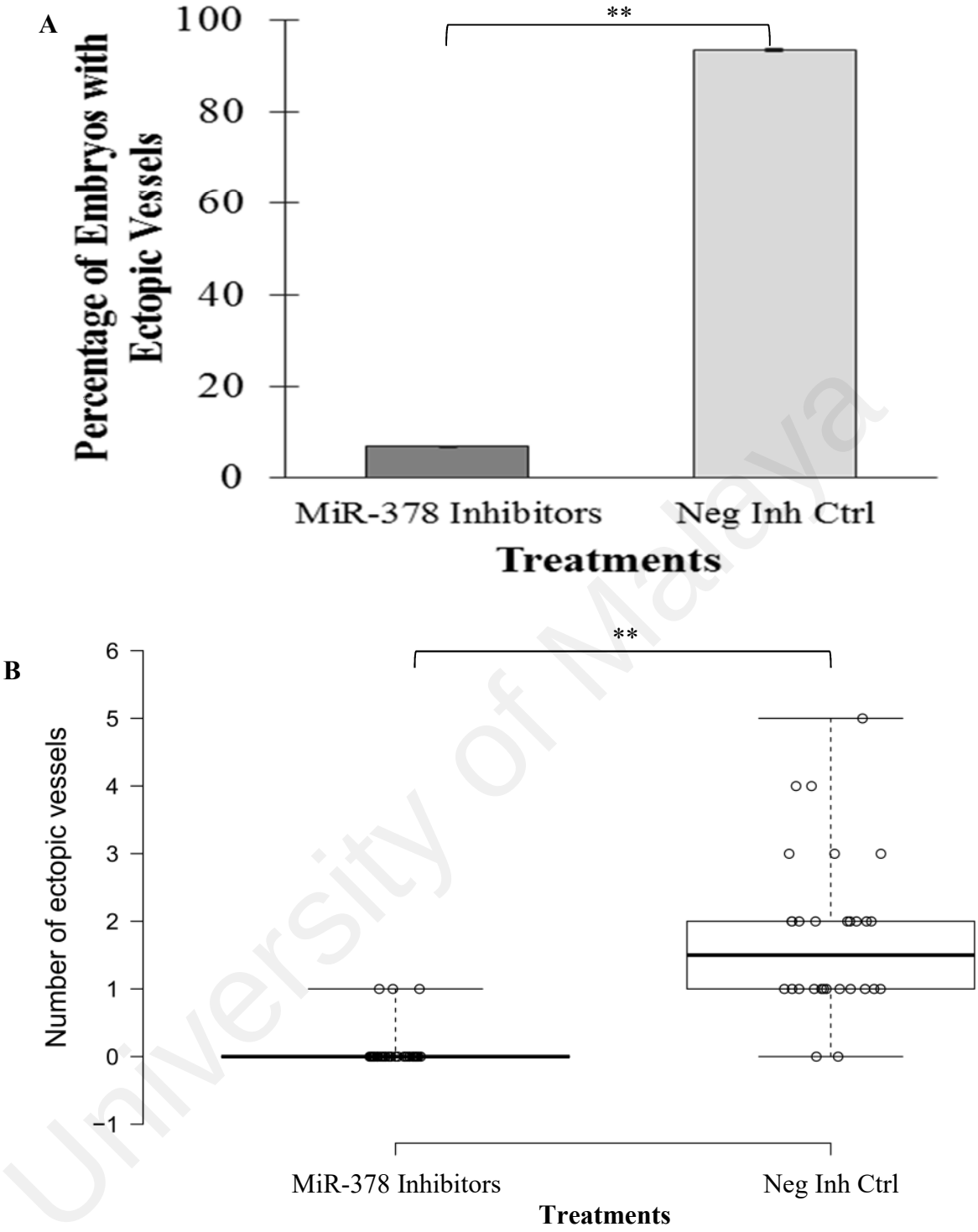

Figure 8.6: Quantification of angiogenic activity using zebrafish embryos. (A) The percentage of embryos with ectopic vessels was computed. **(B)** The number of newly formed ectopic vessels was measured. ** $P < 0.01$

C

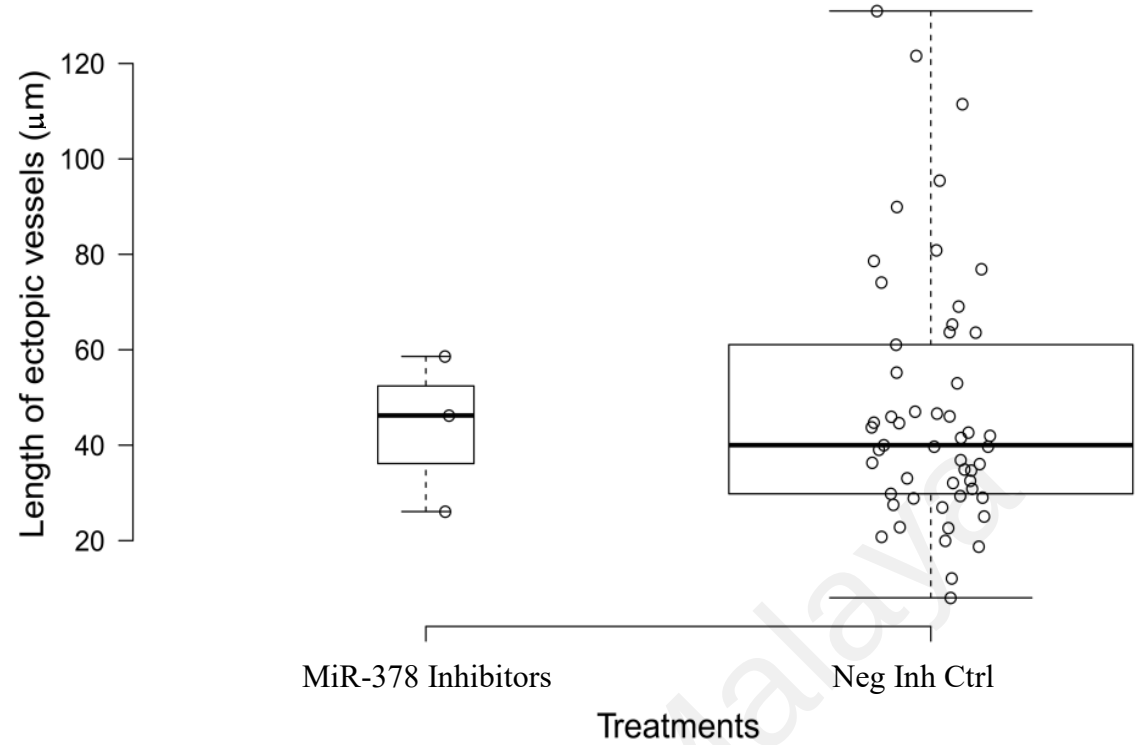

Figure 8.6, continued: (C) The length of newly formed ectopic vessels was measured. ** $P < 0.01$

8.2.2 MiR-1827 Mediates Angiogenesis of NSCLC

In brief, neovascularisation occurred in embryos in which cancer cells had been treated with negative mimics control. A significant decrease in the percentage of embryos carrying ectopic vessels was found with miR-1827 mimics (17%) compared to negative mimics control (65%) cells implantation (Figure 8.8A). MiR-1827-overexpressing A549-I7 cells showed negligible angiogenic responses while control cells induced a robust neovascular response (up to 6 new vessels formed) (Figure 8.7 and Figure 8.8B).

A

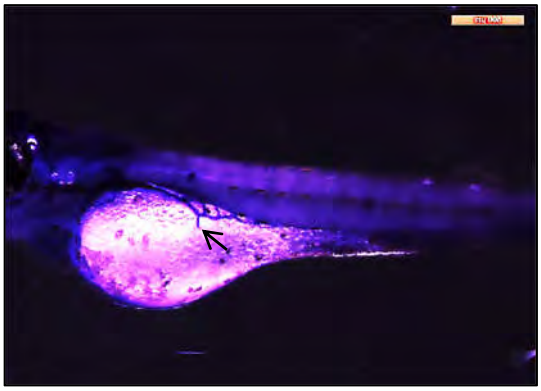

B

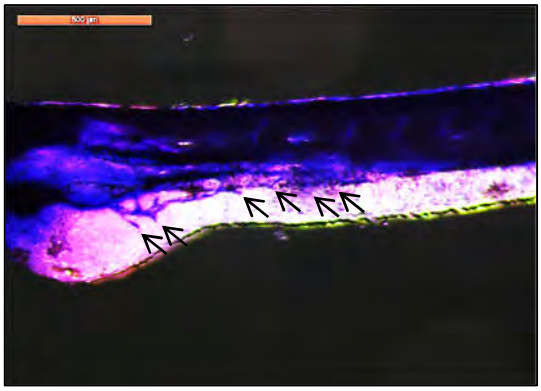

Figure 8.7: Alkaline phosphatase staining of (A) miR-1827 mimics-treated cells-injected and (B) negative mimics control-treated cells-injected embryos. Representative images are shown. Numerous neovessels originating from the SIV basket were seen to migrate and infiltrate the control cell graft, whereas only one neovessel formation was observed in embryos injected with cells transfected with miR-1827 mimics. Black arrows indicate newly formed ectopic vessels from the SIV.

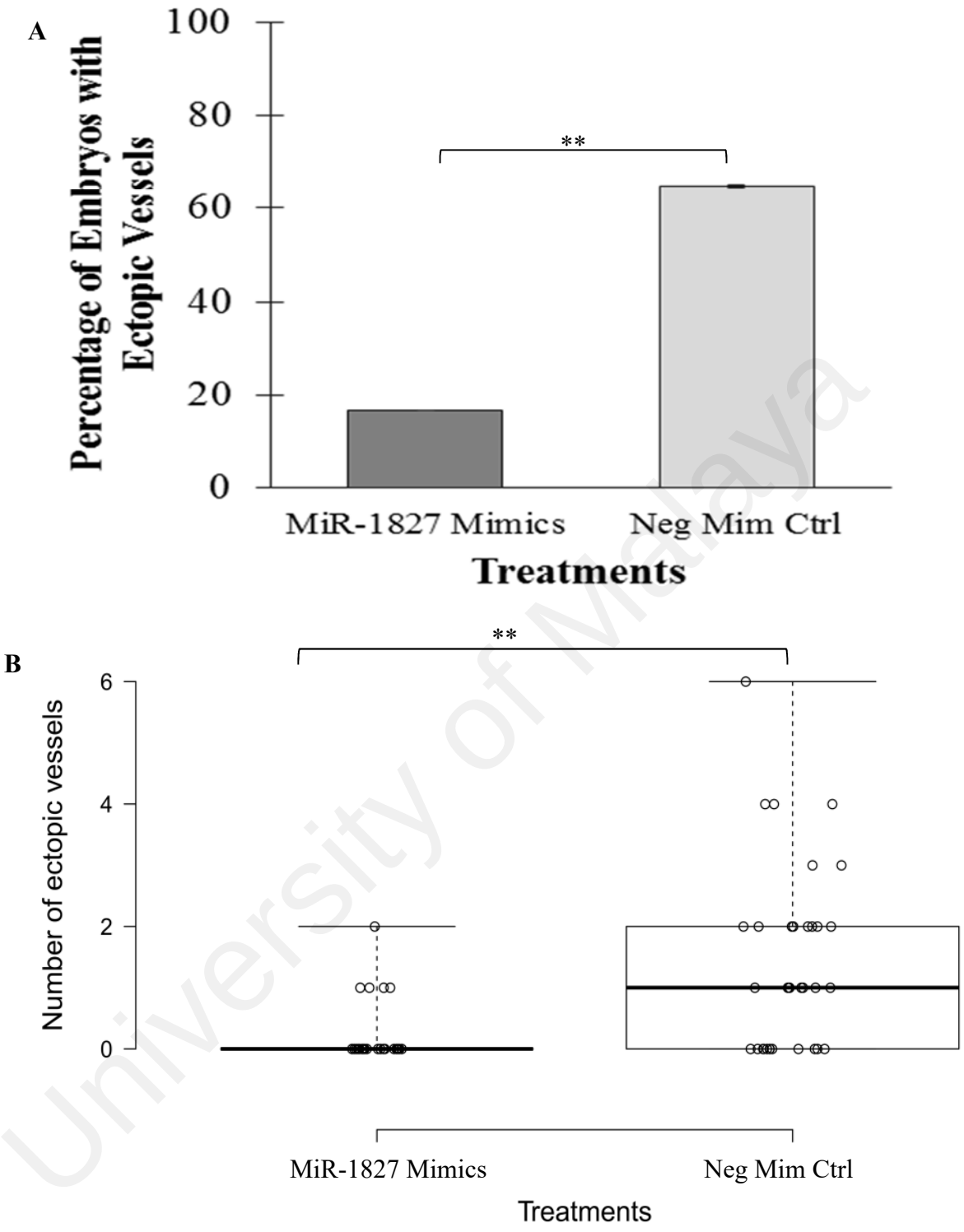

Figure 8.8: Growth of ectopic vessels in zebrafish embryo. (A) Quantification of number of embryos with ectopic vessels. **(B)** Distribution of the total number of neovessels for individual embryo. ** $P < 0.01$

C

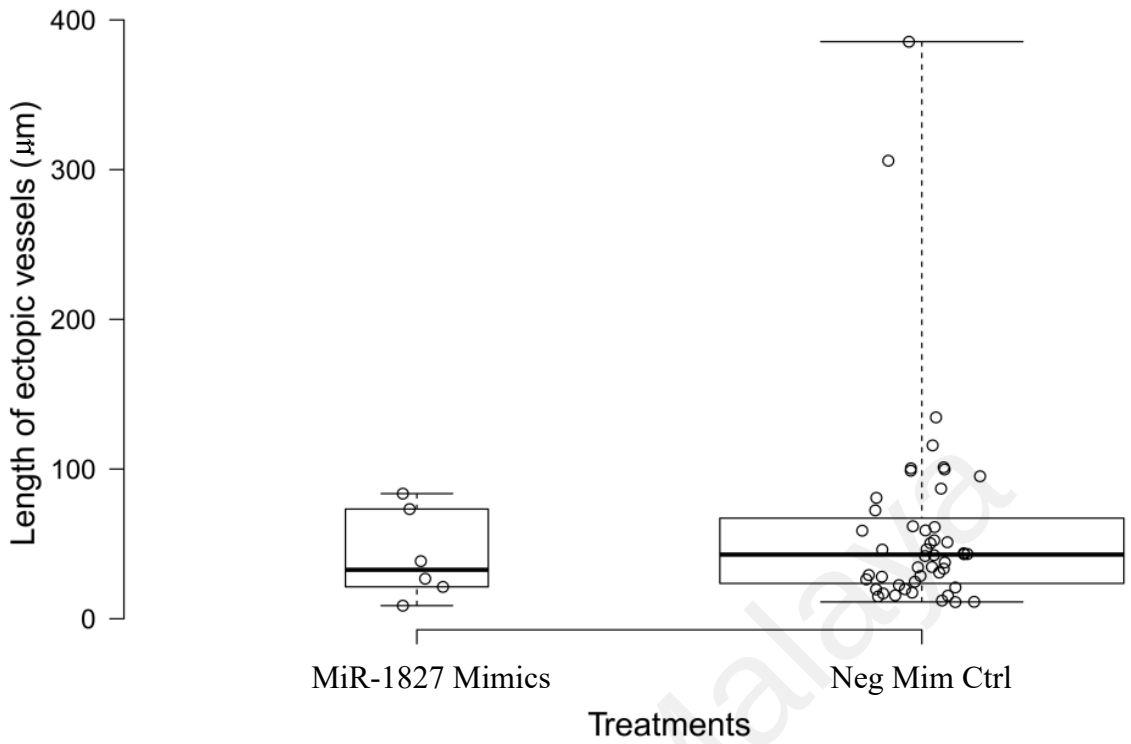

Figure 8.8, continued: (C) Ectopic vessel length was determined by point to point measurement using Fiji.

8.3 Summary

Statistical analyses showed a significant difference between the number of lung focal points derived from miR-378-suppressed and miR-1827-overexpressed A549-I7 cells in comparison to the corresponding control cells. This suggests that miR-378 and miR-1827 govern lung cancer metastasis. Additionally, there was a significantly lower incidence of neovascularisation in embryos injected with A549-I7 cells treated with anti-miR-378 and miR-1827. In consistency with *in vitro* results, miR-378 and miR-1827 were proven to be important miRNAs that regulate angiogenesis in lung cancer.

However, it is well-known that there exists limitation to the *in vivo* metastasis model used here, in which the specific processes such as cell invasion and migration could not be more truthfully represented due to limited resources. It is understood that in order to migrate, cells must first intravasate into the circulation and later extravasate to distant sites, and the fact that tumour cells were found in the tail vein of the embryos

indicates that invasion has taken place. Regardless, in the absence of in depth real-time imaging for analysis, determining precise benchmarks to characterise cell invasion and migration remains controversial. Nonetheless, it was proposed that the threshold to imply cell invasion and migration is the presence of > 3 or 5 cells extravasating per embryo (Teng *et al.*, 2013; Zoni *et al.*, 2015). All in all, the zebrafish embryo model was able to evaluate the metastatic and angiogenic roles of miR-378 and miR-1827 in NSCLC.

CHAPTER 9: DISCUSSION

9.1 Emerging Picture of the Role(s) of MiR-92b, MiR-378 and MiR-1827 in NSCLC Metastasis and Angiogenesis

Cancer arises through somatic evolution which contributes to tumour heterogeneity (Gerlinger *et al.*, 2012; Burrell *et al.*, 2013). The *in vitro* serial selection assay practised in this study is thus useful for isolating cell variants with different degrees of malignancy, and the isolated cell populations can be used to assess properties associated specifically with lung cancer metastasis (Chu *et al.*, 1997). Following the identification of eleven miRNAs that were significantly deregulated in A549-I7 sub-cell line in comparison to A549-NI7 sub-cell line, miR-92b, miR-378 and miR-1827 were validated as miRNAs that play important roles in NSCLC metastasis.

Encoded on human chromosome 1q22, hsa-miR-92b differs by only one nucleotide in its first 20 from miR-92a, a member of the oncogenic miR-17-92 cluster (Hayashita *et al.*, 2005). The promoter of miR-92b has two STAT1 (signal transducer and activator of transcription 1) target sites. In the presence of interferon, STAT1 binds directly to miR-92b promoter regions to regulate miR-92b transcription. Interestingly, interferon gamma (*IFNG*) is a target of miR-92b. Together, they form a feedback loop resulting in the attenuation of interferon effects through STAT1-miR-92b-mediated network (Wang *et al.*, 2010a).

In accordance to past studies (Vosa *et al.*, 2011; Wang *et al.*, 2011a), miR-92b was found to be increased in both A549-I7 and SK-LU-1-I7 cells. However, miR-92b was revealed to not be a major miRNA controlling NSCLC cell invasion, migration and angiogenesis, which contrasts with the findings by Lei *et al.* (Lei *et al.*, 2014). This variation may be attributed to the use of parental cell lines which are composed of unknown percentages of high and low invasive cells, thus giving rise to dissimilarities

in miR-92b levels and its outcomes. MiR-92b has also been found to be up-regulated and functions as an oncogene in several other tumours, including brain primary tumours, colon cancer and ovarian epithelial carcinoma (Nass *et al.*, 2009; Tsuchida *et al.*, 2011; Guo *et al.*, 2013). Studies have shown that miR-92b was associated with G1/S progression in human embryonic stem cells by targeting *CDKN1B* (Sengupta *et al.*, 2009), intestinal epithelial differentiation of C2BBe1 cells by targeting *SLC15A1* (solute carrier family 15 member 1) (Dalmasso *et al.*, 2011), neuroblastoma tumourigenesis by targeting *DKK3* (Dickkopf WNT signalling pathway inhibitor 3) (Haug *et al.*, 2011), growth and cisplastin chemosensitivity of A549 cells by targeting *PTEN* (Li *et al.*, 2013b), invasion and proliferation of glioblastoma cells by targeting *NLK* (Nemo-like kinase) and *SMAD3* (Wang *et al.*, 2013c; Wu *et al.*, 2013c), as well as metastasis and proliferation of hepatocellular carcinoma cells by targeting *SMAD7* (SMAD family member 7) (Zhuang *et al.*, 2016).

The gene encoding hsa-miR-378 is located within intron 1 of *PPARGC1B* (peroxisome proliferator-activated receptor gamma co-activator 1 beta) gene on human chromosome 5q33.1, suggesting that the expression of miR-378 would be in parallel with that of *PPARGC1B*, a transcriptional regulator of oxidative energy metabolism (Lin *et al.*, 2005). Later, it was found out that miR-378 is regulated and transcribed independently from *PPARGC1B* (Hupkes *et al.*, 2014). Nevertheless, embedding in the sequence of the regulator of hepatic lipid synthesis and lipoprotein production, miR-378 was found to affect lipid and xenobiotic metabolism, lipid storage, mitochondrial function and shift towards glycolytic pathway (Warburg effect) (Eichner *et al.*, 2010; Carrer *et al.*, 2012). MiR-378 was also identified as a target of MYC (Feng *et al.*, 2011) and HMOX1 in NSCLC. *HMOX1* overexpression tended to attenuate distal metastasis, while miR-378 enhanced lung metastasis. These observations were supported by an analysis of NSCLC clinical samples in which *HMOX1* expression was lower in lymph

node metastasis than in primary tumour, while miR-378 tended to be non-significantly higher in metastasis. Interestingly, *HMOX1* is a target of miR-378, forming a feedback regulatory loop (Skrzypek *et al.*, 2013).

In this study, miR-378 was found to be up-regulated in both A549-I7 and SK-LU-1-I7 cells compared to A549-NI7 and SK-LU-1-NI7 cells, as with the other cancer types such as acute myeloid leukaemia, diffuse large B-cell lymphoma, gastric cancer, ovarian cancer and renal cell carcinoma (Imig *et al.*, 2011; Liu *et al.*, 2012b; Redova *et al.*, 2012; Qian *et al.*, 2013; Chan *et al.*, 2014). However, miR-378 was found to be down-regulated in basal cell carcinoma, colorectal cancer, cutaneous squamous cell carcinoma, oral cancer and prostate cancer (Guo *et al.*, 2009; Yao *et al.*, 2009; Scapoli *et al.*, 2010; Wang *et al.*, 2010c; Callari *et al.*, 2012; Faltejskova *et al.*, 2012; Mosakhani *et al.*, 2012; Sand *et al.*, 2012a; Sand *et al.*, 2012b; Deng *et al.*, 2013; Fei & Wu, 2013; Chen *et al.*, 2016b). It is also worth mentioning that miR-378 has different expression between tissues and plasma (Tanaka *et al.*, 2009; Wang *et al.*, 2009a; Yu *et al.*, 2014), suggesting that miRNAs are selectively taken up and released by cells.

MiR-378 was shown to promote cell invasion, migration and angiogenesis in liver cancer, nasopharyngeal carcinoma and NSCLC by down-regulating *SUFU*, *TOB2* (transducer of *ERBB2*, 2) and *TUSC2* (tumour suppressor candidate 2) expression (Chen *et al.*, 2012; Ma *et al.*, 2014; Yu *et al.*, 2014), leading to an up-regulation of angiopoietin 1 (ANGPT1), angiopoietin 2 and VEGFA (Pola *et al.*, 2001; Lee *et al.*, 2007; Wang & Olson, 2009b). This is somewhat in agreement with the results demonstrated in this study, where miR-378 was proven to be a significant miRNA that modulates cell invasion and angiogenesis in both A549-NI7 and SK-LU-1-NI7. Nonetheless, it was revealed that miR-378 is dispensable for cell migration during metastasis in NSCLC. Taken together, miR-378 is categorised as an oncomiR and is part of the angiogenic network in lung tumour. Conversely, miR-378 could exhibit

opposite effects in some types of tumours which may be due to the differences of the tumour microenvironment. In colorectal cancer tissue samples, loss of miR-378 expression was associated with advanced clinical stage and lymph node metastasis (Zhang *et al.*, 2014). Besides that, overexpression of miR-378 could significantly inhibit cell invasion and migration in colorectal cancer, gastric cancer and prostate cancer cells (Guo *et al.*, 2009; Yao *et al.*, 2009; Fei & Wu, 2013; Zhang *et al.*, 2014; Chen *et al.*, 2016b).

Hsa-miR-1827 is located in the intergenic region on human chromosome 12q23.1 (Friedlander *et al.*, 2008). To date, miR-1827 was only implicated to be up-regulated in paediatric brain tumours (Liu *et al.*, 2013a) and down-regulated in colorectal cancer (Zhang *et al.*, 2016). MiR-1827 was also found to negatively regulate *MDM2* to suppress tumour growth (Zhang *et al.*, 2016). Thus, this study successfully discovered a novel role of miR-1827 in governing NSCLC cell migration and angiogenesis.

9.2 Signalling Pathways Associated with NSCLC Metastasis and Angiogenesis

To investigate the mechanism taken by miR-378 and miR-1827 to regulate NSCLC cell invasion, migration and angiogenesis, targets of the miRNAs were identified using TargetScan and DIANA-microT-CDS, and functionally annotated by DAVID. The gene targets were illustrated in Chapter 6.0 such that the roles of miR-378 and miR-1827 were integrated into a broader signalling network of metastasis and angiogenesis. Generally, most of the miRNAs target genes are involved in ErbB, HIF-1, Hippo, p53, Rap1, Ras, TGF-β and Wnt signalling pathways to mediate metastatic and angiogenic effects.

9.2.1 Wnt Signalling

Wnt signals are transduced by at least two distinct pathways: the canonical Wnt/β-catenin pathway and β-catenin-independent non-canonical Wnt pathway (Wnt/Ca^{2+} and Wnt/planar cell polarity (PCP)) (Komiya & Habas, 2008). Canonical Wnt signalling regulates cell adhesion by regulating the stability of catenin beta 1, where it is in complex with cadherin 1 and catenin alpha (CTNNA) at the adherens junction (Kemler, 1992; Ilyas & Tomlinson, 1997; Nelson & Nusse, 2004). As miR-1827 was down-regulated in NSCLC and that *WNT*, *FZD* (frizzled) and *LRP5/6* (low density lipoprotein receptor-related protein 5/6) were predicted to be targeted by miR-1827, hence the three components were predicted to be up-regulated and decreases CTNNB1 degradation by the ubiquitination and proteasomal pathways (Yost *et al.*, 1996; Ciechanover, 1998; Liu *et al.*, 2002; You *et al.*, 2004). The accumulation of CTNNB1 in the nucleus causes an up-regulation of transcription of multiple genes such as *MYC* and *VEGF* in angiogenesis (He *et al.*, 1998; Tetsu & McCormick, 1999). Interestingly, *MYC* could be directly targeted by miR-1827. *MYC* is amplified in 2.5-10.0% of NSCLC (Reissmann *et al.*, 1999). It promotes angiogenesis and vasculogenesis by up-regulating the expression of pro-angiogenic factors and by repressing anti-angiogenic factors such as connective tissue growth factor (CTGF) and thrombospondin 1 (THBS1) (Baudino *et al.*, 2002; Dews *et al.*, 2006).

RHO (RAS homolog) GTPases are also activated in the canonical Wnt signalling pathway in lung carcinogenesis (Uematsu *et al.*, 2003; Schlessinger *et al.*, 2009). RHO GTPases regulate cell movement by regulating the dynamic reorganisation of the actin cytoskeleton that directs protrusion (lamellipodia) at the leading edge and retraction at the rear of the cell, as well as involved in focal adhesion and stress fibre formation, all of which are essential in EMT and enable directional migration in metastasis (Ridley & Hall, 1992; Arber *et al.*, 1998; Clark *et al.*, 2000; Cascon *et al.*,

2003; Lamalice *et al.*, 2007; Narumiya *et al.*, 2009; Nelson, 2009; Godde *et al.*, 2010; Spiering & Hodgson, 2011).

On the other hand, the Wnt/Ca^{2+} pathway, mediated by G-protein signalling, has been demonstrated to be regulator of cell migration in mammalian cancer cell lines (Weeraratna *et al.*, 2002; Wang *et al.*, 2010b). Wnt-FZD binding activates phospholipase C (*PLC*) leading to an increase of intracellular Ca^{2+} level and activation of downstream Ca^{2+}-sensitive effectors including protein kinase C (PRKC) and calcium/calmodulin-dependent protein kinase II (CAMK2) (Kuhl *et al.*, 2000). It is worthy to note that *PLC* and *CAMK2* were predicted as miR-1827 gene targets, suggesting that their expression were up-regulated when miR-1827 was down-regulated in NSCLC. This in turn regulates the organisation of the actin cytoskeleton and cell adhesion (Frank *et al.*, 1998; Bourguignon *et al.*, 2006). The low expression of miR-1827 was also predicted to promote the expression of transmembrane VANGL planar cell polarity protein 2 (*VANGL2*) in PCP pathway that transduces extracellular inputs to induce intracellular cytoskeleton rearrangements (Bastock *et al.*, 2003; Strutt, 2003; Jenny *et al.*, 2005). All in all, miR-1827 was predicted to up-regulate the members in all three types of Wnt signalling pathways to modulate adherens junction, cytoskeletal dynamics and focal adhesion in NSCLC metastasis.

9.2.2 ErbB and Ras Signalling

Protein tyrosine kinase 2 (*PTK2*) is activated by angiogenic growth factors, such as fibroblast growth factor (*FGF*) and insulin-like growth factor (*IGF*), which were predicted as targets of miR-1827. Enhanced expression of *PTK2* increases cell migration (Mitra *et al.*, 2005) by regulating the disassembly of focal adhesion through the suppression of RHO activity (Ren *et al.*, 2000; Webb *et al.*, 2004; Owen *et al.*, 2007; Iwanicki *et al.*, 2008).

STAT3 (signal transducer and activator of transcription 3) and *PI3K* (phosphatidylinositol-4,5-bisphosphate 3-kinase) are also activated by the extracellular stimuli. Constitutive *STAT3* expression promoted by upstream signals as well as low level of miR-1827 was expected to induce *VEGF* expression and tumour angiogenesis in NSCLC (Darnell, 1997). *PI3K* is recognised to be involved in initiating actin cytoskeletal rearrangements, cell polarisation and cell migration in many cell types (Liliental *et al.*, 2000). *PI3K* has also been shown to be involved in the secretion of PLAU which degrades plasminogen and MMP9 (matrix metallopeptidase 9) which degrades collagen IV in the ECM that are important for tumour cell invasion (Dunn *et al.*, 2001; Ellerbroek *et al.*, 2001).

Furthermore, as a result of miR-1827 down-regulation, more IKK (inhibitor of nuclear factor kappa B) complex was expected to be recruited to activate NFκB (nuclear factor kappa B). NFκB is involved in up-regulation of TWIST1 (TWIST family bHLH transcription factor 1)-mediated EMT that is critical for cancer cell invasion and metastasis (Huber *et al.*, 2004). The protein exerts its metastasis-promoting effect by up-regulating the transcription of genes known to be important for tumour metastasis, such as *HPSE* (heparanase), *MMP9* and *PLAU* (Grivennikov *et al.*, 2010; Lin *et al.*, 2010). It also down-regulates the expression of collapsin response mediator protein 1 (*CRMP1*), an invasion suppressor gene. In addition, NFκB can promote tumour metastasis through activation of integrin subunit alpha V (*ITGAV*) and integrin subunit beta 3 (*ITGB3*) (Cai *et al.*, 2011). A binding site for NFκB was also identified within the *VEGF* promoter (Pages & Pouyssegur, 2005). Collectively, when miR-1827 was down-regulated in NSCLC, its targeting on growth factor-mediated pathways was expected to be manifested by an increased ability to migrate and induce angiogenesis.

Perhaps a more intriguing interaction would be the regulation of *ERBB4* (Erb-B2 receptor tyrosine kinase 4) by both miR-378 and miR-1827. The two miRNAs were

predicted to have similar inhibitory effects on ERBB4 mRNA (TargetScan total context score of -0.10). Despite that, a stronger interaction with miR-1827 was predicted by DIANA (miR-378: 0.715 while miR-1827: 0.890). Therefore, when miR-378 was up-regulated and miR-1827 was down-regulated in NSCLC, the net result predicted is the up-regulation of *ERBB4*, leading to higher *KRAS* expression. The effect is heightened with the up-regulation of *GRB2* (growth factor receptor-bound protein 2) targeted by low level of miR-1827. Importantly, *KRAS* accounts for 90% of *RAS* mutations in lung adenocarcinomas, with mutations detected in about 25% of all tumours (Forbes *et al.*, 2006; Shigematsu & Gazdar, 2006). These mutations lead to constitutive activation of Ras signaling due to impaired GTPase activity (Riely *et al.*, 2009; Brandao *et al.*, 2012). Located downstream of *KRAS*, novel mutations in *BRAF* (B-RAF proto-oncogene, serine/threonine kinase) were also identified through systematic re-sequencing of oncogenes. They are present in around 2% of lung adenocarcinoma patients and restricted to tumours that did not show *KRAS* mutations (Brose *et al.*, 2002; Naoki *et al.*, 2002). The effector of ErbB signalling pathway, that is, the mitogen-activated protein kinase (MAPK) pathway, plays crucial role in cell motility (Eliceiri *et al.*, 1998). MAPK signalling has also been implicated in endothelial cell proliferation (Meadows *et al.*, 2001) and VEGF-mediated survival (Berra *et al.*, 2000).

9.2.3 Hippo Signalling

CRB (crumbs, cell polarity complex component) is a transmembrane protein that is essential for establishing the apical-basal polarity of a cell (Chen *et al.*, 2010a). Its expression was expected to be elevated when miR-1827 was down-regulated in NSCLC. This promotes the accumulation of WWTR1 (WW domain containing transcriptional regulator 1) and YAP1 (Yes-associated protein) in cytoplasm when they interact with members of the CRB complex, such as AMOT (angiomotin), MPDZ (multiple PDZ domain crumbs cell polarity complex component), MPP5 (membrane palmitoylated

protein 5) and PATJ (PATJ, crumbs cell polarity complex component) (Varelas *et al.*, 2010). The aberrant activation of WWTR1 and YAP1 contributes to anchorage-independent growth, cell invasion and EMT as well as enhances cancer stem cell characteristics (Zhao *et al.*, 2007; Chan *et al.*, 2008; Bhat *et al.*, 2011; Cordenonsi *et al.*, 2011). Moreover, recent ChIP-seq analyses revealed that when WWTR1 and YAP1 fuse with endogenous TEADs (TEA domain transcription factors), most of the target genes are associated with cell migration and ECM organisation (Stein *et al.*, 2015; Zanconato *et al.*, 2015). Apart from TEADs, WWTR1 and YAP1 also interact with SMADs to promote tumourigenesis (Rosenbluh *et al.*, 2012; Hiemer *et al.*, 2014).

9.2.4 HIF-1 and TGF-β Signalling

In addition to hypoxia, *HIF1A* can be induced by numerous stimuli including EGF (epidermal growth factor), FGF, IGF and ERBB2 activation (Zelzer *et al.*, 1998; Feldser *et al.*, 1999; Laughner *et al.*, 2001; Gao *et al.*, 2002; Gao *et al.*, 2004; Li *et al.*, 2004). The modulation of *HIF1A* by growth factors and hypoxia is orchestrated via a parallel-independent pathway (Bermont *et al.*, 2000). Activation of *KRAS*, *MAPK1/3* (mitogen-activated protein kinase 1/3) (Kumar *et al.*, 2007), *PI3K* (Stiehl *et al.*, 2002) and *SRC* (SRC proto-oncogene, non-receptor tyrosine kinase) (Bardos & Ashcroft, 2004) have also been implicated in stimulating normoxic expression of *HIF1A*. Thus, the predicted amplification of the pathways discussed above due to the down-regulation of miR-1827 in NSCLC causes HIF1A to accumulate in tumour cells even under normoxic conditions.

Upon binding to ARNT (aryl hydrocarbon receptor nuclear translocator) in the nucleus, various genes encoding proteins involved in angiogenesis and metastasis are activated (Semenza, 2001; Chun *et al.*, 2002; Semenza, 2002; Safran & Kaelin, 2003). In particular, HIF-1 activates the transcription of genes encoding repressors of CDH1

(*ID2* (inhibitor of DNA binding 2, HLH protein), *SNAI1* (SNAIL family transcriptional repressor 1), *SNAI2*, *TCF3* (transcription factor 3), *ZEB1* and *ZEB2*) and proteins that regulate cell-cell adhesion, cytoskeleton and other characteristics exhibited by epithelial cells (*TGFA* and *VIM*) (Gunaratnam *et al.*, 2003; Esteban *et al.*, 2006; Krishnamachary *et al.*, 2006; Wu *et al.*, 2011a). HIF-1 also activates transcription of genes encoding proteases that degrade (*CTSC* (cathepsin C), *MMP2*, *MMP14* and *PLAUR*) or remodel (*LOX* (lysyl oxidase), *LOXL2* (lysyl oxidase-like 2) and *LOXL4* (lysyl oxidase-like 4)) the ECM at both the primary and secondary sites, motility factors (*GPI* (glucose-6-phosphate isomerase) and *MET*), permeability factors that promote the intravasation of cancer cells into blood vessels (*ANGPT2* and *VEGF*), as well as cell surface (*L1CAM* (L1 cell adhesion molecule)) and secreted (*ANGPTL4* (angiopoietin-like 4)) proteins that stimulate extravasation of cancer cells into the parenchyma at distant sites of metastasis (Erler *et al.*, 2006; Wong *et al.*, 2011; Zhang *et al.*, 2011).

On the contrary, HIF1A is known to be a substrate of E3 ubiquitin ligase under normoxia (Koh *et al.*, 2008). Importantly, the components of the E3 ubiquitin ligase complex, *RBX1* was predicted to be down-regulated while von Hippel-Lindau tumour suppressor (*VHL*) was predicted to be up-regulated in NSCLC. The mechanism of how the balance is achieved and whether it affects HIF1A level is definitely something to ponder about. Nevertheless, the low level of *RBX1* was predicted to promote TGF-β signalling pathway, by facilitating the binding of SMAD2/3 and SMAD4 (SMAD family member 4). Consequently, production of ECM proteins is suppressed and ECM-degrading enzymes are stimulated (Bonnans *et al.*, 2014). Taken together, TGF-β and HIF-1 signalling pathways were predicted to play a part in NSCLC metastasis and angiogenesis.

9.2.5 p53 Signalling

Another key inhibitor of angiogenesis is the *TP53* (tumour protein p53) tumour suppressor gene. TP53 promotes the expression of angiogenesis inhibitors such as *THBS1* and inhibits *VEGFA* expression (Fontanini *et al.*, 1998a; Ravi *et al.*, 2000). Unfortunately, *TP53* is mutated in 60-75% of lung cancer including both SCLC and NSCLC (Devereux *et al.*, 1996) and thus the up-regulation of *HIF1A* was expected to not able to stabilise *TP53* (Zhong *et al.*, 1999). In turn, the loss of *TP53* expression enhances the heterodimerisation of HIF1A with ARNT, thereby up-regulating the expression of *VEGFA* in tumour cells (Zhong *et al.*, 1999).

9.2.6 Rap1 Signalling

Rap1 signalling pathway encompasses the regulators for adherens junction, cell polarity, cytoskeleton and focal adhesion. SRC is a cell-autonomous non-receptor tyrosine kinase that is frequently and aberrantly activated in malignant cancer including NSCLC (Mazurenko *et al.*, 1992; Masaki *et al.*, 2003). The protein mediates adhesion, invasion and motility by activating key components of the focal adhesion complex (BCAR1 (BCAR1, Cas family scaffolding protein), cortactin (CTTN), ezrin (EZR), paxillin (PXN), PTK2, talin (TLN), tensin (TNS) and vinculin (VCL)) and junctional proteins (CTNNB1, catenin delta 1 (CTNND1), gap junction protein alpha 1 (GJA1), junction plakoglobin (JUP), nectin cell adhesion molecule 2 (NECTIN2), OCLN and TJP1) (Thomas & Brugge, 1997; Kikyo *et al.*, 2000; McLachlan *et al.*, 2007; Parsons *et al.*, 2010). TLN is a scaffolding protein that links integrins to the actin cytoskeleton (Morse *et al.*, 2014). Integrins also bind ECM proteins or other adhesion receptors on neighbouring cells (Kim *et al.*, 2011). Moreover, TLN complexes PTK2 and VCL into a functional complex that controls inside-out activation of the integrin and outside-in signalling resulting from matrix binding (Mehrbod *et al.*, 2013).

Additionally, SRC leads to the activation of the ACTR2/3 (ARP2/3 actin-related protein 2/3 homolog) complex via its ability to phosphorylate and activate Wiskott-Aldrich syndrome (WAS) proteins (Park *et al.*, 2005). Members of these protein families facilitate the polymerisation of new actin strands and promote protrusion of the cell's leading edge (Insall & Machesky, 2009). CDC42 (cell division cycle 42) is another small GTPase that is involved in the formation of filopodia consisting of parallel bundles of actin filaments and are involved in sensing the chemotactic gradient (Lamalice *et al.*, 2007). In this study, *RAPGEF5* (Rap guanine nucleotide exchange factor 5) was predicted to be down-regulated by miR-378. Its expression was further reduced by *KRAS*. Hence, Rap1 signalling was predicted to be suppressed. However, the fact that when miR-378 was highly expressed, cells gained the abilities to invade and induce angiogenesis, suggests that Rap1 signalling pathway might not be the major route to metastasis and angiogenesis in NSCLC, or there could be other regulatory elements that counterbalance the inhibitory effects by miR-378 and *KRAS*.

9.3 Regulatory Mechanism of MiR-378 and MiR-1827 in NSCLC Metastasis and Angiogenesis

RBX1, also known as *ROC1* (regulator of cullins 1), is one of the RING components of CRL (cullin-based RING ligase), that is, the largest family of E3 ubiquitin ligases that mediate nearly 20% of ubiquitinated proteins for 26S proteasome degradation (Zhao & Sun, 2013). *RBX1* is evolutionarily conserved from yeast to human (Sun *et al.*, 2001). Human *RBX1* gene consists of 5 exons and 4 introns and it encodes a 13kDa protein (108 amino acids) (Tan *et al.*, 2009). Although the transcription of *RBX1* is often induced by mitogens (Ohta *et al.*, 1999), *RBX1* is, in general, constitutively expressed (Sun *et al.*, 2001). Yet, RBX1 is rapidly ubiquitinated and degraded upon overexpression, but the binding to cullins confers their stabilisation (Ohta *et al.*, 1999). RBX1 is localised in the cytoplasm and nucleus (Jia *et al.*, 2009),

signifying their participation in ubiquitination and degradation of both cytoplasmic and nuclear proteins (Chen *et al.*, 2016a).

RBX1 was reported to be overexpressed in carcinomas of the breast, gastric, liver and lung (Jia *et al.*, 2009; Chen *et al.*, 2015b; Xing *et al.*, 2016). Recent study showed that high *RBX1* expression was associated with advanced TNM stage and lymph node metastasis in NSCLC (Xing *et al.*, 2016). However, little is known about how *RBX1* is regulated at the post-transcriptional level. *RBX1* has only been reported to suppress bladder cancer cell migration by inhibiting EMT through targeting of the *MTOR* (mechanistic target of rapamycin)-inhibitory protein DEPTOR (DEP domain-containing MTOR interacting protein) (Wang *et al.*, 2016a), and *RBX1* was targeted by miR-194 to inhibit cell invasion and migration in gastric cancer (Chen *et al.*, 2015b), in other words, *RBX1* promotes gastric cancer cell invasion and migration. These suggest that *RBX1* could play different roles across different types of cancer.

Here, *RBX1* was shown to be directly targeted by miR-378 and ectopic expression of *RBX1* could overcome increased invasion driven by miR-378 in lung cancer cells. Similarly, silencing of *RBX1* restored the anti-miR-378-suppressed invasion in lung cancer cells. It was thus shown that *RBX1* is functionally involved in miR-378-mediated lung tumour cell invasion. As much as miR-378 was shown to regulate lung cancer cell invasion and angiogenesis, its target *RBX1* was revealed to not be a major player in NSCLC angiogenesis. This could be due to the need for CRL to be activated by the dissociation of CAND1 (cullin-associated and neddylation-dissociated-1) that sequesters cullin/RBX1 heterodimers upon binding to substrate-recognition module (SRM) followed by the neddylation of the cullin, thereby mediating the angiogenic effect in lung cancer cells along with adaptor and substrate receptor proteins (Figure 9.1) (Merlet *et al.*, 2009; Bulatov & Ciulli, 2015). This resulted in the

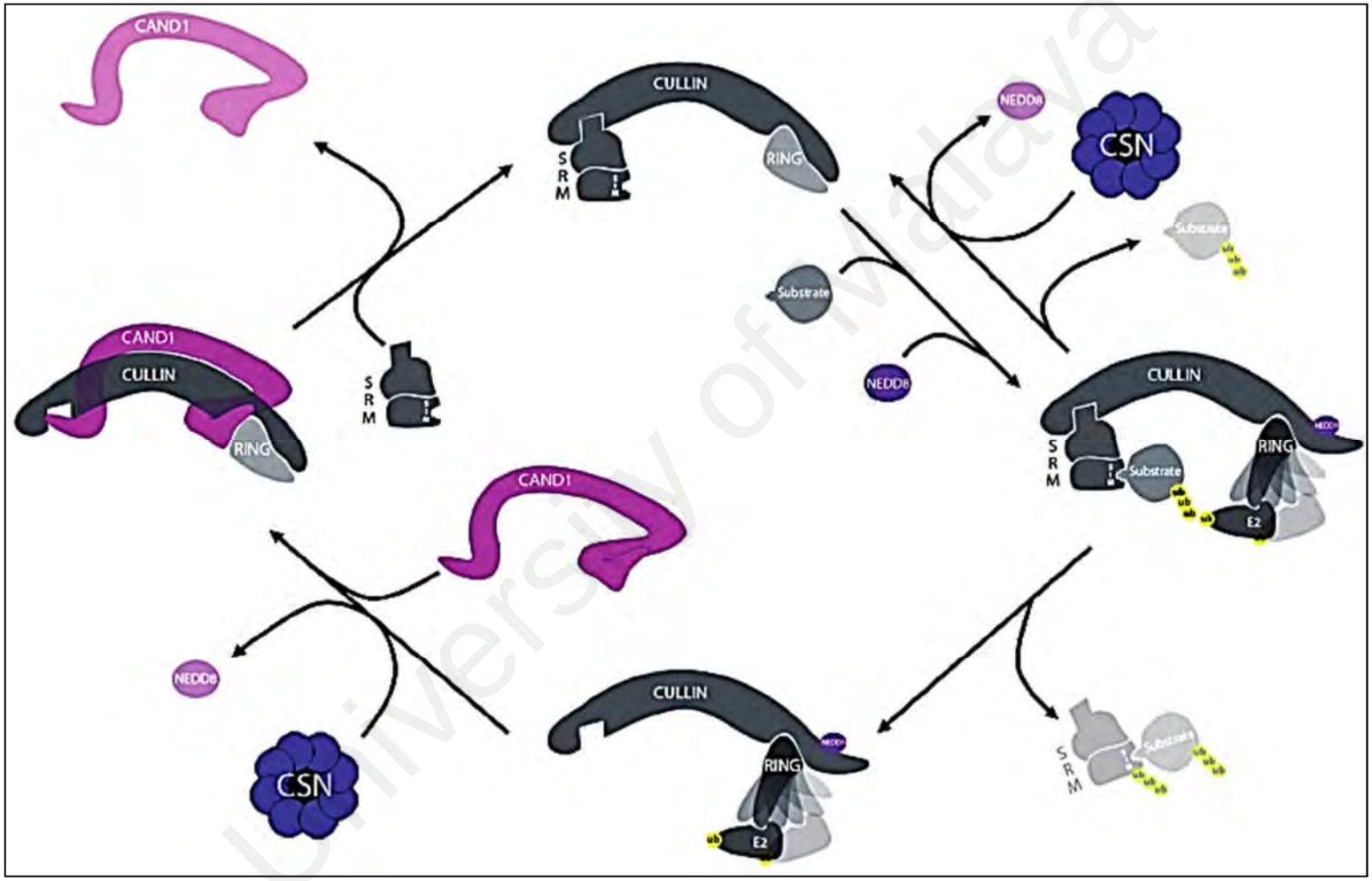

Figure 9.1: The CRL assembly cycle. CAND1 sequesters cullin/RBX1 heterodimers and dissociates upon binding of the SRM. The CRL complex is further activated by neddylation of the cullin subunit. The Cop9 Signalosome (CSN) hydrolyses cullin-NEDD8 conjugate and inactivates CRL complex (Figure reproduced with permission from Merlet *et al*., 2009).

insignificant elevation of the amount of angiogenic factors secreted into TCM, rather than silencing

insignificant elevation of the amount of angiogenic factors secreted into TCM, rather than silencing the gene in HUVEC itself (Tao *et al.*, 2014). *RBX1* also plays a role in HIF-1 signalling pathway to produce VEGF to induce angiogenesis during hypoxia (Weidemann & Johnson, 2008) and the experimental conditions in this study might have been the cause for partial restoration of angiogenic effects. In short, the detailed mechanism of miR-378/*RBX1* signalling merits further research.

A set of *in vitro* functional assays showed that *MYCL1* (MYC lung carcinoma-derived homolog) is a target of miR-1827. A G-to-T variant (rs3134615) in the MYCL1 3'-UTR inhibits its interaction with miR-1827, resulting in a constitutively higher *MYCL1* expression and an increased risk of SCLC (Xiong *et al.*, 2011a). This variant at 5q15.33 significantly influenced the risk of lung cancer differentially by histology, suggesting that genetic factors associated with the risk of SCLC and NSCLC may be different (Broderick *et al.*, 2009; Landi *et al.*, 2009). Interestingly, sharing an identical miR-1827 binding site with *MYCL1*, *MYC* was shown to not be a target of miR-1827 in this study. As explained in Chapter 6.0, this could be due to the choice of cell line used in performing dual luciferase reporter assay and the endogenous level of the gene of interest. Although MYCL1 is structurally similar to MYC (Nau *et al.*, 1985), its expression is only limited to SCLC (Shiraishi *et al.*, 1989) and thus may function differently from MYC (Xiong *et al.*, 2011a).

CRKL (human chromosome 22q11) is located in the region commonly deleted in patients with DiGeorge/ velocardiofacial syndrome (DGS/ VCFS) (Devriendt *et al.*, 1998) and belongs to the CRK family of adaptor proteins, originally discovered in the late 1980s as the oncogene fusion product, v-Crk, of the CT10 chicken retrovirus (Mayer *et al.*, 1988; ten Hoeve *et al.*, 1993). This family of proteins lacks catalytic activity (Mayer *et al.*, 1988) but act as adaptors in diverse signalling pathways that link upstream tyrosine kinase and integrin-dependent signals to downstream effectors (Birge

et al., 1993; Knudsen *et al.*, 1994). However, the understanding of how CRK proteins function during *in vivo* cancer progression is still poorly understood, which may partly be due to the highly pleiotropic nature of CRK signalling (Chodniewicz & Klemke, 2004; Bell & Park, 2012).

CRKL is localised within a region of genomic amplification (Kim *et al.*, 2009), causing a frequent elevated expression in NSCLC (Sriram & Birge, 2011). High level of *CRKL* was also observed in NSCLC cell lines lacking amplification of 22q11.21, suggesting that there exist other mechanisms that contribute to *CRKL* overexpression (Cheung *et al.*, 2011). In this study, *CRKL* was identified as the first target for miR-1827 and the pro-migratory effect achieved by anti-miR-1827 was reversed via silencing of *CRKL* in lung cancer cells. Likewise, when *CRKL* was overexpressed, the anti-migratory effect exerted by miR-1827 was rescued. The results obtained are in accordance with previous findings that *CRKL* is involved in cancer cell migration (Lin *et al.*, 2015; Ye *et al.*, 2015). Nonetheless, no significant evidence from this study showed *CRKL* as a major player in NSCLC angiogenesis. To the best knowledge, there are still no reports that postulate the role of *CRKL* as an angiogenic modulator.

9.4 Zebrafish Xenografts as A Tool to Study Lung Cancer

The teleost zebrafish (*Danio rerio*) represents a promising alternative model in cancer research (Lam *et al.*, 2006). About 71% of human genes have at least one zebrafish orthologue and reciprocally, 69% of zebrafish genes have at least one human orthologue (Viella *et al.*, 2009). Moreover, 82% of the human disease-related genes can be related to at least one zebrafish orthologue (Howe *et al.*, 2013). The zebrafish are inexpensive to generate and easy to maintain long term. The large number of embryos produced from each mating and the optical clarity of the developing embryos allow direct visualisation during embryonic development. For these reasons, zebrafish

embryos have been proposed as an excellent animal model which could bridge the gap between simple cell-based assays and biological validation in whole animals such as rodents (Lieschke & Currie, 2007). Without a functional immune system at the early embryonic stage, immunosuppression is not needed (Lam *et al.*, 2004; Stoletov & Klemke, 2008; Lieschke & Trede, 2009).

Cancer cell transplantation in zebrafish embryos was first demonstrated by transplanting human malignant melanoma cells into the zebrafish embryos and it was found that the cancer cells were not rejected but survived and exhibited motility (Lee *et al.*, 2005; Topczewska *et al.*, 2006). Subsequently, zebrafish xenograft models have been developed through xenotransplantation of fluorescence-labelled human primary tumour cells or cancer cell lines into the yolk sac of 48hpf zebrafish embryos (Figure 9.2) (Lee *et al.*, 2005; Haldi *et al.*, 2006; Topczewska *et al.*, 2006; Nicoli & Presta, 2007; Nicoli *et al.*, 2007). In these models, cancer cells engrafted into the yolk sac were shown to have proliferated and migrated. The yolk sac was proposed to be the ideal site for injection in 2dpf zebrafish embryos because (1) ~50-100 cells from a single injection were retained in the animals and not expelled into the embryo medium, (2) the yolk sac is rich in nutrients which support cell proliferation and (3) migration from this acellular compartment was not likely to occur by passive transport. To exclude the possibility that exogenous feeding could affect experimental results, the zebrafish relied solely on the yolk sac for nutrition (Haldi *et al.*, 2006).

In this study, DiI-labelled A549-I7 cells were injected into the yolk sac of 2dpf zebrafish embryos and the embryos were analysed at 24hpi using confocal microscopy. The spread of cancer cells could be clearly seen throughout the body of the zebrafish embryos which have been injected with negative mimics/ inhibitors control-transfected A549-I7 cells. When dissemination was seen for the high invasive cells, there were significantly more than 5 cell clusters within the fish body. In contrast, A549-I7 cells

that were transfected with miR-378 hairpin inhibitors and miR-1827 mimics transformed cells to a low invasive phenotype and rarely showed cells in the body of the zebrafish embryos. Distant metastasis formation in the zebrafish embryos was remarkably reduced. These observations were in parallel with the invasion and migration potentials assessed *in vitro* using transwell invasion and wound healing assays, where miR-378 regulates cell invasion while miR-1827 modulates cell migration, both of which are important steps in metastasis. Evaluation of metastasis formation in the zebrafish model is thus significantly quicker than in currently used mouse models, where it may take several weeks until metastases become detectable (Waerner *et al.*, 2006).

On the other hand, *in vitro* assays allow analysis of isolated processes that contribute to angiogenesis whereas *in vivo* assays model enable analysis of angiogenesis as a whole (Goodwin, 2007). The zebrafish hence represents a useful system to analyse the development and function of the vasculature since numerous genes and mechanisms of angiogenesis regulation are shared with mammals (Weinstein, 2002; Rubinstein, 2003). By 24hpf, the zebrafish embryos have already developed a functional cardiovascular system (aorta, beating heart, blood and cardinal vein) (Hermkens *et al.*, 2015). However, there has been some debate over the best measure for angiogenesis because, the dorsal aorta and posterior cardinal vein are formed by vasculogenesis while the intersegmental vessels are formed by angiogenesis (Zhong *et al.*, 2001), and the fact that these processes are not separated definitively or temporally in the developing embryos, raises the question whether angiogenesis or vasculogenesis is being measured. There is less debate over the SIV though, because they are commonly accepted to be formed by angiogenesis (Zheng *et al.*, 2007) and angiogenesis-induced SIV were shown to infiltrate the transplanted cancer mass (Figure 9.2) (Nicoli *et al.*, 2007; Ma *et al.*, 2011; Mohseny *et al.*, 2012).

In this study, when the injected embryos were stained for ALP activity, it was observed that negative mimics/ inhibitors control-transfected A549-I7 cells recruited the zebrafish endothelial cells and infiltrated the tumour mass, leading to vessel formation. On the contrary, miR-378 hairpin inhibitors- and miR-1827 mimics-transfected A549-I7 cells did not show significant angiogenic response upon transplantation into 2dpf zebrafish embryos. These results were in accordance with their ability to induce or suppress *in vitro* tube formation, in which the number of branching points and tubes formed by HUVEC were markedly reduced when treated with miR-378 hairpin inhibitors and miR-1827 mimics. Therefore, blood vessel formation can be directly observed and quantified rather easily in the zebrafish embryos using a low-power microscope compared to currently used mouse models, where angiogenesis is detected by immunohistochemistry for markers such as CD31 (Lawson & Weinstein, 2002).

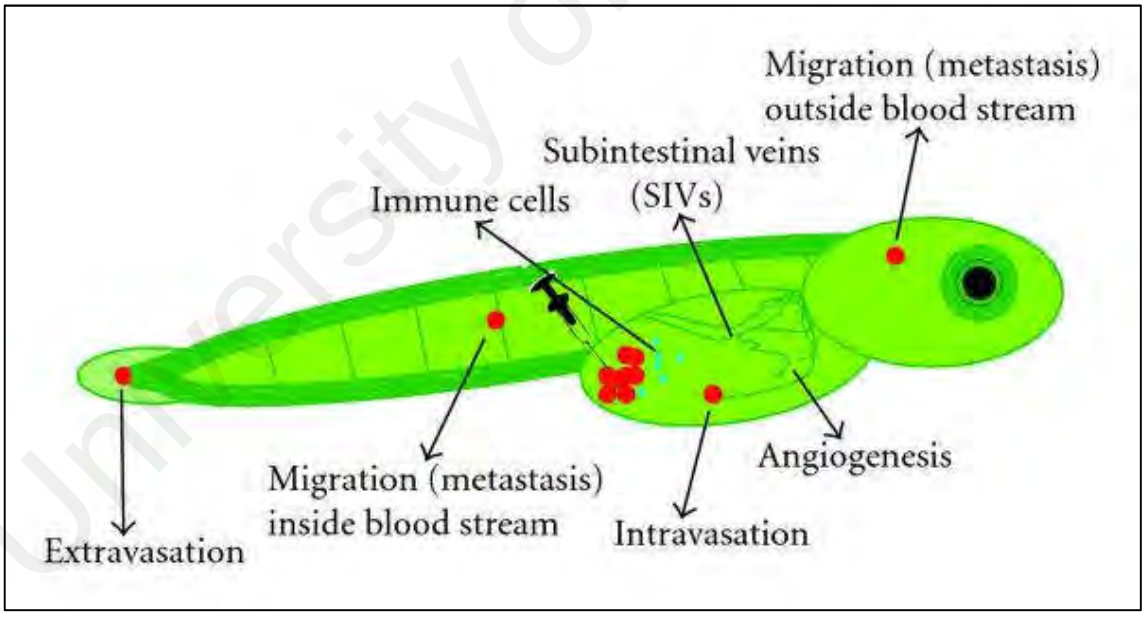

Figure 9.2: Schematic representation of angiogenesis and metastasis in the zebrafish embryo. Cancer cells are labelled in red and injected into the yolk sac of 2dpf transparent embryo (Figure reproduced with permission from Mohseny *et al*., 2012).

CHAPTER 10: CONCLUSION

In summary, the evidences presented in this thesis support miR-378 and miR-1827 as regulators of NSCLC metastasis and angiogenesis, by regulating EMT and potentially modulating ErbB, HIF-1, Hippo, p53, Rap1, Ras, TGF-β and Wnt signalling pathways. In addition, miR-378 was found to target *RBX1* to promote NSCLC cell invasion while miR-1827 was demonstrated to inhibit NSCLC cell migration by directly targeting *CRKL*. Both *RBX1* and *CRKL* were also shown to have a minor role in miR-378- and miR-1827-mediated NSCLC angiogenesis. These findings were extrapolated to *in vivo* conditions and equivalent results were observed.

10.1 Areas of Future Research

This study thus has shown that miR-378 and miR-1827 serve as attractive therapeutic targets in NSCLC. Nonetheless further work on miR-378 and miR-1827 is required. As discussed earlier, the functions of miRNA may be context specific and it may have to be coupled with alterations of expression of other miRNAs to affect the phenotype (Patnaik *et al.*, 2010), therefore the alterations in phenotype upon miRNA overexpression or knockdown should be compared between malignant and non-malignant cells. It is inevitable that there will be concern on the potential toxicity in normal cells, especially with the delivery of miRNA mimics that would lead to overloading of RISC. However, thus far no *in vivo* evidence for toxicity induced by miRNA mimics has been reported, suggesting that the delivery of miRNA was well tolerated (Esquela-Kerscher *et al.*, 2008; Kota *et al.*, 2009; Takeshita *et al.*, 2010; Wiggins *et al.*, 2010). This could be due to (1) pathways activated or repressed by the miRNA mimics are already activated or repressed by the endogenous miRNA, (2) increase in the miRNA expression level by miRNA mimics is insignificant compared to what is already present in normal cells, (3) normal cells are not addicted to oncogenic

pathways (Cheng & Slack, 2012) or (4) normal cells are able to regulate the activity of the miRNA mimics in comparison to cancer cells inability (Bader *et al.*, 2010).

Secondly, assuming miRNA functions are context dependent, then the candidate approach to identifying miRNA targets is a flawed approach. This is because computer algorithms cannot predict context dependent miRNA functions. It is more informative if the miRNA targets could be identified *in vivo* by identifying RNAs that are differentially expressed as a result of miRNA manipulations in normal cells versus cancer cells.

In addition, it is estimated that 90% of evolutionarily conserved miRNA-mRNAs interactions involve a single target site and the inhibitory effect induced by miRNA on its target may merely cause a subtle reduction of protein expression (Bartel, 2009). It is the simultaneous down-regulation of multiple targets by the miRNA that results in the cellular phenotype seen. Most of the time though, mRNAs harbour binding site that could be targeted by several other miRNAs or more than one binding sites to other miRNAs. In such circumstances, only the most abundantly expressed miRNAs have the most significant regulatory potential on their target mRNA binding sites and affect target mRNA stability (Baek *et al.*, 2008; Landthaler *et al.*, 2008; Selbach *et al.*, 2008; Hausser *et al.*, 2009). MicroRNAs that have lower expression can work synergistically to fine-tune target mRNA expression (Bartel & Chen, 2004; Krek *et al.*, 2005; Wu *et al.*, 2010). The mechanism involved in attaining regulation and equilibrium is certainly worth exploring. Therefore, it will be exciting to look into the effects of co-transfecting miR-378 and miR-1827 on *RBX1* and *CRKL* expression, along with effects on cell invasion, migration and angiogenesis. More importantly, a better understanding of the antimiR oligonucleotide mechanism of action is necessary for therapeutic manipulations.

Finally, additional work investigating the long-term effects of miRNA modulations *in vivo* in not only zebrafish but also in rodents are warranted, for the fact that zebrafish can never replace rodents in later stages of cancer research. Its value is to complement cell-based assays at earlier stages.

REFERENCES

Achiwa, H., Yatabe, Y., Hida, T., Kuroishi, T., Kozaki, K., Nakamura, S., … Takanashi, T. (1999). Prognostic significance of elevated cyclooxygenase 2 expression in primary, resected lung adenocarcinomas. *Cancer Research, 5*(5), 1001-1005.

Agarwal, V., Bell, G. W., Nam, J.-W., & Bartel, D. P. (2015). Predicting effective microRNA target sites in mammalian mRNAs. *eLife, 4*, e05005.

Aguirre-Ghiso, J. A. (2007). Models, mechanisms and clinical evidence for cancer dormancy. *Nature Reviews Cancer, 7*(11), 834-846.

Al-Mehdi, A. B., Tozawa, K., Fisher, A. B., Shientag, L., Lee, A., & Muschel, R. J. (2000). Intravascular origin of metastasis from the proliferation of endothelium-attached tumor cells: A new model for metastasis. *Nature Medicine, 6*(1), 100-102.

Almog, N., Henke, V., Flores, L., Hlatky, L., Kung, A. L., Wright, R. D., … Folkman, J. (2006). Prolonged dormancy of human liposarcoma is associated with impaired tumor angiogenesis. *FASEB Journal, 20*(7), 947-949.

Aonuma, M., Saeki, Y., Akimoto, T., Nakayama, Y., Hattori, C., Yoshitake, Y., … Tanaka, N. G. (1999). Vascular endothelial growth factor overproduced by tumour cells acts predominantly as a potent angiogenic factor contributing to malignant progression. *International Journal of Experimental Pathology, 80*(5), 271-281.

Arber, S., Barbayannis, F., Hanser, H., Schneider, C., Stanyon, C. A., Bernard, O., & Caroni, P. (1998). Regulation of actin dynamics through phosphorylation of cofilin by LIM-kinase. *Nature, 393*(6687), 805-809.

Azizah, Ab. M., Nor Saleha, I. T., Noor Hashimah, A., Asmah, Z. A., & Mastulu, W. (2016). Malaysian National Cancer Registry Report 2007-2011. Malaysia Cancer Statistics, Data And Figure [Internet]. *Kuala Lumpur, Malaysia: National Cancer Institute, Ministry of Health.* Retrieved September 9, 2016, from http://nci.moh.gov.my

Baccelli, I., Schneeweiss, A., Riethdorf, S., Stenzinger, A., Schillert, A., Vogel, V., … Trumpp, A. (2013). Identification of a population of blood circulating tumor cells from breast cancer patients that initiates metastasis in a xenograft assay. *Nature Biotechnology, 31*, 539-544.

Bach, P. B., Jett, J. R., Pastorino, U., Tockman, M. S., Swensen, S. J., & Begg, C. B. (2007). Computed tomography screening and lung cancer outcomes. *JAMA, 297*(9), 953-961.

Bader, A. G., Brown, D., & Winkler, M. (2010). The promise of microRNA replacement therapy. *Cancer Research, 70*(18), 7027-7030.

Baek, D., Villen, J., Shin, C., Camargo, F. D., Gygi, S. P., & Bartel, D. P. (2008). The impact of microRNAs on protein output. *Nature, 455*(7209), 64-71.

Bagga, S., Bracht, J., Hunter, S., Massirer, K., Holtz, J., Eachus, R., & Pasquinelli, A. E. (2005). Regulation by let-7 and lin-4 miRNAs results in target mRNA degradation. *Cell, 122*(4), 553-563.

Baish, J. W., & Jain, R. K. (2000). Fractals and cancer. *Cancer Research, 60*(14), 3683-3688.

Bardos, J. I., & Ashcroft, M. (2004). Hypoxia-inducible factor-1 and oncogenic signalling. *Bioessays, 26*(3), 262-269.

Bartel, D. P. (2009). MicroRNAs: Target recognition and regulatory functions. *Cell, 136*(2), 215-233.

Bartel, D. P., & Chen, C. Z. (2004). Micromanagers of gene expression: The potentially widespread influence of metazoan microRNAs. *Nature Reviews Genetics, 5*(5), 396-400.

Bastock, R., Strutt, H., & Strutt, D. (2003). Strabismus is asymmetrically localised and binds to Prickle and Dishevelled during *Drosophila* planar polarity patterning. *Development, 130*(13), 3007-3014.

Baudino, T. A., McKay, C., Pendeville-Samain, H., Nilsson, J. A., Maclean, K. H., White, E. L., … Cleveland, J. L. (2002). c-Myc is essential for vasculogenesis and angiogenesis during development and tumor progression. *Genes & Development, 16*(19), 2530-2543.

Beitzinger, M., & Meister, G. (2010). MicroRNAs: From decay to decoy. *Cell, 140*(5), 612-614.

Bell, E. S., & Park, M. (2012). Models of Crk adaptor proteins in cancer. *Genes & Cancer, 3*(5-6), 341-352.

Bergers, G., & Benjamin, L. E. (2003). Tumorigenesis and the angiogenic switch. *Nature Reviews Cancer, 3*(6), 401-410.

Bermont, L., Lamielle, F., Fauconnet, S., Esumi, H., Weisz, A., & Adessi, G. L. (2000). Regulation of vascular endothelial growth factor expression by insulin-like growth factor-I in endometrial adenocarcinoma cells. *International Journal of Cancer, 85*(1), 117-123.

Berra, E., Milanini, J., Richard, D. E., Le Gall, M., Vinals, F., Gothie, E., … Pouyssegur, J. (2000). Signaling angiogenesis via p42/p44 MAP kinase and hypoxia. *Biochemistry & Pharmacology, 60*(8), 1171-1178.

Bhat, K. P., Salazar, K. L., Balasubramaniyan, V., Wani, K., Heathcock, L., Hollingsworth, F., … Aldape, K. D. (2011). The transcriptional coactivator TAZ regulates mesenchymal differentiation in malignant glioma. *Genes & Development, 25*(24), 2594-2609.

Birge, R. B., Fajardo, J. E., Reichman, C., Shoelson, S. E., Songyang, Z., Cantley, L. C., & Hanafusa, H. (1993). Identification and characterization of a high-affinity interaction between v-Crk and tyrosine-phosphorylated paxillin in CT10-transformed fibroblasts. *Molecular and Cellular Biology, 13*(8), 4648-4656.

Bishop, J. A., Benjamin, H., Cholakh, H., Chajut, A., Clark, D. P., & Westra, W. H. (2010). Accurate classification of non-small cell lung carcinoma using a novel microRNA-based approach. *Clinical Cancer Research, 16*(2), 610-619.

Bonnans, C., Chou, J., & Werb, Z. (2014). Remodelling the extracellular matrix in development and disease. *Nature Reviews Molecular Cell Biology, 15*(12), 786-801.

Borczuk, A. C., Kim, H. K., Yegen, H. A., Friedman, R. A., & Powell, C. A. (2005). Lung adenocarcinoma global profiling identifies type II transforming growth factor-beta receptor as a repressor of invasiveness. *American Journal of Respiratory and Critical Care Medicine, 172*(6), 729-737.

Bourguignon, L. Y., Gilad, E., Brightman, A., Diedrich, F., & Singleton, P. (2006). Hyaluronan-CD44 interaction with leukemia-associated RhoGEF and epidermal growth factor receptor promotes Rho/Ras co-activation, phospholipase C epsilon-Ca^{2+} signaling, and cytoskeleton modification in head and neck squamous cell carcinoma cells. *The Journal of Biological Chemistry, 281*(20), 14026-14040.

Brandao, G. D. A., Brega, E. F., & Spatz, A. (2012). The role of molecular pathology in non-small-cell lung carcinoma- Now and in the future. *Current Oncology, 19*(Suppl 1), S24-S32.

Broderick, P., Wang, Y., Vijayakrishnan, J., Matakidou, A., Spitz, M. R., Eisen, T., Amos, C. I., & Houlston, R. S. (2009). Deciphering the impact of common genetic variation on lung cancer risk: A genome-wide association study. *Cancer Research, 69*(16), 6633-6641.

Brose, M., Volpe, R., Feldman, M., Kumar, M., Rishi, I., Gerrero, R., … Weber, B. L. (2002). *BRAF* and *RAS* mutations in human lung cancer and melanoma. *Cancer Research, 62*(23), 6997-7000.

Brown, P. D., Bloxidge, R. E., Stuart, N. S., Gatter, K. C., & Carmichael, J. (1993). Association between expression of ativated 72-kilodalton gelatinase and tumor spread in non-small-cell lung carcinoma. *Journal of the National Cancer Institute, 85*(7), 574-578.

Bulatov, E., & Ciulli, A. (2015). Targeting Cullin-RING E3 ubiquitin ligases for drug discovery: Structure, assembly and small-molecule modulation. *The Biochemical Journal, 467*(3), 365-386.

Burrell, R. A., McGranahan, N., Bartek, J., & Swanton, C. (2013). The causes and consequences of genetic heterogeneity in cancer evolution. *Nature, 501*(7467), 338-345.

Burri, P. H., Hlushchuk, R., & Djonov, V. (2004). Intussusceptive angiogenesis: Its emergence, its characteristics, and its significance. *Developmental Dynamics, 231*(3), 474-488.

Cai, J., Wu, J., Zhang, H., Fang, L., Huang, Y., Yang, Y., … Li, M. (2013). MiR-186 downregulation correlates with poor survival in lung adenocarcinoma, where it interferes with cell-cycle regulation. *Cancer Research, 73*(2), 756-766.

Cai, Z., Tchou-Wong, K.-M., & Rom, W. N. (2011). NF-kappaB in lung tumorigenesis. *Cancers (Basel), 3*(4), 4258-4268.

Callari, M., Dugo, M., Musella, V., Marchesi, E., Chiorino, G., Grand, M. M., … De Cecco, L. (2012). Comparison of microarrray platforms for measuring differential microRNA expression in paired normal/cancer colon tissues. *PLoS One, 7*(9), e45105.

Cao, G., Li, F., & Du, T. (2016). MicroRNA-365 inhibits growth, invasion and metastasis of lung cancer by targeting *NRP1* expression. *International Journal of Clinical & Experimental Pathology, 9*(2), 1081-1092.

Capes-Davis, A., Theodosopoulos, G., Atkin, I., Drexler, H. G., Kohara, A., MacLeod, R. A., … Freshney, R. I. (2010). Check your cultures! A list of cross-contaminated or misidentified cell lines. *International Journal of Cancer, 127*(1), 1-8.

Carmeliet, P. (2000a). Mechanisms of angiogenesis and arteriogenesis. *Nature Medicine, 6*(4), 389-395.

Carmeliet, P. (2000b). *VEGF* gene therapy: Stimulating angiogenesis or angioma-genesis? *Nature Medicine, 6*(10), 1102-1103.

Carmeliet, P., & Jain, R. K. (2011a). Molecular mechanisms and clinical applications of angiogenesis. *Nature, 473*(7347), 298-307.

Carmeliet, P., & Jain, R. K. (2011b). Principles and mechanisms of vessel normalization for cancer and other angiogenic diseases. *Nature Reviews Drug Discovery, 10*(6), 417-427.

Carrer, M., Liu, N., Grueter, C. E., Williams, A. H. Frisard, M. I., Hulver, M. W., Bassel-Duby, R., & Olson, E. N. (2012). Control of mitochondrial metabolism and systemic energy homeostasis by microRNAs 378 and 378*. *Proceedings of the National Academy of Sciences of the United States of America, 109*(38), 15330-15335.

Casaluce, F., Sgambato, A., Maione, P., Rossi, A., Ferrara, C., Napolitano, A., … Gridelli, C. (2013). ALK inhibitors: A new targeted therapy in the treatment of advanced NSCLC. *Targeted Oncology, 8*(1), 55-67.

Casamassimi, A., de Nigris, F., Schiano, C., & Napoli, C. (2015). Endothelial cell tube formation on basement membrane to study cancer neoangiogenesis. In M. Slevin & G. McDowell (Eds.), *Handbook of Vascular Biology Techniques* (Vol. 12, pp. 13-22). Dordrecht, The Netherlands: Springer Publishing.

Cascon, I., Giraudo, E., Caccavari, F., Napione, L., Bertotti, E., Collard, J. G., Serini, G., & Bussolino, F. (2003). Temporal and spatial modulation of GTPases during *in vitro* formation of capillary vascular network: Adherens junctions and myosin light chain as targets of Rac1 and RhoA. *The Journal of Biological Chemistry, 278*(50), 50702-50713.

Ceppi, P., Mudduluru, G., Kumarswamy, R., Rapa, I., Scagliotti, G. V., Papotti, M., & Allgayer, H. (2010). Loss of miR-200c expression induces an aggressive, invasive, and chemoresistant phenotype in non-small cell lung cancer. *Molecular Cancer Research, 8*(9), 1207-1216.

Cha, S.-T., Chen, P.-S., Johansson, G., Chu, C. Y., Wang, M. Y., Jeng, Y. M., … Kuo, M. L. (2010). MicroRNA-519c suppresses hypoxia-inducible factor-1alpha expression and tumor angiogenesis. *Cancer Research, 70*(7), 2675-2685.

Chambers, A. F., Groom, A. C., & MacDonald, I. C. (2002). Dissemination and growth of cancer cells in metastatic sites. *Nature Reviews Cancer, 2*(8), 563-572.

Chan, J. K., Kiet, T. Y., Blansit, K., Ramasubbaiah, R., Hilton, J. F., Kapp, D. S., & Matei, D. (2014). MiR-378 as a biomarker for response to anti-angiogenic treatment in ovarian cancer. *Gynecologic Oncology, 133*(3), 568-574.

Chan, S. W., Lim, C. J., Guo, K., Ng, C. P., Lee, I., Hunziker, W., Zeng, Q., & Hong, W. (2008). A role for TAZ in migration, invasion, and tumorigenesis of breast cancer cells. *Cancer Research, 68*(8), 2592-2598.

Chandrasoma, P. T. C. (1998). The lung: III. Neoplasms. In P. T. C. Chandrasoma (Ed.), *Concise Pathology* (3rd ed.). New York, NY: McGraw-Hill.

Chen, C. L., Gajewski, K. M., Hamaratoglu, F., Bossuyt, W., Sansores-Garcia, L., Tao, C., & Halder, G. (2010a). The apical-basal cell polarity determinant Crumbs regulates Hippo signaling in *Drosophila*. *Proceedings of the National Academy of Sciences of the United States of America, 107*(36), 15810-15815.

Chen, G., Umelo, I. A., Lv, S., Teugels, E., Fostier, K., Kronenberger, P., … De Greve, J. (2013). MiR-146a inhibits cell growth, cell migration and induces apoptosis in non-small cell lung cancer cells. *PLoS One, 8*(3), e60317.

Chen, H-Y., Liu, C-C., & Chen, R-H. (2016a). Cul3-KLHL20 ubiquitin ligase: Physiological functions, stress responses, and disease implications. *Cell Division, 11*, 5.

Chen, L. T., Xu, S. D., Xu, H., Zhang, J. F., Ning, J. F., & Wang, S. F. (2012). MicroRNA-378 is associated with non-small cell lung cancer brain metastasis by promoting cell migration, invasion and tumor angiogenesis. *Medical Oncology, 29*(3), 1673-1680.

Chen, Q. G., Zhou, W., Han, T., Du, S. Q., Li, Z. H., Zhang, Z., Shan, G. Y., & Kong, C. Z. (2016b). MiR-378 suppresses prostate cancer cell growth through downregulation of *MAPK1 in vitro* and *in vivo*. *Tumour Biology, 37*(2), 2095-2103.

Chen, Q. Y., Jiao, D. M., Wu, Y. Q., Chen, J., Wang, J., Tang, X. L., … Wang, Z. (2016c). MiR-206 inhibits HGF-induced epithelial-mesenchymal transition and angiogenesis in non-small cell lung cancer via c-Met/PI3k/Akt/mTOR pathway. *Oncotarget, 7*(14), 18247-18261.

Chen, T., Xu, C., Chen, J., Ding, C., Xu, Z., Li, C., & Zhao, J. (2015a). MicroRNA-203 inhibits cellular proliferation and invasion by targeting *Bmi1* in non-small cell lung cancer. *Oncology Letters, 9*(6), 2639-2646.

Chen, X., Wang, Y., Zang, W., Du, Y., Li, M., & Zhao, G. (2015b). MiR-194 targets *RBX1* gene to modulate proliferation and migration of gastric cancer cells. *Tumour Biology, 36*(4), 2393-2401.

Chen, Y., Zhu, X., Zhang, X., Liu, B., & Huang, L. (2010b). Nanoparticles modified with tumor-targeting scFv deliver siRNA and miRNA for cancer therapy. *Molecular Therapy, 18*(9), 1650-1656.

Chendrimada, T. P., Finn, K. J., Ji, X., Baillat, D., Gregory, R. I., Liebhaber, S. A., Pasquinelli, A. E., & Shiekhattar, R. (2007). MicroRNA silencing through RISC recruitment of eIF6. *Nature, 447*(7146), 823-828.

Cheng, C. J., & Slack, F. J. (2012). The duality of oncomiR addiction in the maintenance and treatment of cancer. *The Cancer Journal, 18*(3), 232-237.

Cheung, H. W., Du, J., Boehm, J. S., He, F., Weir, B. A., Wang, X., … Hahn, W. C. (2011). Amplification of *CRKL* induces transformation and epidermal growth factor receptor inhibitor resistance in human non-small cell lung cancers. *Cancer Discovery, 1*(7), 608-625.

Childs, S., Chen, J. N., Garrity, D. M., & Fishman, M. C. (2002). Patterning of angiogenesis in the zebrafish embryo. *Development, 129*(4), 973-982.

Chin, L. J., Ratner, E., Leng, S., Zhai, R., Nallur, S., Babar, I., … Weidhaas, J. B. (2008). A SNP in a let-7 microRNA complementary site in the *KRAS* 3' untranslated region increases non-small cell lung cancer risk. *Cancer Research, 68*(20), 8535-8540.

Chodniewicz, D., & Klemke, R. L. (2004). Regulation of integrin-mediated cellular responses through assembly of a CAS/Crk scaffold. *Biochimica et Biophysica Acta*, 1692(2-3), 63-76.

Choi. J. H., Kim, H. C., Lim, H. Y., Nam, D. K., Kim, H. S., Yi, J. W., … Hahn, M. H. (2001). Vascular endothelial growth factor in the serum of patients with non-small cell lung cancer: Correlation with platelet and leucocyte counts. *Lung Cancer, 33*(2-3), 171-179.

Chou, Y. T., Lin, H. H., Lien, Y. C., Wang, Y. H., Hong, C. F., Kao, Y. R., … Wu, C. W. (2010). EGFR promotes lung tumorigenesis by activating miR-7 through a Ras/ERK/Myc pathway that targets the *Ets2* transcriptional repressor ERF. *Cancer Research, 70*(21), 8822-8831.

Chu, Y. W., Yang, P. C., Yang, S. C., Shyu, Y. C., Hendrix, M. J., Wu, R., & Wu, C. W. (1997). Selection of invasive and metastatic subpopulations from a human lung adenocarcinoma cell line. *American Journal of Respiratory Cell and Molecular Biology, 17*(3), 353-360.

Chun, Y.-S., Kim, M.-S., & Park, J.-W. (2002). Oxygen-dependent and -independent regulation of HIF-1alpha. *Journal of Korean Medical Science, 17*(5), 581-588.

Ciechanover, A. (1998). The ubiquitin-proteasome pathway: On protein death and cell life. *The EMBO Journal, 17*(24), 7151-7160.

Cittelly, D. M., Das, P. M., Salvo, V. A., Fonseca, J. P., Burow, M. E., & Jones, F. E. (2010a). Oncogenic HER2Δ16 suppresses miR-15a/16 and deregulates *BCL-2* to promote endocrine resistance of breast tumors. *Carcinogenesis, 31*(12), 2049-2057.

Cittelly, D. M., Das, P. M., Spoelstra, N. S., Edgerton, S. M., Richer, J. K., Thor, A. D., & Jones, F. E. (2010b). Downregulation of miR-342 is associated with tamoxifen resistant breast tumors. *Molecular Cancer, 9*, 317.

Ciuleanu, T., Brodowicz, T., Zielinski, C., Kim, J. H., Krzakowski, M., Laack, E., … Belani, C. P. (2009). Maintenance pemetrexed plus best supportive care versus placebo plus best supportive care for non-small-cell lung cancer: A randomised, double-blind, phase 3 study. *The Lancet, 374*(9699), 1432-1440.

Clark, E. A., Golub, T. R., Lander, E. S., & Hynes, R. O. (2000). Genomic analysis of metastasis reveals an essential role for *RhoC*. *Nature, 406*(6795), 532-535.

Condeelis, J., & Pollard, J. W. (2006). Macrophages: Obligate partners for tumor cell migration, invsion, and metastasis. *Cell, 124*(2), 263-266.

Copin, M. C., Buisine, M. P., Leteurtre, E., Marquette, C. H., Porte, H., Aubert, J. P., Gosselin, B., & Porchet, N. (2001). Mucinous bronchioloalveolar carcinomas display a specific pattern of mucin gene expression among primary lung adenocarcinomas. *Human Pathology, 32*(3), 274-281.

Cordenonsi, M., Zanconato, F., Azzolin, L., Forcato, M., Rosato, A., Frasson, C., … Piccolo, S. (2011). The Hippo transducer TAZ confers cancer stem cell-related traits on breast cancer cells. *Cell, 147*(4), 759-772.

Cortez, M. A., Valdecanas, D., Zhang, X., Zhan, Y., Bhardwaj, V., Calin, G. A., … Welsh, J. W. (2014). Therapeutic delivery of miR-200c enhances radiosensitivity in lung cancer. *Molecular Therapy, 22*(8), 1494-1503.

Crawford, H. C., Fingleton, B. M., Rudolph-Owen, L. A., Goss, K. J., Rubinfeld, B., Polakis, P., & Matrisian, L. M. (1999). The metalloproteinase matrilysin is a target of beta-catenin transactivation in intestinal tumors. *Oncogene, 18*(18), 2883-2891.

Crawford, M., Brawner, E., Batte, K., Yu, L., Hunter, M. G., Otterson, G. A., … Nana-Sinkam, S. P. (2008). MicroRNA-126 inhibits invasion in non-small cell lung carcinoma cell lines. *Biochemical and Biophysical Research Communications, 373*(4), 607-612.

Cui, Z., & Hu, Y. (2016). MicroRNA-124 suppresses *Slug*-mediated lung cancer metastasis. *European Review for Medical and Pharmacological Sciences, 20*(18), 3802-3811.

Dacic, S., Kelly, L., Shuai, Y., & Nikiforova, M. N (2010). MiRNA expression profiling of lung adenocarcinoma: Correlation with mutational status. *Modern Pathology, 23*(12), 1577-1582.

Dalmasso, G., Nguyen, H. T., Yan, Y., Laroui, H., Charania, M. A., Obertone, T. S., Sitaraman, S. V., & Merlin, D. (2011). MicroRNA-92b regulates expression of the oligopeptide transporter PepT1 in intestinal epithelial cells. *American Journal of Physiology. Gastrointestinal and Liver Physiology, 300*(1), G52-G59.

Darnell, J. E. J. (1997). STATs and gene regulation. *Science, 277*(5332), 1630-1635.

De Craene, B., & Berx, G. (2013). Regulatory networks defining EMT during cancer initiation and progression. *Nature Reviews Cancer, 13*(2), 97-110.

Deng, H., Guo, Y., Song, H., Xiao, B., Sun, W., Liu, Z., … Guo, J. (2013). MicroRNA-195 and microRNA-378 mediate tumor growth suppression by epigenetical regulation in gastric cancer. *Gene, 518*(2), 351-359.

Denli, A. M., Tops, B. B. J., Plasterk, R. H. A., Ketting, R. F., & Hannon, G. J. (2004). Processing of primary microRNAs by the Microprocessor complex. *Nature, 432*(7014), 231-235.

Devereux, T. R., Taylor, J. A., & Barrett, J. C. (1996). Molecular mechanisms of lung cancer. Interaction of environmental and genetic factors. Giles F. Filley Lecture. *Chest, 109*(3 Suppl), 14S-19S.

DeVore, R. (2000). *A randomized phase II trial comparing RhuMAb VEGF (recombinant humanized monoclonal antibody to vascular endothelial cell growth factor) plus Carboplatinum/ Paclitaxel (CP) to CP alone in patients with stage IIIB/IV NSCLC.* Paper presented at the 36th ASCO Annual Meeting, New Orleans, Louisiana.

Devriendt, K., Fryns, J. P., Mortier, G., van Thienen, M. N., & Keymolen, K. (1998). The annual incidence of DiGeorge/velocardiofacial syndrome. *Journal of Medical Genetics, 35*(9), 789-790.

Dews, M., Homayouni, A., Yu, D., Murphy, D., Sevignani, C., Wentzel, E., … Thomas-Tikhonenko, A. (2006). Augmentation of tumor angiogenesis by a Myc-activated microRNA cluster. *Nature Genetics, 38*(9), 1060-1065.

Ding, L., Getz, G., Wheeler, D. A., Mardis, E. R., McLellan, M. D., Cibulskis, K., … Wilson, R. K. (2008). Somatic mutations affect key pathways in lung adenocarcinoma. *Nature, 455*(7216), 1069-1075.

Duncavage, E., Goodgame, B., Sezhiyan, A., Govindan, R., & Pfeifer, J. (2010). Use of microRNA expression levels to predict outcomes in resected stage I non-small cell lung cancer. *Journal of Thoracic Oncology, 5*(11), 1755-1763.

Dunn, S. E., Torres, J. V., Oh, J. S., Cykert, D. M., & Barrett, J. C. (2001). Up-regulation of urokinase-type plasminogen activator by insulin-like growth factor-I depends upon phosphatidylinositol-3 kinase and mitogen-activated protein kinase. *Cancer Research, 61*(4), 1367-1374.

Edmonds, M. D., Boyd, K. L., Moyo, T., Mitra, R., Duszynski, R. Arrate, M. P., … Eischen, C. M. (2016). MicroRNA-31 initiates lung tumorigenesis and promotes mutant *KRAS*-driven lung cancer. *The Journal of Clinical Investigation, 126*(1), 349-364.

Eichner, L. J., Perry, M. C., Dufour, C. R., Bertos, N., Park, M., St-Pierre, J., & Giguere, V. (2010). MiR-378 (*) mediates metabolic shift in breast cancer cells via the PGC-1β/ERRγ transcriptional pathway. *Cell Metabolism, 12*(4), 352-361.

Eiring, A., Harb, J. G., Neviani, P., Garton, C., Oaks, J. J., Spizzo, R., … Perroti, D. (2010). MiR-328 functions as an RNA decoy to modulate hnRNP E2 regulation of mRNA translation in leukemic blasts. *Cell, 140*(5), 652-655.

Eliceiri, B. P., Klemke, R., Stromblad, S., & Cheresh, D. A. (1998). Integrin αvβ3 requirement for sustained mitogen-activated protein kinase activity during angiogenesis. *The Journal of Cell Biology, 140*(5), 1255-1263.

Ellerbroek, S. M., Halbleib, J. M., Benavidez, M., Warmka, J. K., Wattenberg, E. V., Stack, S., & Hudson, L. G. (2001). Phosphatidylinositol 3-kinase activity in epithelial growth factor-stimulated matrix metalloproteinase-9 production and cell surface association. *Cancer Research, 61*(5), 1855-1861.

Elmen, J., Lindow, M., Schutz, S., Lawrence, M., Petri, A., Obad, S., … Kauppinen, S. (2008). LNA-mediated microRNA silencing in non-human primates. *Nature, 452*(7189), 896-899.

Erler, J. T., Bennewith, K. L., Nicolau, M., Dornhofer, N., Kong, C., Le, Q.-T., … Giaccia, A. J. (2006). Lysyl oxidase is essential for hypoxia-induced metastasis. *Nature, 440*, 1222-1226.

Erler, J. T., & Weaver, V. M. (2009). Three-dimensional context regulation of metastasis. *Clinical & Experimental Metastasis, 26*(1), 35-49.

Esquela-Kerscher, A., & Slack, F. J. (2006). Oncomirs- MicroRNAs with a role in cancer. *Nature Reviews Cancer, 6*(4), 259-269.

Esquela-Kerscher, A., Trang, P., Wiggins, J. F., Patrawala, L., Cheng, A., Ford, L., … Slack, F. J. (2008). The let-7 microRNA reduces tumor growth in mouse models of lung cancer. *Cell Cycle, 7*(6), 759-764.

Esteban, M. A., Tran, M. G., Harten, S. K., Hill, P., Castellanos, M. C., Chandra, A., … Maxwell, P. H. (2006). Regulation of E-cadherin expression by VHL and hypoxia-inducible factor. *Cancer Research, 66*(7), 3567-3575.

Evans, T. (2012). Utility of hypertension as a surrogate marker for efficacy of antiangiogenic therapy in NSCLC. *Anticancer Research, 32*(11), 4629-4638.

Faltejskova, P., Svoboda, M., Srutova, K., Mlcochova, J., Besse, A., Nekvindova, J., … Slaby, O. (2012). Identification and functional screening of microRNAs highly deregulated in colorectal cancer. *Journal of Cellular and Molecular Medicine, 16*(11), 2655-2666.

Fei, B., & Wu, H. (2013). MiR-378 inhibits progression of human gastric cancer MGC-803 cells by targeting *MAPK1 in vitro*. *Oncology Research, 20*(12), 557-564.

Feinberg, A. P. (2007). Phenotypic plasticity and the epigenetics of human disease. *Nature, 447*(7143), 433-440.

Feldser, D., Agani, F., Iyer, N. V., Pak, B., Ferreira, G., & Semenza, G. L. (1999). Reciprocal positive regulation of hypoxia-inducible factor 1alpha and insulin-like growth factor 2. *Cancer Research, 59*(16), 3915-3918.

Feng, M., Li, Z., Aau, M., Wong, C. H., Yang, X., & Yu, Q. (2011). Myc/miR-378/TOB2/cyclin D1 functional module regulates oncogenic transformation. *Oncogene, 30*(19), 2242-2251.

Ferlay, J., Soerjomataram, I., Ervik, M., Dikshit, R., Eser, S., Mathers, C., … Bray, F. (2014). GLOBOCAN 2012 v1.1, Cancer incidence and mortality worldwide: IARC CancerBase No. 11 [Internet]. *Lyon, France: International Agency for Research on Cancer*. Retrieved September 9, 2016, from http://globocan.iarc.fr

Fidler, I. J. (1973). Selection of successive tumor lines for metastasis. *Nature: New Biology, 242*(118), 148-149.

Fidler, I. J. (1978). Tumor heterogeneity and the biology of cancer invasion and metastasis. *Cancer Research, 38*(9), 2651-2660.

Fidler, I. J. (1989). Origin and biology of cancer metastasis. *Cytometry, 10*(6), 673-680.

Fidler, I. J. (2003). The pathogenesis of cancer metastasis: The 'seed and soil' hypothesis revisited. *Nature Reviews Cancer, 3*(6), 453-458.

Fidler, I. J., & Kripke, M. L. (1977). Metastasis results from preexisting variant cells within a malignant tumor. *Science, 197*(4306), 893-895.

Foldes-Papp, Z., Konig, K., Studier, H., Buckle, R., Breunig, H. G., Uchugonova, A., & Kostner, G. M. (2009). Trafficking of mature miRNA-122 into the nucleus of liver cells. *Current Pharmaceutical Biotechnology, 10*(6), 569-578.

Folkman, J. (1971). Tumor angiogenesis: Therapeutic implications. *The New England Journal of Medicine, 285*(21), 1182-1186.

Fontanini, G., Boldrini, L., Vignati, S., Chine, S., Basolo, F., Silvestri, V., … Bevilacqua, G. (1998a). Bcl2 and p53 regulate vascular endothelial growth factor (VEGF)-mediated angiogenesis in non-small cell lung carcinoma. *European Journal of Cancer, 34*(5), 718-723.

Fontanini, G., De Laurentiis, M., Vignati, S., Chine, S., Lucchi, M., Silvestri, V., … Ciardiello, F. (1998b). Evaluation of epidermal growth factor-related growth factors and receptors and of neoangiogenesis in completely resected stage I-IIIA non-small-cell lung cancer: Amphiregulin and microvessel count are independent prognostic indicators of survival. *Clinical Cancer Research, 4*(1), 241-249.

Fontanini, G., Lucchi, M., Vignati, S., Mussi, A., Ciardiello, F., De Laurentiis, M., … Bevilacqua, G. (1997). Angiogenesis as a prognostic indicator of survival in non-small-cell lung carcinoma: A prospective study. *Journal of the National Cancer Institute, 89*(12), 881-886.

Forbes, S., Clements, J., Dawson, E., Bamford, S., Webb, T., Dogan, A., … Stratton, M. R. (2006). COSMIC 2005. *British Journal of Cancer, 94*(2), 318-322.

Foss, K. M., Sima, C., Ugolini, D., Neri, M., Allen, K. E., & Weiss, G. J. (2011). MiR-1254 and miR-574-5p: Serum-based microRNA biomarkers for early-stage non-small cell lung cancer. *Journal of Thoracic Oncology, 6*(3), 482-488.

Frank, S. R., Hatfield, J. C., & Casanova, J. E. (1998). Remodelling of the actin cytoskeleton is coordinately regulated by protein kinase C and the ADP-ribosylation factor nucleotide exchange factor ARNO. *Molecular Biology of the Cell, 9*(11), 3133-3146.

Friedlander, M. R., Chen, W., Adamidi, C., Maaskola, J., Einspanier, R., Knewspel, S., & Rajewsky, N. (2008). Discovering microRNAs from deep sequencing data using miRDeep. *Nature Biotechnology, 26*(4), 407-415.

Friedman, R. C., Farh, K. K., Burge, C. B., & Bartel, D. P. (2009). Most mammalian mRNAs are conserved targets of microRNAs. *Genome Research, 19*(1), 92-105.

Fujisawa, T., Rubin, B., Suzuki, A., Patel, P. S., Gahl, W. A., Joshi, B. H., & Puri, R. K. (2012). Cysteamine suppresses invasion, metastasis and prolongs survival by inhibiting matrix metalloproteinases in a mouse model of human pancreatic cancer. *PLoS One, 7*(4), e34437.

Fukumura, D., Duda, D. G., Munn, L. L., & Jain, R. K. (2010). Tumour microvasculature and microenvironment: Novel insights through intravital imaging in pre-clinical models. *Microcirculation, 17*(3), 206-225.

Gallardo, E., Navarro, A., Vinolas, N., Marrades, R. M., Diaz, T., Gel, B., … Monzo, M. (2009). MiR-34a as a prognostic marker of relapse in surgically resected non-small-cell lung cancer. *Carcinogenesis, 30*(11), 1903-1909.

Gao, N., Ding, M., Zheng, J. Z., Zhang, Z., Leonard, S. S., Liu, K. J., … Jiang, B. H. (2002). Vanadate-induced expression of hypoxia-inducible factor 1alpha and vascular endothelial growth factor through phosphatidylinositol 3-kinase/Akt pathway and reactive oxygen species. *The Journal of Biological Chemistry, 277*(35), 31963-31971.

Gao, N., Shen, L., Zhang, Z., Leonard, S. S., He, H., Zhang, X. G., … Jiang, B. H. (2004). Arsenite induces HIF-1alpha and VEGF through PI3K, Akt and reactive oxygen species in DU145 human prostate carcinoma cells. *Molecular and Cellular Biochemistry, 255*(1-2), 33-45.

Garofalo, M., Di Leva, G., Romano, G., Nuovo, G., Suh, S. S. Ngankeu, A., … Croce, C. M. (2009). MiR-221&222 regulate TRAIL resistance and enhance tumorigenicity through *PTEN* and *TIMP3* downregulation. *Cancer Cell, 16*(6), 498-509.

Garzon, R., Marcucci, G., & Croce, C. M. (2010). Targeting microRNAs in cancer: Rationale, strategies and challenges. *Nature Reviews Drug Discovery, 9*(10), 775-789.

Geback, T., Schulz, M. M., Koumoutsakos, P., & Detmar, M. (2009). TScratch: A novel and simple software tool for automated analysis of monolayer wound healing assays. *Biotechniques, 46*(4), 265-274.

Gerlinger, M., Rowan, A. J., Horswell, S., Larkin, J., Endesfelder, D., Gronroos, E., … Swanton, C. (2012). Intratumor heterogeneity and branched evolution revealed by multiregion sequencing. *The New England Journal of Medicine, 366*, 883-892.

Giard, D. J., Aaronson, S. A., Todaro, G. J., Arnstein, P., Kersey, J. H., Dosik, H., & Parks, W. P. (1973). *In vitro* cultivation of human tumors: Establishment of cell lines derived from a series of solid tumors. *Journal of National Cancer Institute, 51*(5), 1417-1423.

Giraldez, A. J., Mishima, Y., Rihel, J., Grocock, R. J., Van Dongen, S., Inoue, K., … Schier, A. F. (2006). Zebrafish miR-430 promotes deadenylation and clearance of maternal mRNAs. *Science, 312*(5770), 75-79.

Godde, N. J., Galea, R. C., Elsum, I. A., & Humbert, P. O. (2010). Cell polarity in motion: Redefining mammary tissue organization through EMT and cell polarity transitions. *Journal of Mammary Gland Bioogy and Neoplasia, 15*(2), 149-168.

Goh, P. P., Sze, D. M., & Roufogalis, B. D. (2007). Molecular and cellular regulators of cancer angiogenesis. *Current Cancer Drug Targets, 7*(8), 743-758.

Goldsmith, K. T., Listinsky, C. M., & Garver, J., R. I. (1991). Serum response heterogeneity among nonsmall cell lung cancer cell lines. *The American Journal of Pathology, 139*(4), 939-947.

Gonzalez, S., Pisano, D. G., & Serrano, M. (2008). Mechanistic principles of chromatin remodeling guided by siRNAs and miRNAs. *Cell Cycle, 7*(16), 2601-2608.

Goodwin, A. M. (2007). *In vitro* assays of angiogenesis for assessment of angiogenic and anti-angiogenic agents. *Microvascular Research, 74*(2-3), 172-183.

Gradl, D., Kuhl, M., & Wedlich, D. (1999). The Wnt/Wg signal transducer beta-catenin controls fibronectin expression. *Molecular and Cellular Biology, 19*(8), 5576-5587.

Gridelli, C., Ardizzoni, A., Ciardiello, F., Hanna, N., Heymach, J. V., Perrone, F., … De Marinis, F. (2008). Second-line treatment of non-small cell lung cancer. *Journal of Thoracic Oncology, 3*(4), 430-440.

Grivennikov, S. I., Greten, F. R., & Karin, M. (2010). Immunity, inflammation and cancer. *Cell, 140*(6), 883-899.

Gu, Y., Cheng, Y., Song, Y., Zhang, Z., Deng, M., Wang, C., … He, Z. (2014). MicroRNA-493 suppresses tumor growth, invasion and metastasis of lung cancer by regulating *E2F1*. *PLoS ONE, 9*(8): e102602.

Gunaratnam, L., Morley, M., Franovic, A., de Paulsen, N., Mekhail, K., Parolin, D. A., … Lee, S. (2003). Hypoxia inducible factor activates the transforming growth factor-alpha/epidermal growth factor receptor growth stimulatory pathway in VHL(-/-) renal cell carcinoma cells. *The Journal of Biological Chemistry, 278*(45), 44966-44974.

Guo, F., Tian, J., Lin, Y., Jin, Y., Wang, L., & Cui, M. (2013). Serum microRNA-92 expression in patients with ovarian epithelial carcinoma. *The Journal of International Medical Research*, *41*(5), 1456-1461.

Guo, J., Miao, Y., Xiao, B., Huan, R., Jiang, Z., Meng, D, & Wang, Y. (2009). Differential expression of microRNA species in human gastric cancer versus non-tumorous tissues. *Journal of Gastroenterology and Hepatology, 24*(4), 652-657.

Gupta, G. P., & Massague, J. (2006). Cancer metastasis: Building a framework. *Cell, 127*(4), 679-695.

Hai, J., Zhu, C. Q., Bandarchi, B., Wang, Y. H., Navab, R., Shepherd, F. A. … Tsao, M. S. (2012). L1 cell adhesion molecule promotes tumorigenicity and metastatic potential in non-small cell lung cancer. *Clinical Cancer Research, 18*(7), 1914-1924.

Haldi, M., Ton, C., Seng, W. L., & McGrath, P. (2006). Human melanoma cells transplanted into zebrafish proliferates, migrates, produce melanin, from masses and stimulate angiogenesis in zebrafish. *Angiogenesis, 9*(3), 139-151.

Han, H. S., Son, S. M., Yun, J., Jo, Y. N., & Lee, O. J. (2014). MicroRNA-29a suppresses the growth, migration, and invasion of lung adenocarcinoma cells by targeting carcinoembryonic antigen-related cell adhesion molecule 6. *FEBS Letters, 588*(20), 3744-3750.

Han, J., Lee, Y., Yeom, K. H., Kim, Y. K., Jin, H., & Kim, V. N. (2004). The Drosha-DGCR8 complex in primary microRNA processing. *Genes & Development, 18*(24), 3016-3027.

Hanahan, D., & Folkman, J. (1996). Patterns and emerging mechanisms of the angiogenic switch during tumorigenesis. *Cell, 86*(3), 353-364.

Hanahan, D., & Weinberg, R. A. (2011). Hallmarks of cancer: The next generation. *Cell, 144*(5), 646-674.

Haug, B. H., Henriksen, J. R., Buechner, J., Geerts, D., Tomte, E., Kogner, P., … Einvik, C. (2011). MYCN-regulated miRNA-92 inhibits secretion of the tumor suppressor DICKKOPF-3 (DKK3) in neuroblastoma. *Carcinogenesis, 32*(7), 1005-1012.

Hausser, J., Landthaler, M., Jaskiewicz, L., Gaidatzis, D., & Zavolan, M. (2009). Relative contribution of sequence and structure features to the mRNA binding of Argonaute/EIF2C-miRNA complexes and the degradation of miRNA targets. *Genome Research, 19*(11), 2009-2020.

Hayashita, Y., Osada, H., Tatematsu, Y., Yamada, H., Yanagisawa, K., Tomida, S., … Takahashi, T. (2005). A polycistronic microRNA cluster, miR-17-92, is overexpressed in human lung cancers and enhances cell proliferation. *Cancer Research, 65*(21), 9628-9632.

He, T. C., Sparks, A. B., Rago, C., Hermeking, H., Zawel, L., da Costa, L. T., … Kinzler, K. W. (1998). Identification of *c-MYC* as a target of the APC pathway. *Science, 281*(5382), 1509-1512.

He, X. Y., Chen, J. X., Zhang, Z., Li, C. L., Peng, Q. L., & Peng, H. M. (2010). The let-7a microRNA protects from growth of lung carcinoma by suppression of *k-Ras* and *c-Myc* in nude mice. *Journal of Cancer Research and Clinical Oncology, 136*(7), 1023-1028.

Heller, G., Weinzierl, M., Noll, C., Babinsky, V., Ziegler, B., Altenberger, C., … Zochbauer-Muller, S. (2012). Genome-wide miRNA expression profiling identifies miR-9-3 and miR-193a as targets for DNA methylation in non-small cell lung cancers. *Clinical Cancer Research, 18*(6), 1619-1629.

Henschke, C. I., & Yankelevitz, D. F. (2008). CT screening for lung cancer: Update 2007. *The Oncologist, 13*(1), 65-78.

Hermkens, D. M. A., Duckers, H. J., & Schulte-Merker, S. (2015). Vascular development in the zebrafish. In M. H. H. Schmidt & S. Liebner (Eds.), *Endothelial Signaling in Development and Disease* (Vol. 14, pp. 47-56). New York, NY: Springer-Verlag.

Hiemer, S. E., Szymaniak, A. D., & Varelas, X. (2014). The transcriptional regulators TAZ and YAP direct transforming growth factor β-induced tumorigenic phenotypes in breast cancer cells. *The Journal of Biologial Chemistry, 289*(19), 13461-13474.

Holm, C., Gineitis, D., McConville, G., & Kazlauskas, A. (1996). Expression of PDGF, VEGF and their receptors in non-small cell lung tumor lines. *International Journal of Oncology, 9*(5), 1077-1086.

Holmgren, L., O'Reilly, M. S., & Folkman, J. (1995). Dormancy of micrometastases: Balanced proliferation and apoptosis in the presence of angiogenesis suppression. *Nature Medicine, 1*(2), 149-153.

Howe, K., Clark, M. D., Torroja, C. F., Torrance, J., Berthelot, C., Muffato, M., … Stemple, D. L. (2013). The zebrafish reference genome sequence and its relationship to the human genome. *Nature, 496*(7446), 498-503.

Hu, H., Li, S., Liu, J., & Ni, B. (2012). MicroRNA-193b modulates proliferation, migration, and invasion of non-small cell lung cancer cells. *Acta Biochimica et Biophysica Sinica, 44*(5), 424-430.

Hu, H., Wang, B., Borde, M., Nardone, J., Maika, S., Allred, L., … Rao, A. (2006). Foxp1 is an essential transcriptional regulator of B cell development. *Nature Immunology, 7*(8), 819-826.

Hu, H., Xu, Z., Li, C., Xu, C., Lei, Z., Zhang, H. T., & Zhao, J. (2016). MiR-145 and miR-203 represses TGF-β-induced epithelial-mesenchymal transition and invasion by inhibiting *SMAD3* in non-small cell lung cancer cells. *Lung Cancer, 97*, 87-94.

Hu, J., Cheng, Y., Li, Y., Jin, Z., Pan, Y., Liu, G., … Feng, Y. (2014a). MicroRNA-128 plays a critical role in human non-small cell lung cancer tumourigenesis, angiogenesis and lymphangiogenesis by directly targeting vascular endothelial growth factor-C. *European Journal of Cancer, 50*(13), 2336-2350.

Hu, J., Qiu, M., Jiang, F., Zhang, S., Yang, X., Wang, J., … Yin, R. (2014b). MiR-145 regulates cancer stem-like properties and epithelial-to-mesenchymal transition in lung adenocarcinima-initiating cells. *Tumour Biology, 35*(9), 8953-8961.

Huang, B., Luo, W., Sun, L., Zhang, Q., Jiang, L., Chang, J., … Wang, E. (2013). MiRNA-125a-3p is a negative regulator of the RhoA-actomyosin pathway in A549 cells. *International Journal of Oncology, 42*(5), 1734-1742.

Huang, D. W., Sherman, B. T., & Lempicki, R. A. (2009). Systematic and integrative analysis of large gene lists using DAVID bioinformatics resources. *Nature Protocols, 4*(1), 44-57.

Huang, R. Y., Guilford, P., & Thiery, J. P. (2012). Early events in cell adhesion and polarity during epithelial-mesenchymal transition. *Journal of Cell Science, 125*(Pt 19), 4417-4422.

Huang, T., She, K., Peng, G., Wang, W., Huang, J., Li, J., … He, J. (2016). MicroRNA-186 suppresses cell proliferation and metastasis through targeting *MAP3K2* in non-small cell lung cancer. *International Journal of Oncology*, *49*(4), 1437-1444.

Huber, M. A., Beug, H., & Wirth, T. (2004). Epithelial-mesenchymal transition: NF-kappaB takes center stage. *Cell Cycle, 3*(12), 1477-1480.

Hughes, P., Marshall, D., Reid, Y., Parkes, H., & Gelber, C. (2007). The costs of using unauthenticated, over-passaged cell lines: How much more data do we need? *Biotechniques, 43*(5), 577-578, 581-582.

Humphreys, D. T., Westman, B. J., Martin, D. I., & Preiss, T. (2005). MicroRNAs control translation initiation by inhibiting eukaryotic initiation factor 4E/cap and poly(A) tail function. *Proceedings of the National Academy of Sciences of the United States of America, 102*(47), 16961-16966.

Hunter, J. (1861). *The Works of John Hunter. Volume II. Observations in Comparative Anatomy* (Vol. 2). London, England: John van Voorst.

Hupkes, M., Sotoca, A. M., Hendriks, J. M., van Zoelen, E. J., & Dechering, K. J. (2014). MicroRNA miR-378 promotes BMP2-induced osteogenic differentiation of mesenchymal progenitor cells. *BMC Molecular Biology, 15*, 1.

Hurst, D. R., Edmonds, M. D., & Welch, D. R. (2009). MetastamiR: The field of metastasis-regulatory microRNA is spreading. *Cancer Research, 69*(19), 7495-7498.

Hwang, H. W., Wentzel, E. A., & Mendell, J. T. (2007). A hexanucleotide element directs microRNA nuclear import. *Science, 315*(5808), 97-100.

Hwang, J. H., Voortman, J., Giovannetti, E., Steinberg S. M., Leon, L. G., Kim, Y. T., … Giaccone, G. (2010). Identification of microRNA-21 as a biomarker for chemoresistance and clinical outcome following adjuvant therapy in resectable pancreatic cancer. *PLoS One, 5*(5), e10630.

Ilyas, M., & Tomlinson, I. P. (1997). The interactions of APC, E-cadherin and beta-catenin in tumour development and progression. *The Journal of Pathology, 182*(2), 128-137.

Imig, J., Motsch, N., Zhu, J. Y., Barth, S., Okoniewski, M., Reineke, T., … Grasser, F. A. (2011). MicroRNA profiling in Epstein-Barr virus-associated B-cell lymphoma. *Nucleic Acids Research, 39*(5), 1880-1893.

Incoronato, M., Urso, L., Portela, A., Laukkanen, M. O., Soini, Y., Quintavalle, C., … Condorelli, G. (2011). Epigenetic regulation of miR-122 expression in lung cancer. *PLoS One, 6*(11), e27722.

Insall, R. H., & Machesky, L. M. (2009). Actin dynamics at the leading edge: From simple machinery to complex networks. *Developmental Cell, 17*(3), 310-322.

Isobe, T., Herbst, R. S., & Onn, A. (2005). Current management of advanced non-small cell lung cancer: Targeted therapy. *Seminars in Oncology, 32*(3), 315-328.

Iwanicki, M. P., Vomastek, T., Tilghman, R. W., Martin, K. H., Banerjee, J., Wedegaertner, P. B., & Parsons, J. T. (2008). FAK, PDZ-RhoGEF and ROCKII cooperate to regulate adhesion movement and trailing-edge retraction in fibroblasts. *Journal of Cell Science, 121*, 895-905.

Jain, R. K. (2005). Normalization of tumor vasculature: An emerging concept in antiangiogenic therapy. *Science, 307*(5706), 58-62.

Jain, R. K., & Styllanopoulos, T. (2010). Delivering nanomedicine to solid tumors. *Nature Reviews Clinical Oncology, 7*(11), 653-664.

Jeffries, C. D., Fried, H. M., & Perkins, D. O. (2011). Nuclear and cytoplasmic localization of neural stem cell microRNAs. *RNA, 17*(4), 675-686.

Jenny, A., Reynolds-Kenneally, J., Das, G., Burnett, M., & Mlodzik, M. (2005). Diego and Prickle regulate Frizzled planar cell polarity signalling by competing for Dishevelled binding. *Nature Cell Biology, 7*(7), 691-697.

Jeon, H. M., Sohn, Y. W., Oh, S. Y., Kim, S. H., Beck, S., Kim, S., & Kim, H. (2011). ID4 imparts chemoresistance and cancer stemness to glioma cells by derepressing miR-9*-mediated suppression of *SOX2*. *Cancer Research, 71*(9), 3410-3421.

Jeong, H. C., Kim, E. K., Lee, J. H., Lee, J. M., Yoo, H. N., & Kim, J. K. (2011). Aberrant expression of let-7a in the blood of non-small cell lung cancer patients. *Molecular Medicine Reports, 4*(2), 383-387.

Jia, L., Soengas, M. S., & Sun, Y. (2009). ROC1/RBX1 E3 ubiquitin ligase silencing suppresses tumor cell growth via sequential induction of G2-M arrest, apoptosis, and senescence. *Cancer Research, 69*(12), 4974-4982.

Jiang, L., Huang, Q., Zhang, S., Zhang, Q., Chang, J., Qiu, X., & Wang, E. (2010). Hsa-miR-125a-3p and hsa-miR-125a-5p are downregulated in non-small cell lung cancer and have inverse effects on invasion and migration of lung cancer cells. *BMC Cancer, 10*, 318.

Jiang, L., & Qiu, X. (2013). MicroRNAs in invasion and metastasis in lung cancer. In C. Lopez-Camarillo & E. Arechaga-Ocampo (Eds.), *Oncogenomics and Cancer Proteomics- Novel Approaches in Biomarkers Discovery and Therapeutic Targets in Cancer* (pp. 123-138). Rijeka, Croatia: InTechOpen.

Johnson, S. M., Grosshans, H., Shingara, J., Byrom, M., Jarvis, R., Cheng, A., … Slack, F. J. (2005). *RAS* is regulated by the let-7 microRNA family. *Cell, 120*(5), 635-647.

Joyce, J. A., & Pollard, J. W. (2009). Microenvironmental regulation of metastasis. *Nature Reviews Cancer, 9*(4), 239-252.

Jung, J. H., Jung, C. K., Choi, H. J., Jun, K. H., Yoo, J., Kang, S. J., & Lee, K. Y. (2009). Diagnostic utility of expression of claudins in non-small cell lung cancer: Different expression profiles in squamous cell carcinomas and adenocarcinomas. *Pathology, Research and Practice, 205*(6), 409-416.

Kalluri, R., & Weinberg, R. A. (2009). The basics of epithelial-mesenchymal transition. *The Journal of Clinical Investigation, 119*(6), 1420-1428.

Kano, A. (2015). Tumor cell secretion of soluble factor(s) for specific immunosuppression. *Scientific Reports, 5*, 8913.

Karlsson, J., von Hofsten, J., & Olsson, P. E. (2001). Generating transparent zebrafish: A refined method to improve detection of gene expression during embryonic development. *Marine Biotechnology, 3*(6), 522-527.

Kasinski, A. L., Kelnar, K., Stahlhut, C., Orellana, E., Zhao, J., Shimer, E., … Slack F. J. (2015). A combinatorial microRNA therapeutics approach to suppressing non-small cell lung cancer. *Oncogene, 34*(27), 3547-3555.

Ke, Y., Zhao, W., Xiong, J., & Cao, R. (2013). MiR-149 inhibits non-small-cell lung cancer cells EMT by targeting *FOXM1*. *Biochemistry Research International*, *2013*, 506731.

Kemler, R. (1992). Classical cadherins. *Seminars in Cell Biology, 3*(3), 149-155.

Khraiwesh, B., Arif, M. A., Seumel, G. I., Ossowski, S., Weigel, D., Reski, R., & Frank, W. (2010). Transcriptional control of gene expression by microRNAs. *Cell, 140*(1), 112-122.

Khvorova, A., Reynolds, A., & Jayasena, S. D. (2003). Functional siRNAs and miRNAs exhibit strand bias. *Cell, 115*(2), 209-216.

Kidd, M. E., Shumaker, D. K., & Ridge, K. M. (2014). The role of vimentin intermediate filaments in the progression of lung cancer. *American Journal of Respiratory Cell and Molecular Biology, 50*(1), 1-6.

Kienast, Y., von Baumgarten, L., Fuhrmann, M., Klinkert, W. E., Goldbrunner, R., Herms, J., & Winkler, F. (2010). Real-time imaging reveals the single steps of brain metastasis formation. *Nature Medicine, 16*(1), 116-122.

Kikyo, M., Matozaki, T., Kodama, A., Kawabe, H., Nakanishi, H., & Takai, Y. (2000). Cell-cell adhesion-mediated tyrosine phosphorylation of nectin-2delta, an immunoglobulin-like cell adhesion molecule at adherens junctions. *Oncogene, 19*(35), 4022-4028.

Kim, D. H., Saetrom, P., Snove Jr., O., & Rossi, J. J. (2008a). MicroRNA-directed transcriptional gene silencing in mammalian cells. *Proceedings of the National Academy of Sciences of the United States of America, 105*(42), 16230-16235.

Kim, E. S., Hirsh, V., Mok, T., Socinski, M. A., Gervais, R., Wu, Y. L., … Douillard, J. Y. (2008b). Gefitinib versus docetaxel in previously treated non-small-cell lung cancer (INTEREST): A randomised phase III trial. *The Lancet, 372*(9352), 1809-1818.

Kim, J., Yu, W., Kovalski, K., & Ossowski, L. (1998). Requirement for specific proteases in cancer cell intravasation as revealed by a novel semiquantitative PCR-based assay. *Cell, 94*(3), 353-362.

Kim, S. H., Turnbull, J., & Guimond, S. (2011). Extracellular matrix and cell signalling: The dynamic cooperation of integrin, proteoglycan and growth factor receptor. *The Journal of Endocrinology, 209*(2), 139-151.

Kim, Y. H., Kwei, K. A., Girard, L., Salari, K., Kao, J., Pacyna-Gengelbach, M., … Pollack, J. R. (2009). Genomic and functional analysis identifies *CRKL* as an oncogene amplified in lung cancer. *Oncogene, 29*(10), 1421-1430.

Kiriakidou, M., Tan, G. S., Lamprinaki, S., De Planell-Saguer, M., Nelson, P. T., & Mourelatos, Z. (2007). An mRNA m7G cap binding-like motif within human *Ago2* represses translation. *Cell, 129*(6), 1141-1151.

Klopp, A. H., Spaeth, E. L., Dembinski, J. L., Woodward, W. A., Munshi, A., Meyn, R. E., … Marini, F. C. (2007). Tumor irradiation increases the recruitment of circulating mesenchymal stem cells into the tumor microenvironment. *Cancer Research, 67*(24), 11687-11695.

Knudsen, B. S., Feller, S. M., & Hanafusa, H. (1994). Four proline-rich sequences of the guanine-nucleotide exchange factor C3G bind with unique specificity to the first Src homology 3 domain of *Crk*. *The Journal of Biological Chemistry, 269*(52), 32781-32787.

Koh, M. Y., Darnay, B. G., & Powis, G. (2008). Hypoxia-associated factor, a novel E3-ubiquitin ligase, binds and ubiquitinates hypoxia-inducible factor 1alpha, leading to its oxygen-independent degradation. *Molecular and Cellular Biology, 28*(23), 7081-7095.

Komiya, Y., & Habas, R. (2008). Wnt signal transduction pathways. *Organogenesis, 4*(2), 68-75.

Kos, M., & Dabrowski, A. (2002). Tumour's angiogenesis- The function of VEGF and bFGF in colorectal cancer. *Annales Universitatis Mariae Curie-Sklodowska, 57*(2), 556-561.

Kota, J., Chivukula, R. R., O'Donnell, K. A., Wentzel, E. A., Montgomery, C. L., Hwang, H. W., … Mendell, J. T. (2009). Therapeutic microRNA delivery suppresses tumorigenesis in a murine liver cancer model. *Cell, 137*(6), 1005-1017.

Krek, A., Grun, D., Poy, M. N., Wolf, R., Rosenberg, L., Epstein, E. J., … Rajewsky, N. (2005). Combinatorial microRNA target predictions. *Nature Genetics, 37*(5), 495-500.

Krishnamachary, B., Zagzag, D., Nagasawa, H., Rainey, K., Okuyama, H., Baek, J. H., & Semenza, G. L. (2006). Hypoxia-inducible factor-1-dependent repression of E-cadherin in von Hippel-Lindau tumor suppressor-null renal cell carcinoma mediated by TCF3, ZFHX1A, and ZFHX1B. *Cancer Research, 66*(5), 2725-2731.

Krist, B., Florczyk, U., Pietraszek-Gremplewicz, K., Jozkowicz, A., & Dulak, J. (2015). The role of miR-378a in metabolism, angiogenesis, and muscle biology. *International Journal of Endocrinology, 2015*, 281756.

Krutzfeldt, J., Rajewsky, N., Braich, R., Rajeev, K. G., Tuschl, T., Manoharan, M., & Stoffel, M. (2005). Silencing of microRNAs *in vivo* with "antagomirs". *Nature, 438*(7068), 685-689.

Kuhl, M., Sheldahl, L. C., Malbon, C. C., & Moon, R. T. (2000). Ca(2+)/calmodulin-dependent protein kinase II is stimulated by Wnt and Frizzled homologs and promotes ventral cell fates in *Xenopus*. *The Journal of Biological Chemistry, 275(17)*, 12701-12711.

Kumar, S., & Weaver, V. M. (2009). Mechanics, malignancy, and metastasis: The force journey of a tumor cell. *Cancer Metastasis Rev*iews, *28*(1-2). 113-127.

Kumar, S. M., Yu, H., Edwards, R., Chen, L., Kazianis, S., Brafford, P., … Xu, X. (2007). Mutant V600E *BRAF* increases hypoxia inducible factor-1alpha expression in melanoma. *Cancer Research, 67*(7), 3177-3184.

Kumarswamy, R., Mudduluru, G., Ceppi, P., Muppala, S., Kozlowski, M., Niklinski, J., … Allgayer, H. (2012). MicroRNA-30a inhibits epithelial-to-mesenchymal transition by targeting *Snai1* and is downregulated in non-small cell lung cancer. *International Journal of Cancer, 130*(9), 2044-2053.

Kunner, R., Muley, T., Meister, M., Ruschhaupt, M., Buness, A., Xu, E. C., … Hoffmann, H. (2009). Global gene expression analysis reveals specific patterns of cell junctions in non-small cell lung cancer subtypes. *Lung Cancer, 63*(1), 32-38.

Laack, E., Kohler, A., Kugler, C., Dierlamm, T., Knuffmann, C., Vohwinkel, G., … Hossfeld, D. K. (2002). Pretreatment serum levels of matrix metalloproteinase-9 and vascular endothelial growth factor in non-small-cell lung cancer. *Annals of Oncology, 13*(10), 1550-1557.

Lam, S. H., Chua, H. L., Gong, Z., Lam, T. J., & Sin, Y. M. (2004). Development and maturation of the immune system in zebrafish, *Danio rerio*: A gene expression profiling, *in situ* hybridization and immunological study. *Developmental & Comparative Immunology, 28*(1), 9-28.

Lam, S. H., Wu, Y. L., Vega, V. B., Miller, L. D., Spitsbergen, J., Tong, Y., … Gong, Z. (2006). Conservation of gene expression signatures between zebrafish and human liver tumors and tumor progression. *Nature Biotechnology, 24*(1), 73-75.

Lamalice, L., Le Boeuf, F., & Huot, J. (2007). Endothelial cell migration during angiogenesis. *Circulation Research, 100*, 782-794.

Landi, M. T., Chatterjee, N., Yu, K., Goldin, L. R., Goldstein, A. M., Rotunno, M., … Caporaso, N. E. (2009). A genome-wide association study of lung cancer identifies a region of chromosome 5p15 associated with risk for adenocarcinoma. *American Journal of Human Genetics, 85*(5), 679-691.

Landi, M. T., Zhao, Y., Rotunno, M., Koshiol, J., Liu, H., Bergen, A. W., … Wang, E. (2010). MicroRNA expression differentiates histology and predicts survival of lung cancer. *Clinical Cancer Research, 16*(2), 430-441.

Landthaler, M., Gaidatzis, D., Rothballer, A., Chen, P. Y., Soll, S. J., Dinic, L., … Tuschl, T. (2008). Molecular characterization of human Argonaute-containing ribonucleoprotein complexes and their bound target mRNAs. *RNA, 14*(12), 2580-2596.

Laughner, E., Taghavi, P., Chiles, K., Mahon, P. C., & Semenza, G. L. (2001). HER2 (neu) signaling increases the rate of hypoxia-inducible factor 1alpha (HIF-1alpha) synthesis: Novel mechanism for HIF-1-mediated vascular endothelial growth factor expression. *Molecular and Cellular Biology, 21*(12), 3995-4004.

Lawson, N. D., & Weinstein, B. M. (2002). Arteries and veins: Making a difference with zebrafish. *Nature Reviews Genetics, 3*(9), 674-682.

Lecomte, N., Njardarson, J. T., Nagorny, P., Yang, G., Downey, R., Ouerfelli, O., … Danishefsky, S. J. (2011). Emergence of potent inhibitors of metastasis in lung cancer via syntheses based on migrastatin. *Proceedings of the National Academy of Sciences of the United States of America, 108*(37), 15074-15078.

Lee, D. Y., Deng, Z., Wang, C. H., & Yang, B. B. (2007). MicroRNA-378 promotes cell survival, tumor growth, and angiogenesis by targeting *SuFu* and *Fus-1* expression. *Proceedings of the National Academy of Sciences of the United States of America, 104*(51), 20350-20355.

Lee, J. M., Yoo, J. K., Yoo, H., Jung, H. Y., Lee, D. R., Jeong, H. C., … Kim, J. K. (2013). The novel miR-7515 decreases the proliferation and migration of human lung cancer cells by targeting *c-Met*. *Molecular Cancer Research, 11*(1), 43-53.

Lee, L. M., Seftor, E. A., Bonde, G., Cornell, R. A., & Hendrix, M. J. (2005). The fate of human malignant melanoma cells transplanted into zebrafish embryos: Assessment of migration and cell division in the absence of tumor formation. *Developmental Dynamics, 233*(4), 1560-1570.

Lee, R. C., Feinbaum, R. L., & Ambros, V. (1993). The *C. elegans* heterochronic gene *lin-4* encodes small RNAs with antisense complementarity to lin-14. *Cell, 75*(5), 843-854.

Lee, Y., Kim, M., Han, J., Yeom, K.-Y., Lee, S., Baek, S. H., & Kim, V. N. (2004). MicroRNA genes are transcribed by RNA polymerase II. *The EMBO Journal, 23*(20), 4051-4060.

Lei, L., Huang, Y., & Gong, W. (2014). Inhibition of miR-92b suppresses nonsmall cell lung cancer cells growth and motility by targeting *RECK*. *Molecular and Cellular Biochemistry*, 387(1-2), 171-176.

Lepinske, M. (1996). BSA and restriction enzyme digestions. *Promega Notes*, *60*, 28.

Leslie, E. M., Ghibellini, G., Nezasa, K., & Brouwer, K. L. (2007). Biotransformation and transport of the tobacco-specific carcinogen 4-(methylnitrosamino)-1-(3-pyridyl)-1-butanone (NNK) in bile duct-cannulated wild-type and Mrp2/Abcc2-deficient (TR) Wistar rats. *Carcinogenesis, 28*(12), 2650-2656.

Li, J., Davidson, G., Huang, Y., Jiang, B.-H., Shi, X., Costa, M., & Huang, C. (2004). Nickel compounds act through phosphatidylinositol-3-kinase/Akt-dependent, $p70^{S6k}$-independent pathway to induce hypoxia inducible factor transactivation and *Cap43* expression in mouse epidermal C141 cells. *Cancer Research, 64*(1), 94-101.

Li, J., Song, Y., Wang, Y., Luo, J., & Yu, W. (2013a). MicroRNA-148a suppresses epithelial-to-mesenchymal transition by targeting *ROCK1* in non-small cell lung cancer cells. *Molecular and Cellular Biochemistry, 380*(1), 277-282.

Li, J., Tan, Q., Yan, M., Liu, L., Lin, H., Zhao, F., … Yao, M. (2014). MiRNA-200c inhibits invasion and metastasis of human non-small cell lung cancer by directly targeting ubiquitin specific peptidase 25. *Molecular Cancer, 13*, 166.

Li, J., Yu, T., Cao, J., Liu, L., Liu, Y., Kong, H. W., … Yan, M. X. (2015a). MicroRNA-148a suppresses invasion and metastasis of human non-small-cell lung cancer. *Cellular Physiology and Biochemistry, 37*(5), 1847-1856.

Li, Q., Han, Y., Wang, C., Shan, S., Wang, Y., Zhang, J., & Ren, T. (2015b). MicroRNA-125b promotes tumor metastasis through targeting tumor protein 53-induced nuclear protein 1 in patients with non-small-cell lung cancer. *Cancer Cell International, 15*, 84-93.

Li, Y., Chen, P., Zu, L., Liu, B., Wang, M., & Zhou, Q. (2016). MicroRNA-338-3p suppresses metastasis of lung cancer cells by targeting the EMT regulator *Sox4*. *American Journal of Cancer Research, 6*(2), 127-140.

Li, Y., Li, L., Guan, Y., Liu, X., Meng, Q., & Guo, Q. (2013b). MiR-92b regulates the cell growth, cisplatin chemosensitivity of A549 non small cell lung cancer cell line and target *PTEN*. *Biochemical and Biophysical Research Communications, 440*(4), 604-610.

Li, Y., Zhang, D., Chen, C., Ruan, Z., Li, Y., & Huang, Y. (2012a). MicroRNA-212 displays tumor-promoting properties in non-small cell lung cancer cells and targets the hedgehog pathway receptor *PTCH1*. *Molecular Biology of the Cell, 23*(8), 1423-1434.

Li, Y. J., Zhang, Y. X., Wang, P. Y., Chi, Y. L., Zhang, C., Ma, Y., … Xie, S. Y. (2012b). Regression of A549 lung cancer tumors by anti-miR-150 vector. *Oncology Reports, 27*(1), 129-134.

Liao, D., & Johnson, R. S. (2007). Hypoxia: A key regulator of angiogenesis in cancer. *Cancer Metastasis Reviews, 26*(2), 281-290.

Liao, J. Y., Ma, L. M., & Guo, Y. H., Zhang, Y. C., Zhou, H., Shao, P., … Qu, L. H. (2010). Deep sequencing of human nuclear and cytoplasmic small RNAs reveals an unexpectedly complex subcellular distribtution of miRNAs and tRNA 3' trailers. *PLoS One, 5*(5), e10563.

Lieber, M., Smith, B., Szakal, A., Nelson-Rees, W., & Todaro, G. (1976). A continuous tumor-cell line from a human lung carcinoma with properties of type II alveolar epithelial cells. *International Journal of Cancer, 17*(1), 62-70.

Lieschke, G. J., & Currie, P. D. (2007). Animal models of human disease: Zebrafish swim to view. *Nature Reviews Genetics, 8*(5), 353-367.

Lieschke, G. J., & Trede, N. S. (2009). Fish immunology. *Current Biology, 19*(16), 678-682.

Liliental, J., Moon, S. Y., Lesche, R., Mamillapalli, R., Li, D., Zheng, Y., … Wu, H. (2000). Genetic deletion of the *Pten* tumour suppressor gene promotes cell motility by activation of Rac1 and Cdc42 GTPases. *Current Biology, 10*(7), 401-404.

Lim, L. P., Lau, N. C., Garrett-Engele, P., Grimson, A., Schelter, J. M., Castle, J., … Johnson, J. M. (2005). Microarray analysis shows that some microRNAs downregulate large numbers of target mRNAs. *Nature, 433*, 769-773.

Lin, J., Yang, R., Tarr, P. T., Wu, P. H., Handschin, C., Li, S., … Spiegelman, B. M. (2005). Hyperlipidemic effects of dietary saturated fats mediated through PGC-1beta coactivation of *SREBP*. *Cell, 120*(2), 261-273.

Lin, Q., Sun, M. Z., Guo, C., Shi, J., Chen, X., & Liu, S. (2015). *CRKL* overexpression suppresses *in vitro* proliferation, invasion and migration of murine hepatocarcinoma Hca-P cells. *Biomedicine & Pharmacotherapy, 69*, 11-17.

Lin, S. Y., Yang, J., Everett, A. D., Clevenger, C. V., Koneru, M., Mishra, P. J., … Glod, J. (2008). The isolation of novel mesenchymal stromal cell chemotactic factors from the conditioned medium of tumor cells. *Experimental Cell Research, 314*(17), 3107-3117.

Lin, Y., Bai, L., Chen, W., & Xu, S. (2010). The NF-kappaB activation pathways, emerging molecular targets for cancer prevention and therapy. *Expert Opinion on Therapeutic Targets, 14*(1), 45-55.

Ling, B., Wang, G. X., Long, G., Qiu, J. H., & Hu, Z. L. (2012). Tumor suppressor miR-22 suppresses lung cancer cell progression through post-transcriptional regulation of *ErbB3*. *Journal of Cancer Research and Clinical Oncology, 138*(8), 1355-1361.

Liu, B., Wu, X., Liu, B., Wang, C., Liu, Y, Zhou, Q., & Xu, K. (2012a). MiR-26a enhances metastasis potential of lung cancer cells via AKT pathway by targeting *PTEN*. *Biochimica et Biophysica Acta, 1822*(11), 1692-1704.

Liu, C., Li, Y., Semenov, M., Han, C., Baeg, G. H., Tan, Y., … He, X. (2002). Control of beta-catenin phosphorylation/degradation by a dual-kinase mechanism. *Cell, 108*(6), 837-847.

Liu, C., Yang, H., Xu, Z., Li, D., Zhou, M., Xiao, K., … Zhou, R. (2015). MicroRNA-548I is involved in the migration and invasion of non-small cell lung cancer by targeting the AKT1 signaling pathway. *Journal of Cancer Research and Clinical Oncology, 141*(3), 431-441.

Liu, F., Xiong, Y., Zhao, Y., Tao, L., Zhang, Z., Zhang, H., … Yang, Y. (2013a). Identification of aberrant microRNA expression pattern in pediatric gliomas by microarray. *Diagnostic Pathology, 8*, 158.

Liu, H., Zhu, L., Liu, B., Yang, L., Meng, X., Zhang, W., … Xiao, H. (2012b). Genome-wide microRNA profiles identify miR-378 as a serum biomarker for early detection of gastric cancer. *Cancer Letters, 316*(2), 196-203.

Liu, J., Rivas, F. V., Wohlschlegel, J., Yates 3rd, J. R., Parker, R., & Hannon, G. J. (2005a). A role for the P-body component GW182 in microRNA function. *Nature Cell Biology, 7*(12), 1261-1266.

Liu, J., Valencia-Sanchez, M. A., Hannon, G. J., & Parker, R. (2005b). MicroRNA-dependent localization of targeted mRNAs to mammalian P-bodies. *Nature Cell Biology, 7*(7), 719-723.

Liu, L., Shao, X., Gao, W., Zhang, Z., Liu, P., Wang, R., … Shu, Y. (2012c). MicroRNA-133b inhibits the growth of non-small-cell lung cancer by targeting the epidermal growth factor receptor. *The FEBS Journal, 279*(20), 3800-3812.

Liu, X. H., Lu, K. H., Wang, K. M., Sun, M., Zhang, E. B., Yang, J. S., … Wang, Z. X. (2012d). MicroRNA-196a promotes non-small cell lung cancer cell proliferation and invasion through targeting *HOXA5*. *BMC Cancer, 12*, 348.

Liu, Z. L., Wang, H., Liu, J., & Wang, Z. X. (2013b). MicroRNA-21 (miR-21) expression promotes growth, metastasis, and chemo- or radioresistance in non-small cell lung cancer cells by targeting *PTEN*. *Molecular and Cellular Biochemistry, 372*(1-2), 35-45.

Lopez-Camarillo, C., Marchat, L. A., Arechaga-Ocampo, E., Perez-Plasencia, C., del Moral-Hernandez, O., Castaneda-Ortiz, E. J., & Rodriguez-Cuevas, S. (2012). MetastamiRs: Non-coding microRNAs driving cancer invasion and metastasis. *International Journal of Molecular Sciences, 13*(2), 1347-1379.

Loprevite, M., Varesco, L., Favoni, R., Ferrara, G., Moro, F., Ottaggio, L., … Ardizzoni, A. (1997). Analysis of *K-ras*, *p53*, *bcl-2* and *Rb* expression in non-small cell lung cancer cell lines. *International Journal of Oncology, 11*(6), 1203-1208.

Lorenzi, P. L., Reinhold, W. C., Varma, S., Hutchinson, A. A., Pommier, Y., Chanock, S. J., & Weinstein, J. N. (2009). DNA fingerprinting of the NCI-60 cell line panel. *Molecular Cancer Therapeutics, 8*(4), 713-724.

Lu, Y., Govindan, R., Wang, L., Liu, P. Y., Goodgame, B., Wen, W., … You, M. (2012). MicroRNA profiling and prediction of recurrence/relapse-free survival in stage I lung cancer. *Carcinogenesis, 33*(5), 1046-1054.

Lu, Y., Xiao, J., Lin, H., Bai, Y., Luo, X., Wang, Z., & Yang, B. (2009). A single anti-microRNA antisense oligodeoxyribonucleotide (AMO) targeting multiple microRNAs offers an improved approach for microRNA interference. *Nucleic Acids Research, 37*(3), e24.

Luo, W., Huang, B., Li, Z., Li, H., Sun, L., Zhang, Q., … Wang, E. (2013). MicroRNA-449a is downregulated in non-small cell lung cancer and inhibits migration and invasion by targeting *c-Met*. *PLoS One, 8*(5), e64759.

Lutz, W., Leon, J., & Eilers, M. (2002). Contributions of *Myc* to tumorigenesis. *Biochimica et Biophysica Acta*, *1602*(1), 61-71.

Luzzi, K. J., MacDonald, I. C., Schmidt, E. E., Kerkvliet, N., Morris, V. L., Chambers, A. F., & Groom, A. C. (1998). Multistep nature of metastatic inefficiency: Dormancy of solitary cells after successful extravasation and limited survival of early micrometastases. *The American Journal of Pathology, 153*(3), 865-873.

Ma, A. C. H., Guo, Y., He, A. B. L., & Leung, A. Y. H. (2011). Modeling tumor angiogenesis with zebrafish. In D. T. Simionescu & A. Simionescu (Eds.), *Vasculogenesis and Angiogenesis- From Embryonic Development to Regenerative Medicine* (pp. 133-144). Rijeka, Croatia: InTechOpen.

Ma, J., Lin, J., Qian, J., Qian, W., Yin, J., Yang, B., … Deng, Z. (2014). MiR-378 promotes the migration of liver cancer cells by down-regulating *Fus* expression. *Cellular Physiology and Biochemistry, 34*(6), 2266-2274.

Ma, Y., Fan, M., Dai, L., Kang, X., Liu, Y., Sun, Y., … Chen, K. (2015). The expression of TTF-1 and Napsin A in early-stage lung adenocarcinoma correlates with the results of surgical treatment. *Tumour Biology, 36*(10), 8085-8092.

Mao, G., Liu, Y., Fang, X., Liu, Y., Fang, L., Lin, L., … Wang, N. (2015). Tumor-derived microRNA-494 promotes angiogenesis in non-small cell lung cancer. *Angiogenesis, 18*(3), 373-382. 5

Marcon, E., Babak, T., Chua, G., Hughes, T., & Moens, P. B. (2008). MiRNA and piRNA localization in the male mammalian meiotic nucleus. *Chromosome Research, 16*(2), 243-260.

Masaki, T., Igarashi, K., Tokuda, M., Yukimasa, S., Han, F., Jin, Y. J., … Kuriyama, S. (2003). Pp60c-src activation in lung adenocarcinoma. *European Journal of Cancer, 39*(10), 1447-1455.

Masters, J. R., Thomson, J. A., Daly-Burns, B., Reid, Y. A., Dirks, W. G., Packer, P., … Debenham, P. G. (2001). Short tandem repeat profiling provides an international reference standard for human cell lines. *Proceedings of the National Academy of Sciences of the United States of America, 98*(14), 8012-8017.

Matsuyama, W., Hashiguchi, T., Mizoguchi, A., Iwami, F., Kawabata, M., Arimura, K., & Osame, M. (2000). Serum levels of vascular endothelial growth factor dependent on the stage progression of lung cancer. *Chest, 118*(4), 948-951.

Mattern, J., Koomagi, R., & Volm, M. (1995). Vascular endothelial growth-factor expression and angiogenesis in nonsmall cell lung carcinomas. *International Journal of Oncology, 6*(5), 1059-1062.

Mayer, B. J., Hamaguchi, M., & Hanafusa, H. (1988). A novel viral oncogene with structural similarity to phospholipase C. *Nature, 332*(6161), 272-275.

Mazurenko, N. N., Kogan, E. A., Zborovskaya, I. B., & Kisseljov, F. L. (1992). Expression of pp60c-src in human small cell and non-small cell lung carcinomas. *European Journal of Cancer, 28*(2-3), 372-377.

McLachlan, R. W., Kraemer, A., Helwani, F. M., Kovacs, E. M., & Yap, A. S. (2007). E-cadherin adhesion activates c-Src signaling at cell-cell contacts. *Molecular Biology of the Cell, 18*(8), 3214-3223.

Meadows, K. N., Bryant, P., & Pumiglia, K. (2001). Vascular endothelial growth factor induction of the angiogenic phenotype requires *Ras* activation. *The Journal of Biological Chemistry, 276*(52), 49289-49298.

Mehrbod, M., Trisno, S., & Mofrad, M. R. (2013). On the activation of integrin αIIbβ3: Outside-in and inside-out pathways. *Biophysical Journal, 105*(6), 1304-1315.

Mendelsohn, J., & Baselga, J. (2003). Status of epidermal growth factor receptor antagonists in the biology and treatment of cancer. *Journal of Clinical Oncology, 21*(14), 2787-2799.

Menon, L. G., Picinich, S., Koneru, R., Gao, H., Lin, S. Y., Koneru, M., … Banerjee, D. (2007). Differential gene expression associated with migration of mesenchymal stem cells to conditioned medium from tumor cells or bone marrow cells. *Stem Cells, 25*(2), 520-528.

Merlet, J., Burger, J., Gomes, J. E., & Pintard, L. (2009). Regulation of cullin-RING E3 ubiquitin-liagases by neddylation and dimerization. *Cellular and Molecular Life Sciences, 66*(11-12), 1924-1938.

Mitra, S. K., Hanson, D. A., & Schlaepfer, D. D. (2005). Focal adhesion kinase: In command and control of cell motility. *Nature Reviews Molecular Cell Biology, 6*(1), 56-68.

Mohseny, A. B., Hogendoorn, P. C. W., & Cleton-Jansen, A.-M. (2012). Osteosarcoma models: From cell lines to zebrafish. *Sarcoma, 2012,* 417271.

Mok, T. S., Wu, Y. L., Thongprasert, S., Yang, C. H., Chu, D. T., Saijo, N., … Fukuoka, M. (2009). Gefitinib or carboplatin-paclitaxel in pulmonary adenocarcinoma. *The New England Journal of Medicine, 361*(10), 947-957.

Morse, E. M., Brahme, N. N., & Calderwood, D. A. (2014). Integrin cytoplasmic tail interactions. *Biochemistry, 53*(5), 810-820.

Mosakhani, N., Sarhadi, V. K., Borze, I., Karjalainen-Lindsberg, M. L., Sundstrom, J., Ristamaki, R., … Knuutila, S. (2012). MicroRNA profiling differentiates colorectal cancer according to *KRAS* status. *Genes, Chromosomes & Cancer, 51*(1), 1-9.

Nagashio, R., Ueda, J., Ryuge, S., Nakashima, H., Jiang, S.-X., Kobayashi, M., … Sato, Y. (2015). Diagnostic and prognostic significances of MUC5B and TTF-1 expressions in resected non-small cell lung cancer. *Scientific Reports, 5*, 8649.

Nagrath, S., Sequist, L. V., Maheswaran, S., Bell, D. W., Irimia, D., Ulkus, L., … Toner, M. (2007). Isolation of rare circulating tumour cells in cancer patients by microchip technology. *Nature, 450*(7173), 1235-1239.

Naoki, K., Chen, T. H., Richards, W. G., Sugarbaker, D. J., & Meyerson, M. (2002). Missense mutations of the *BRAF* gene in human lung adenocarcinoma. *Cancer Research, 62*(23), 7001-7003.

Narumiya, S., Tanji, M., & Ishizaki, T. (2009). Rho signaling, ROCK and mDia1, in transformation, metastasis and invasion. *Cancer Metastasis Reviews, 28*(1-2), 65-76.

Nass, D., Rosenwald, S., Meiri, E., Gilad, S., Tabibian-Keissar, H., Schlosberg, A., … Rosenfeld, N. (2009). MiR-92b and miR-9/9* are specifically expressed in brain primary tumors and can be used to differentiate primary from metastatic brain tumors. *Brain Pathology, 19*(3), 375-383.

Nau, M. M., Brooks, B. J., Battey, J., Sausville, E., Gazdar, A. F., Kirsch, I. R., … Minna, J. D. (1985). *L-myc*, a new *myc*-related gene amplified and expressed in human small cell lung cancer. *Nature, 318*(6041), 69-73.

Naumov, G. N., Akslen, L. A., & Folkman, J. (2006). Role of angiogenesis in human tumor dormancy: Animal models of the angiogenic switch. *Cell Cycle, 5*(16), 1779-1787.

Nelson, W. J. (2009). Remodeling epithelial cell organization: Transitions between front-rear and apical-basal polarity. *Cold Spring Harbor Perspectives in Biology, 1*(1), a000513.

Nelson, W. J., & Nusse, R. (2004). Convergence of Wnt, beta-catenin, and cadherin pathways. *Science, 303*(5663), 1483-1487.

Nguyen, D. X., Bos, P. D., & Massague, J. (2009). Metastasis: From dissemination to organ-specific colonization. *Nature Reviews Cancer, 9*(4), 274-284.

Nguyen, D. X., & Massague, J. (2007). Genetic determinants of cancer metastasis. *Nature Reviews Genetics, 8*(5), 341-352.

Nguyen, P. L., Niehans, G. A., Cherwitz, D. L., Kim, Y. S., & Ho, S. B. (1996). Membrane-bound (*MUC1*) and secretory *(MUC2*, *MUC3*, and *MUC4*) mucin gene expression in human lung cancer. *Tumour Biology, 17*(3), 176-192.

Nicoli, S., & Presta, M. (2007). The zebrafish/tumor xenograft angiogenesis assay. *Nature Protocols, 2*(11), 2918-2923.

Nicoli, S., Ribatti, D., Cotelli, F., & Presta, M. (2007). Mammalian tumor xenograft induce neovascularization in zebrafish embryos. *Cancer Research, 67*(7), 2927-2931.

Nieto, M. A. (2013). Epithelial plasticity: A common theme in embryonic and cancer cells. *Science, 342*(6159), 1234850.

Nowell, P. C. (1976). The clonal evolution of tumor cell populations. *Science, 194*(4260), 23-28.

O'Reilly, M. S., Holmgren, L., Chen, C., & Folkman, J. (1996). Angiostatin induces and sustains dormancy of human primary tumours in mice. *Nature Medicine, 2*(6), 689-692.

Ohrt, T., Mutze, J., Staroske, W., Weinmann, L., Hock, J., Crell, K., … Schwille, P. (2008). Fluorescence correlation spectroscopy and fluorescence cross-correlation spectroscopy reveal the cytoplasmic origination of loaded nucelar RISC *in vivo* in human cells. *Nucleic Acids Research, 36*(20), 6439-6449.

Ohta, T., Michel, J. J., & Xiong, Y. (1999). Association with cullin partners protects ROC proteins from proteasome-dependent degradation. *Oncogene, 18*(48), 6758-6766.

Ohta, Y., Endo, Y., Tanaka, M., Shimizu, J., Oda, M., Hayashi, Y., … Sasaki, T. (1996). Significance of vascular endothelial growth factor messenger RNA expression in primary lung cancer. *Clinical Cancer Research, 2*(8), 1411-1416.

Oliveros, J. C. (2015). Venny. An interactive tool for comparing lists with Venn's diagrams [Internet]. Retrieved March 15, 2016, from http://bioinfogp.cnb.csic.es/tools/venny

Orom, U. A., Nielsen, F. N., & Lund, A. H. (2008). MicroRNA-10a binds the 5'UTR of ribosomal protein mRNAs and enhances their translation. *Molecular Cell, 30*(4), 460-471.

Osada, H., & Takahashi, T. (2007). MicroRNAs in biological processes and carcinogenesis. *Carcinogenesis, 28*(1), 2-12.

Owen, K. A., Pixley, F. J., Thomas, K. S., Vicente-Manzanares, M., Ray, B. J., Horwitz, A. F., … Bouton, A. H. (2007). Regulation of lamellipodial persistence, adhesion turnover, and motility in macrophages by focal adhesion kinase. *The Journal of Cell Biology, 179*(6), 1275-1287.

Pacurari, M., Addison, J. B., Bondalapati, N., Wan, Y. W., Luo, D., Qian, Y., … Guo, N. L. (2013). The microRNA-200 family targets multiple non-small cell lung cancer prognostic markers in H1299 cells and BEAS-2B cells. *International Journal of Oncology, 43*(2), 548-560.

Pages, G., & Pouyssegur, J. (2005). Transcriptional regulation of the vascular endothelial growth factor gene- A concert of activating factors. *Cardiovascular Research, 65*(3), 564-573.

Paget, S. (1889). The distribution of secondary growths in cancer of the breast. *The Lancet, 133*(3421), 571-573.

Palmer, T. D., Ashby, W. J., Lewis, J. D., & Zijlstra, A. (2011). Targeting tumor cell motility to prevent metastasis. *Advanced Drug Delivery Reviews, 63*(8), 568-581.

Paraskevopoulou, M. D., Georgakilas, G., Kostulas, N., Vlachos, I. S., Vergoulis, T., Reczko, M., … Hatzigeorgiou, A. G. (2013). DIANA-microT web server v5.0: Service integration into miRNA functional analysis workflows. *Nucleic Acids Research, 41*9(Web Server issue), W169-173.

Park, D. H., Jeon, H. S., Lee, S. Y., Choi, Y. Y., Lee, H. W., Yoon, S., … Son, J. W. (2015). MicroRNA-146a inhibits epithelial mesenchymal transition in non-small cell lung cancer by targeting insulin receptor substrate 2. *International Journal of Oncology, 47*(4), 1545-1553.

Park, S. J., Suetsugu, S., & Takenawa, T. (2005). Interaction of HSP90 to N-WASP leads to activation and protection from proteasome from proteasome-dependent degradation. *The EMBO Journal, 24*(8), 1557-1570.

Parsons, J. T., Horwitz, A. R., & Schwartz, M. A. (2010). Cell adhesion: Integrating cytoskeletal dynamics and cellular tension. *Nature Reviews Molecular Cell Biology, 11*(9), 633-643.

Pasquinelli, A. E. (2012). MicroRNAs and their targets: Recognition, regulation and an emerging reciprocal relationship. *Nature Reviews Genetics, 13*(4), 271-282.

Patnaik, S. K., Kannisto, E., & Yendamuri, S. (2010). Overexpression of microRNA miR-30a or miR-191 in A549 lung cancer or BEAS-2B normal lung cell lines does not alter phenotype. *PLoS One, 5*(2), e9219.

Peifer, M., & Polakis, P. (2000). Wnt signaling in oncogenesis and embryogenesis: A look outside the nucleus. *Science, 287* (5458), 1606-1609.

Peinado, H., Olmeda, D., & Cano, A. (2007). Snail, Zeb and bHLH factors in tumour progression: An alliance against the epithelial phenotype? *Nature Reviews Cancer, 7*(6), 415-428.

Pelengaris, S., & Khan, M. (2003). The many faces of *c-MYC*. *Archives of Biochemistry and Biophysics, 416*(2), 129-136.

Peng, Y., & Croce, C. M. (2016). The role of microRNAs in human cancer. *Signal Transduction and Targeted Therapy, 1*, 15004.

Pepper, M. S., Mandriota, S. J., & Montesano, R. (2002). Angiogenesis-regulating cytokines. In T.-P. D. Fan & E. C. Kohn (Eds.), *The New Angiotherapy* (pp. 7-40). New York, NY: Humana Press.

Pillai, R. S., Bhattacharyya, S. N., Artus, C. G., Zoller, T., Cougot, N., Basyuk, E., … Filipowicz, W. (2005). Inhibition of translational initiation by Let-7 microRNA in human cells. *Science, 309*(5740), 1573-1576.

Pirker, R., Pereira, J. R., Szczesna, A., von Pawel, J., Krzakowski, M., Ramlau., R., … Gatzemeler, U. (2009). Cetuximab plus chemotherapy in patients with advanced non-small-cell lung cancer (FLEX): An open-label randomised phase III trial. *The Lancet, 373*(9674), 1525-1531.

Place, R. F., Li, L. C., Pookot, D., Noonan, E. J., & Dahiya, R. (2008). MicroRNA-373 induces expression of genes with complementary promoter sequences. *Proceedings of the National Academy of Sciences of the United States of America, 105*(5), 1608-1613.

Pola, R., Ling, L. E., Silver, M., Corbley, M. J., Kearney, M., Blake Pepinsky, R., … Isner, J. M. (2001). The morphogen Sonic hedgehog is an indirect angiogenic agent upregulating two families of angiogenic growth factors. *Nature Medicine, 7*(6), 706-711.

Politz, J. C., Hogan, E. M., & Pederson, T. (2009). MicroRNAs with a nucleolar location. *RNA, 15*(9), 1705-1715.

Popper, H. H. (2016). Progression and metastasis of lung cancer. *Cancer Metastasis Reviews, 35*, 75-91.

Pouliot, N., Pearson, H. B., & Burrows, A. (2013). Investigating metastasis using *in vitro* platforms: Madame Curie Bioscience Database [Internet]. *Austin, TX: Landes Bioscience*. Retrieved December 13, 2016, from http://www.ncbi.nlm.nih.gov/books/NBK100379/

Proctor, R. N. (2001). Tobacco and the global lung cancer epidemic. *Nature Reviews Cancer, 1*(1), 82-86.

Puissegur, M. P., Mazure, N. M., Bertero, T., Pradelli, L., Grosso, S., Robbe-Sermesant, K., … Mari, B. (2011). MiR-210 is overexpressed in late stages of lung cancer and mediates mitochondrial alterations associated with modulation of *HIF-1* activity. *Cell Death and Differentiation, 18*(3), 465-478.

Qi, J., Rice, S. J,, Salzberg, A. C., Runkle, E. A., Liao, J., Zander, D. S., & Mu, D. (2012). MiR-365 regulates lung cancer and developmental gene thyroid transcription factor 1. *Cell Cycle, 11*(1), 177-186.

Qian, J., Lin, J., Qian, W., Ma, J. C., Qian, S. X., Li, Y., … Deng, Z. Q. (2013). Overexpression of miR-378 is frequent and may affect treatment outcomes in patients with acute myeloid leukemia. *Leukemia Research, 37*(7), 765-768.

Qu, J., Li, M., An, J., Zhao, B., Zhong, W., Gu, Q., … Hu, C. (2015). MicroRNA-33b inhibits lung adenocarcinoma cell growth, invasion, and epithelial-mesenchymal transition by suppressing Wnt/β-catenin/ZEB1 signaling. *International Journal of Oncology, 47*(6), 2141-2152.

Rabinowits, G., Gercel-Taylor, C., Day, J. M., Taylor, D. D., & Kloecker, G. H. (2009). Exosomal microRNA: A diagnostic marker for lung cancer. *Clinical Lung Cancer, 10*(1), 42-46.

Rai, K., Takigawa, N., Ito, S., Kashihara, H., Ichihara, E., Yasuda, T., … Kiura, K. (2011). Liposomal delivery of microRNA-7-expressing plasmid overcomes epidermal growth factor receptor tyrosine kinase inhibitor-resistance in lung cancer cells. *Molecular Cancer Therapeutics, 10*(9), 1720-1727.

Raponi, M., Dossey, L., Jatkoe, T., Wu, X., Chen, G., Fan, H., & Beer, D. G. (2009). MicroRNA classifiers for predicting prognosis of squamous cell lung cancer. *Cancer Research, 69*(14), 5776-5783.

Ravi, R., Mookerjee, B., Bhujwalla, Z. M., Sutter, C. H., Artemov, D., Zeng, Q., … Bedi, A. (2000). Regulation of tumor angiogenesis by p53-induced degradation of hypoxia-inducible factor 1alpha. *Genes & Development, 14*(1), 34-44.

Redova, M., Poprach, A., Nekvindova, J., Iliev, R., Radova, L., Lakomy, R., … Slaby, O. (2012). Circulating miR-378 and miR-451 in serum are potential biomarkers for renal cell carcinoma. *Journal of Translational Medicine, 10*, 55.

Reid, G., Williams, M., Kirschner, M. B., Mugridge, N., Weiss, J., Brahmbhatt, H., … van Zandwijk, N. (2015). Targeted delivery of a synthetic microRNA-based mimic as an approach to cancer therapy. *Cancer Research, 75*(15 Suppl), 3976.

Reinhold, H. S., & van den Berg-Blok, A. (1984). Factors influencing the neovascularization of experimental tumours. *Biorheology, 21*(4), 493-501.

Reissmann, P. T., Koga, H., Figlin, R. A., Holmes, E. C., Slamon, D. J., & The Lung Cancer Study Group (1999). Amplification and overexpression of the cyclin D1 and epidermal growth factor receptor genes in non-small-cell-lung cancer. *Journal of Cancer Research and Clinical Oncology, 125*(2), 61-70.

Rekhtman, N., Ang, D. C., Sima, C. S., Travis, W. D., & Moreira, A. L. (2011). Immunohistochemical algorithm for differentiation of lung adenocarcinoma and squamous cell carcinoma based on large series of whole-tissue sections with validation in small specimens. *Modern Pathology, 24*, 1348-1359.

Ren, X., Kiosses, W. B., Sieg, D. J., Otey, C. A., Schlaepfer, D. D., & Schwartz, M. A. (2000). Focal adhesion kinase suppresses Rho activity to promote focal adhesion turnover. *Journal of Cell Science, 113*(Pt 20), 3673-3678.

Ridley, A., & Hall, A. (1992). The small GTP-binding protein Rho regulates the assembly of focal adhesions and actin stress fibers in response to growth factors. *Cell, 70*(3), 389-399.

Ridley, A. J. (2011). Life at the leading edge. *Cell, 145*(7), 1012-1022.

Ridley, A. J., Schwartz, M. A., Burridge, K., Firtel, R. A., Ginsberg, M. H., Borisy, G., … Horwitz, A. R. (2003). Cell migration: Integrating signals from front to back. *Science, 302*(5651), 1704-1709.

Riely, G. J., Marks, J., & Pao, W. (2009). *KRAS* mutations in non-small cell lung cancer. *Proceedings of the American Thoracic Society, 6*(2), 201-205.

Rigoutsos, I. (2009). New tricks for animal microRNAs: Targeting of amino acid coding regions at conserved and nonconserved sites. *Cancer Research, 69*(8), 3245-3248.

Rodriguez, A., Griffiths-Jones, S., Ashurst, J. L., & Bradley, A. (2004). Identification of mammalian microRNA host genes and transcription units. *Genome Research, 14*(10), 1902-1910.

Rosenbluh, J., Nijhawan, D., Cox, A. G., Li, X., Neal, J. T., Schafer, E. J., … Hahn, W. C. (2012). β-catenin-driven cancers require a YAP1 transcriptional complex for survival and tumorigenesis. *Cell, 151*(7), 1457-1473.

Roth, C., Kasimir-Bauer, S., Pantel, K., & Schwarzenbach, H. (2011). Screening for circulating nucleic acids and caspase activity in the peripheral blood as potential diagnostic tools in lung cancer. *Molecular Oncology, 5*(3), 281-291.

Roybal, J. D., Zang, Y., Ahn, Y. H., Yang, Y., Gibbons, D. L., Baird, B. N., … Kurie, J. M. (2011). MiR-200 inhibits lung adenocarcinoma cell invasion and metastasis by targeting *Flt1*/*VEGFR1*. *Molecular Cancer Research, 9*(1), 25-35.

Rubinstein, A. L. (2003). Zebrafish: From disease modeling to drug discovery. *Current Opinion in Drug Discovery & Development, 6*(2), 218-223.

Ruppender, N. S., Merkel, A. R., Martin, T. J., Mundy, G. R., Sterling, J. A., & Guelcher, S. A. (2010). Matrix rigidity induces osteolytic gene expression of metastatic breast cancer cells. *PLoS One, 5*(11), e15451.

Sachdeva, M., & Mo, Y. Y. (2010). MicroRNA-145 suppresses cell invasion and metastasis by directly targeting *mucin1*. *Cancer Research, 70*(1), 378-387.

Safran, M., & Kaelin, W. G. J. (2003). HIF hydroxylation and the mammalian oxygen-sensing pathway. *The Journal of Clinical Investigation, 111*(6), 779-783.

Sand, M., Skrygan, M., Georgas, D., Sand, D., Hahn, S. A., Gambichler, T., … Bechara, F. G. (2012a). Microarray analysis of microRNA expression in cutaneous squamous cell carcinoma. *Journal of Dermatological Science, 68*(3), 119-126.

Sand, M., Skrygan, M., Sand, D., Georgas, D., Hahn, S. A., Gambichler, T., … Bechara, F. G. (2012b). Expression of microRNAs in basal cell carcinoma. *The British Journal of Dermatology, 167*(4), 847-855.

Sandler, A., Gray, R., Perry, M. C., Brahmer, J., Schiller, J. H., Dowlati, A., … Johnson, D. H. (2006). Paclitaxel-carboplatin alone or with bevacizumab for non-small-cell lung cancer. *The New England Journal of Medicine, 355*(24), 2542-2550.

Sayed, D., & Abdellatif, M. (2011). MicroRNAs in development and disease. *Physiological Reviews, 91*(3), 827-887.

Scagliotti, G., Hanna, N., Fossella, F., Sugarman, K., Blatter, J., Peterson, P., … Shepherd, F. A. (2009). The differential efficacy of pemetrexed according to NSCLC histology: A review of two phase III studies. *The Oncologist, 14*(3), 253-263.

Scapoli, L., Palmieri, A., Lo Muzio, L., Pezzetti, F., Rubini, C., Girardi, A., … Carinci, F. (2010). MicroRNA expression profiling of oral carcinoma identifies new markers of tumor progression. *International Journal of Immunopathology and Pharmacology, 23*(4), 1229-1234.

Schindelin, J., Arganda-Carreras, I., Frise, E., Kaynig, V., Longair, M., Pietzsch, T., … Cardona, A. (2012). Fiji: An open sourse platform for biological-image analysis. *Nature Methods, 9*(7), 676-682.

Schlessinger, K., Hall, A., & Tolwinski, N. (2009). Wnt signaling pathways meet Rho GTPases. *Genes & Development, 23*(3), 265-277.

Schreiber, G., & McCrory, D. C. (2003). Performance characteristics of different modalities for diagnosis of suspected lung cancer: Summary of published evidence. *Chest, 123*(1 Suppl), 115S-128S.

Schwarz, D. S., Hutvagner, G., Du, T., Xu, Z., Aronin, N., & Zamore, P. D. (2003). Asymmetry in the assembly of the RNAi enzyme complex. *Cell, 115*(2), 199-208.

Seftor, E. A., Seftor, R. E., & Hendrix, M. J. (1990). Selection of invasive and metastatic subpopulations from a heterogeneous human melanoma cell line. *Biotechniques, 9*(3), 324-331.

Seike, M., Goto, A., Okano, T., Bowman, E. D., Schetter, A. J., Horikawa, I., … Harris, C. C. (2009). MiR-21 is an EGFR-regulated anti-apoptotic factor in lung cancer in never-smokers. *Proceedings of the National Academy of Sciences of the United States of America, 106*(29), 12085-12090.

Selbach, M., Schwanhausser, B., Thierfelder, N., Fang, Z., Khanin, R., & Rajewsky, N. (2008). Widespread changes in protein synthesis induced by microRNAs. *Nature, 455*(7209), 58-63.

Semenza, G. L. (2001). HIF-1 and mechanisms of hypoxia sensing. *Current Opinion in Cell Biology, 13*(2), 167-171.

Semenza, G. L. (2002). Involvement of hypoxia-inducible factor 1 in human cancer. *Internal Medicine, 41*(2), 79-83.

Sengupta, S., Nie, J., Wagner, R. J., Yang, C., Stewart, R., & Thomson, J. A. (2009). MicroRNA 92b controls the G1/S checkpoint gene *p57* in human embryonic stem cells. *Stem Cells, 27*(7), 1524-1528.

Shen, S., Yue, H., Li, Y., Qin, J., Li, K., Liu, Y., & Wang, J. (2014). Upregulation of miR-136 in human non-small cell lung cancer cells promotes Erk1/ 2 activation by targeting *PPP2R2A*. *Tumour Biology, 35*(1), 631-640.

Shepherd, F. A., Rodrigues, P. J., Ciuleanu, T., Tan, E. H., Hirsh, V., Thongprasert, S., … National Cancer Institute of Canada Clinical Trials Group (2005). Erlotinib in previously treated non-small-cell lung cancer. *The New England Journal of Medicine, 353*(2), 123-132.

Shigematsu, H., & Gazdar, A. F. (2006). Somatic mutations of epidermal growth factor receptor signaling pathway in lung cancers. *International Journal of Cancer, 118*(2), 257-262.

Shimanuki, Y., Takahashi, K., Cui, R., Hori, S., Takahashi, F., Miyamoto, H., & Fukurchi, Y. (2005). Role of serum vascular endothelial growth factor in the prediction of angiogenesis and prognosis for non-small cell lung cancer. *Lung, 183*(1), 29-42.

Shin, S., Cha, H. J., Lee, E. M., Lee, S. J., Seo, S. K., Jin, H. O., … An, S. (2009). Alteration of miRNA profiles by ionizing radiation in A549 human non-small cell lung cancer cells. *International Journal of Oncology, 35*(1), 81-86.

Shiraishi, M., Noguchi, M., Shimosato, Y., & Sekiya, T. (1989). Amplification of protooncogenes in surgial specimens of human lung carcinomas. *Cancer Research, 49*(23), 6474-6479.

Shubik, P. (1982). Vascularization of tumors: A review. *Journal of Cancer Research and Clinical Oncology, 103*(3), 211-226.

Sikora, J., Slodkowska, J., Radomyski, A., Giedronowicz, D., Kobos, J., Kupis, W., & Rudzinski, P. (1997). Immunohistochemical evaluation of tumour angiogenesis in adenocarcinoma and squamous cell carcinoma of the lung. *Roczniki Akademii Medycznej w Bialymstoku, 42*(Suppl 1), 271-279.

Skrzypek, K., Tertil, M., Golda, S., Ciesla, M., Weglarczyk, K., Collet, G., … Dulak, J. (2013). Interplay between heme oxygenase-1 and miR-378 affects non-small cell lung carcinoma growth, vascularization, and metastasis. *Antioxidants & Redox Signaling, 19*(7), 644-660.

Sotillo, E., & Thomas-Tikhonenko, A. (2011). Shielding the messenger (RNA): MicroRNA-based anticancer therapies. *Pharmacology & Therapeutics, 131*(1), 18-32.

Spiering, D., & Hodgson, L. (2011). Dynamics of the Rho-family small GTPases in actin regulation and motility. *Cell Adhesion & Migration, 5*(2), 170-180.

Spira, A., Beane, J., Shah, V., Liu, G., Schembri, F., Yang, X., … Brody, J. S. (2004). Effects of cigarette smoke on the human airway epithelial cell transcriptome. *Proceedings of the National Academy of Sciences of the United States of America, 101*(27), 10143-10148.

Sriram, G., & Birge, R. B. (2011). Emerging roles for *Crk* in human cancer. *Genes & Cancer, 1*(11), 1132-1139.

Stark, A., Lin, M. F., Kheradpour, P., Pedersen, J. S., Parts, L., Carlson, J. W., … Kellis, M. (2007). Discovery of functional elements in 12 *Drosophila* genomes using evolutionary signatures. *Nature, 450*(7167), 219-232.

Steeg, P. S. (2006). Tumor metastasis: Mechanistic insights and clinical challenges. *Nature Medicine, 12*(8), 895-904.

Stefanou, D., Batistatou, A., Arkoumani, E., Ntzani, E., & Agnantis, N. J. (2004). Expression of vascular endothelial growth factor (VEGF) and association with microvessel density in small-cell and non-small-cell lung carcinomas. *Histology and Histopathology, 19*(1), 37-42.

Stein, C., Bardet, A. F., Roma, G., Bergling, S., Clay, I., Ruchti, A., … Bauer, A. (2015). YAP1 exerts its transcriptional control via TEAD-mediated activation of enhancers. *PLoS Genetics, 11*(8), e1005465.

Stenbygaard, L. E., Sorensen, J. B., & Olsen, J. E. (1997). Metastatic pattern at autopsy in non-resectable adenocarcinoma of the lung- A study from a cohort of 259 consecutive patients treated with chemotherapy. *Acta Oncologica, 36*(3), 301-306.

Stiehl, D. P., Jelkmann, W., Wenger, R. H., & Hellwig-Burgel, T. (2002). Normoxic induction of the hypoxia-inducible factor 1alpha by insulin and interleukin-1beta involves the phosphatidylinositol 3-kinase pathway. *FEBS Letters, 512*(1-3), 157-162.

Stoletov, K., & Klemke, R. (2008). Catch of the day: Zebrafish as a human cancer model. *Oncogene, 27*(33), 4509-4520.

Stott, S. L., Lee, R. J., Nagrath, S., Yu, M., Miyamoto, D. T., Ulkus, L., … Maheswaran, S. (2010). Isolation and characterization of circulating tumor cells from patients with localized and metastatic prostate cancer. *Science Translational Medicine, 2*(25), 25ra23.

Strutt, D. (2003). Frizzled signalling and cell polarisation in *Drosophila* and vertebrates. *Development, 130*(19), 4501-4513.

Sullivan, R., & Graham, C. H. (2007). Hypoxia-driven selection of the metastatic phenotype. *Cancer Metastasis Reviews, 26*(2), 319-331.

Sun, M., Hong, S., Li, W., Wang, P., You, J., Zhang, X., … Zhang, C. (2016). MiR-99a regulates ROS-mediated invasion and migration of lung adenocarcinoma cells by targeting *NOX4*. *Oncology Reports, 35*(5), 2755-2766.

Sun, Y., Tan, M., Duan, H., & Swaroop, M. (2001). SAG/ROC/Rbx/Hrt, a zinc RING finger gene family: Molecular cloning, biochemical properties, and biological functions. *Antioxidants & Redox Signaling, 3*(4), 635-650.

Takamizawa, J., Konishi, H., Yanagisawa, K., Tomida, S., Osada, H., Endoh, H., … Takahashi, T. (2004). Reduced expression of the let-7 microRNAs in human lung cancers in association with shortened postoperative survival. *Cancer Research, 64*(11), 3753-3756.

Takanami, I., Tanaka, F., Hashizume, T., & Kodaira, S. (1997). Pulmonary adenocarcinoma angiogenesis. *International Journal of Oncology, 10*(1), 101-106.

Takeda, A., Stoeltzing, O., Ahmad, S. A., Reinmuth, N., Liu, W., Parikh, A., … Ellis, L. M. (2002). Role of angiogenesis in the development and growth of liver metastasis. *Annals of Surgical Oncology, 9*(7), 610-616.

Takeshita, F., Patrawala, L., Osaki, M., Takahashi, R. U., Yamamoto, Y., Kosaka, N., … Ochiya, T. (2010). Systemic delivery of synthetic microRNA-16 inhibits the growth of metastatic prostate tumors via downregulation of multiple cell-cycle genes. *Molecular Therapy, 18*(1), 181-187.

Takigawa, N., Segawa, Y., Fujimoto, N., Hotta, K., & Eguchi, K. (1998). Elevated vascular endothelial growth factor levels in sera of patients with lung cancer. *Anticancer Research, 18*(2B), 1251-1254.

Tamura, M., Ohta, Y., Kajita, T., Kimura, K., Go, T., Oda, M., … Watanabe, G. (2001). Plasms VEGF concentration can predict the tumor angiogenic capacity in non-small cell lung cancer. *Oncology Reports, 8*(5), 1097-1102.

Tan, M., Davis, S. W., Saunders, T. L., Zhu, Y., & Sun, Y. (2009). *RBX1/ROC1* disruption results in early embryonic lethality due to proliferation failure, partially rescued by simultaneous loss of *p27*. *Proceedings of the National Academy of Sciences of the United States of America, 106*(15), 6203-6208.

Tanaka, F., Ishikawa, S., Yanagihara, K., Miyahara, R., Kawano, Y., Li, M., … Wada, H. (2002). Expression of angiopoietins and its clinical significance in non-small cell lung cancer. *Cancer Research, 62*(23), 7124-7129.

Tanaka, F., Otake, Y., Yanagihara, K., Kawano, Y., Miyahara, R., Li, M., … Wada, H. (2001). Evaluation of angiogenesis in non-small cell lung cancer: Comparison between anti-CD34 antibody and anti-CD105 antibody. *Clinical Cancer Research, 7*(11), 3410-3415.

Tanaka, M., Oikawa, K., Takanashi, M., Kudo, M., Ohyashiki, J., Ohyashiki, K., & Kuroda, M. (2009). Down-regulation of miR-92 in human plasma is a novel marker for acute leukemia patients. *PLoS One, 4*(5), e5532.

Tao, W. T., Wu, J. F., Yu, G. Y., Wang, R., Wang, K., Li, L. H., … Jia, L. J. (2014). Suppression of tumor angiogenesis by targeting the protein neddylation pathway. *Cell Death & Disease, 5*, e1059.

ten Hoeve, J., Morris, C., Heisterkamp, N., & Groffen, J. (1993). Isolation and chromosomal localization of *CRKL*, a human *crk*-like gene. *Oncogene, 8*(9), 2469-2474.

Teng, Y., Xie, X., Walker, S., White, D. T., Mumm, J. S., & Cowell, J. K. (2013). Evaluating human cancer cell metastasis in zebrafish. *BMC Cancer, 13*, 453.

Tetsu, O., & McCormick, F. (1999). Beta-catenin regulates expression of cyclin D1 in colon carcinoma cells. *Nature, 398*(6726), 422-426.

Thiery, J. P., Acloque, H., Huang, R. Y. J., & Nieto, M. A. (2009). Epithelial-mesenchymal transitions in development and disease. *Cell, 139*(5), 871-890.

Thiery, J. P., & Sleeman, J. P. (2006). Complex networks orchestrate epithelial-mesenchymal transitions. *Nature Reviews Molecular Cell Biology, 7*, 131-142.

Thomas, S. M., & Brugge, J. S. (1997). Cellular functions regulated by Src family kinases. *Annual Review of Cell and Developmental Biology, 13*, 513-609.

Topczewska, J. M., Postovit, L. M., Margaryan, N. V., Sam, A., Hess, A. R., Wheaton, W. W., … Hendrix, M. J. (2006). Embryonic and tumorigenic pathways converge via nodal signaling: Role in melanoma aggressiveness. *Nature Medicine, 12*(8), 925-932.

Trang, P., Medina, P. P., Wiggins, J. F., Ruffino, L., Kelnar, K., Omotola, M., … Slack, F. J. (2010). Regression of murine lung tumors by the let-7 microRNA. *Oncogene, 29*(11), 1580-1587.

Trang, P., Wiggins, J. F., Daige, C. L., Cho, C., Omotola, M., Brown, D., … Slack, F. J. (2011). Systemic delivery of tumor suppressor microRNA mimics using a neutral lipid emulsion inhibits lung tumors in mice. *Molecular Therapy, 19*(6), 1116-1122.

Travis, W. D., Brambilla, E., Muller-Hermelink, H. K., & Harris, C. C. (2004). World Health Organization classification of tumours. Pathology and genetics of tumours of the lung, pleura, thymus and heart [Internet]. *Lyon, France: International Agency for Research on Cancer Press*. Retrieved September 9, 2016, from www.iarc.fr/who-bluebooks

Travis, W. D., Brambilla, E., Noguchi, M., Nicholson, A. G., Geisinger, K. R., Yatabe, Y., … Yankelewitz, D. (2011). International association for the study of lung cancer/american thoracic society/european respiratory society international multidisciplinary classification of lung adenocarcinoma. *Journal of Thoracic Oncology, 6*(2), 244-285.

Travis, W. D., Travis, L. B., & Devesa, S. S. (1995). Lung cancer. *Cancer, 75*(1 Suppl), 191-202.

Tsuchida, A., Ohno, S., Wu, W., Borjigin, N., Fujita, K., Aoki, T., … Kuroda, M. (2011). MiR-92 is a key oncogenic component of the miR-17-92 cluster in colon cancer. *Cancer Science, 102*(12), 2264-2271.

Turner, B. M., Cagle, P. T., Sainz, I. M., Fukuoka, J., Shen, S. S., & Jagirdar, J. (2012). Napsin A, a new marker for lung adenocarcinoma, is complementary and more sensitive and specific than thyroid transcription factor 1 in the differential diagnosis of primary pulmonary carcinoma: Evaluation of 1674 cases by tissue microarray. *Archives of Pathology & Laboratory Medicine, 136*(2), 163-171.

Uematsu, K., He, B., You, L., Xu, Z., McCormick, F., & Jablons, D. M. (2003). Activation of the Wnt pathway in non small cell lung cancer: Evidence of dishevelled overexpression. *Oncogene, 22*(46), 7218-7221.

Uramoto, H., Yamaada, S., & Tanaka, F. (2013). Angiogenesis of lung cancer utilizes existing blood vessels rather than developing new vessels using signals from carcinogenesis. *Anticancer Research, 33*(5), 1913-1916.

Utoguchi, N., Mizuguchi, H., Saeki, K., Ikeda, K., Tsutsumi, Y., Nakagawa, S., & Mayumi, T. (1995). Tumor-conditioned medium increases macromolecular permeability of endothelial cell monolayer. *Cancer Letters, 89*(1), 7-14.

Valastyan, S., & Weinberg, R. A. (2011). Tumor metastasis: Molecular insights and evolving paradigms. *Cell, 147*(2), 275-292.

Valcourt, U., Kowanetz, M., Niimi, H., Heldin, C. H., & Moustakas, A. (2005). TGF-beta and the Smad signaling pathway support transcriptomic reprogramming during epithelial-mesenchymal transition. *Molecular Biology of the Cell, 16*(4), 1987-2002.

van der Ent, W., Burrello, C., de Lange, M. J., van der Velden, P. A., Jochemsen, A. G., Jager, M. J., & Snaar-Jagalska, B. E. (2015). Embryonic zebrafish: Different phenotypes after injection of human uveal melanoma cells. *Ocular Oncology and Pathology, 1*(3), 170-181.

van der Veldt, A. A. M., Lubberink, M., Bahce, I., *et al.* (2012). Rapid decrease in delivery of chemotherapy to tumors after anti-VEGF therapy: Implications for scheduling of anti-angiogenic drugs. *Cancer Cell, 21*(1), 82-91.

Varelas, X., Samavarchi-Tehrani, P., Narimatsu, M., Weiss, A., Cockburn, K., Larsen, B. G., … Wrana, J. L. (2010). The Crumbs complex couples cell density sensing to Hippo-dependent control of the TGF-β-SMAD pathway. *Developmental Cell, 19*(6), 831-844.

Viella, A. J., Severin, J., Ureta-Vidal, A., Heng, L., Durbin, R., & Birney, E. (2009). EnsemblCompara Gene Trees: Complete, duplication-aware phylogenetic trees in vertebrates. *Genome Research, 19*(2), 327-335.

Voortman, J., Goto, A., Mendibourne, J., Sohn, J. J., Schetter, A. J., Saito, M., … Giaccone, G. (2010). MicroRNA expression and clinical outcomes in patients treated with adjuvant chemotherapy after complete resection of non-small cell lung carcinoma. *Cancer Research, 70*(21), 8288-8298.

Vosa, U., Vooder, T., Kolde, R., Fischer, K., Valk, K., Tonisson, N., … Annilo, T. (2011). Identification of miR-374a as a prognostic marker for survival in patients with early-stage nonsmall cell lung cancer. *Genes, Chromosomes & Cancer, 50*(10), 812-822.

Waerner, T., Alacakaptan, M., Tamir, I., Oberauer, R., Gal, A., Brabletz, T., … Beug, H. (2006). ILEI: A cytokine essential for EMT, tumor formation, and late events in metastasis in epithelial cells. *Cancer Cell, 10*(3), 227-239.

Wang, C., Wang, X., Liang, H., Wang, T., Yan, X., Cao, M., … Chen, X. (2013a). MiR-203 inhibits cell proliferation and migration of lung cancer cells by targeting *PKCα*. *PLoS One, 8*(9), e73985.

Wang, G., Wang, Y., Teng, M., Zhang, D., Li, L., & Liu, Y. (2010a). Signal transducers and activators of transcription-1 (STAT1) regulates microRNA transcription in interferon gamma-stimulated HeLa cells. *PLoS One, 5*(7), e11794.

Wang, H., Guan, X., Tu, Y., Zheng, S., Long, J., Li, S., … Zhang, Y. (2015a). MicroRNA-29b attenuates non-small cell lung cancer metastasis by targeting matrix metalloproteinase 2 and *PTEN*. *Journal of Experimental & Clinical Cancer Research, 34*, 59.

Wang, H., Zhu, Y., Zhao, M., Wu, C., Zhang, P., Tang, L., … Liu, G. (2013b). MiRNA-29c suppresses lung cancer cell adhesion to extracellular matrix and metastasis by targeting integrin β1 and matrix metalloproteinase2 (*MMP2*). *PLoS One, 8*(8), e70192.

Wang, K., Wang, X., Zou, J., Zhang, A., Wan, Y., Pu, P., … Wang, Y. (2013c). MiR-92b controls glioma proliferation and invasion through regulating Wnt/beta-catenin signaling via Nemo-like kinase. *Neuro-Oncology, 15*(5), 578-588.

Wang, K., Zhang, S., Marzolf, B., Troisch, P., Brightman, A., Hu, Z., … Galas, D. J. (2009a). Circulating microRNAs, potential biomarkers for drug-induced liver injury. *Proceedings of the National Academy of Sciences of the United States of America, 106*(11), 4402-4407.

Wang, L., & Wang, J. (2012). MicroRNA-mediated breast cancer metastasis: From primary site to distant organs. *Oncogene, 31*(20), 2499-2511.

Wang, L. G., Ni, Y., Su, B. H., Mu, X. R., Shen, H. C., & Du, J. J. (2013d). MicroRNA-34b functions as a tumor suppressor and acts as a nodal point in the feedback loop with *Met*. *International Journal of Oncology, 42*(3), 957-962.

Wang, M., Wang, J., Deng, J., Li, X., Long, W., & Chang, Y. (2015b). MiR-145 acts as a metastasis suppressor by targeting metadherin in lung cancer. *Medical Oncology, 32*(1), 344.

Wang, Q., Symes, A. J., Kane, C. A., Freeman, A., Nariculam, J., Munson, P., … Ahmed, A. (2010b). A novel role for Wnt/Ca2+ signaling in actin cytoskeleton remodeling and cell motility in prostate cancer. *PLoS One, 5*(5), e10456.

Wang, R., Wang, Z. X., Yang, J. S., Pan, X., De, W., & Chen, L. B. (2011a). MicroRNA-451 functions as a tumor suppressor in human non-small cell lung cancer by targeting ras-related protein 14 (*RAB14*). *Oncogene, 30*(23), 2644-2658.

Wang, S., & Olson, E. N. (2009b). AngiomiRs- Key regulators of angiogenesis. *Current Opinion in Genetics & Development, 19*(3), 205-211.

Wang, W., Chen, H., Liu, Z., Qu, P., Lan, J., Chen, H., … Qiu, J. (2016a). Regulator of cullins-1 expression knockdown suppresses the malignant progression of muscle-invasive transitional cell carcinoma by regulating mTOR/DEPTOR pathway. *British Journal of Cancer, 114*(3), 305-313.

Wang, X., Ling, C., Bai, Y., & Zhao, J. (2011b). MicroRNA-206 is associated with invasion and metastasis of lung cancer. *The Anatomical Record, 294*(1), 88-92.

Wang, X., Liu, Y., Liu, X., Yang, J., Teng, G., Zhang, L., & Zhou, C. (2016b). MiR-124 inhibits cell proliferation, migration and invasion by directly targeting *SOX9* in lung adenocarcinoma. *Oncology Reports, 35*(5), 3115-3121.

Wang, X., Zhang, Y., Fu, Y., Zhang, J., Yin, L., Pu, Y., & Liang, G. (2014). MicroRNA-125b may function as an oncogene in lung cancer cells. *Molecular Medicine Reports, 11*(5), 3880-3887.

Wang, Y., Yang, H., Liu, H., Huang, J., & Song, X. (2009c). Effect of staurosporine on the mobility and invasiveness of lung adenocarcinoma A549 cells: An *in vitro* study. *BMC Cancer, 9*, 174.

Wang, Y. X., Zhang, X. Y., Zhang, B. F., Yang, C. Q., Chen, X. M., & Gao, H. J. (2010c). Initial study of microRNA expression profiles of colonic cancer without lymph node metastasis. *Journal of Digestive Diseases, 11*(1), 50-54.

Wang, Y. Y., Ren, T., Cai, Y. Y., & He, X. Y. (2013e). MicroRNA let-7a inhibits the proliferation and invasion of nonsmall cell lung cancer cell line 95D by regulating *K-Ras* and *HMGA2* gene expression. *Cancer Biotherapy & Radiopharmaceuticals, 28*(2), 131-137.

Wang, Z., Chen, Z., Gao, Y., Li, N., Li, B., Tan, F., … He, J. (2011c). DNA hypermethylation of microRNA-34b/c has prognostic value for stage I non-small cell lung cancer. *Cancer Biology & Therapy, 11*(5), 490-496.

Wang, Z., Li, Y., Ahmad, A., Azmi, A. S., Kong, D., Banerjee, S., & Sarkar, F. H. (2010d). Targeting miRNAs involved in cancer stem cell and EMT regulation: An emerging concept in overcoming drug resistance. *Drug Resistance Updates, 13*(4-5), 109-118.

Webb, D. J., Donais, K., Whitmore, L. A., Thomas, S. M., Turner, C. E., Parsons, J. T., & Horwitz, A. F. (2004). FAK-Src signalling through paxillin, ERK and MLCK regulates adhesion disassembly. *Nature Cell Biology, 6*(2), 154-161.

Webster, R. J., Giles, K. M., Price, K. J., Zhang, P. M., Mattick, J. S., & Leedman, P. J. (2009). Regulation of epidermal growth factor receptor signaling in human cancer cells by microRNA-7. *The Journal of Biological Chemistry, 284*(9), 5731-5741.

Weeraratna, A. T., Jiang, Y., Hostetter, G., Rosenblatt, K., Duray, P., Bittner, M., & Trent, J. M. (2002). Wnt5a signaling directly affects cell motility and invasion of metastatic melanoma. *Cancer Cell, 1*(3), 279-288.

Weidemann, A., & Johnson, R. S. (2008). Biology of HIF-1alpha. *Cell Death and Differentiation, 15*(4), 621-627.

Weinberg, R. A. (2007). Moving out: Invasion and metastasis. In E. Jeffcock, E. Zayatz & R. K. Mickey (Eds.), *The Biology of Cancer* (Vol. 1, pp. 587-654). New York, NY: Garland Science.

Weinstein, B. (2002). Vascular cell biology *in vivo*: A new piscine paradigm? *Trends in Cell Biology, 12*(9), 439-445.

Weiss, L. (1990). Metastatic inefficiency. *Advances in Cancer Research, 54*, 159-211.

Weiss, L. (1992a). Biomechanical interactions of cancer cells with the microvasculature during hematogenous metastasis. *Cancer Metastasis Reviews, 11*(3-4), 227-235.

Weiss, L., Harlos, J. P., & Elkin, G. (1989). Mechanism of mechanical trauma to Ehrlich ascites tumor cells *in vitro* and its relationship to rapid intravascular death during metastasis. *International Journal of Cancer, 44*(1), 143-148.

Weiss, L., Nannmark, U., Johansson, B. R., & Bagge, U. (1992b). Lethal deformation of cancer cells in the microcirculation: A potential rate regulator of hematogenous metastasis. *International Journal of Cancer, 50*(1), 103-107.

Weiss, L., Orr, F. W., & Honn, K. W. (1988). Interactions of cancer cells with the microvasculature during metastasis. *FASEB Journal, 2*(1), 12-21.

Wesley, U. V., Tiwari, S., & Houghton, A. N. (2004). Role for dipeptidyl peptidase IV in tumor suppression of human non small cell lung carcinoma cells. *International Journal of Cancer, 109*(6), 855-866.

Wheatley-Price, P., & Shepherd, F. A. (2008). Targeting angiogenesis in the treatment of lung cancer. *Journal of Thoracic Oncology, 3*(10), 1173-1184.

Wheelock, M. J., Knudsen, K. A., & Johnson, K. R. (1996). Membrane-cytoskeleton interactions with cadherin cell adhesion proteins: Roles of catenins as linker proteins. In W. J. Nelson (Ed.), *Current Topics in Membranes* (Vol. 43, pp. 169-185). Massachusetts, MA: Academic Press.

Wheelock, M. J., Shintani, Y., Maeda, M., Fukumoto, Y., & Johnson, K. R. (2008). Cadherin switching. *Journal of Cell Science, 121*(Pt 6), 727-736.

Wiggins, J. F., Ruffino, L., Kelnar, K., Omotola, M., Patrawala, L., Brown, D., & Bader, A. G. (2010). Development of a lung cancer therapeutic based on the tumor suppressor microRNA-34. *Cancer Research, 70*(14), 5923-5930.

Williams, R., Kline, M., & Smith, R. (1996). BSA and restriction enzyme digestions. *Promega Notes*, *59*, 46.

Winter, J., Jung, S., Keller, S., Gregory, R. I., & Diederichs, S. (2009). Many roads to maturity: MicroRNA biogenesis pathways and their regulation. *Nature Cell Biology, 11*(3), 228-234.

Wolf, K., Mazo, I., Leung, H., Engelke, K., von Andrian, U. H., Deryugina, E. I., … Friedl, P. (2003). Compensation mechanism in tumor cell migration: Mesenchymal-amoeboid transition after blocking of pericellular proteolysis. *The Journal of Cell Biology, 160*(2), 267-277.

Wong, C. C., Gilkes, D. M., Zhang, H., Chen, J., Wei, H., Chaturvedi, P., … Semenza, G. L. (2011). Hypoxia-inducible factor 1 is a master regulator of breast cancer metastatic niche formation. *Proceedings of the National Academy of Sciences of the United States of America, 108*(39), 16369-16374.

Wong, C. W., Lee, A., Shientag, L., Yu, J., Dong, Y., Kao, G., … Muschel, R. J. (2001). Apoptosis: An early event in metastatic inefficiency. *Cancer Research, 61*(1), 333-338.

Wood, S. L., Pernemalm, M., Crosbie, P. A., & Whetton, A. D. (2014). The role of the tumor-microenvironment in lung cancer- Metastasis and its relationship to potential therapeutic targets. *Cancer Treatment Reviews*, *40*(4), 558-566.

Wu, H., Liu, Y., Shu, X. O., & Cai, Q. (2016). MiR-374a suppresses lung adenocarcinoma cell proliferation and invasion by targeting *TGFA* gene expression. *Carcinogenesis*, *37*(6), 567-575.

Wu, L., & Belasco, J. G. (2005). Micro-RNA regulation of the mammalian *lin-28* gene during neuronal differentiation of embryonal carcinoma cells. *Molecular and Cellular Biology, 25*(21), 9198-9208.

Wu, M. Z., Tsai, Y. P., Yang, M. H., Huang, C. H., Chang, S. Y., Chang, C. C., … Wu, K. J. (2011a). Interplay between HDAC3 and WDR5 is esential for hypoxia-induced epithelial-mesenchymal transition. *Molecular Cell, 43*(5), 811-822.

Wu, S., Huang, S., Ding, J., Zhao, Y., Liang, L., Liu, T., … He, X. (2010). Multiple microRNAs modulate *p21Cip1/Waf1* expression by directly targeting its 3' untranslated region. *Oncogene, 29*(15), 2302-2308.

Wu, X., Liu, T., Fang, O., Leach, L. J., Hu, X., & Luo, Z. (2013a). MiR-194 suppresses metastasis of non-small cell lung cancer through regulating expression of *BMP1* and *p27(kip1)*. *Oncogene*, *33*(12), 1506-1514.

Wu, Y., Crawford, M., Mao, Y., Lee, R. J., Davis, I. C., Elton, T. S., … Nana-Sinkam, S. P. (2013b). Therapeutic delivery of microRNA-29b by cationic lipoplexes for lung cancer. *Molecular Therapy. Nucleic Acids, 2*, e84.

Wu, Y., Crawford, M., Yu, B., Mao, Y., Nana-Sinkam, S. P., & Lee, L. J. (2011b). MicroRNA delivery by cationic lipoplexes for lung cancer therapy. *Molecular Pharmaceutics, 8*(4), 1381-1389.

Wu, Z. B., Cai, L., Lin, S. J., Lu, J. L., Yao, Y., & Zhou, L. F. (2013c). The miR-92b functions as a potential oncogene by targeting on *Smad3* in glioblastomas. *Brain Research, 1529*, 16-25.

Xing, R., Chen, K-B., Xuan, Y., Feng, C., Xue, M., & Zeng, Y-C. (2016). RBX1 expression is an unfavorable prognostic factor in patients with non-small cell lung cancer. *Surgical Oncology, 25*(3), 147-151.

Xiong, F., Wu, C., Chang, J., Yu, D., Xu, B., Yuan, P., … Lin, D. (2011a). Genetic variation in an miRNA-1827 binding site in *MYCL1* alters susceptibility to small-cell lung cancer. *Cancer Research, 71*(15), 5175-5181.

Xiong, S., Zheng, Y., Jiang, P., Liu, R., Liu, X., & Chu, Y. (2011b). MicroRNA-7 inhibits the growth of human non-small cell lung cancer A549 cells through targeting *BCL-2*. *International Journal of Biological Sciences, 7*(6), 805-814.

Xu, L., Wen, Z., Zhou, Y., Liu, Z., Li, Q., Fei, G., … Ren, T. (2013a). MicroRNA-7-regulated TLR9 signaling-enhanced growth and metastatic potential of human lung cancer cells by altering the phosphoinositide-3-kinase, regulatory subunit 3/Akt pathway. *Molecular Biology of the Cell, 24*(1), 42-55.

Xu, M., & Wang, Y. Z. (2013b). MiR-133a suppresses cell proliferation, migration and invasion in human lung cancer by targeting *MMP-14*. *Oncology Reports, 30*(3), 1398-1404.

Yanaihara, N., Caplen, N., Bowman, E., Seike, M., Kumamoto, K., Yi, M., … Harris, C. C. (2006). Unique microRNA molecular profiles in lung cancer diagnosis and prognosis. *Cancer Cell, 9*(3), 189-198.

Yang, Y., Liu, L., Cai, J., Wu, J., Guan, H., Zhu, X., … Li, M. (2013). Targeting *Smad2* and *Smad3* by miR-136 suppresses metastasis-associated traits of lung adenocarcinoma cells. *Oncology Research, 21*(6), 345-352.

Yao, Y., Suo, A. L., Li, Z. F., Liu, L. Y. Tian, T., Ni, L., … Huang, C. (2009). MicroRNA profiling of human gastric cancer. *Molecular Medicine Reports, 2*(6), 963-970.

Yap, S. H. (2012). *Identification and Characterization of MicroRNAs Involved in the Invasion and Migration Properties of Lung, Prostate and Breast Cancer Cells* (Unpublished Master's thesis). University of Malaya, Kuala Lumpur.

Ye, Z. B., Ma, G., Zhao, Y. H., Xiao, Y., Zhan, Y., Jing, C., … Yu, S. J. (2015). MiR-429 inhibits migration and invasion of breast cancer cells *in vitro*. *International Journal of Oncology, 46*(2), 531-538.

Yilmaz, M., & Christori, G. (2009). EMT, the cytoskeleton, and cancer cell invasion. *Cancer Metastasis Reviews, 28*(1-2), 15-33.

Yilmaz, M., & Christori, G. (2010). Mechanisms of motility in metastasizing cells. *Molecular Cancer Research, 8*(5), 629-642.

Yost, C., Torres, M., Miller, J. R., Huang, E., Kimelman, D., & Moon, R. T. (1996). The axis-inducing activity, stability, and subcellular distribution of beta-catenin is regulated in *Xenopus* embryos by glycogen synthase kinase 3. *Genes & Development, 10*(12), 1443-1454.

You, J., Li, Y., Fang, N., Liu, B., Zu, L., Chang, R., … Zhou, Q. (2014). MiR-132 suppresses the migration and invasion of lung cancer cells via targeting the EMT regulator *ZEB2*. *PLoS One, 9*(3), e91827.

You, L., He, B., Xu, Z., Uematsu, K., Mazieres, J., Mikami, I., … Jablons, D. M. (2004). Inhibition of Wnt-2-mediated signaling induces programmed cell death in non-small-cell lung cancer cells. *Oncogene, 23*(36), 6170-6174.

Yu, B. L., Peng, X. H., Zhao, F. P., Liu, X., Lu, J., Wang, L., … Li, X. P. (2014). MicroRNA-378 functions as an onco-miR in nasopharyngeal carcinoma by

repressing *TOB2* expression. *International Journal of Oncology, 44*(4), 1215-1222.

Yu, C. J., Shih, J. Y., Lee, Y. C., Shun, C. R., Yuan, A., & Yang, P. C. (2005). Sialyl Lewis antigens: Association with MUC5AC protein and correlation with post-operative recurrence of non-small cell lung cancer. *Lung Cancer, 47*(1), 59-67.

Yu, L., Todd, N. W., Xing, L., Xie, Y., Zhang, H., Liu, Z., … Jiang, F. (2010). Early detection of lung adenocarcinoma in sputum by a panel of microRNA markers. *International Journal of Cancer, 127*(12), 2870-2878.

Yu, M., Ting, D. T., Stott, S. L., Wittner, B. S., Ozsolak, F., Paul, S., … Haber, D. A. (2012). RNA sequencing of pancreatic circulating tumour cells implicates WNT signalling in metastasis. *Nature, 487*(7408), 510-513.

Yu, S. L., Chen, H. Y., Chang, G. C., Chen, C. Y., Chen, H. W., Singh, S., … Yang, P. C. (2008). MicroRNA signature predicts survival and relapse in lung cancer. *Cancer Cell, 13*(1), 48-57.

Yuan, A., Yang, P. C., Yu, C. J., Lee, Y. C., Yao, Y. T., Chen, C. L., … Luh, K. T. (1995). Tumour angiogenesis correlates with histological type and metastasis in non-small cell lung cancer. *American Jorunal of Respiratory and Critical Care Medicine, 152*(6 Pt 1), 2157-2162.

Zanconato, F., Forcato, M., Battilana, G., Azzolin, L., Quaranta, E., Bodega, B., … Piccolo, S. (2015). Genome-wide association between YAP/TAZ/TEAD and AP-1 at enhancers drives oncogenic growth. *Nature Cell Biology, 17*(9), 1218-1227.

Zavadil, J., Narasimhan, M., Blumenberg, M., & Schneider, R. J. (2007). Transforming growth factor-beta and microRNA:mRNA regulatory networks in epithelial plasticity. *Cells, Tissues, Organs, 185*(1-3), 157-161.

Zeidman, I. (1961). The fate of circulating tumor cells. I. Passage of cells through capillaries. *Cancer Research, 21*, 38-39.

Zelzer, E., Levy, Y., Kahana, C., Shilo, B. Z., Rubinstein, M., & Cohen, B. (1998). Insulin induces transcription of target genes through the hypoxia-inducible factor HIF-1alpha/ARNT. *The EMBO Journal, 17*(17), 5085-5094.

Zhan, C., Yan, L., Wang, L., Sun, Y., Wang, X., Lin, Z., … Wang, Q. (2015). Identification of immunohistochemical markers for distinguishing lung

adenocarcinoma from squamous cell carcinoma. *Journal of Thoracic Disease*, *7*(8), 1398-1405.

Zhang, C., Liu, J., Tan, C., Yue, X., Zhao, Y., Peng, J., … Feng, Z. (2016). MicroRNA-1827 represses MDM2 to positively regulate tumor suppresor p53 and suppress tumorigenesis. *Oncotarget*, *7*(8), 8783-8796.

Zhang, G. J., Zhou, H., Xiao, H. X., Li, Y., & Zhou, T. (2014). MiR-378 is an independent prognostic factor and inhibits cell growth and invasion in colorectal cancer. *BMC Cancer, 14*, 109.

Zhang, H., Wong, C. C., Wei, H., Gilkes, D. M., Korangath, P., Chaturvedi, P., … Semenza, G. L. (2011). HIF-1-dependent expression of angiopoietin-like 4 and *L1CAM* mediates vascular metastasis of hypoxic breast cancer cells to the lungs. *Oncogene, 31*(14), 1757-1770.

Zhang, H., Zhu, X., Li, N., Li, D., Sha, Z., Zheng, X., & Wang, H. (2015a). MiR-125a-3p targets *MTA1* to suppress NSCLC cell proliferation, migration, and invasion. *Acta Biochimica et Biophysica Sinica, 47*(7), 496-503.

Zhang, J. G., Wang, J. J., Zhao, F., Liu, Q., Jiang, K., & Yang, G. H. (2010). MicroRNA-21 (miR-21) represses tumor suppressor *PTEN* and promotes growth and invasion in non-small cell lung cancer (NSCLC). *Clinica Chimica Acta, 411*(11-12), 846-852.

Zhang, Y. J., Xu, F., Zhang, Y. J., Li, H. B., Han, J. C., & Li, L. (2015b). MiR-206 inhibits non small cell lung cancer cell proliferation and invasion by targeting *SOX9*. *International Journal of Clinical and Experimental Medicine, 8*(6), 9107-9113.

Zhao, B., Wei, X., Li, W., Udan, R. S., Yang, Q., Kim, J., … Guan, K. L. (2007). Inactivation of YAP oncoprotein by the Hippo pathway is involved in cell contact inhibition and tissue growth control. *Genes & Developmet, 21*(21), 2747-2761.

Zhao, Y., & Sun, Y. (2013). Cullin-RING ligases as attractive anti-cancer targets. *Current Pharmaceutical Design, 19*(18), 3215-3225.

Zheng, L., Ling, P., Wang, Z., Niu, R., Hu, C., Zhang, T., & Lin, X. (2007). A novel polypeptide from shark cartilage with potent anti-angiogenic activity. *Cancer Biology & Therapy, 6*(5), 775-780.

Zhong, H., De Marzo, A. M., Laughner, E., Lim, M., Hilton, D. A., Zagzag, D., … Simons, J. W. (1999). Overexpression of hypoxia-inducible factor 1alpha in common human cancers and their metastases. *Cancer Research, 59*(22), 5830-5835.

Zhong, T. P., Childs, S., Leu, J. P., & Fishman, M. C. (2001). Gridlock signalling pathway fashions the first embryonic artery. *Nature, 414*(6860), 216-220.

Zhu, X., Li, D., Yu, F., Jia, C., Xie, J., Ma, Y., … Fan, L. (2016). MiR-194 inhibits the proliferation, invasion, migration, and enhances the chemosensitivity of non-small cell lung cancer cells by targeting forkhead box A1 protein. *Oncotarget, 7*(11), 13139-13152.

Zhuang, L. K., Yang, Y. T., Ma, X., Han, B., Wang, Z. S., Zhao, Q. Y., … Qu, Z. Q. (2016). MicroRNA-92b promotes hepatocellular carcinoma progression by targeting *Smad7* and is mediated by long non-coding RNA XIST. *Cell Death & Disease, 7*, e2203.

Zoni, E., van der Horst, G., van de Merbel, A. F., Chen, L., Rane, J. K., Pelger, R. C., … van der Pluijm, G. (2015). MiR-25 modulates invasiveness and dissemination of human prostate cancer cells via regulation of αv- and α6-integrin expression. *Cancer Research*, *75*(11), 2326-2336.

LIST OF PUBLICATIONS AND PAPERS PRESENTED

Publications

1. Ho, C. S., Yap, S. H., Phuah, N. H., Lionel In, L. A., & Noor Hasima, N. (2014). MicroRNAs associated with tumour migration, invasion and angiogenic properties in A549 and SK-LU-1 human lung adenocarcinoma cells. *Lung Cancer, 83*(2014), 154-162. (ISI/SCOPUS Indexed Publication; Impact Factor: 3.767)

2. Ho, C. S., Suzita, M. N., & Noor Hasima, N. (2017). MiR-378 and miR-1827 regulate tumour invasion, migration and angiogenesis in human lung adenocarcinoma by targeting *RBX1* and *CRKL*, respectively. *Journal of Cancer*. (ACCEPTED) (ISI/SCOPUS Indexed Publication; Impact Factor: 3.609)

Papers presented

1. Ho, C. S., & Noor Hasima, N. (2014). MicroRNAs associated with tumour migration, invasion and angiogenic properties in A549 and SK-LU-1 human lung adenocarcinoma cells. 19th Biological Sciences Graduate Congress (BSGC). Singapore. (Poster)

2. Ho, C. S., & Noor Hasima, N. (2015). MicroRNAs associated with tumour migration, invasion and angiogenic properties in A549 and SK-LU-1 human lung adenocarcinoma cells. 6th Regional Conference on Molecular Medicine (RCMM) in conjunction with 2nd National Conference for Cancer Research. Kuala Lumpur, Malaysia. (Poster)

3. Ho, C. S., & Noor Hasima, N. (2016). MicroRNAs associated with tumour migration, invasion and angiogenic properties in human lung adenocarcinoma. International Postgraduate Research Awards Seminar (InPRAS). Kuala Lumpur, Malaysia. (Oral)

Lung Cancer 83 (2014) 154–162

Contents lists available at ScienceDirect

Lung Cancer

journal homepage: www.elsevier.com/locate/lungcan

MicroRNAs associated with tumour migration, invasion and angiogenic properties in A549 and SK-Lu1 human lung adenocarcinoma cells

Chai San Ho [a], Seow Hui Yap [a], Neoh Hun Phuah [a], Lionel L.A. In [a], Noor Hasima [a,b,*]

[a] Institute of Biological Sciences, Division of Genetics and Molecular Biology, Faculty of Science, University of Malaya, 50603 Kuala Lumpur, Malaysia [b] Centre for Research in Biotechnology for Agriculture (CEBAR), University of Malaya, 50603 Kuala Lumpur, Malaysia

article info

Article history:
Received 29 May 2013
Received in revised form
20 November 2013
Accepted 27 November 2013

Keywords:
MicroRNA
Non-small cell lung cancer
Migration
Invasion
Angiogenesis
Metastasis

abstract

Objectives: Dysregulation in miRNA expression contributes towards the initiation and progression of metastasis by regulating multiple target genes. In this study, variations in miRNA expression profiles were investigated between high and low invasive NSCLC cell lines followed by identification of miRNAs with targets governing NSCLC's metastatic potential.

Materials and methods: Two NSCLC sub-cell lines possessing opposing migration and invasion properties were established using serial transwell invasion assays. Global miRNA expression profiles were obtained using microarray followed by RT-qPCR validation. Target prediction and pathway enrichment analyses were conducted on dysregulated miRNAs using DIANA-mirPath, DIANA-microT 4.0 and TargetScan 5.2 softwares. Metastatic effects of dysregulated miRNAs were evaluated using wound healing assay, invasion assay and HUVEC angiogenesis assay following transfection with mimics and inhibitors.

Results: A total of eleven differentially expressed miRNAs were revealed from microarray analyses, with four miRNAs validated through RT-qPCR. Three of these miRNAs were further selected for biological function validations, with only two modulating metastasis. A pathway model describing interactions between miRNAs and metastasis highlighted four major pathways: non-canonical Wnt/PCP, TGF- , MAPK and integrin-FAK-Src signalling cascade.

Conclusion: These results provide a list of potential candidate metastatic markers during the classifica-tion of NSCLCs and a platform for the development of bio-therapeutics targeting these miRNA control elements.

1. Introduction

Lung cancer is the leading cause of cancer-related-deaths in males and second in females worldwide [1]. The major cause of cancer-related-deaths in lung cancer patients is attributed to its ability to metastasize to distant organs through mechanisms, which are not yet fully understood [2]. Non-small cell lung cancer (NSCLC) accounts for 85% of lung cancer patients and two-third of these patients were diagnosed at late stages when the cancer had undergone local or distant metastasis with poor prognosis [3]. The fact that metastasis accounted for high lung cancer mortality rates was supported in a recent study which indicated an overall poor progno-sis in patients with NSCLC and concurrent distant metastasis with 12% and 0% for a 3- and 5-year survival rate, respectively [4].

Progression from localized tumours to metastatic cancers involves the enhancement of migration, invasion and angiogenesis properties. Even though numerous factors and cellular signalling events promoting these processes such as epithelial to mes-enchymal transition (EMT), focal adhesion dynamics, actomyosin polymerization, integrin-FAK-Src signalling, Rho-GTPases super-family signalling, transforming growth factor- (TGF-), Wnt/PCP, phosphatidylinositol 3-kinase (PI3K)/AKT, Notch signalling and others have been reported, little is known about the role that epi-genetic elements such as microRNAs (miRNAs) play during the regulation of these events [5–8].

MiRNAs are attractive candidates as upstream regulators of tumourigenesis and metastasis because they post-transcriptionally regulate numerous target genes, thereby potentially enabling inter-vention at multiple steps of the invasion-metastasis cascade [9]. Past studies have shown that dsyregulation in miRNA expression is associated with lung cancer through malignant transformation, angiogenesis and tumour metastasis [10]. Recent studies have implicated the involvement of several miRNAs which play impor-tant roles in cancer progression, for example miR-10b acts as a

* Corresponding author at: Institute of Biological Sciences, Division of Genet-ics and Molecular Biology, Faculty of Science, University of Malaya, 50603 Kuala Lumpur, Malaysia. Tel.: +60 3 79675921; fax: +60 3 79675908.
E-mail address: hasima@um.edu.my (N. Hasima).

0169-5002/$ – see front matter © 2013 Elsevier Ireland Ltd. All rights reserved.
http://dx.doi.org/10.1016/j.lungcan.2013.11.024

APPENDIX A: TaqMan MiRNA Assay Details

Assay Names	MiRBase ID	MiRBase Accession Numbers	ABI Assay ID	MiRNA Sequences (5'-3')
Hsa-miR-92b	Xtr-miR-92b	MI0004899 (Stem Loop)	007028_mat	UAC AGA AGG AUC GGG AUG UUG UGC ACU GUU GUC CUU UCU CCU GCC AAU AUU GCA CUC GUC CCG GCC UCC UGC G
		MIMAT0003658		UAU UGC ACU CGU CCC GGC CUC
Rno-miR-422b	Hsa-miR-378a-3p	MI0000786 (Stem Loop)	001314	AGG GCU CCU GAC UCC AGG UCC UGU GUG UUA CCU AGA AAU AGC ACU GGA CUU GGA GUC AGA AGG CCU
		MIMAT0000732		ACU GGA CUU GGA GUC AGA AGG C
Hsa-miR-671-5p	Hsa-miR-671-5p	MI0003760 (Stem Loop)	197646_mat	GCA GGU GAA CUG GCA GGC CAG GAA GAG GAG GAA GCC CUG GAG GGG CUG GAG GUG AUG GAU GUU UUC CUC CGG UUC UCA GGG CUC CAC CUC UUU CGG GCC GUA GAG CCA GGG CUG GUG C
		MIMAT0003880		AGG AAG CCC UGG AGG GGC UGG AG
Hsa-miR-1827	Hsa-miR-1827	MI0008195 (Stem Loop)	002814	UCA GCA GCA CAG CCU UCA GCC UAA AGC AAU GAG AAG CCU CUG AAA GGC UGA GGC AGU AGA UUG AAU
		MIMAT0006767		UGA GGC AGU AGA UUG AAU

APPENDIX B: RNA QC by Agilent TapeStation

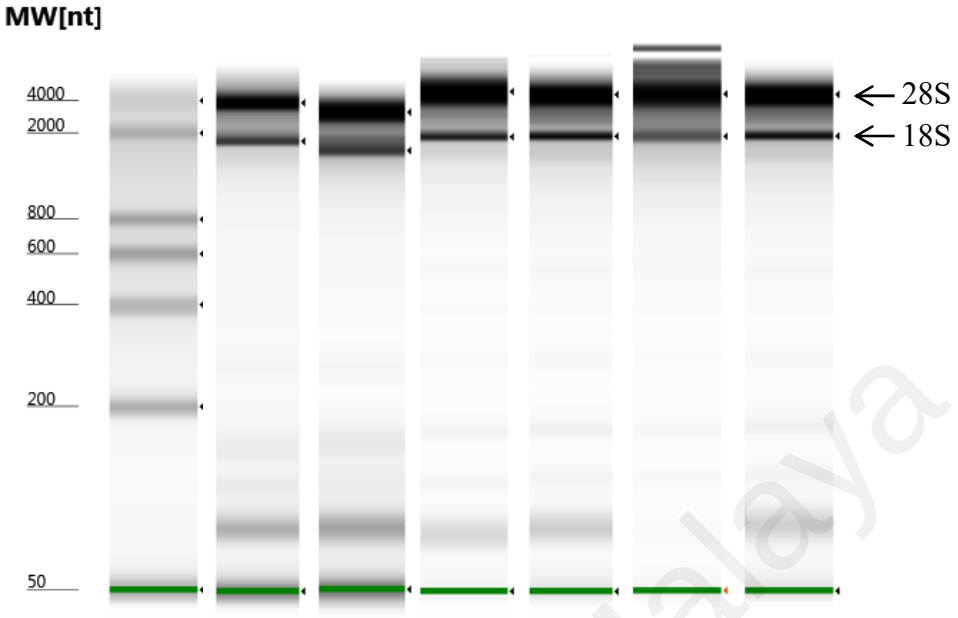

From left to right: Lane 1 (L1): Ladder; L2: SK-LU-1-I7 Replicate 1 (RIN: 9.6); L3: SK-LU-1-I7 Replicate 2 (RIN: 9.6); L4: SK-LU-1-I7 Replicate 3 (RIN: 9.6); L5: SK-LU-1-NI7 Replicate 1 (RIN: 9.7); L6: SK-LU-1-NI7 Replicate 2 (RIN: 9.3); L7: SK-LU-1-NI7 Replicate 3 (RIN: 9.5).

Sub-cell Lines	Replicates	RIN Value	28S/18S rRNA Ratio
SK-LU-1-I7	1	9.6	2.79
	2	9.6	1.85
	3	9.6	1.73
SK-LU-1-NI7	1	9.7	2.25
	2	9.3	2.62
	3	9.5	1.78

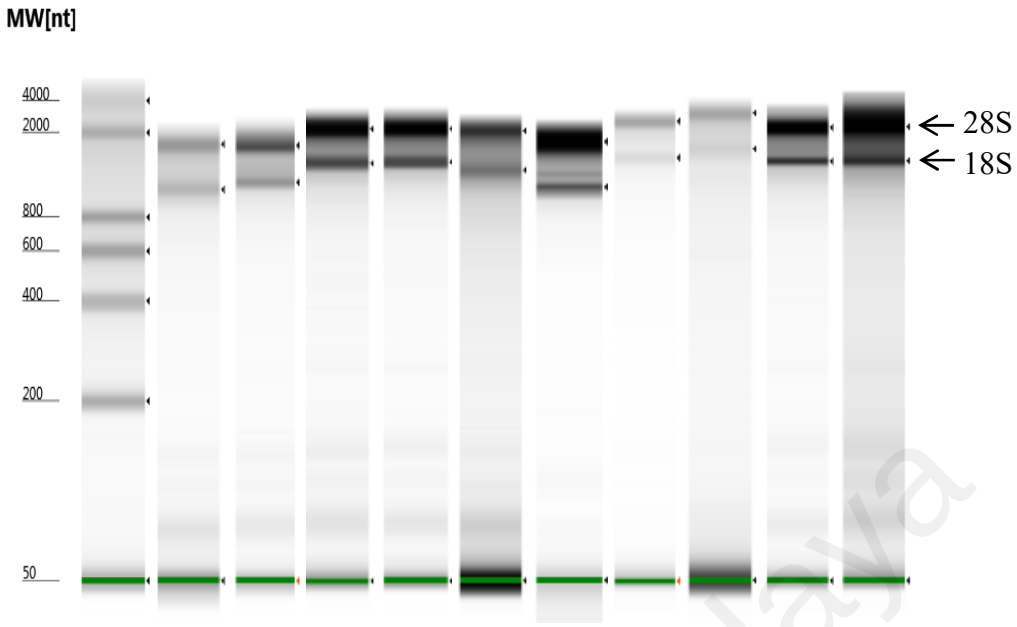

From left to right (A549-NI7): L1: Ladder; L2: MiR-92b Mimics (RIN: 8.2); L3: MiR-378 Mimics (RIN: 9.1); L4: MiR-1827 Mimics (RIN: 9.3); L5: Negative Mimics Control (RIN: 9.4); L6: MiR-92b Hairpin Inhibitors (RIN: 7.7); L7: MiR-378 Hairpin Inhibitors (RIN: 9.7); L8: MiR-1827 Hairpin Inhibitors (RIN: 8.0); L9: Negative Inhibitors Control (RIN: 7.0); L10: Mock Control (RIN: 9.5); L11: Untreated Control (RIN: 9.7).

Sub-cell Line	Treatments	RIN Value	28S/18S rRNA Ratio
A549-NI7	MiR-92b Mimics	8.2	1.5
	MiR-378 Mimics	9.1	2.0
	MiR-1827 Mimics	9.3	2.3
	Negative Mimics Control	9.4	2.8
	MiR-92b Inhibitors	7.7	1.8
	MiR-378 Inhibitors	9.7	3.6
	MiR-1827 Inhibitors	8.0	2.7
	Negative Inhibitors Control	7.0	2.1
	Mock† Control	9.5	2.3
	Untreated Control	9.7	2.5

†Mock: Transfection reagent only

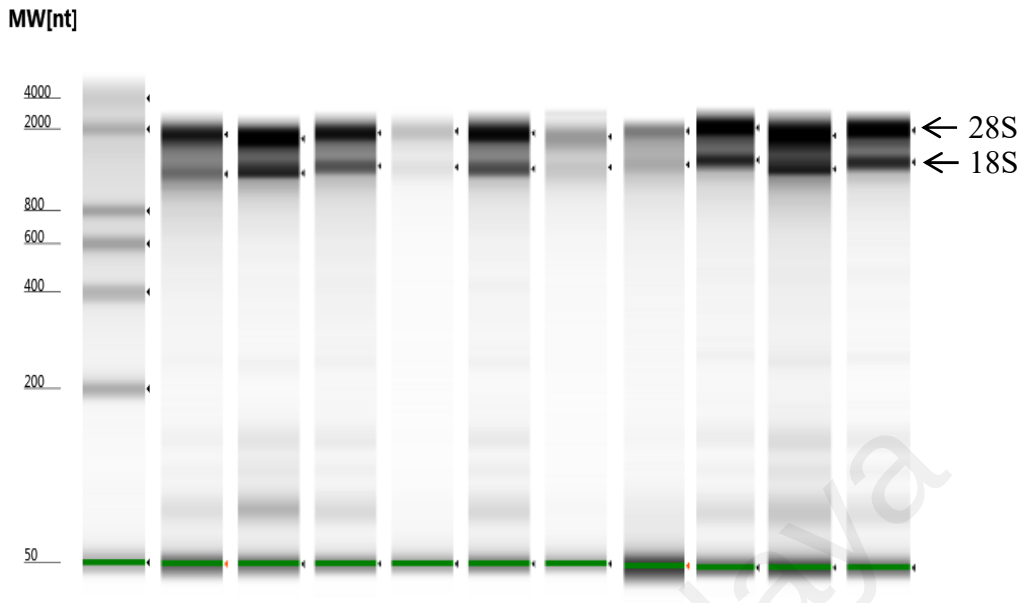

From left to right (SK-LU-1-NI7): L1: Ladder; L2: MiR-92b Mimics (RIN: 7.4); L3: MiR-378 Mimics (RIN: 9.1); L4: MiR-1827 Mimics (RIN: 8.3); L5: Negative Mimics Control (RIN: 8.3); L6: MiR-92b Hairpin Inhibitors (RIN: 8.8); L7: MiR-378 Hairpin Inhibitors (RIN: 7.2); L8: MiR-1827 Hairpin Inhibitors (RIN: 7.3); L9: Negative Inhibitors Control (RIN: 9.1); L10: Mock Control (RIN: 8.9); L11: Untreated Control (RIN: 9.2).

Sub-cell Line	Treatments	RIN Value	28S/18S rRNA Ratio
SK-LU-1-NI7	MiR-92b Mimics	7.4	2.3
	MiR-378 Mimics	9.1	2.3
	MiR-1827 Mimics	8.3	2.0
	Negative Mimics Control	8.3	2.1
	MiR-92b Inhibitors	8.8	2.3
	MiR-378 Inhibitors	7.2	1.9
	MiR-1827 Inhibitors	7.3	1.7
	Negative Inhibitors Control	9.1	2.2
	Mock† Control	8.9	2.1
	Untreated Control	9.2	2.2

†Mock: Transfection reagent only

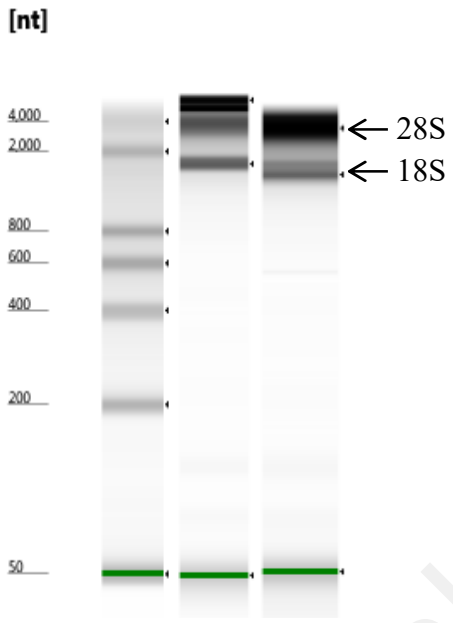

From left to right: L1: Ladder; L2: A549 (RIN: 9.7); L3: SK-LU-1 (RIN: 9.6).

Cell Lines	RIN Value	28S/18S rRNA Ratio
A549	9.7	3.6
SK-LU-1	9.6	2.7

APPENDIX C: RNA QC by NanoDrop 2000

Sub-cell Lines	Replicates	Concentration (ng/µL)	A_{260}	A_{280}	$A_{260/280}$	$A_{260/230}$
SK-LU-1-I7	1	428.1	10.702	5.547	1.93	1.37
	2	1050.3	26.258	13.137	2.00	2.19
	3	413.6	10.340	5.290	1.95	1.88
SK-LU-1-NI7	1	184.1	4.601	2.445	1.88	1.76
	2	498.4	12.459	6.541	1.90	2.20
	3	248.8	6.220	3.255	1.91	1.42

Sub-cell Line	Treatments	Concentration (ng/µL)	A_{260}	A_{280}	$A_{260/280}$	$A_{260/230}$
A549-NI7	MiR-92b Mimics	31.0	0.774	0.493	1.57	1.71
	MiR-378 Mimics	69.5	1.737	0.939	1.85	1.73
	MiR-1827 Mimics	59.4	1.485	0.790	1.88	1.81
	Negative Mimics Control	72.5	1.814	1.098	1.65	1.87
	MiR-92b Inhibitors	28.9	0.722	0.459	1.57	1.73
	MiR-378 Inhibitors	60.8	1.521	0.809	1.88	1.46
	MiR-1827 Inhibitors	119.3	2.981	1.775	1.68	1.84
	Negative Inhibitors Control	69.0	1.725	1.025	1.68	2.01
	Mock Control	123.2	3.079	1.889	1.63	1.72
	Untreated Control	66.6	1.666	1.026	1.62	2.06

Sub-cell Line	Treatments	Concentration (ng/µL)	A_{260}	A_{280}	$A_{260/280}$	$A_{260/230}$
SK-LU-1-NI7	MiR-92b Mimics	75.6	1.890	1.162	1.63	1.32
	MiR-378 Mimics	73.5	1.838	0.925	1.99	1.48
	MiR-1827 Mimics	55.3	1.382	0.710	1.95	1.58
	Negative Mimics Control	72.2	1.805	1.004	1.80	1.75
	MiR-92b Inhibitors	150.5	3.762	1.867	2.02	1.39
	MiR-378 Inhibitors	127.2	3.179	1.571	2.02	1.41
	MiR-1827 Inhibitors	149.4	3.736	1.863	2.00	1.57
	Negative Inhibitors Control	43.4	1.084	0.606	1.79	1.92
	Mock Control	48.2	1.206	0.658	1.83	2.31
	Untreated Control	37.5	0.938	0.486	1.93	1.61

Cell Lines	Concentration (ng/µL)	A_{260}	A_{280}	$A_{260/280}$	$A_{260/230}$
A549	1457.9	36.447	17.755	2.05	2.14
SK-LU-1	2429.9	60.749	29.403	2.07	2.19

Cell Lines	Samples (3'UTR)	Concentration (ng/µL)	A_{260}	A_{280}	$A_{260/280}$	$A_{260/230}$
A549	Purified RBX1	70.8	1.416	0.726	1.95	0.43
	Purified MYC	119.0	2.381	1.321	1.80	0.25
	Purified CRKL	106.8	2.136	1.126	1.90	0.92
SK-LU-1	Purified RBX1	47.5	0.951	0.493	1.93	0.76
	Purified MYC	54.4	1.088	0.552	1.97	0.37
	Purified CRKL	70.7	1.414	0.748	1.89	1.18

Samples (3'-UTR)	Concentration (ng/µL)	A_{260}	A_{280}	$A_{260/280}$	$A_{260/230}$
Purified Cut RBX1	25.1	0.502	0.252	1.99	0.14
Purified Cut MYC	23.7	0.474	0.253	1.87	0.99
Purified Cut CRKL	41.1	0.823	0.460	1.79	0.20

Samples	Concentration (ng/µL)	A_{260}	A_{280}	$A_{260/280}$	$A_{260/230}$
Purified pmirGLO	66.7	1.335	0.685	1.95	2.20
Purified Cut pmirGLO (1)	15.0	0.300	0.145	2.01	0.12
Purified Cut pmirGLO (2)	16.2	0.324	0.166	1.95	0.78
Purified Cut pmirGLO (3)	18.7	0.374	0.194	1.93	0.41

Colonies (WT RBX1 3'-UTR)	Concentration (ng/µL)	A_{260}	A_{280}	$A_{260/280}$	$A_{260/230}$
1	89.1	1.783	0.977	1.83	1.88
2	81.7	1.634	0.880	1.86	2.05
3	88.9	1.777	0.961	1.85	2.10
4	98.2	1.964	1.074	1.83	1.96
5	79.6	1.591	0.956	1.66	1.96

Colonies (WT MYC 3'-UTR)	Concentration (ng/µL)	A_{260}	A_{280}	$A_{260/280}$	$A_{260/230}$
1	76.7	1.534	0.813	1.89	1.57
2	57.8	1.156	0.600	1.93	1.85
3	52.5	1.050	0.556	1.89	1.57
4	53.7	1.074	0.568	1.89	1.63
5	49.8	0.995	0.532	1.87	1.40

Colonies (WT CRKL 3'-UTR)	Concentration (ng/µL)	A_{260}	A_{280}	$A_{260/280}$	$A_{260/230}$
1	43.9	0.878	0.681	1.29	0.83
2	93.3	1.867	1.289	1.45	1.90
3	92.1	1.842	1.251	1.47	2.31
4	103.4	2.068	1.405	1.47	1.75

Colonies (MT RBX1 3'-UTR)	Concentration (ng/µL)	A_{260}	A_{280}	$A_{260/280}$	$A_{260/230}$
1	175.3	3.506	1.904	1.84	2.32
2	371.3	7.426	4.026	1.84	1.95
3	550.8	11.017	5.961	1.85	1.87
4	395.5	7.909	4.275	1.85	1.87
5	177.9	3.558	1.932	1.84	1.84

Colonies (MT MYC 3'-UTR)	Concentration (ng/µL)	A_{260}	A_{280}	$A_{260/280}$	$A_{260/230}$
1	212.7	4.255	2.886	1.47	1.72
2	265.7	5.313	3.440	1.54	1.80
3	275.2	5.504	3.568	1.54	1.73

APPENDIX D: MiRNA Mimics and Hairpin Inhibitors Transfection Optimisation

(1) A549-NI7

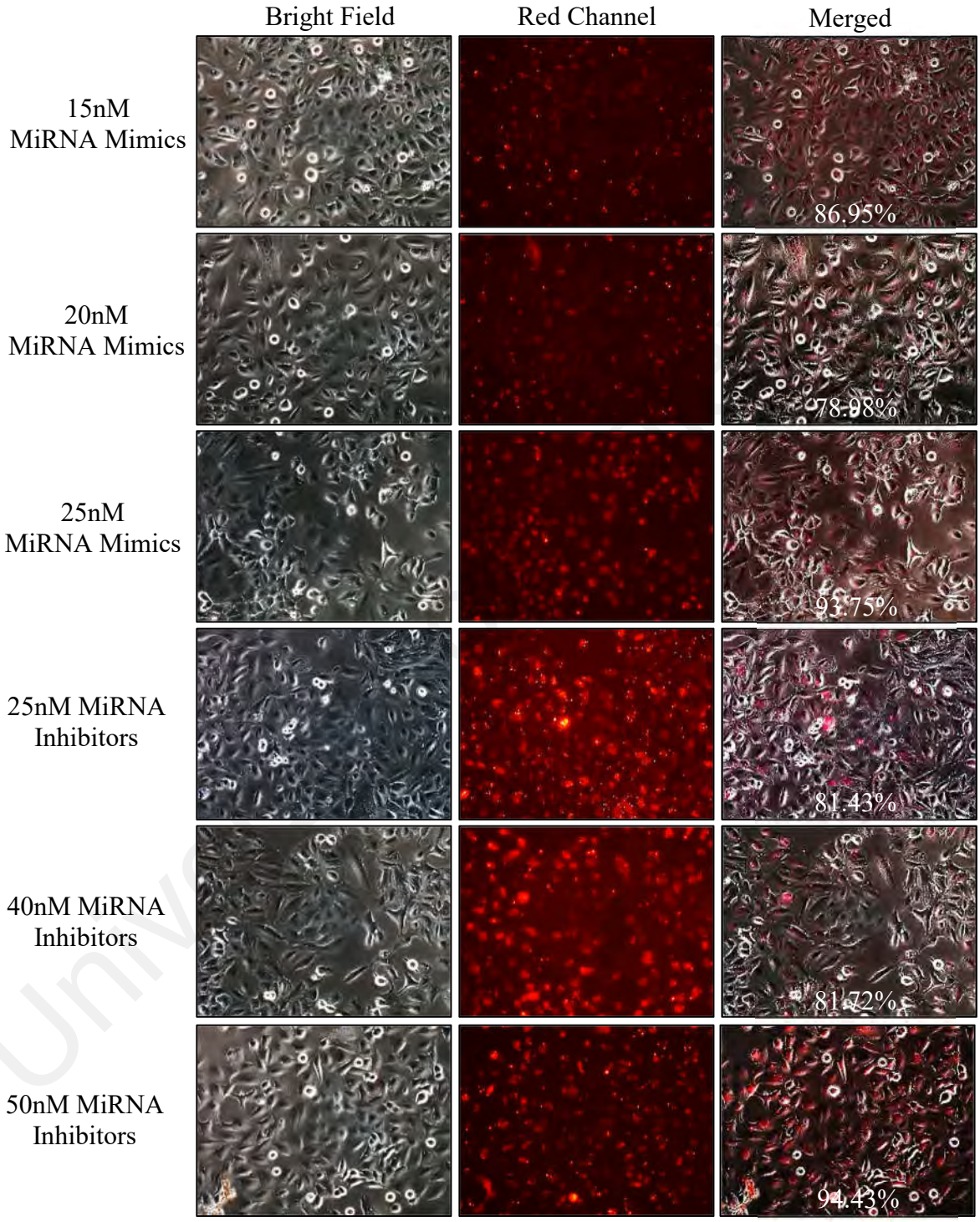

(2) SK-LU-1-NI7

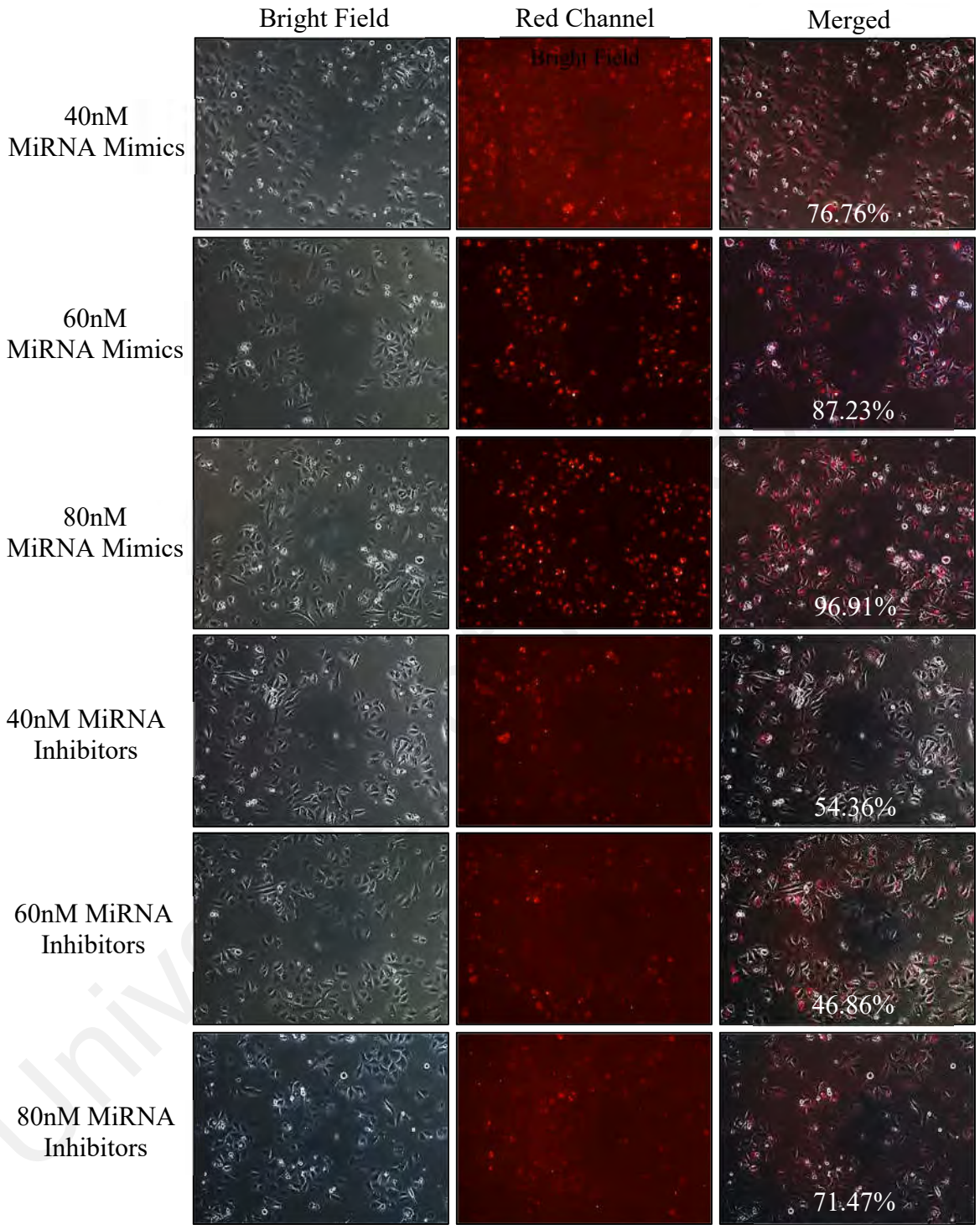
Bright Field
Red Channel
Merged
40nM MiRNA Mimics
60nM MiRNA Mimics
80nM MiRNA Mimics
40nM MiRNA Inhibitors
60nM MiRNA Inhibitors
80nM MiRNA Inhibitors
76.76%
87.23%
96.91%
54.36%
46.86%
71.47%

APPENDIX E: Tube Formation Assay Controls

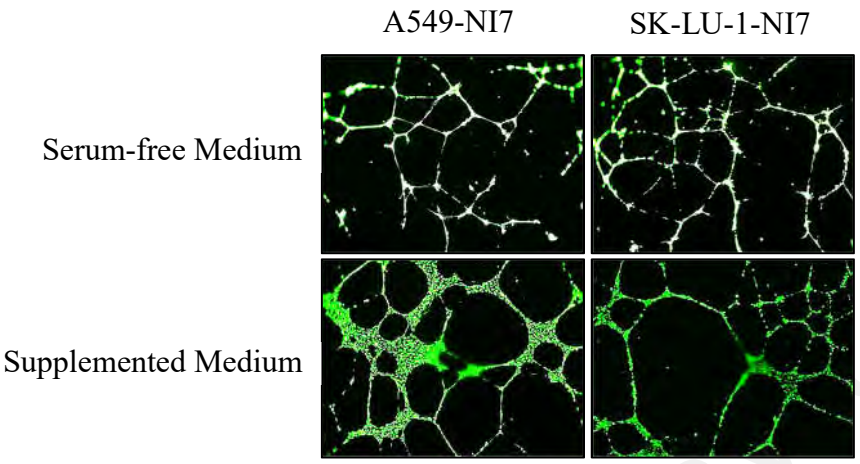

Parameters	Average Number of Branching Points		Average Number of Tubes	
	A549-NI7	SK-LU-1-NI7	A549-NI7	SK-LU-1-NI7
Serum-free Medium	64 ± 5	58 ± 6	131 ± 12	128 ± 9
Supplemented Medium	113 ± 2	112 ± 3	244 ± 7	242 ± 6

APPENDIX F: Data Analysis with the WimTube Module

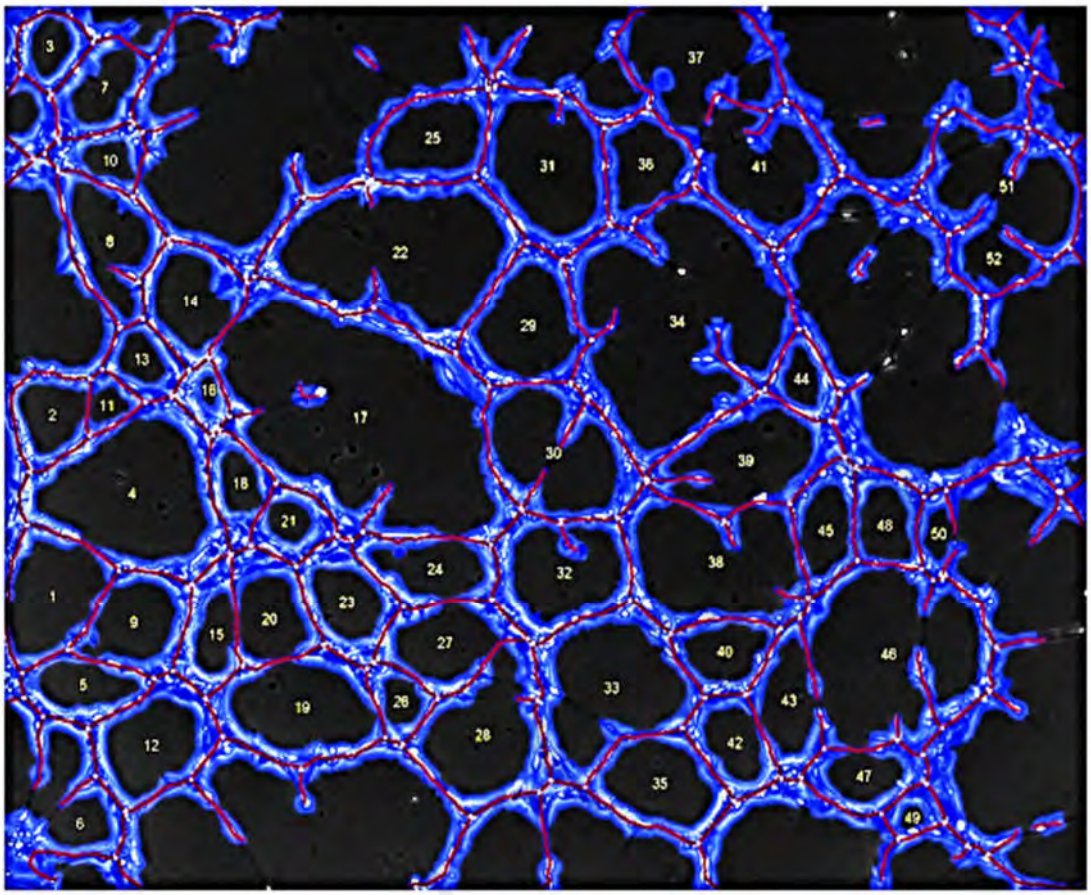

†Tubes are shown in red, the cell-covered area in blue. The branching points are shown as white dots. The numbers indicate a closed loop of tubes.

Covered area (%): The percentage of covered area, that is the percentage of tubular structure in the whole area of the image. It is calculated by dividing the total number of pixels of the image by the pixels that belong to the tubular structure.

Total loops: An area of the background enclosed (or almost) by the tubular structure. **Mean loop area (px):** For each loop, the area (number of pixels) enclosed by it is considered as its area. So, the mean loop area is the arithmetic mean of the area of all the loops.

Mean loop perimeter (px): For each loop, the pixels that belong to its edge (pixels that are in contact with the blue tubular structure) are considered its border. The number of

pixels of this border is its perimeter and the mean loop perimeter is the arithmetic mean of the perimeter of all loops.

Total tube length (px): The length in pixels of the whole tubular structure.

Total tubes: The number of tubes on the image. A tube is considered to be the part of the tubular structure between two branching points or a branching point and a loose end.

Total branching points: The branching points are parts of the skeleton where three or more tubes converge.

APPENDIX G: Hypothetical Gene Targets Details

(1) MiR-378

Gene Symbol	Gene ID	Representative Transcript
ERBB4	ENSG00000178568	ENST00000342788.4
NKX3-1	ENSG00000167034	ENST00000380871.4
PAX8	ENSG00000125618	ENST00000263335.7
PLA2G12A	ENSG00000123739	ENST00000243501.5
RAD51	ENSG00000051180	ENST00000423169.2
RAPGEF5	ENSG00000136237	ENST00000401957.2
RBX1	ENSG00000100387	ENST00000216225.8
SKP2	ENSG00000145604	ENST00000274255.6

(2) MiR-1827

Gene Symbol	Gene ID	Representative Transcript
ADCY2	ENSG00000078295	ENST00000338316.4
AR	ENSG00000169083	ENST00000374690.3
ATM	ENSG00000149311	ENST00000452508.2
BBC3	ENSG00000105327	ENST00000341983.4
BCL2L1	ENSG00000171552	ENST00000376062.2
BCR	ENSG00000186716	ENST00000305877.8
BDKRB2	ENSG00000168398	ENST00000306005.3
CAMK2A	ENSG00000070808	ENST00000348628.6
CCNG1	ENSG00000113328	ENST00000340828.2
CDKN1B	ENSG00000111276	ENST00000228872.4
CRB2	ENSG00000148204	ENST00000373631.3
CRKL	ENSG00000099942	ENST00000354336.3
CYCS	ENSG00000172115	ENST00000305786.2
E2F2	ENSG00000007968	ENST00000361729.2
ERBB4	ENSG00000178568	ENST00000342788.4
FAS	ENSG00000026103	ENST00000352159.4
FGF18	ENSG00000156427	ENST00000274625.5
FGF20	ENSG00000078579	ENST00000180166.5
FZD3	ENSG00000104290	ENST00000240093.3
FZD5	ENSG00000163251	ENST00000295417.3
GRB2	ENSG00000177885	ENST00000392563.1
GSK3β	ENSG00000082701	ENST00000264235.8
IGF1	ENSG00000017427	ENST00000337514.6
IKBKG	ENSG00000073009	ENST00000393549.2
LAMC2	ENSG00000058085	ENST00000264144.4
LIMD1	ENSG00000144791	ENST00000273317.4
LLGL2	ENSG00000073350	ENST00000392550.3

Table, continued

Gene Symbol	Gene ID	Representative Transcript
LRP6	ENSG00000070018	ENST00000261349.4
MDM2	ENSG00000135679	ENST00000462284.1
MDM4	ENSG00000198625	ENST00000391947.2
MITF	ENSG00000187098	ENST00000328528.6
MYC	ENSG00000136997	ENST00000377970.2
NCOA4	ENSG00000138293	ENST00000452682.1
NF2	ENSG00000186575	ENST00000347330.5
NFATC3	ENSG00000072736	ENST00000329524.4
NFATC4	ENSG00000100968	ENST00000413692.2
NKD1	ENSG00000140807	ENST00000268459.3
PAK1	ENSG00000149269	ENST00000278568.4
PLCG1	ENSG00000124181	ENST00000244007.3
PLEKHG5	ENSG00000171680	ENST00000377725.1
PPP2R2A	ENSG00000221914	ENST00000380737.3
PTGS2	ENSG00000073756	ENST00000367468.5
RALBP1	ENSG00000017797	ENST00000383432.3
RCHY1	ENSG00000163743	ENST00000451788.1
RXRB	ENSG00000204231	ENST00000374685.4
STAT3	ENSG00000168610	ENST00000585517.1
STAT5B	ENSG00000173757	ENST00000293328.3
STK36	ENSG00000163482	ENST00000295709.3
STK4	ENSG00000101109	ENST00000372801.1
SUFU	ENSG00000107882	ENST00000369902.3
THBS1	ENSG00000137801	ENST00000260356.5
TP73	ENSG00000078900	ENST00000378280.1
TPM3	ENSG00000143549	ENST00000368531.2
VANGL2	ENSG00000162738	ENST00000368061.2
VHL	ENSG00000134086	ENST00000256474.2
WNT2B	ENSG00000134245	ENST00000369686.5
WNT3A	ENSG00000154342	ENST00000284523.1
WNT5B	ENSG00000111186	ENST00000397196.2
WNT9B	ENSG00000158955	ENST00000290015.2

APPENDIX H: Full Length mRNAs Sequence

(1) RBX1

```
1    GUGCGCUGCU GCGCAGGCGC GGUGGUCGGA CGACAGACCG UGUGUUUCCA AAAUGGCGGC
61   AGCGAUGGAU GUGGAUACCC CGAGCGGCAC CAACAGCGGC GCGGGCAAGA AGCGCUUUGA
121  AGUGAAAAAG UGGAAUGCAG UAGCCCUCUG GGCCUGGGAU AUUGUGGUUG AUAACUGUGC
181  CAUCUGCAGG AACCACAUUA UGGAUCUUUG CAUAGAAUGU CAAGCUAACC AGGCGUCCGC
241  UACUUCAGAA GAGUGUACUG UCGCAUGGGG AGUCUGUAAC CAUGCUUUUC ACUUCCACUG
301  CAUCUCUCGC UGGCUCAAAA CACGACAGGU GUGUCCAUUG GACAACAGAG AGUGGGAAUU
361  CCAAAAGUAU GGGCACUAGG AAAAGACUUC UUCCAUCAAG CUUAAUUGUU UUGUUAUUCA
421  UUUAAUGACU UUCCCUGCUG UUACCUAAUU ACAAAUUGGA UGGAACUGUG UUUUUUUCUG
481  CUUUGUUUUU UCAGUUUGCU GUUUCUGUAG CCAUAUUGUA UUCUGUGUCA AAUAAAGUCC
541  AGUUGGAUUC UGGAACGGAU GCUCUCUCUU GUGUAUGUGA ACAAAGUGAA CAUAAAUGAA
601  GAGUCUCCCC UUCCAAGGCU GAAAACUCAG CUUUUGAAAG UGAAAUGUUU GUUCAUCGGG
661  GCCAGAGCAG GGUUGUCCUC UGAGCGCAUC ACUUAGUGAC GAGGAAUCCA ACAGCUCAAG
721  GCAGAGUGUG GAUCACCGGC UCCCGAAAAC AGCAGUCAGC CCUUCUUUCU CCUGUGUGAC
781  AGCAGUGGGC AGCUGAAAGA GGGAAGAAUG UGGGAUUCAG UCAUCAAACC CAGUUCUGAG
841  UCCUGGUUCC ACAGCUUGGG UACUGAUGGC AAUCUUGGCC AAGUUGUCUC UCUACUCUGA
901  ACUUUC
```

†Underlined bases are the 3'-UTR of RBX1 mRNA
†Bases highlighted are the target sequence that interacts with miR-378 seed sequence

(2) MYC

```
   1 GACCCCCGAG CUGUGCUGCU CGCGGCCGCC ACCGCCGGGC CCCGGCCGUC CCUGGCUCCC
  61 CUCCUGCCUC GAGAAGGGCA GGGCUUCUCA GAGGCUUGGC GGGAAAAAGA ACGGAGGGAG
 121 GGAUCGCGCU GAGUAUAAAA GCCGGUUUUC GGGGCUUUAU CUAACUCGCU GUAGUAAUUC
 181 CAGCGAGAGG CAGAGGGAGC GAGCGGGCGG CCGGCUAGGG UGGAAGAGCC GGGCGAGCAG
 241 AGCUGCGCUG CGGGCGUCCU GGGAAGGGAG AUCCGGAGCG AAUAGGGGGC UUCGCCUCUG
 301 GCCCAGCCCU CCCGCUGAUC CCCCAGCCAG CGGUCCGCAA CCCUUGCCGC AUCCACGAAA
 361 CUUUGCCCAU AGCAGCGGGC GGGCACUUUG CACUGGAACU UACAACACCC GAGCAAGGAC
 421 GCGACUCUCC CGACGCGGGG AGGCUAUUCU GCCCAUUUGG GGACACUUCC CCGCCGCUGC
 481 CAGGACCCGC UUCUCUGAAA GGCUCUCCUU GCAGCUGCUU AGACGCUGGA UUUUUUUCGG
 541 GUAGUGGAAA ACCAGCAGCC UCCCGCGACG AUGCCCCUCA ACGUUAGCUU CACCAACAGG
 601 AACUAUGACC UCGACUACGA CUCGGUGCAG CCGUAUUUCU ACUGCGACGA GGAGGAGAAC
 661 UUCUACCAGC AGCAGCAGCA GAGCGAGCUG CAGCCCCCGG CGCCCAGCGA GGAUAUCUGG
 721 AAGAAAUUCG AGCUGCUGCC CACCCCGCCC CUGUCCCCUA GCCGCCGCUC CGGGCUCUGC
 781 UCGCCCUCCU ACGUUGCGGU CACACCCUUC UCCCUUCGGG GAGACAACGA CGGCGGUGGC
 841 GGGAGCUUCU CCACGGCCGA CCAGCUGGAG AUGGUGACCG AGCUGCUGGG AGGAGACAUG
 901 GUGAACCAGA GUUUCAUCUG CGACCCGGAC GACGAGACCU UCAUCAAAAA CAUCAUCAUC
 961 CAGGACUGUA UGUGGAGCGG CUUCUCGGCC GCCGCCAAGC UCGUCUCAGA GAAGCUGGCC
1021 UCCUACCAGG CUGCGCGCAA AGACAGCGGC AGCCCGAACC CCGCCCGCGG CCACAGCGUC
1081 UGCUCCACCU CCAGCUUGUA CCUGCAGGAU CUGAGCGCCG CCGCCUCAGA GUGCAUCGAC
1141 CCCUCGGUGG UCUUCCCCUA CCCUCUCAAC GACAGCAGCU CGCCCAAGUC CUGCGCCUCG
1201 CAAGACUCCA GCGCCUUCUC UCCGUCCUCG GAUUCUCUGC UCUCCUCGAC GGAGUCCUCC
1261 CCGCAGGGCA GCCCCGAGCC CCUGGUGCUC CAUGAGGAGA CACCGCCCAC CACCAGCAGC
1321 GACUCUGAGG AGGAACAAGA AGAUGAGGAA GAAAUCGAUG UUGUUUCUGU GGAAAAGAGG
1381 CAGGCUCCUG GCAAAAGGUC AGAGUCUGGA UCACCUUCUG CUGGAGGCCA CAGCAAACCU
1441 CCUCACAGCC CACUGGUCCU CAAGAGGUGC CACGUCUCCA CACAUCAGCA CAACUACGCA
1501 GCGCCUCCCU CCACUCGGAA GGACUAUCCU GCUGCCAAGA GGGUCAAGUU GGACAGUGUC
1561 AGAGUCCUGA GACAGAUCAG CAACAACCGA AAAUGCACCA GCCCCAGGUC CUCGGACACC
1621 GAGGAGAAUG UCAAGAGGCG AACACACAAC GUCUUGGAGC GCCAGAGGAG GAACGAGCUA
1681 AAACGGAGCU UUUUUGCCCU GCGUGACCAG AUCCCGGAGU UGGAAAACAA UGAAAAGGCC
1741 CCCAAGGUAG UUAUCCUUAA AAAAGCCACA GCAUACAUCC UGUCCGUCCA AGCAGAGGAG
1801 CAAAAGCUCA UUUCUGAAGA GGACUUGUUG CGGAAACGAC GAGAACAGUU GAAACACAAA
1861 CUUGAACAGC UACGGAACUC UUGUGCGUAA GGAAAAGUAA GGAAAACGAU UCCUUCUAAC
1921 AGAAAUGUCC UGAGCAAUCA CCUAUGAACU UGUUUCAAAU GCAUGAUCAA AUGCAACCUC
1981 ACAACCUUGG CUGAGUCUUG AGACUGAAAG AUUUAGCCAU AAUGUAAACU GCCUCAAAUU
```

2041 GGACUUUGGG CAUAAAAGAA CUUUUUUAUG CUUACCAUCU UUUUUUUUUC UUUAACAGAU
2101 UUGUAUUUAA GAAUUGUUUU UAAAAAAUUU UAAGAUUUAC ACAAUGUUUC UCUGUAAAUA
2161 UUGCCAUUAA AUGUAAAUAA CUUUAAUAAA ACGUUUAUAG CAGUUACACA GAAUUUCAAU
2221 CCUAGUAUAU AGUACCUAGU AUUAUAGGUA CUAUAAACCC UAAUUUUUUU UAUUUAAGUA
2281 CAUUUUGCUU UUUAAAGUUG AUUUUUUUCU AUUGUUUUUA GAAAAAAUAA AAUAACUGGC
2341 AAAUAUAUCA UUGAGCCAAA UCUUAAAAAA AAAAAAAAA

†Underlined bases are the 3'-UTR of MYC mRNA
†Bases highlighted are the target sequence that interacts with miR-1827 seed sequence

(3) CRKL

1 CGGAGGGGGA GGUGGCUGCC GCUUCUCCCG CGUCCGCCAU UUUGUUGCUG UGGCUAUUGG
61 GAACAAGCUG GGCAAAAGCA CCCCGGAGGC GCGACGCUCC UUCGAGUUCG GUGCCUCGUG
121 UGACGGCGGG GGUCGGUGAA GACCCGUCGA GCUGCGGCGC CGGCGCGUUC CAGGCCGGGA
181 GUCACUGGAG GCACCCCUGG GACGCCGAGC AGCCCGAGAA CCCCGGGGUG GCCUCCGCUG
241 CGGCUCGGGU UUGCCUGCCC CGACCCCCCG GCUCUGCCGU GCAUUCCCGG GCGGCUCUCU
301 CCGUGUGGCG GCCCCGGAGC AGGCGGGCGG CGUCGGAGGA UGCUGCGGGC CCGGAGCCGA
361 GAGGAAAGUG CUGGCCCAGC CCUCUGAGCG CUCCUCGAGG UGUGCGAGAG GCCCUUCCUC
421 GGCCCCAAAG CCGUCUGCCG GGCUAAGGCG UGCAGAGCAG GCGAGGACAG CCGCCGCCCC
481 UACCGCCGCA GAGUCCCCGG UCCAACACCA UGUCCUCCGC CAGGUUCGAC UCCUCGGACC
541 GCUCCGCCUG GUAUAUGGGG CCGGUGUCUC GCCAGGAGGC GCAGACCCGG CUCCAGGGCC
601 AGCGCCACGG UAUGUUCCUC GUCCGCGAUU CUUCCACCUG CCCUGGGGAC UAUGUGCUGU
661 CGGUGUCCGA GAACUCGCGG GUCUCCCACU ACAUCAUCAA CUCGCUGCCC AACCGCCGUU
721 UUAAGAUCGG GGACCAGGAA UUUGACCAUU UGCCGGCCCU GCUGGAGUUU UACAAGAUCC
781 ACUACCUGGA CACCACCACC CUCAUCGAGC CUGCGCCCAG GUAUCCAAGC CCACCAAUGG
841 GAUCUGUCUC AGCACCCAAC CUGCCUACAG CAGAAGAUAA CCUGGAAUAU GUACGGACUC
901 UGUAUGAUUU UCCUGGGAAU GAUGCCGAAG ACCUGCCCUU UAAAAAGGGU GAGAUCCUAG
961 UGAUAAUAGA GAAGCCUGAA GAACAGUGGU GGAGUGCCCG GAACAAGGAU GGCCGGGUUG
1021 GGAUGAUUCC UGUCCCUUAU GUCGAAAAGC UUGUGAGAUC CUCACCACAC GGAAAGCAUG
1081 GAAAUAGGAA UUCCAACAGU UAUGGGAUCC CAGAACCUGC UCAUGCAUAC GCUCAACCUC
1141 AGACCACAAC UCCUCUACCU GCAGUUUCCG GUUCUCCUGG GGCAGCAAUC ACCCCUUUGC
1201 CAUCCACACA GAAUGGACCU GUCUUUGCGA AAGCAAUCCA GAAAAGAGUA CCCUGUGCUU
1261 AUGACAAGAC UGCCUUGGCA UUAGAGGUUG GUGACAUCGU GAAAGUCACA AGGAUGAAUA
1321 UAAAUGGCCA GUGGGAAGGC GAAGUGAACG GGCGCAAAGG GCUUUUCCCC UUUACGCACG
1381 UCAAAAUCUU UGACCCUCAA AACCCAGAUG AAAACGAGUG AUUGCUGUUG CCCUGUUUCC
1441 UGCUGCUUUG UUGUUCUGCC UGUCCUAGUC UCCUUUGAAG UGGGAAAGCA UUUUCUCUCA
1501 UAGGCAAGUC ACACUGCAUU GCCGAAGUCC AGCUUUCUGC AGACUGGCAG UCGCACACAC
1561 AUUUGGAAUG CACACAGCGG CUGCCUCCUG AUGUUUGUAU CAUAGUCGUA UUGUCAAAGA
1621 GUAGCCGAUU UUAGAGUUCU UUUGGAUCAU AAACUGGAAA UACUGAUGGA AGCACACAAG
1681 UGGAGAGAAG UUGACAUGGA AAGGGUCUUC CUUCUCAUUG CUGCCCGUUU GUACAUGGGA
1741 CUGAUUCUGU UGUGUUCACC AGAGAAAGCU UGAGGCCAUG GCGAGAUACU GCAUGUUUGC
1801 UGUUCCACAA AGCAGUGGCU UAGCUGCCAU CUUGCUUUUC UUUGGACAAC AGGAAGUGAA
1861 CCUUAAGGAA GAGAGAAUUC UGUUCUAAAA CUCCAAAAUC UGGCUUUUUU UUUUCUUUUG
1921 UUUUGGUUUG GUUUUGGAAA ACUAAUUAAU UAGACUUGUG UGGGGGUUUU UUUUUGUUUU
1981 GUUUUGUUUG UUUUGUUUUG UUUUUUUGAG ACGGUGUCUC GCUGCAUCAC CCAGGCUGGA
2041 GUGCAGUGGC GCAAUCUCGC CUUCCUGCAG UCUCCGCCUC CUGAGUUCAA GCGAUUCUCC
2101 UGCCUCAGCC UCCCAAGUAG CUGGGACUGC AGGCGCGCAC ACCACGCCCA GCUAAUUUUU
2161 GUAUUUUUAG UAGAGACGGG GUUUCAUCAU GUUGACCAGG CUGGUCUCAA ACUCCUGACU
2221 UCAGGUGAUC CACCCGCCUU CAGCCUCCCA ACGUGCUGGG AUUACAGCCG UGAGCCGCCG
2281 CGCCUGGCCU AGACUUGUGU GUUCUAAACA GGUUAAGUAG CAGGUUGGGU UUUUAUGAUA
2341 GUGCAAGGAA UGACUCAUGC CUCUGAGCUU CUAAACUGAA GCUGCUGUAA CUAAAGGAAU
2401 CUGAAAAGAA CAACCCUGAA GCAGAGGCCU UUAUUGUCUU GGUUGCCAGU AGUACCUUGU
2461 UUUGCCAUGU AGCAGACAAC ACACAAAAUA AUGCAGUUGU GGUGUGCCAU GCUAUGUGCA
2521 CAGCCCCUUG GAUUACUUUG UUUUAAAAAG CAUCAGAGUU GGGGGUACUU UAGGGAAACC
2581 UUUGCUUACC UUGUUUUGCC AGUGAUAAGA GCAGUGGGUU GGAGGGCACU UGGCCAGUUU
2641 UCUGUUCAGC UUUUCAGUGA AUGUACCCCU UUAAGGUUCA GACUUAAACU UCCUUAAAAA
2701 GUGGCGUUGU UCAUAGAAUC GUUGGACUCA UUAAUGAAUC GUUCAACUCC ACUCACUGAA
2761 GCCCAGACCU CCGUGCCCAG GCCCAAUCUC GUCAGGCUGC CAGAGAAAGU UGGUGCUGCU
2821 CAUACUGGUC UCACAGUCUA AGUAAGUGUC UGUGAUGCUC CCAAGCAAAG GAAAUGCAAG
2881 CUCUGGAAAU UCGUUAAUGU AUUUGAUGUC UUAGUGUUUU AGUGACUAGG GAGACCAUUA

2941 ACUAGUUUAU CAUUAACCAC UUAUCAGUGU AUUGAUGUUA AAGCAUUUCC CUGUUAGCUA
3001 AAAGAGGCCU GUUCAUACAA GCCAACUGGU AUAUACGUGU GGUUCAUCCA UCAUCUGCUG
3061 CACAUAGCAG ACUAGAAUUC UGGGAACCCU GUGCAAUUCA GUCUGCUCUC CCUUGUGGAC
3121 CCUGGUAAAG AAAAGCCUCA GCUCAUAGUG AACACAGCAG ACCUAGAAAU GUAGCAGCAG
3181 CCUACUGAGU AGCUUUCAUU UACUGAUCAU CUGCUGUGAC UGUGGCCCUG UCUGGAGGUU
3241 CCUAGGUUUU GAGAUUUAGA GCAAUGCAUU CUGGAGACAG AACCAGCAGA ACAGCCAUUU
3301 UUCAAUUUUU CUUUAAAUCA GUAUUCCAUC AGGCAGAUAA CUGCUGUAUU CAUGAAUCUU
3361 GAGAGUGUUC CUGAGACAGA AUUAAUGGUC AUUUGGGAAA ACUAUCGCCA UGGCUUCCCA
3421 UCUGUGGUUU UCCUCUAAAA GCCUUGGAGA UUAGCCCUUC CUUGCCAGUG AGAACGGUGA
3481 CCGCCUCCUG CUCUGCACGG UCUGCGGCAG UUGCCGCUUC UGGUUAGGUG UGUCAGGUUG
3541 GCUUAUUUUG GGUUCAGGCC UGGCGUAGCA CCCACAAGUG GCAGACAUAU CACAAGAGUC
3601 CCCAGACUCU GCCUAGAAAC AGUGUUUGCC CUUUGGCCAG UGACGUGGUU CAUCCCGGCC
3661 CAUGUUGAGC CAUGAGUGGA GUUUCCAACA GAGGGAGGAA UGUGUGCCUU GUUCAAGGAG
3721 GGCACGACCC UUAGGCCUUU UUCAACCAGA UUUAGCUGAA GGGCUUGACA CCUUUGAAUU
3781 ACAGCAGUUG ACUCAGAGUG CAAGAAGUCU GGCCAUUUUG GAAAGCAAGG UUUCCUUUCA
3841 GCCCUGUCUA CUGACCAAUA CCCCGACUCA CCUUGUGUGG CGCACUUCAG AAUCAGAUAU
3901 ACCUAGAGUA UACCUGUGGU UUGGUUUUAU AAUUAAUCAG CUCGUUACUU CAGCCCAUGA
3961 AAAUGGCAUC CAGGGCUGCC AGGAGAUUCA GAGCUCAAAA CAAGGCGAGC UUGAGUUCUG
4021 CACUCCAGAU AUGUGCCAAA ACUAGUAAAA CUUAACGGAC UUACAACCUU GUCAGUUUUU
4081 UUAAUGAGGC AGGGAUACUC UGUUUUUCAC ACUAAACAUA UGAAUGCAGC ACUGCUGCCU
4141 CAGCUCAGCU UCGUGCCUGG GUUCCCCACU GGUCUGGGAA GACUGUUGUG CUCCAUAGAG
4201 CAGUGCACAU CUGACCCAGA GGGUGGGUGU UCAUAACUGC UACUUGCUCU GCUCUACCAU
4261 GUUUAAAGAA AUAUUUGGAU GUUAAAUUAA CUCACUAUGG UUUUUCACCU GGGAAGGAAA
4321 CAAAUUACGU ACUAGAGGGC AUUGACUGGU UAAAAACUUG UGUAUCCCGG GAAGGACCUG
4381 CGGUACAGGA GUCAGCCAUG UCUGUGCUGU GUGGAACCAC CUGAUGACAU GGUUAACGAG
4441 GAAGACGAUG UGUUGACCGG CUGCCGUUUG AGGACUUUGG UCACCCAGAC UAGACACCUU
4501 CUGUGCUCAU GUUUGGAAAG CUGAAAGGGA AGGACAGCUG UGCCCUCCUG GGAGCUCAUG
4561 UGUCCCUGGC GCUGUGCUAG CUUUCCUUUA CAGCUGUUUA CAGACAAGGC AGGCCUGAGG
4621 CAGAUGGCCA CUGCUCUUGU GAUGUUUGCU CAGAGGAAUA UGAACAUUUU AUUUUUGAAA
4681 AGGGAUGAUG UGGUUUUUUG CCAGGUGUUU AUAAUUAAUC CUUUAAUAUU AUGGUUAUUA
4741 ACCUCUUAAA CAUGAAUGAA UUCUUGAUUG UUUUAACACA GUACCUAAGA CUAAUGCUUU
4801 CUGUGGACAC CACUGAGCUC UGCCUCAACU CCACCCUCUG CGACCGGAGG ACUAUGCCCC
4861 UAGUAACUGC UGUCGGUGUG GACGCUGUGC UGGUUCUGUU UUCUAAAGGA GCAGAAGGAC
4921 AGGUCUCUGA GACAGGAUCG UUGUCCCUAC AGGAGGAACA GUGGCCUUGC UUCUUAGACG
4981 GUCUUCACUG UGUGUUUUAA AACAACAACA ACAACAACAA CAACAACAUA AAACUCUUUU
5041 GACCUGUAAC UUAAAGAUCA UAAACUUCAG GCAAUAAUAU UUUCUGUGUA AGCUUUUAAA
5101 AUUAUUUUUG GGGAUCAUAG CUUGUUUUAU UUUGUGCUAU AAAAUUAACA GUAUUAAAUG
5161 ACUUAUAUUC UUAGAAUACA UCGAGUGUCU UUUCUUAACA GAUUAGUGCC UUUUUAUUUU
5221 UGUAUUCCGU UUUACGUUAC UGGUCCCAGC AUCAAAACCC UUGUUUCCAU GGCCUGUUUG
5281 UAUAUUGUCU CAAUAAAACU UGCAUCAGCC GGUGGUGGCG GCAGCAAAAA AAAAAA

†Underlined bases are the 3'-UTR of CRKL mRNA
†Bases highlighted are the target sequence that interacts with miR-1827 seed sequence

APPENDIX I: Primers Properties

(1) WT RBX1 3'-UTR

Primer pair 1

	Sequence (5'->3')	Template strand	Length	Start	Stop	Tm	GC%	Self complementarity	Self 3' complementarity
Forward primer	CATACACAAGAGAGAGCATCCG	Plus	22	330	351	58.62	50.00	2.00	2.00
Reverse primer	CTTCAGAAGAGTGTACTGTCGC	Minus	22	664	643	58.76	50.00	7.00	2.00
Product length	335								

Products on potentially unintended templates

>NM_014248.3 Homo sapiens ring-box 1, E3 ubiquitin protein ligase (RBX1), mRNA

```
product length = 335
Forward primer  1    CATACACAAGAGAGAGCATCCG  22
Template        577  ......................  556

Reverse primer  1    CTTCAGAAGAGTGTACTGTCGC  22
Template        243  ......................  264
```

(2) MT RBX1 3'-UTR

Primer sequences:

Primer Name	Primer Sequence (5' to 3')
	5'-gcatccgttccagaatccaacgttcatttatttgacacagaatacaatatggctacagaaacagc-3'
g102t_t103g_c104a_c105a_a106c_	5'-gctgtttctgtagccatattgtattctgtgtcaaataaatgaacgttggattctggaacggatgc-3'

Oligonucleotide information:

Primer Name	Length (nt.)	Tm	Duplex Energy at 65 °C	Energy Cost of Mismatches
	65	78.56°C	-79.00 kcal/mole	7.87%
g102t_t103g_c104a_c105a_a106c_	65	78.56°C	-71.77 kcal/mole	10.99%

Primer-template duplexes:

Primer Name	Primer-Template Duplex
	tttgctgtttctgtagccatattgtattctgtgtcaaataaagtccagttggattctggaacggatgctct
	3'-cgacaaagacatcggtataacataagacacagtttatttacttgcaacctaagaccttgcctacg-5'
	5'-gctgtttctgtagccatattgtattctgtgtcaaataaatgaacgttggattctggaacggatgc-3'
g102t_t103g_c104a_c105a_a106c_	aaacgacaaagacatcggtataacataagacacagtttatttcaggtcaacctaagaccttgcctacgaga

(3) WT MYC 3'-UTR

Primer pair 2

	Sequence (5'->3')	Template strand	Length	Start	Stop	Tm	GC%	Self complementarity	Self 3' complementarity
Forward primer	GGATTGAAATTCTGTGTAACTGCT	Plus	24	25	48	57.74	37.50	5.00	1.00
Reverse primer	TGTTGCGGAAACGACGAGAA	Minus	20	421	402	60.53	50.00	5.00	0.00
Product length	397								

Products on intended target

>NM_002467.4 Homo sapiens v-myc avian myelocytomatosis viral oncogene homolog (MYC), mRNA

```
product length = 397
Forward primer  1     GGATTGAAATTCTGTGTAACTGCT  24
Template        2222  ........................  2199

Reverse primer  1     TGTTGCGGAAACGACGAGAA  20
Template        1826  ....................  1845
```

(4) MT MYC 3'-UTR

Primer sequences:

Primer Name	Primer Sequence (5' to 3')
	5'-gcataaaaaagttcttttatgcccaaagtccaattttcttaagtttacattatggctaaatctttcagtctcaagac-3'
g102t_c103a_c104a_t105g_c106a_	5'-gtcttgagactgaaagatttagccataatgtaaacttaagaaaattggactttgggcataaaagaacttttttatgc-3'

Oligonucleotide information:

Primer Name	Length (nt.)	Tm	Duplex Energy at 65 °C	Energy Cost of Mismatches
	77	78.49°C	-75.32 kcal/mole	11.80%
g102t_c103a_c104a_t105g_c106a_	77	78.49°C	-76.32 kcal/mole	10.78%

Primer-template duplexes:

Primer Name	Primer-Template Duplex
	tgagtcttgagactgaaagatttagccataatgtaaacttaagaaaattggactttgggcataaaagaacttttttatgctta
	3'-cagaactctgactttctaaatcggtattacatttgaattcttttaacctgaaacccgtattttcttgaaaaaatacg-5'
	5'-gtcttgagactgaaagatttagccataatgtaaacttaagaaaattggactttgggcataaaagaacttttttatgc-3'
t105g_c106a_	
	actcagaactctgactttctaaatcggtattacatttgacggagtttaacctgaaacccgtattttcttgaaaaaatacgaat

(5) WT CRKL 3'-UTR

Primer pair 6

	Sequence (5'->3')	Template strand	Length	Start	Stop	Tm	GC%	Self complementarity	Self 3' complementarity
Forward primer	GCAGTTATGAACACCCACCCT	Plus	21	113	133	60.27	52.38	4.00	0.00
Reverse primer	ATCAGCTCGTTACTTCAGCCC	Minus	21	417	397	60.13	52.38	4.00	0.00
Product length	305								

Products on intended target

>NM_005207.3 Homo sapiens v-crk avian sarcoma virus CT10 oncogene homolog-like (CRKL), mRNA

```
product length = 305
Forward primer  1     GCAGTTATGAACACCCACCCT  21
Template        4240  ......................  4220

Reverse primer  1     ATCAGCTCGTTACTTCAGCCC  21
Template        3936  ......................  3956
```

(6) MT Control

Primer sequences:

Primer Name	Primer Sequence (5' to 3')
	5'-cccgtcgtgtagataactacgatacgggag-3'
a102a_t103t_c104c_t105t_a106a_	5'-ctcccgtatcgtagttatctacacgacggg-3'

Oligonucleotide information:

Primer Name	Length (nt.)	Tm	Duplex Energy at 65 °C	Energy Cost of Mismatches
	30	80.87°C	-46.38 kcal/mole	.00%
a102a_t103t_c104c_t105t_a106a_	30	80.87°C	-46.77 kcal/mole	.00%

Primer-template duplexes:

Primer Name	Primer-Template Duplex
	gccctcccgtatcgtagttatctacacgacggggag
	3'-gagggcatagcatcaatagatgtgctgccc-5'
	5'-ctcccgtatcgtagttatctacacgacggg-3'
a102a_t103t_c104c_t105t_a106a_	
	cgggagggcatagcatcaatagatgtgctgccctc

APPENDIX J: Restriction Enzymes Map

(1) pmirGLO-WT RBX1 3' UTR (HindIII)

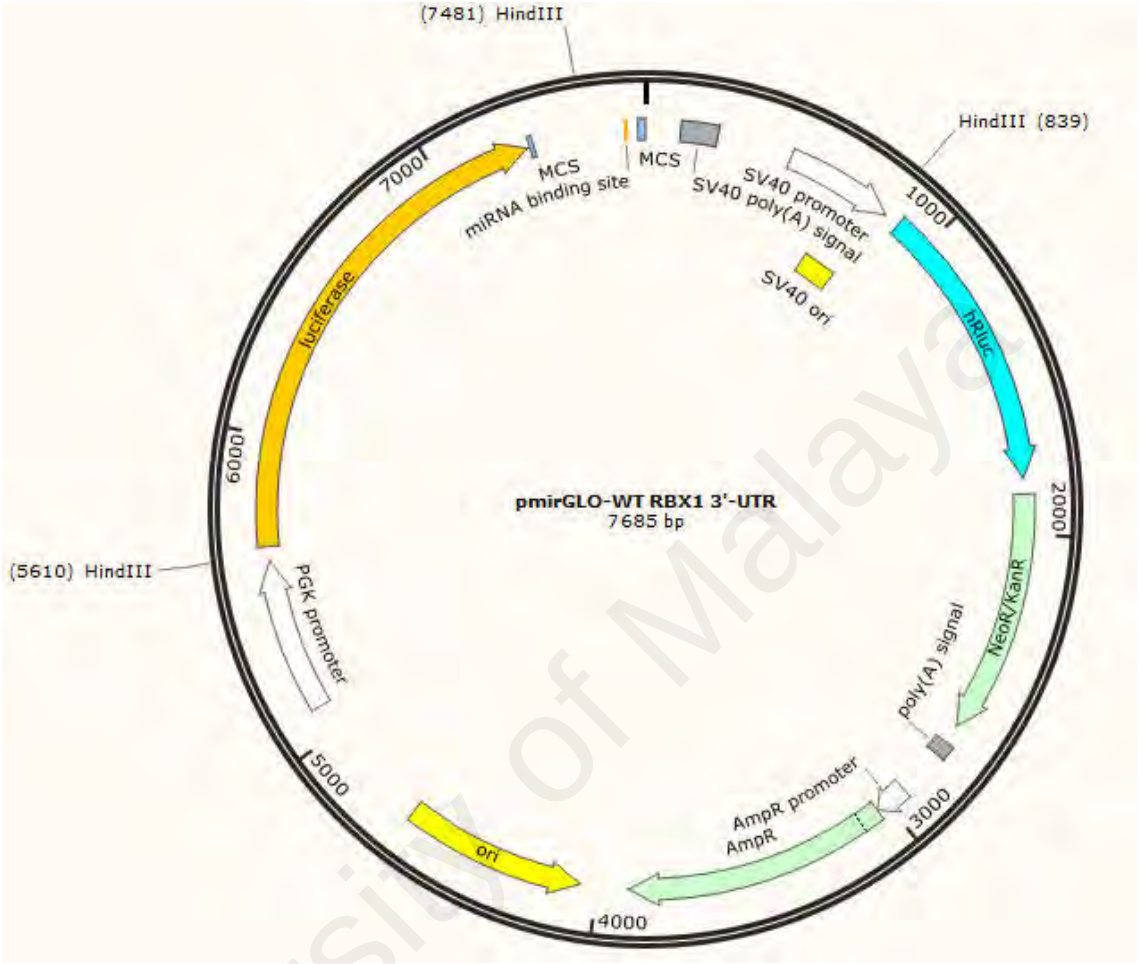

(2) pmirGLO-WT MYC 3'-UTR (SspI)

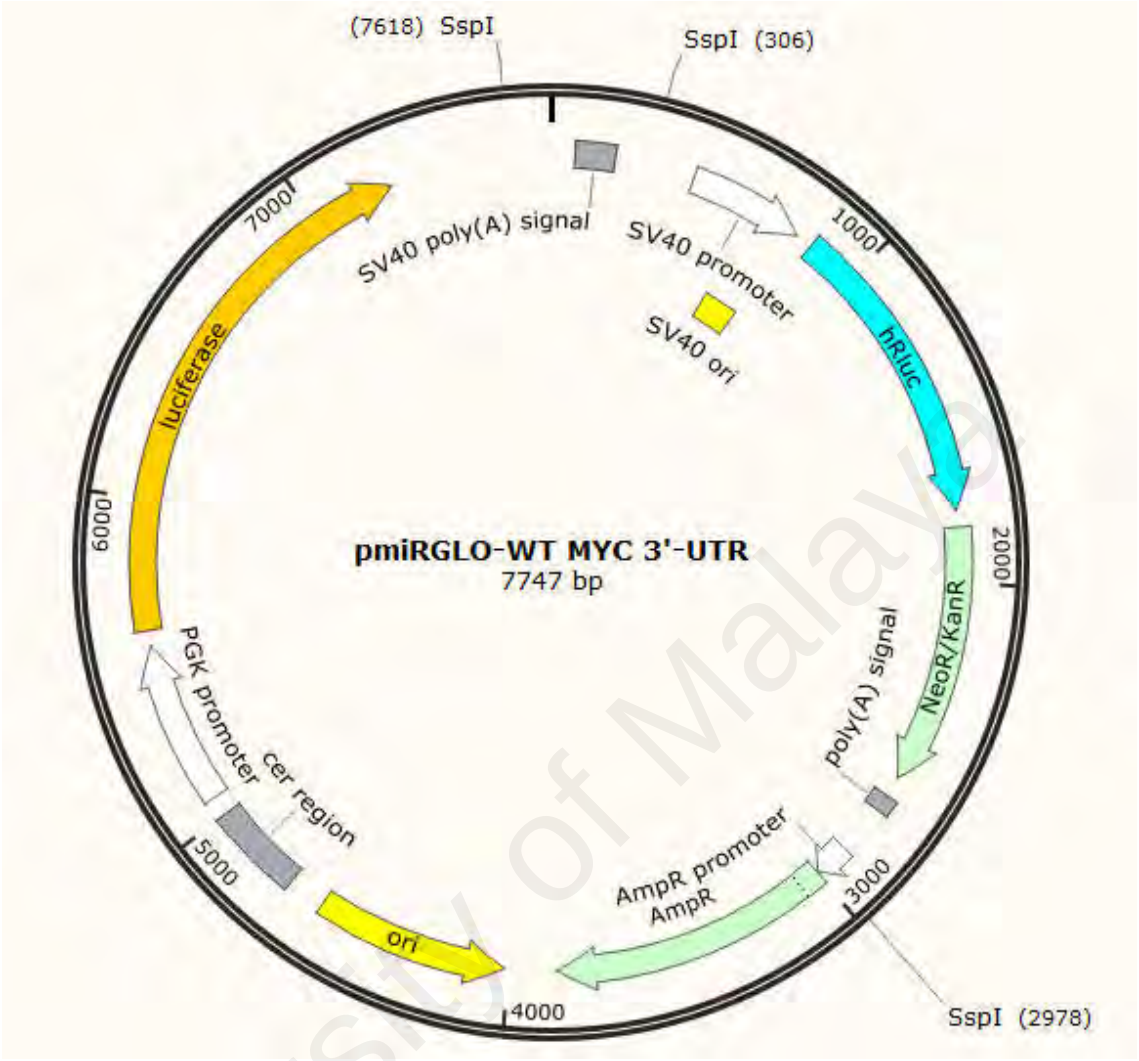

(3) pmirGLO-WT CRKL 3'-UTR (SpeI)

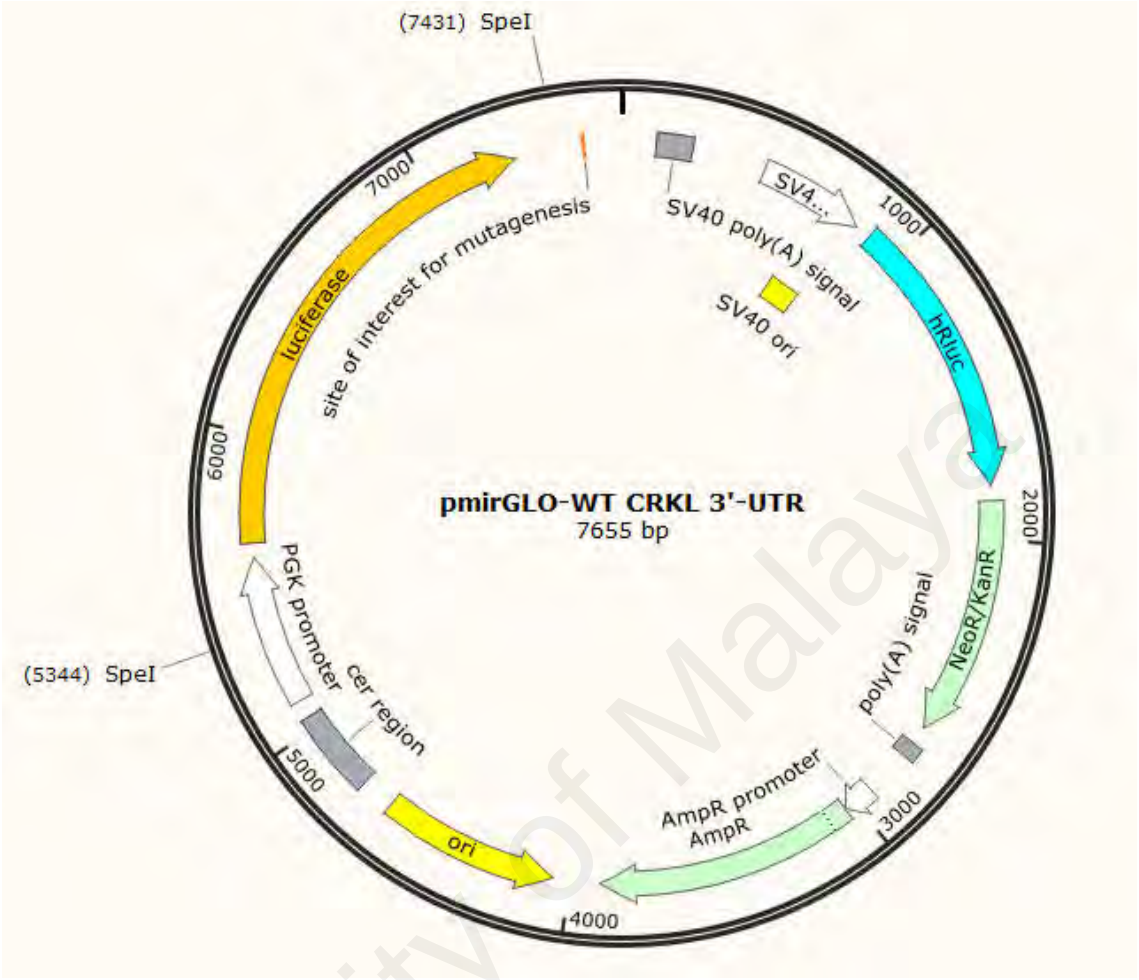

APPENDIX K: SiRNAs Transfection Optimisation

(1) A549

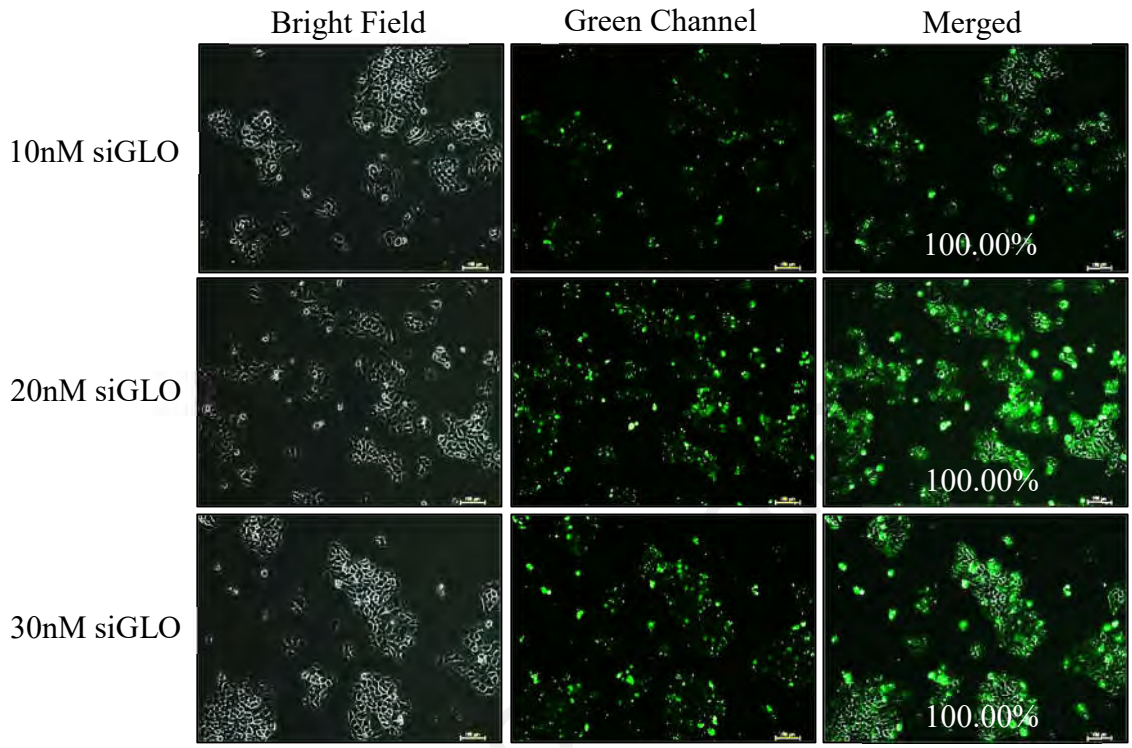

(2) SK-LU-1

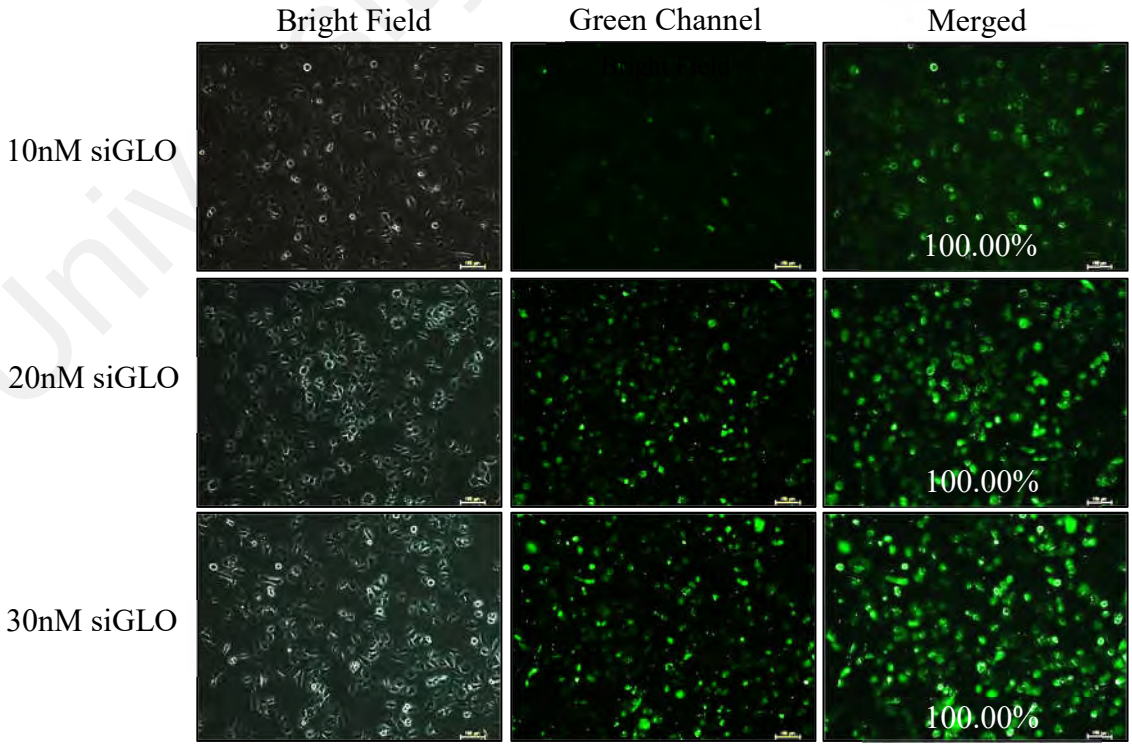

APPENDIX L: Western Blots

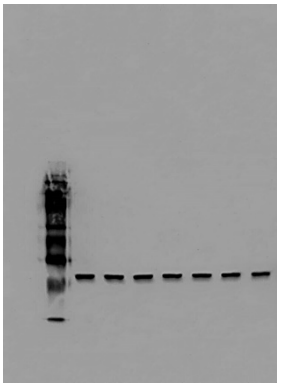

Fig 5.16
A549 GAPDH_1

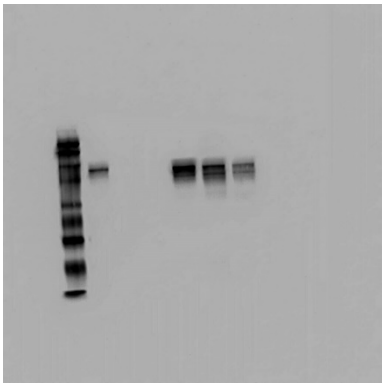

Fig 5.16
A549 CTNNB1

Fig 5.16
A549 GAPDH_2

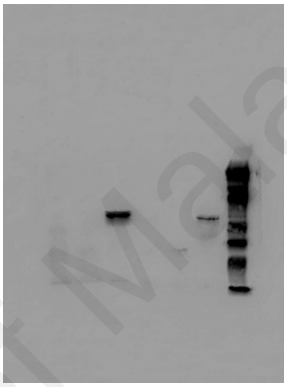

Fig 5.16
A549 VIM

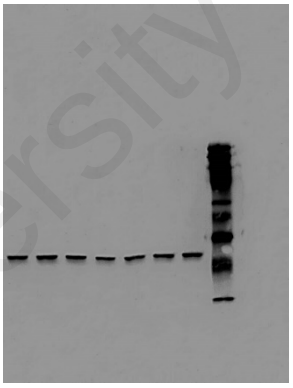

Fig 5.16
SK-LU-1 GAPDH_1

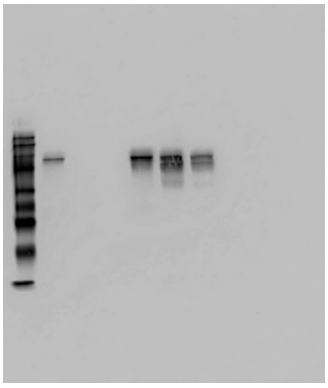

Fig 5.16
SK-LU-1 CTNNB1

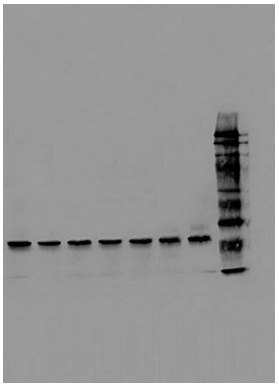

Fig 5.16
SK-LU-1 GAPDH_2

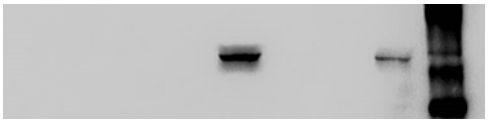

Fig 5.16
SK-LU-1 VIM

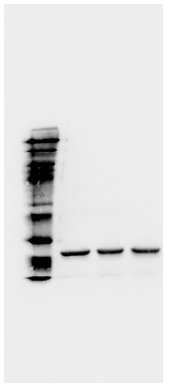

Fig 7.1
A549 GAPDH

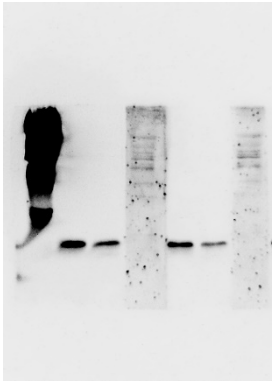

Fig 7.1
A549 RBX1_1

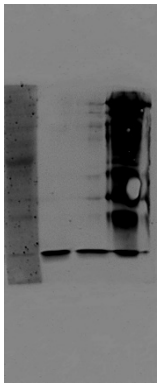

Fig 7.1
A549 RBX1_2

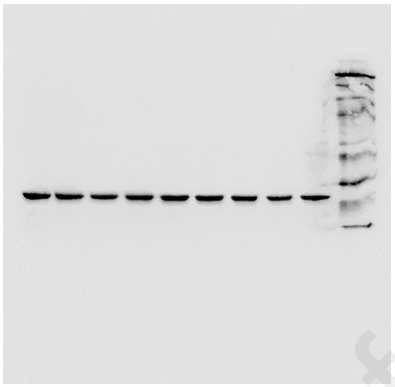

Fig 7.1
SK-LU-1 GAPDH

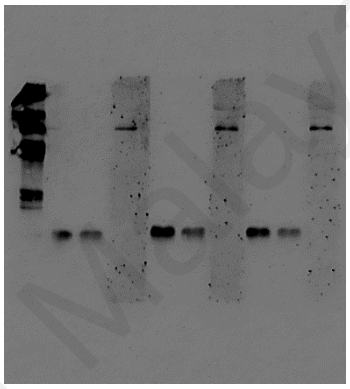

Fig 7.1
SK-LU-1 RBX1

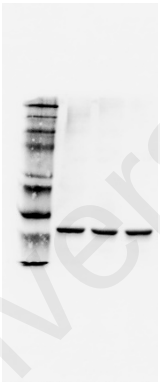

Fig 7.5
A549 GAPDH

Fig 7.5
A549 RBX1

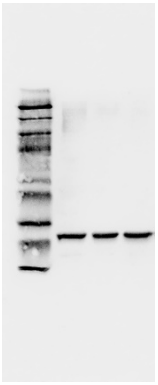

Fig 7.5
SK-LU-1 GAPDH

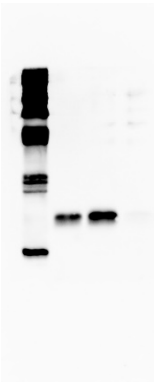

Fig 7.5
SK-LU-1 RBX1

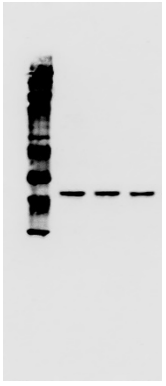

Fig 7.9
A549 GAPDH

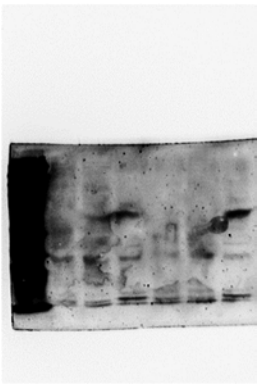

Fig 7.9
A549 CRKL

Fig 7.9
SK-LU-1 GAPDH

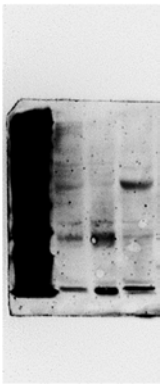

Fig 7.9
SK-LU-1 CRKL

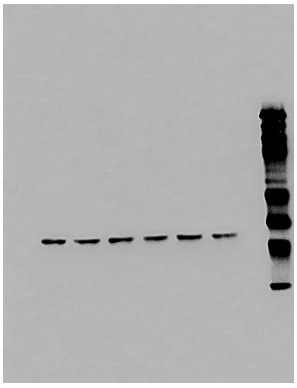

Fig 7.13
A549 GAPDH

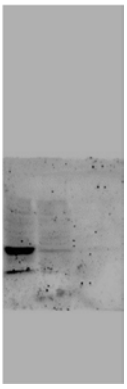

Fig 7.13
A549 CRKL

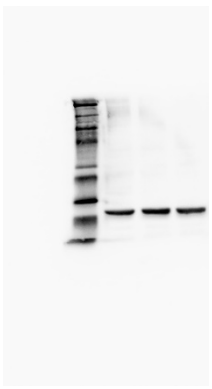

Fig 7.13
SK-LU-1 GAPDH

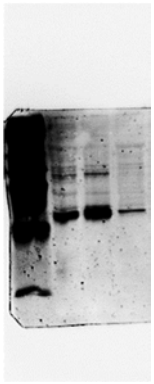

Fig 7.13
SK-LU-1 CRKL

APPENDIX M: Ethics Approval

UNIVERSITY OF MALAYA
KUALA LUMPUR

12th May 2015

Assoc. Professor Dr. Noor Hasima Nagoor Pitchai
Institute of Biological Sciences
Faculty of Science

Dear Researcher,

Development of miRNA-based therapeutics for highly invasive human non-small cell lung cancer (NSCLC)

This is to inform you that the FOM Institutional Animal Care and Use Committee, University of Malaya (FOM IACUC) has approved your Animal Use Protocol with the above mentioned title for a duration of one (1) year until **May 2016.**

Please be advised that should you require changes to be made to the approved protocol, you are responsible to submit an application for amendments. Failure to do so may result in the Approval of your Animal Research Protocol being withdrawn by FOM IACUC.

Your Ethics Reference no. : **2015-160505/IBS/R/NHNP**

Thank you.

Yours sincerely,

Professor Dr. Sim Si Mui
Chairperson
Faculty of Medicine Institutional Animal Care and Use Committee (FOM IACUC)

Faculty of Medicine Institutional Animal Care and Use Committee (FOM IACUC)
Deputy Dean (Research), Faculty of Medicine, University of Malaya, 50603, Kuala Lumpur, MALAYSIA
Tel: (603) 7967 7515 • Fax: (603) 7956 8841• E-mail: fom-iacuc@ummc.edu.my
• Website: http://resfom.um.edu.my

APPENDIX N: A549-I7 Cells Labelling